STATE OF ARKANSAS

ARKANSAS GEOLOGICAL COMMISSION

Norman F. Williams, State Geologist

MISCELLANEOUS PUBLICATION 18-C

CONTRIBUTIONS TO THE GEOLOGY OF ARKANSAS

VOLUME III

Edited by

John David McFarland, III

Little Rock, Arkansas
1988

STATE OF ARKANSAS

ARKANSAS GEOLOGICAL COMMISSION

Norman F. Williams, State Geologist

MISCELLANEOUS PUBLICATION 18-C

CONTRIBUTIONS TO THE GEOLOGY OF ARKANSAS

VOLUME III

Edited by

John David McFarland, III

Little Rock, Arkansas
1988

STATE OF ARKANSAS
Bill Clinton, Governor

ARKANSAS GEOLOGICAL COMMISSION
Norman F. Williams, State Geologist

COMMISSIONERS

C. S. Williams, Chairman ..... Mena

Dr. Richard Cohoon ..... Russellville

John A. Moritz ..... Bauxite

John Gray ..... El Dorado

David J. Baumgardner ..... Little Rock

Dr. David Vosburg ..... State University

W. W. Smith ..... Black Rock

PREFACE

The papers included in this publication were submitted to the Arkansas Geological Commission editor during 1987. Unforeseen delays resulted in a slow publication schedule. Several people worked on this volume: Molly Snyder, Sheila Curd, and Norma Lynn Kover typed the manuscripts; Susan Young, Walter Mayfield, and Joel Whiteside drafted various figures (most of the figures were supplied by the authors); and, Adrian Hunter and Kay Tyler printed, collated, and bound this book. Thanks also goes C. G. Stone and B. R. Haley for their time in reviewing the submitted papers and their editorial suggestions.

John David McFarland, III
Editor

TABLE OF CONTENTS

TIDAL-FLAT DEPOSITS OF THE PLATTIN LIMESTONE (MIDDLE ORDOVICIAN), NORTHERN ARKANSAS

By W. W. Craig[1], M. J. Deliz[2], and K. J. Legendre[3]

[1] Department of Geology and Geophysics, University of New Orleans, New Orleans, LA 70148; [2] CLK Company 1615 Poydras St., 5th Floor, New Orleans, LA 70112; [3] 5509 Wilton Drive, Apt. A, New Orleans, LA 70122

ABSTRACT

The Plattin Limestone (Middle Ordovician) of northern Arkansas is a mud-rich rock with a characteristically laminate fabric similar to that of the Andros Island tidal flat sediments ("Andros-type" lamination of Hardie and Ginsburg [1977]). This fabric is interpreted to result from the influence of deposition of cyanobacterial mats. The most common Plattin lithic types are interlaminated lime mudstone and peloid lime packstone/grainstone, faintly laminated lime mudstone, flat-pebble breccia, and Tetradium-bearing lime wackestone/packstone. Mudcracks and calcite pseudomorphs after evaporites are abundant.

The Plattin is unconformity bounded as evidenced by sharp contacts exhibiting truncation of beds and smaller features, thin basal sandy zones, lithic and faunal isolation from subjacent and superjacent units, and overstep relationships.

The bulk of the Plattin was deposited on a nearly featureless tidal flat bordered by a shallow-water platform of low energy. The distribution of lithic types indicates that the flat was higher to the west. Although evaporites are common in the Plattin, sabkhas did not develop on the Plattin tidal flat. Seasonal or longer term dry periods concentrated tidal flat brines through evaporation, resulting in the deposition of evaporite porphyroblasts within the sediment. Intervening wetter periods dissolved the evaporite minerals. The tidal flat sediment apparently became semi-lithified soon after deposition because molds of evaporite crystals persisted to become casted by calcite.

Initial Plattin strata record high intertidal to supratidal deposition on the eroded surface of the Joachim Dolomite and St. Peter Sandstone. Continued transgression resulted in the deposition in the east of the outcrop belt of fossiliferous wackestone of the low intertidal-subtidal environment. Intertidal and supratidal deposits prevailed to the west. This initial transgression was followed by a progradation that brought laminated, mudcracked, evaporite-trace-bearing tidal flat deposits over the subtidal sediments of the lower Plattin. Renewed transgression resulted in widespread distribution of Tetradium-bearing subtidal rocks across the area. Progradational deposits mark the final phase of Plattin deposition preserved in outcrop. The Plattin was gently warped and eroded before deposition of the overlying Kimmswick Limestone.

INTRODUCTION

The Middle Ordovician Plattin Limestone is a medium-dark gray to light-olive gray to olive black, ultra-fine-grained Tetradium-bearing rock that is characterized by micrite in the form of both undisturbed sediment and as the major constituent of peloid and intraclast grains that are either scattered through the micritic matrix or concentrated in layers. Dolomite beds are present, but subordinate. It is remarkable that unlike many other Paleozoic limestones in which the texture of the original sediment was micrite, very little of the Plattin

Mississippian	Boone Formation
	St Joe Limestone
Devonian	Sylamore Sandstone
	Clifty Formation
	Penters Chert
Silurian	Lafferty Limestone
	St. Clair Limestone
	Cason button shale
	Brassfield Limestone
Upper Ordovician	Cason Phosphate beds
	Fernvale Limestone
Middle Ordovician	Kimmswick Limestone
	Plattin Limestone
	Joachim Dolomite
	St. Peter Sandstone
	Everton Formation
Lower Ordovician	Powell Dolomite

FIGURE 1. *Stratigraphic column in study area.*

micrite has been recrystallized into microspar. Prior to modern limestone classifications, geologists referred to such texture as lithographic. In the early part of this century the Plattin was examined extensively for economic lithographic stone, but unfortunately the abundance of void-filling calcite spar (fenestrae) too commonly interrupts the lithographic character of the rock (Miser, 1922).

The stratigraphic position of the Plattin is shown in Figure 1. Essentially coeval strata of strikingly similar character occur throughout the midcontinent and northeastern United States and adjacent Canada (Mukherji, 1969; Walker, 1973; Cressman and Noger, 1976; Stith, 1979; Amsden, 1983). These rocks record the presence of widespread carbonate tidal flats and associated shallow-subtidal environments during this time.

The Plattin ranges in thickness from 0 to 250 feet (76m) in northern Arkansas. The thickest sections of Plattin were reported by Miser (1922) from along Polk Bayou, north of Batesville, Independence County (Figure 2). The limestone thins in outcrop to the west; in central Newton County it occurs in only a few places as a thin unit, generally less than one foot (.3m) in thickness, between the Everton Formation below and various overlying units (Figure 1). The Plattin has not been reported in outcrop west of Jasper, Newton County (Figure 2).

Miser (1922) was the first to establish the Plattin, as well as subjacent and superjacent strata, on a firm lithic basis. In more recent studies, the Plattin of northern Arkansas is included in reports of the super-St. Peter Ordovician rocks by Freeman (1966a) and Young and others (1972a). These reports, which are broad in scope and based on observations concentrated in Independence, Izard, and Stone Counties, outlined the general lithic character of the Plattin and demonstrated its peritidal origin.

Studies on the formation originating at the University of New Orleans began in the late 1970's. The objectives of these studies were to provide a detailed, bed-by-bed description of the Plattin throughout its area of outcrop and to interpret whatever vertical and lateral trends might be present. The results of these investigations were reported by Jee (1981, 1984), Deliz (1984) and Legendre (1987). The reader is referred to these reports for detailed descriptions of the sections on which this paper is based.

FORMATIONAL CONTACTS

The Plattin is underlain by the Joachim Dolomite throughout Independence, Izard, and most of Stone County. At the Barkshed South locality in western Stone County (Figure 2), the Joachim is absent and the Plattin directly overlies the St. Peter Sandstone. With the possible exception of the section at Gilbert, this condition appears to persist across Searcy County and into eastern Newton County. From here westward, the Plattin is either absent or preserved as slivers between the Everton Formation below and different overlying units. One notable example, first brought to our attention by O.A. Wise of the Arkansas Geological Commission, is the roadcut along Arkansas highway 7 north of Jasper in central Newton County (Figure 2). Here a few inches of Plattin occur between the Jasper Limestone Member of the uppermost Everton and the St.

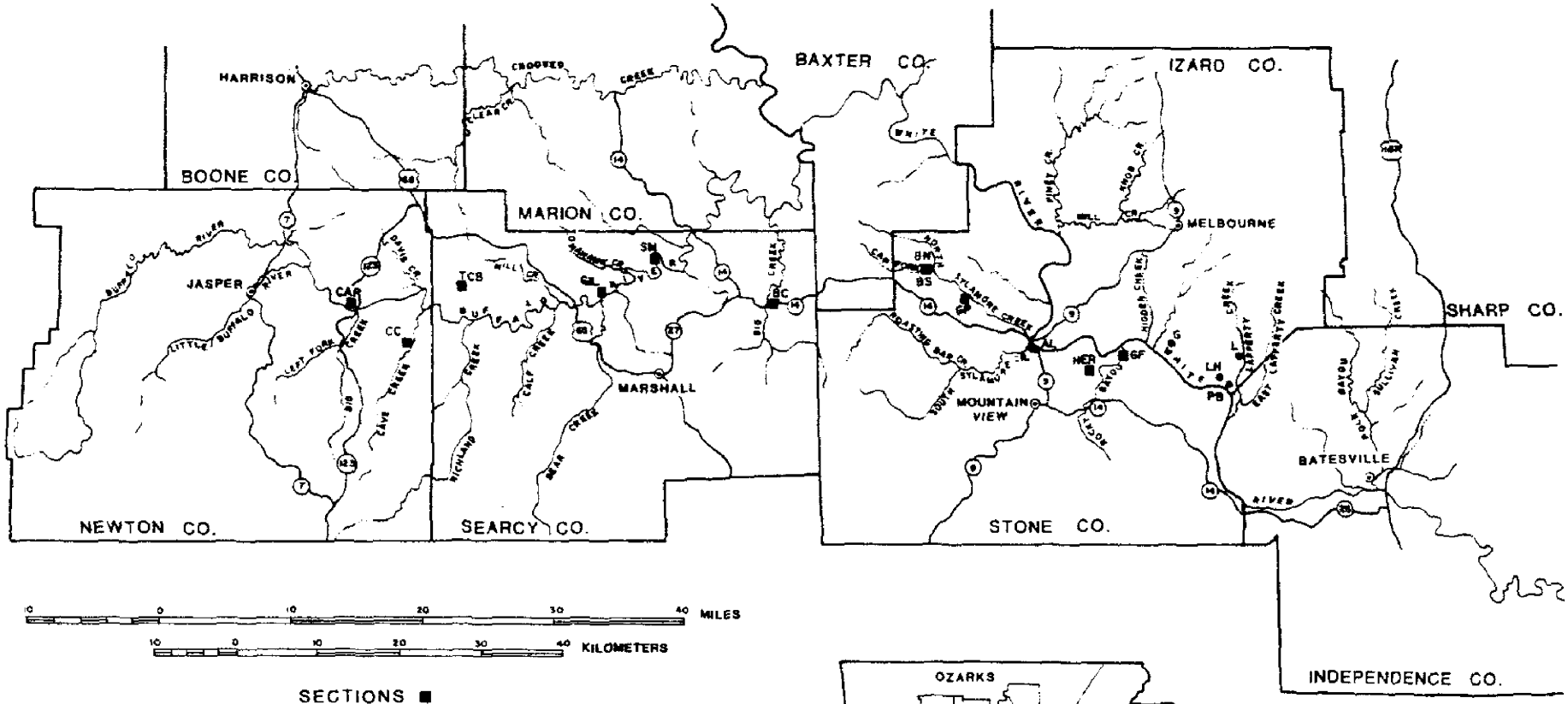

SECTIONS ■

CAR: CARVER
CC: CAVE CREEK
TCB: TRIBUTARY CANE BRANCH
GIL: GILBERT
SM: SOUTH MAUMEE
BC: BEAR CREEK
BN: BARKSHED NORTH
BS: BARKSHED SOUTH
GP: GUNNER POOL
HER: HERPEL
GF: GUION FERRY

JEE'S SECTIONS ●

AL: ALLISON
L: LAFFERTY
G: GUION
LH: LOVE HOLLOW
PB: PENTERS BLUFF

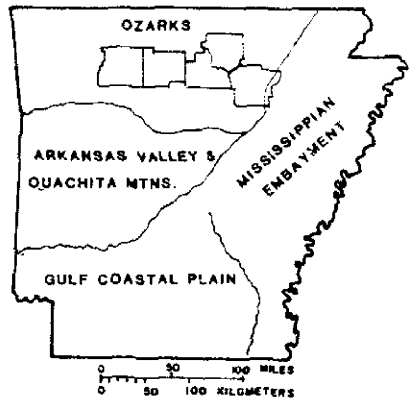

FIGURE 2. INDEX MAP

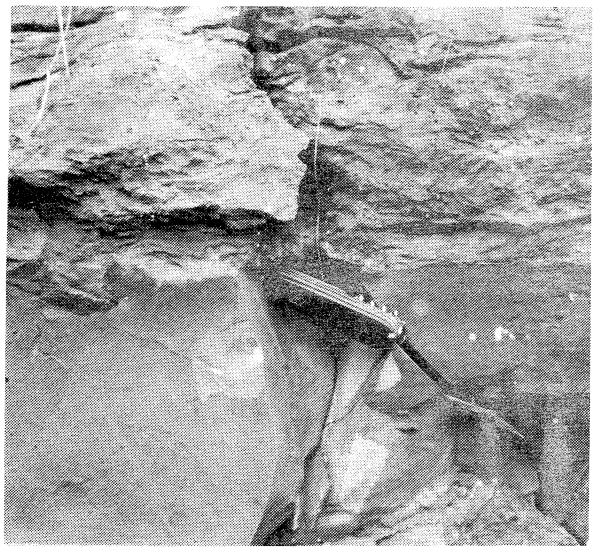

FIGURE 3. *Outcrop photograph of Plattin-Kimmswick(?) "welded" contact at Gilbert. Note the contrast of grain size across contact. Knife rests on finely crystalline dolostone (lithic type 1) of Plattin.*

Joe Limestone. At the Gilbert section, approximately 2.0 feet (0.6m) of dolostone lies between the St. Peter and rock of definite Plattin lithology. If this dolostone is assigned to the Joachim, then it represents the westernmost reported occurrence of Joachim in outcrop in northern Arkansas.

The Plattin is overlain by the Kimmswick Limestone in Independence, Izard, and eastern Stone Counties. Reports of Kimmswick in outcrop west of Mountain View have not been confirmed, although Deliz (1984) reports the possible occurrence of Kimmswick between the Plattin and Fernvale at Gilbert. In Searcy and Newton Counties, the Plattin is commonly overlain by the Upper Ordovician Fernvale Limestone, or where the Fernvale is absent, by younger units.

There has been considerable discussion on the nature of the contacts between the super-St. Peter Ordovician units (Figure 1) of northern Arkansas (Freeman, 1966b, 1972; Young and others, 1972a,b; Craig, 1975; Craig and others, 1984). In his classic report on the manganese deposits of the Batesville district, Miser (1922) placed unconformities between each of the units even though their contacts appeared "even" to him. Miser's decision, which was followed by most

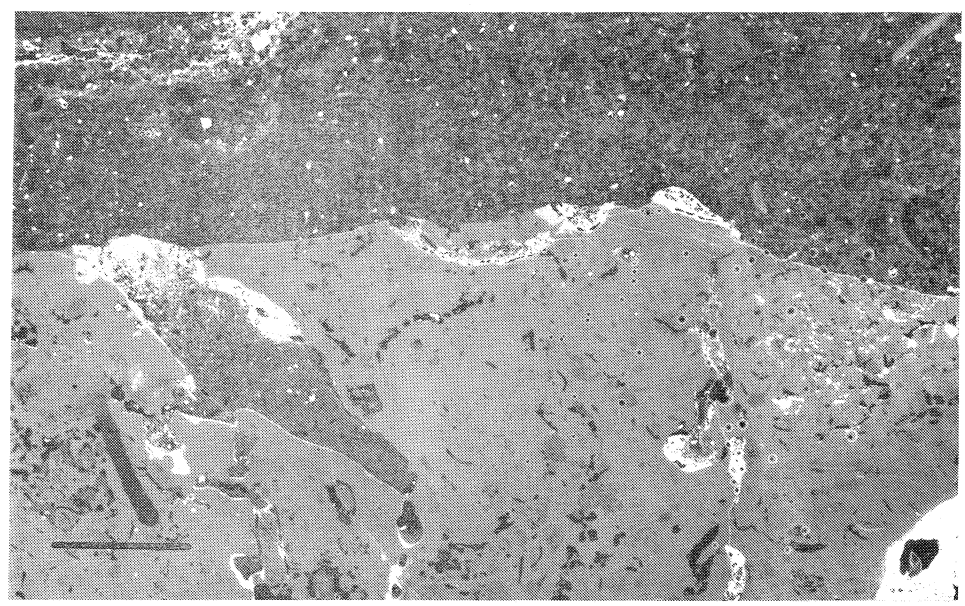

FIGURE 4. *Negative print of acetate peel of the sharp, scalloped Plattin-Kimmswick contact at Guion Ferry. The uppermost Plattin is sparsely fossiliferous and the upper surface contains borings. Bar is 6mm.*

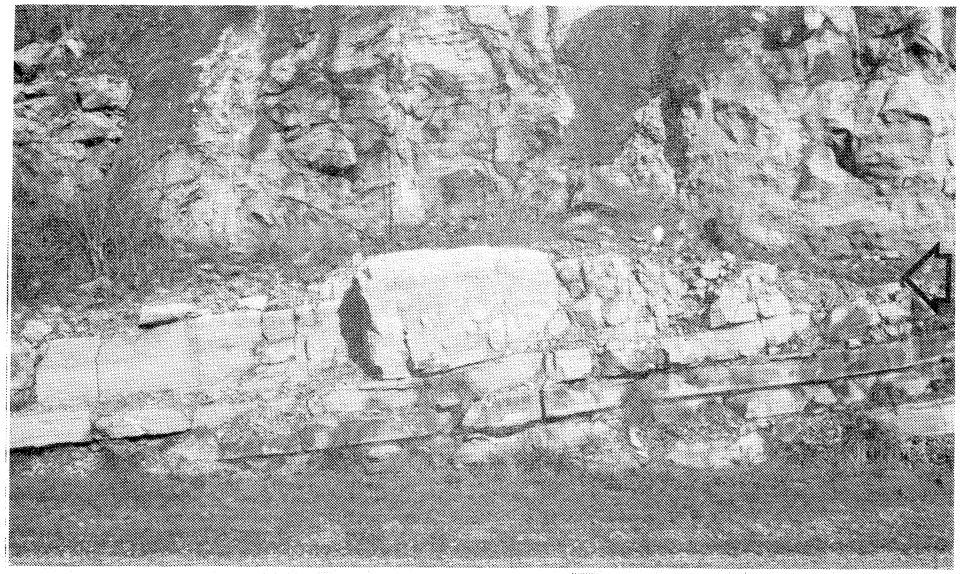

FIGURE 5. *Angular unconformity at Bear Creek between the Plattin and Fernvale. At least 12.5 feet (3.8m) has been removed from top of Plattin at this locality. Arrow points to contact. Thick, light-colored bed below the contact is approximately 3 feet (0.9m) thick.*

later geologists, was strongly influenced by E.O. Ulrich's determination that the units were separated faunally.

The micrite-rich Plattin contrasts sharply with the fine to coarse-grained bioclastic limestone of the Kimmswick (Figure 3). The contact between the two formations is commonly "welded"; that is, it occurs within a single bed with no separation across a bedding plane. It is universally abrupt, shows small-scale truncation features at the contact, and can show small-scale scalloping of the upper surface of the Plattin. In addition to the truncation features, patches of Kimmswick rock type occur within the Plattin up to several inches below the contact. "Welded" contacts between the Plattin and Kimmswick are well displayed at the Guion Ferry (Figure 4) and Herpel sections.

Freeman (1966b) interpreted these contact features to be products of a "micro-karst" surface that formed on a lithified Plattin during a period of subaerial erosion. Young and others (1972a,b) concluded that the Plattin-Kimmswick surface might represent a brief period of subaerial exposure, lithification, and reworking, but that it was unnecessary to call on a prolonged period of erosion or the removal of a significant amount of rock. These authors concluded that the sharp contact was a "facies inconformity" that resulted from the transgression of the subtidal Kimmswick lithotope over the intertidal or supratidal lithotope of the Plattin. Young and others interpreted Freeman's "micro-karst" as a gradational or intercalated passage from the Plattin into the Kimmswick, or as mixing due to burrowing.

The Plattin-Kimmswick contact resembles the scalloped/planar erosional surfaces interpreted by Read and Grover (1977) as products of a prograded, early cemented tidal flat or tidal flat platform. Such a model, which essentially embodies the ideas of Young and others, would explain the features seen at the Plattin-Kimmswick contact without involving the removal by erosion of a measurable amount of rock. There are, however, sections where it can be demonstrated that a few feet, and possible a few tens of feet, of rock were removed from the top of the Plattin prior to the deposition of the Kimmswick. Freeman (1972) and Craig and others (1984) have described and illustrated an angular contact between the Plattin and Kimmswick vividly displayed in a roadcut on the Love Hollow road west of Cushman, Independence County. Here it can

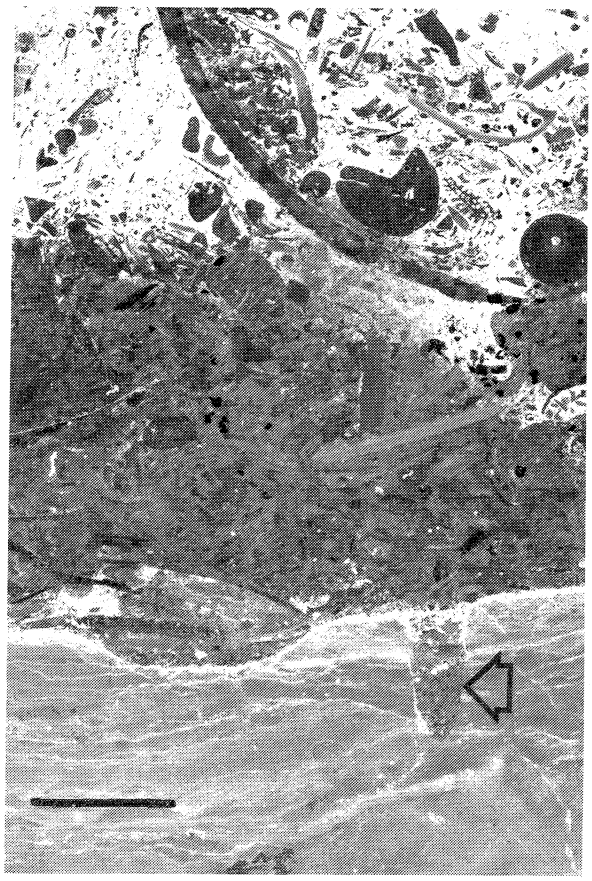

FIGURE 6. *Negative print of acetate peel of Plattin-Fernvale "welded" contact at Cave Creek. White residue separates the two formations. Uppermost Plattin is laminated dolostone; lower Fernvale is coarse bioclastic limestone. White area in Fernvale is phosphate replacement. Arrow points to Fernvale-filled boring in top of Plattin. Bar is 4mm.*

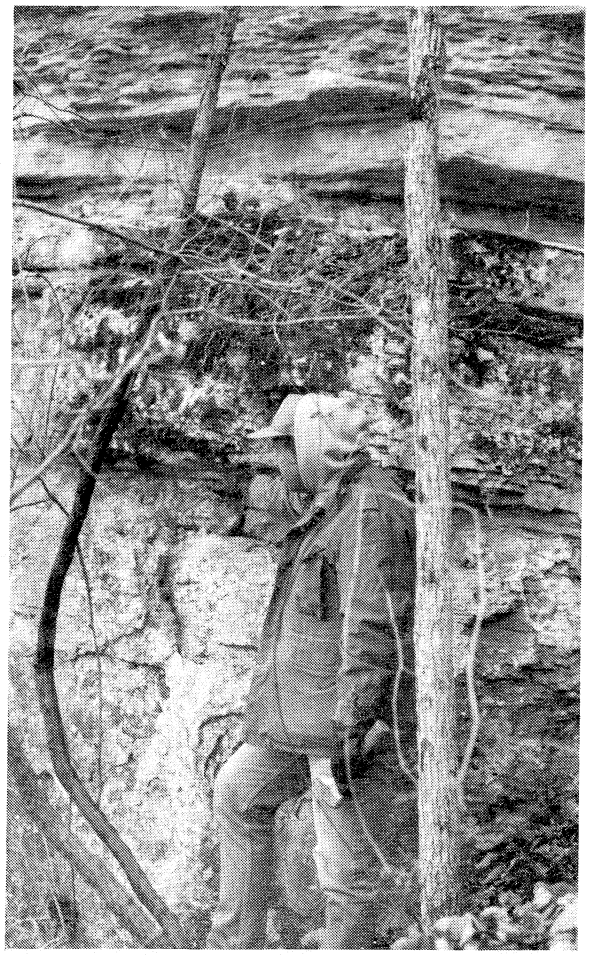

FIGURE 7. *Joachim-Plattin contact at Gunner Pool (at level of geologist's hand). Note contrast of thick bedding below and slabby bedding above.*

be demonstrated that the Plattin was broadly warped and eroded prior to Kimmswick deposition. At the Big Creek section of this study, a similar angular relationship occurs between the Plattin and, in absence of the Kimmswick, the overlying Upper Ordovician Fernvale Limestone (Figure 5). Deliz (1984) has determined that a minimum of 12.5 feet (3.8m) has been removed from the top of the Plattin at this locality. Although the warping of the Plattin at Big Creek could have taken place after deposition of the Kimmswick, it probably represents the same pre-Kimmswick event recorded along the Love Hollow road. The absence of the Kimmswick at Big Creek is attributed to post-Kimmswick-pre-Fernvale erosion. The Plattin-Fernvale contact at Big Creek is "welded" and exhibits the same features as the Plattin-Kimmswick contact in those places where the Kimmswick is present.

"Welded" contacts between the Plattin and Fernvale also occur at the Tributary Cane Branch, Cave Creek and Carver (Figure 6) sections, and between the Plattin and an overlying bioclastic limestone, possibly the Kimmswick, at the Gilbert section.

The contact between the Joachim and Plattin is placed where the succession becomes dominantly limestone, a level that is easily recognized in the field by the change

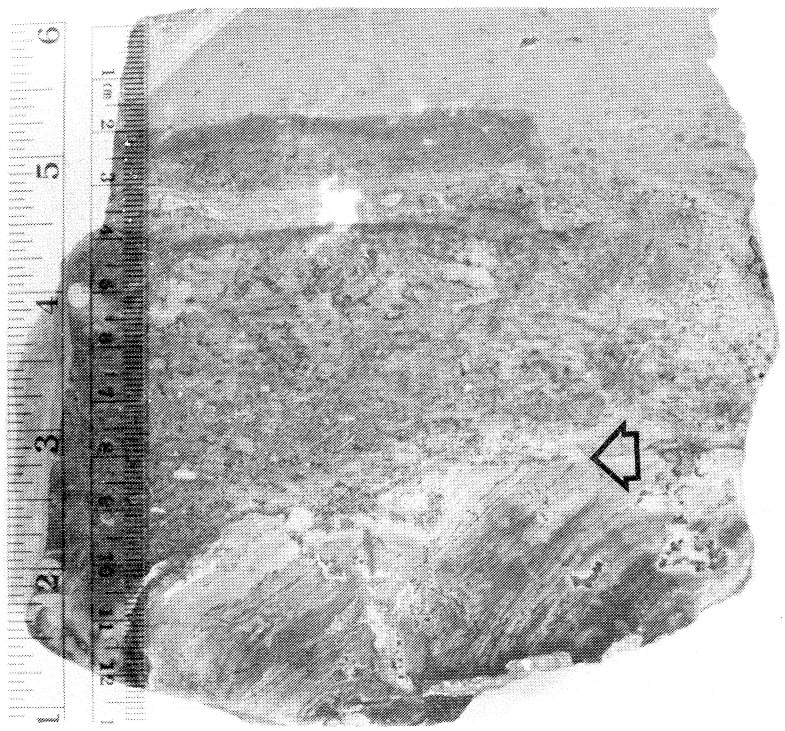

FIGURE 8. *Polished slab of Joachim-Plattin contact at Guion Ferry (arrow). Basal Plattin is quartz-sandy peloid-intraclast dolomite packstone/grainstone overlain by light-colored, mudcracked, evaporite-bearing lime mudstone (lithic type 3). Scale is in millimeters and inches.*

from thick-bedded dolomite to slabby, thin-bedded limestone (Figure 7). Using such a separation of the two units places in the base of the Plattin some beds containing pervasive dolomite. These beds are few, however, and usually contain undolomitized limestone allochems and lenses. Similar beds also occur at unpredictable levels higher in the formation. The separation also results in rare, thin beds of dolomitic limestone in the upper part of the Joachim. The uppermost bed of Joachim at Gunner Pool, as well as a bed approximately 4.0 ft. (1.2m) below the contact at Guion Ferry, are examples. Even though this separation does not result in a complete lithic distinction between the two units, it is chosen because of certain physical features associated with it.

One of these physical features is the change in bed thickness mentioned above. A high content of detrital mud delivered during Plattin deposition gives rise to the unit's numerous shale breaks and slabby bedding, features which are uncharacteristic of the Joachim. Other features associated with the contact as defined above suggest an interval of erosion between the two units. At Guion Ferry the Joachim-Plattin contact is marked by a planar truncation of stromatolites in the uppermost Joachim. The basal Plattin is a two-inch (5cm) dolomitized conglomeratic zone containing subangular to angular dolomite clasts up to pebble size and fine to medium sand-sized quartz grains (Figure 8). The conglomerate grades up into interlaminated lime mudstone and peloid lime packstone/grainstone (lithic type 6, described below).

Similar quartz-sandy conglomeratic zones of a few inches thick characterize the base of the Plattin at Herpel and Gunner Pool. At Herpel the conglomeratic zone is in sharp contact with dolomitized lithic type 6 of the Joachim below and grades up into undolomitized lithic type 6 of the Plattin. At Gunner Pool the uppermost Joachim is an

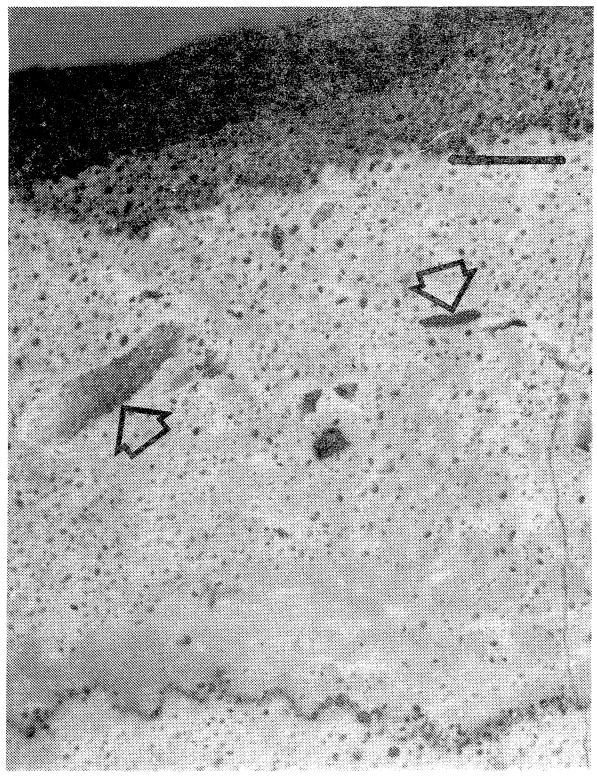

FIGURE 9. *Polished surface of basal Plattin at Barkshed South, where Plattin directly overlies the St. Peter Sandstone and contains rounded quartz grains and pebble-sized quartz arenite clasts (arrows). Bar is 4mm.*

intraclast-peloid lime packstone/grainstone (like lithic type 4, described below) containing rare, thin, disrupted mud-cracked lime mudstone laminae and quartz-sandy patches. It is overlain in abrupt contact by a sandy conglomeratic zone of the basal Plattin containing angular pebble-sized clasts of dark limestone derived from below. The conglomeratic zone grades up into an intraclast-peloid lime packstone/ grainstone (lithic type 4).

The Barkshed localities are interesting in that 43 feet (13m) of the Joachim is present between the St. Peter and Plattin at the Barkshed North section, whereas less than one mile (0.6km) away at Barkshed South, the Plattin rests directly on the St. Peter. The Plattin is approximately the same thickness at both localities suggesting that the absence of the Joachim at Barkshed South is not simply failure to dolomitize the basal portion of the section. There is nothing remarkable about the Joachim-Plattin contact at Barkshed North. Lithic type 6 overlies the dolomite of the Joachim in a simple bedding plane contact without an intervening conglomeratic zone. At Barkshed South the contact is slightly undulatory and the basal Plattin is sandy and contains pebbles of quartz arenite apparently derived from the underlying St. Peter (Figure 9). The Plattin and St. Peter are also in contact at Bear Creek, South Maumee, Tributary Cane Branch, Cave Creek and Carver. At the latter three localities a thin shale (1-3 inches) intervenes between the two units (Plate 7:B). At South Maumee the contact is undulatory

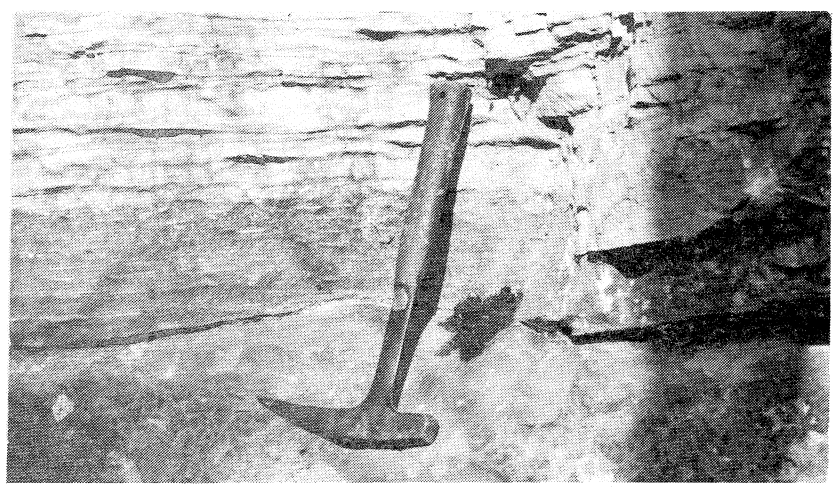

FIGURE 10. *St. Peter-Plattin contact at South Maumee. Rock hammer rests on undulating upper surface of St. Peter. Notice lower Plattin onlapping small St. Peter high to left of hammer. Dark bed at base of Plattin is sandstone with light-colored discontinuous laminae of lime mudstone.*

(Figure 10) and topography on top of the St. Peter causes a differential thickness of two to four inches (5 to 10cm) in the basal bed of the sandy lime mudstone to limy sandstone of the Plattin. At Bear Creek the contact is sharp and the basal Plattin is sand free.

The Plattin-Kimmswick contact is almost certainly unconformable. The angular relationship that the Plattin exhibits with overlying units indicates that prior to deposition of the Kimmswick, the Plattin was broadly warped and truncated by subaerial erosion. The erosional surface must have been reasonably smooth because there is no indication of large-scale topography on top of the Plattin. A similar history is probable for the Joachim prior to Plattin deposition. This would explain the abrupt disappearance of the Joachim between the two Barkshed localities, its erratic thickness from place to place, and its general disappearance to the west. In support of this, Jee (1981) has illustrated from his section at Penters Bluff (Figure 2) along the White River an apparent slight angular relationship between the Joachim and Plattin.

Faunal occurrences provide additional evidence on the nature of the Joachim-Plattin contact. As mentioned previously, Ulrich (in Miser, 1922) reported that the two units were isolated faunally. Ongoing conodont studies at the University of New Orleans show that the Joachim is dominated by elements of Plectodina and Leptochirognathus, whereas Plattin conodonts consist almost entirely of members of Erismodus and Curtognathus. This distinctive change in the conodont succession occurs exactly at the level of the sandy, conglomeratic zone in the base of the Plattin. This dissimilarity of faunas could have resulted from a change in environments across the contact, but judging from a comparison of their lithic types, the bulk of the two units appear to be products of quite similar intertidal and supratidal environments, a conclusion that would seem to rule out ecologic control. The observed faunal change is, however, compatible with a break in deposition between the two units.

Both Jee (1981, 1984) and Legendre (1987) report the presence in the Plattin of intraformational "welded" surfaces. These

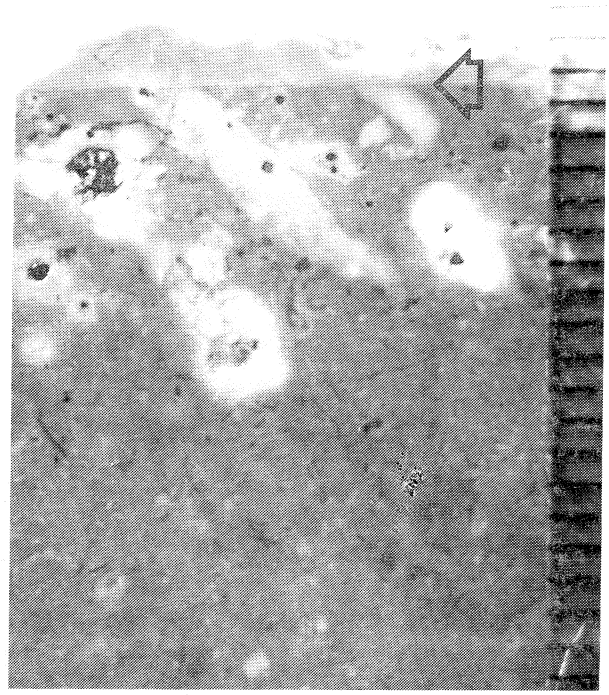

FIGURE 11. *Polished slab of sharp intraformational contact (arrow) in Plattin (HER-38). Lithic type 6 is overlain by lithic type 3. Notice truncation of intraclasts below the contact. Light areas are bleached halos surrounding oxidized pyrite. Scale is in millimeters.*

surfaces are sharp and exhibit truncation (Figure 11). Because they do not separate units that are lithically and faunally distinct, these surfaces are not believed to carry the temporal significance of the formational contacts. They probably represent early cemented tidal flat surfaces similar to those reported by Read and Grover (1977).

LITHIC TYPES

The dominant portion of the Plattin is characterized by features that identify cryptalgal fabric as defined by Aitken (1967). Prime among these are fine-scale planar and wavy laminations and a variety of so-called "birdseyes", an early descriptive term for unsupported void spaces filled by calcite spar. Tebbutt and others (1965) redesignated these openings as fenestrae, which they defined as "...a primary or penecontemporaneous gap in

rock framework, larger than grain-supported interstices... completely or partially filled by secondarily introduced sediment or cement." Logan (1974, p. 214, Table 2) categorized fenestrae as laminoid, irregular, or tubular and further divided each type into fine, medium, and coarse, depending on their thickness. Conversely, Shinn (1968, 1983a,b) has argued that the term fenestrae be restricted to two types of voids: planar-shaped, generally unconnected openings that are more or less parallel to lamination and bubble-shaped openings that are generally randomly distributed in the rock. These features he attributes to shrinkage and expansion, gas bubble formation, air escaping during flooding and wrinkling of cyanobacterial (blue-green algal) mats. Shinn believes that these features are preserved almost exclusively in upper intertidal and supratidal sediments and thus their presence in rock serves as an indicator of those environments even in the absence of other diagnostic features. He proposed that all other calcite-filled voids, which commonly resemble "true fenestrae" described above, be called "pseudo-fenestrae". Because identification of fenestrae as defined by Shinn requires genetic interpretation, we have not followed his scheme. Instead, we use the term fenestrae in the original objective sense of Tebbutt and others (1965). The spar-filled voids that create the Plattin fenestrae have several origins, including burrows, desiccation structures. dissolution of evaporites and mollusc shells, molds of algal filaments and ameoboid interstices between compacted peloids and intraclasts.

The lithic subdivisions presented below are abstracted from more detailed classifications presented by Jee (1981, 1984), Deliz (1984) and Legendre (1987).

1. **Finely crystalline dolostone/ calcareous dolostone.** Lithic type 1 is a yellowish gray, brownish gray to shades of light and olive gray, medium-bedded to thick-bedded, structureless dolostone. Dolomite grains are subhedral to euhedral, very fine grained (decimicron sized) and equigranular, imparting a "sucrosic" appearance to the rock. Minor amounts of fine-grained to medium-grained, subangular to well-rounded quartz sand can be present. Pyrite crystals and associated iron staining are common.

Calcareous dolostones (those dolostones with 10-50% calcite) are also present, particularly in the western part of the study area. Dolomitization is selective in these samples and ghosts of replaced allochems and minor lime mudstone laminae (mm size) can be present. The lithic types commonly replaced include numbers 3 (lime mudstone), 4 (intraclast-peloid lime packstone/grainstone), and 6 (interlaminated lime mudstone and peloid lime packstone/grainstone). Calcite pseudomorphs after halite and very fine-grained euhedral quartz crystals can be present within lime mudstone laminations. Medium-grained, rounded quartz sand is locally abundant. Disarticulated ostracode and trilobite skeletons are of scattered occurrence.

2. **Laminated dolostone** (Plate 1:A). Lithic type 2 is a yellowish gray to light-brownish gray, thin-bedded to medium-bedded, unfossiliferous, externally and internally laminated dolostone. Laminations are very thin (<1mm), slightly undulatory, and result from alternation of very fine-grained and fine-grained (decimicron-sized) unequigranular, subhedral to euhedral dolomite.

3. **Lime mudstone** (Plate 1:B-D). Lithic type 3 is an externally thin-bedded to thick-bedded, internally homogeneous to faintly laminated fenestral lime mudstone. Subtle laminations are caused by difference in grain size among coarser mud-size or silt-size particles as well as rare, thin (<0.5mm), discontinuous, densely packed peloid laminae. Fine (1-5cm) mud-cracks, fine sheet cracks, calcite pseudomorphs after both halite and gypsum, and fine to medium laminoid to irregular fenestrae can be present. Angular and linear boundaries of some fenestrae suggest that their origin is the filling of molds left by the solution of porphyroblastic evaporite crystals that became linked laterally as they grew in the sediment (Plate 1:D). Prior to filling, the molds were slightly to grossly deformed by compaction and caving. In places the rock is completely shattered by desiccation, imparting an intraclastic texture to some intervals (Plate 1:B). Fossils include sparse disarticulated and articulated ostracode valves, and more rarely

trilobite and mollusc fragments. Fine to very-fine euhedral dolomite is sparsely disseminated through the rock, or more concentrated along rare to common stylolites.

4. **Intraclast-peloid lime packstone/grainstone** (Plate 1:E). Lithic type 4 is a thin-bedded to thick-bedded allochemical rock in which either peloids or intraclasts are the dominant grains. Fine to medium, laminoid to irregular fenestrae can be locally abundant. Horizontal tubular burrows are also present. Peloids are poorly to well sorted and exhibit open to dense packing. Intraclasts, which internally are fenestral lime mudstone or peloid packstone, are fine sand to small pebble sized, subangular (polygonal) to well rounded and can have their long axis at any angle to bedding; many, however, have their long axis aligned parallel to bedding and overlie medium laminoid fenestrae. Allochems occur in layers that can be normally or inversely graded and can be partially recrystallized to microspar. Locally abundant are very fine-grained to medium-grained, subangular to well-rounded quartz sand, ooids with radial or concentric fabric and coated grains. The rock can contain disseminated very fine-grained subhedral dolomite and iron-stained pyrite crystals. Fossils include sparse disarticulated ostracode valves (locally abundant) and rare fragments of trilobites and pelecypods.

5. **Peloid-intraclast lime wackestone or wackestone/packstone** (Plate 2:A). Lithic type 5 is much like lithic type 4, but has a greater lime mud content. The muddier portions can contain fine mudcracks, sheet cracks, angular spar-supported clasts, calcite pseudomorphs after evaporites, medium-sized irregular fenestrae, or can be dense and homogeneous. Medium-grained, well-rounded quartz, disseminated very fine-grained anhedral to euhedral dolomite, and iron-stained pyrite crystals are present to locally common. Burrowing is suggested by mottled areas containing micrite and peloids and by vertical tubular fenestrae. Fossils include rare to locally common disarticulated ostracode valves, trilobite fragments, and tentaculitids(?).

6. **Interlaminated lime mudstone and peloid lime packstone/grainstone** (Plate 2:B-D; Plate 3:A-C; Plate 4:A,B). Lithic type 6 is externally thick bedded, and internally contains thin wavy to planar laminae (Plate 2:B). Lime mud laminae are on the average thicker than peloid laminae, the former generally ranging from 0.5-3.0mm, with a maximum of 1.0cm, and the latter commonly less than 1.0mm, but in some examples up to 5.0mm. Mudstone laminae commonly contain fine mudcracks (Plate 2:C; Plate 3:B), fine sheet cracks, calcite pseudomorphs after halite (Plate 3:A; Plate 4:B) and selenite (Plate 2:D; Plate 4:A), and fine to medium laminoid and irregular fenestrae. Some of the latter appear to be evaporite casts, as suggested for similar fenestrae in lithic type 3 (Plate 2:C,D; Plate 3:B,C). Peloid laminae are laterally discontinuous; mud laminae are of greater lateral extent (Plate 2:C; Plate 3:A,B). Commonly associated with this lithic type are laminae up to a few inches thick of lithic type 4 (intraclast-peloid lime packstone/grainstone). Very fine subhedral to euhedral dolomite crystals are sparsely disseminated through the rock and can be concentrated along stylolites. Sparse to common ostracode valves and minor amounts of trilobite and mollusc skeletons are present.

7. **Mollusc lime wackestone** (Plate 4:C,D). Lithic type 7 is a medium-bedded to thick-bedded, unlaminated, burrow-mottled, matrix-supported rock in which skeletal allochems are sparse to common. The most abundant allochems are dominated pelecypod valves and fragments (recrystallized to calcite spar), steinkerns and fragments of gastropods (also recrystallized), and articulated and disarticulated ostracode valves; skeletal fragments of trilobites, brachiopods, and crinozoans are minor. Some examples contain conical fossils tentatively identified as tenticulitids (Plate 4:D). Some intervals contain vertical burrows; peloids and minor sand-sized intraclasts occur in patches that appear burrow related. Sparse calcite pseudomorphs after halite are present in places. Euhedral to subhedral dolomite is sparsely disseminated throughout the rock and can be concentrated along stylolites.

8. **Skeletal lime wackestone/packstone** (Plate 5:A). Lithic type 8 is a medium-bedded to thick-bedded, unlaminated, matrix-rich limestone in which skeletal fragments are locally abundant, generally

diverse, and include pieces of the calcareous alga Hedstroemia,individual and aggregate corallites of the tabulate coral Tetradium (not in growth position), crinozoan plates and spines, fragments of bryozoans, trilobites, molluscs, tentaculitids(?), articulated and disarticulated valves of ostracodes and brachiopods, and fine indeterminate bioclasts. Mottled areas filled by cryptocrystalline to very finely crystalline dolomite and prominent concentrations of peloids and minor sand-sized intraclasts are common. Sparse pyrite and very-fine crystals of doubly-terminated quartz can be present.

9. **Oold-peloid lime grainstone/ packstone** (Plate 5:B-D; Plate 6:A). Lithic type 9 is a medium-bedded to thick-bedded limestone in which ooids with radial or concentric structure are a common allochem. Peloids, coated grains, and intraclasts can be common to locally abundant. Ooids can be almost totally micritized. Allochems are generally well rounded, well sorted, locally densely packed and can be cross laminated (Plate 5:B). Intraclasts, where present, are fine sand to pebble size, subangular (polygonal) to well rounded and composed of lime mudstone or peloid packstone. Many have their long axis aligned parallel to bedding. Scoured lime mudstone laminations are rare. Medium-laminoid and horizontal tubular fenestrae can be present, as well as grains of medium-sized, well-rounded quartz and very fine-sized subhedral dolomite. The rock is sparsely fossiliferous, with scattered occurrences of disarticulated and fragmented ostracode valves, high-spired gastropods, and pelecypods.

10. **Stromatolitic limestone** (Plate 6:B,C). Lithic type 10 consists of medium-bedded to thin bedded, internally laminated, vertically stacked hemispheroids of the LLH-C and SH-V types of Logan and others (1964). Hemispheroids are of varying sizes, with amplitudes up to 25cm and diameters of 35cm (Plate 6:C). This rock, which is characterized by geometry rather than petrology, is formed of a variety of lithic types, dominant among which is lithic type 6 (interlaminated lime mudstone and peloid lime packstone/grainstone) (Plate 6:B). Lime mudstone laminae are commonly irregular, discontinuous, undulose, wispy, and are thin (0.5-3.0mm). Thicker laminae may be present and generally contain fine mudcracks, sheet cracks, calcite pseudomorphs after halite, and fine to medium irregular fenestrae. Peloid laminae, which may be as thin as 0.5mm, are commonly well sorted, densely packed, may exhibit normal or inverse grading, commonly possess laminoid and irregular fenestrae, and contain subangular (polygonal) to well-rounded, fine-sand to pebble-sized intraclasts, many of which have their long axis aligned parallel to bedding and overlie prominent laminoid fenestrae. Coated grains, ooids, and disarticulated ostracode valves are rare, but may occur in some peloid laminae. Very fine-grained, subhedral to euhedral dolomite grains are sparsely disseminated throughout the rock, but are somewhat more concentrated in the peloid laminae.

11. **Coral lime boundstone** (Plate 7:A). Lithic type 11 is characterized by upright colonies of the tabulate coral Tetradium, apparently in growth position. The coral framework is surrounded by a matrix of skeletal lime wackestone identical to lithic type 8.

12. **Calcareous shale or argillaceous limestone** (Plate 7:B,C). Detrital clay is admixed at different levels in the Plattin, forming rocks that range from argillaceous lime mudstone to calcareous shale. These shaley units range in thickness from 1/4 inch to 20 inches (0.6-50cm) in the western part of the study area, where they are most common, to approximately 1cm in the east.

ANALYSIS OF DEPOSITIONAL ENVIRONMENTS

The Plattin possesses a multitude of textures and structures that are similar to those of modern carbonate tidal flats. These include desiccation features, such as mudcracks, sheet cracks, intraclast breccias and conglomerates, teepee structures, and evidence of evaporite deposition. Other hall marks of modern carbonate tidal flat sediments are also notably displayed, including stromatolites, a wide variety of fenestral fabric, smooth and crinkled millimeter laminations, and abundant peloids.

Modern tidal flats have been studied in a variety of climatic settings: Andros Island,

Bahamas, a humid climate with 45 inches (114cm) average annual rainfall (Shinn and others, 1969; Hardie, 1977); Shark Bay, Western Australia, a semi-arid climate with 9 inches (23cm) average annual rainfall (Logan and others, 1974); and the Trucial Coast, Persian Gulf, an arid climate with 1.5 inches (<4cm) average annual rainfall (Kendall and Skipworth, 1968; Purser, 1973). Based on these studies, Shinn (1983a, 1986) has provided excellent summaries on tidal flat deposition.

The term tidal flat is applied to strandline expanses that are subaerially exposed for greater or lesser amounts of time. The consensus is that most sediment is delivered to the flat during periodic meteorological tides rather than diurnal, lower energy astronomical tides (Shinn, 1986). Tidal Flat investigators have generally divided this nearshore, tidally influenced region into three zones: supratidal (above mean high tide); intertidal (between mean high tide and mean low tide); and subtidal (below mean low tide). Because different workers have different definitions of these levels, and because seasonal variations (including storms) along coasts will cause zonal boundaries to shift during the year, Ginsburg and others (1977) have elaborated on a scheme, called the exposure index, that compares tidal flat sediments in relation to the amount of time the sediments are exposed subaerially. By considering textures, structures, and organic activity, all of which are strongly influenced by the amount of subaerial exposure, an exposure index can be assigned to modern sediment and, by analogy, to the rock record. For Andros Island, where the exposure index was determined, the surface above mean high water (supratidal) is exposed more than 85% of the time and the surface between mean high water and mean low water (intertidal) is exposed between 25% and 85% of the time. Ginsburg and others (1977, Figure 4) demonstrated that great similarity exists between the organic and inorganic structures developed in sediments deposited in the supratidal and high intertidal realms. Although some subtidal environments are distinctive, in general it is equally difficult to separate sediments deposited in this zone from those of low intertidal origin. In view of these problems, in the following interpretation of Plattin lithic types we divide the tidal flat into: supratidal-high intertidal, low intertidal-subtidal, and subtidal.

Below we analyze the depositional environment of each lithic type except lithic type 12: calcareous shale or argillaceous limestone. Lithic type 12 represents the influx of detrital mud at different times during Plattin deposition, and as such is not diagnostic of any specific depositional environment. Limey shale and clayey limestone is more common in western sections.

SUPRATIDAL-HIGH INTERTIDAL

Lithic type 1 - finely crystalline dolostone: There is a tendency to interpret dolomite in the record as supratidal because it is documented as an early replacement of calcium carbonate on present-day supratidal flats of Andros Island (Shinn and others, 1965). In addition, evaporation of tidal flat waters, such as in the sabkhas of the Persian Gulf (Bush, 1973), leads to the precipitation of calcium carbonate and calcium sulfate, thus enhancing the magnesium to calcium ratio and producing dolomitizing fluids. In the latter example, however, the supratidal sabkhas have prograded seaward and lie above calcium carbonate subtidal lagoonal sediments, which in the normal circulations of the brines are almost totally replaced by dolomite. To add to the mystery of modern dolomite formation, little dolomite is forming within the supratidal zone of Shark Bay even though sediments are saturated with magnesium-rich brines apparently produced by the evaporation of tidal flat groundwaters (Logan, 1974).

The lesson from these examples is that the only clue for the environment of deposition of dolostone or dolomitic limestone is the relict structures of its calcium carbonate precursor. Structureless, pervasively dolomitized rock, such as some of lithic type 1, provides no such clue. Much of lithic type 1, however, is calcareous dolostone in which allochemical ghosts and/or partially dolomitized to undolomitized laminae of mudcracked, evaporite-trace-bearing lime mudstone are preserved. These examples indicate that the most commonly dolomitized Plattin lithic types are numbers 3, 4, and 6, which we consider to

be dominantly high intertidal to supratidal. The interlaminated dolomite and micrite prominently developed in the High Bridge Group of Kentucky, interpreted by Cressman and Noger (1976) as supratidal, is similar to some of our lithic type 1, as is Jee's (1984) lithofacies 7 (interlaminated, dolomitic and lime mudstone) of the Plattin Limestone in Izard and Independence Counties, Arkansas.

Lithic type 2 - laminated dolostone: Little diagnostic remains of this rock except its millimeter laminations, which are distinctly visible in outcrop (Plate 1:A). It resembles rock interpreted by different authors as supratidal dolomite (Matter, 1967; Roehl, 1967; Laporte, 1967; Lucia, 1972; Gebelein and Hoffman, 1973). Cressman and Noger (1976) identified a similar rock, which they termed "laminated finely crystalline dolomite", from the High Bridge Group of Kentucky. Our lithotype 2 is the same as Jee's (1984) lithofacies 8 (faintly laminated, dolomitic mudstone) from Izard and Independence Counties, Arkansas, and Walker's (1973) lithology 2 from the Black River Group of New York.

The very thin planar to sightly undulose laminations are interpreted to be cyanobacterial in origin. Similar layering was designated as smooth flat laminations by Hardie and Ginsburg (1977), who found it to be characteristic of levee crests on Andros Island. Ginsburg and others (1977) assign an exposure index of >90 to this type lamination.

Lithic type 3 - lime mudstone: Most intertidal and supratidal lime mud in the Plattin probably originated in subtidal environments as soft peloids that upon onshore transport and compaction disintegrated and lost much of their identity. This is suggested by a subtle peloid texture preserved in many of the Plattin mud rocks. Hardie and Ginsburg (1977) observed a similar "clotted" texture in the mud laminae of the Andros Island tidal flat.

Some examples of lithic type 3 are structureless and apparently homogeneous. Homogeneous lime mudstone occurs in layers up to approximately eight feet (2.4m) in thickness and is most common in western sections (TCB and CC, Figures 21, 22). The greater percentage of Plattin mid rock, however, is to some extent heterogeneous and exhibits at least some combination of a variety of textures and structures. This heterogeneous mudstone is either faintly laminated (Plate 1:C or unlaminated, both types of which are commonly mudcracked and/or contain calcite pseudomorphs after evaporites (Plate 1:B). Ostracodes (mostly leperditids) are common to locally abundant in rocks that exhibit desiccation features. Rarely, both laminated and unlaminated varieties can be burrow mottled and/or possess a sparse fauna of diverse nature.

It is apparent that heterogeneous lithic type 3 is gradational with a number of other lithic types, and in fact is found interbedded with other types on a scale too small to be represented in our columnar sections (Figures 13-23). The subtle laminations found in many examples of lithic type 3 are caused by either a slight difference in color and texture between the coarser mud-sized grains or by rare, discontinuous peloid laminae. Faintly laminated lithic type 3 is similar to lithic type 6, the major difference between the two being that faintly laminated lithic type 3 is dominantly lime mid with only subordinate peloid laminae. Alternating discontinuous peloid laminae and continuous mud laminae occur on the western side of Andros Island. This type of laminate fabric is so common to the Andros Island intertidal and supratidal environments that Hardie and Ginsburg (1977) have referred to it as "Andros-type" lamination. Although the peloid and mud laminae commonly occur as couplets on Andros Island, as well as in lithic type 6 of the Plattin, successive mud laminae without intervening peloid ones also are present. Hardie and Ginsburg (1977) interpret each "Andros-type" lamination as the product of a single storm that carried mud and peloids from offshore subtidal environments onto the tidal flat. The mud layer is deposited first as an algal "stick-on", a layer that is trapped on the surface of the wetted algal mat, and the peloids are deposited later in the surface swales of the mat as the storm peak wanes. Successive mud layers, which characterize faintly laminated lithic type 3, would be products of lesser storms that did not entrain quantities of peloids. Faintly laminated lithic type 3 possesses both smooth flat lamination and disrupted flat lamination of Harkie and Ginsburg (1977). The former, in

which mudcracks are rare to absent, is characteristic of levee and beach crest surfaces on Andros Island; the latter, in which the abundance of fine mud cracks, sheet cracks, and fenestrae interrupt lamination, is common on levee and beach ridge backslopes. These features collectively suggest for faintly laminated lithic type 3 an exposure index (Ginsburg and others, 1977) of <90, which is characteristic of supratidal conditions. Traces of evaporites, which are important aspects of faintly laminated lithic type 3, also indicate a high intertidal to supratidal environment. A similar environment is suggested for most of those heterogeneous varieties of lithic type 3 that are apparently unlaminated but possess mudcracks and traces fo evaporites. Both laminated and unlaminated varieties of lithic type 3 discussed above are commonly associated with lithic types 4 and 6 in the lower portions of the Plattin, an occurrence which strengthens their interpretation as products of the supratidal and high intertidal environments.

Heterogeneous lithic type 3 encompasses Jee's (1984) lithofacies 2 and 4 (tubular fenestral, lime mudstone to peloidal, lime wackestone and homogeneous, lime mudstone) from the Plattin of Izard and Independence Counties, Arkansas. Cressman and Noger (1976) designated similar rock types from the High Bridge Group of Kentucky as "laminated micrite" and "micrite containing tubiform burrows," which they interpreted as supratidal and intertidal, respectively.

A few examples of heterogeneous lithic type 3, both faintly laminated and unlaminated, can contain scattered burrows and/or a sparse, though diverse, fauna. Burrows are evidenced by patches of peloids, calcite spar, or dolomitic mottles. Some of these burrowed and/or fossiliferous rocks also can have mudcracks and evidences of evaporites. Burrowed and/or fossiliferous mud rocks, which are most common in the upper portions of the thicker sections (Figures 13, 14, and 18) where they are associated with lithic types 7 and 8, possibly were deposited lower on the tidal flat than other types of heterogeneous lithic type 3. These rocks bear some resemblance to Jee's (1984) lithofacies 12 (dolomite mottled, lime mudstone) and rocks Cressman and Noger (1976) termed "micrite containing dolomite-filled burrows."

Homogeneous lithic type 3 provides little evidence for environmental interpretation. However, its association with heterogeneous lithic type 3 suggests an environment high on the tidal flat under conditions not conducive to development or preservation of textural details.

Lithic types 4 and 5 - intraclast-peloid lime packstone/grainstone and peloid-intraclast lime wackestone or wackestone/packstone: Both lithic types 4 and 5 are characterized by intraclastic grains that range from fine-sand size to about one inch (2.5 cm) in long dimension. They are similar in shape to the flat-pebble gravels of Andros Island (Hardie and Ginsburg, 1977). Lithic type 4 is a volumetrically important rock in western sections (from section BC westward, Figures 18-23), where it dominates intervals up to 10 feet (3m) thick. It is less prevalent in eastern sections (Figures 13-17). Lithic type 5, which is less common than lithic type 4, is not recorded east of the Big Creek section.

Intraclasts form from indurated or semi-indurated crusts that are bound by cyanobacterial mats or by early cementation, generally aragonite, or a combination of the two. Clasts are produced when cyanobacteria-bound sediments dry and develop polygonal shrinkage cracks. Clasts also develop when the force of crystallization accompanying continued cementation by aragonite and/or evaporites brecciates the crust. Once formed, clasts can be moved from their place of formation by wave action, storm surge, or by undercutting resulting from lateral migration of tidal channels. According to Shinn (1983a), most clasts are derived from the supratidal environment, but they can also form in intertidal (Hardie and Ginsburg, 1977) and subtidal (Hagan and Logan, 1974) settings. Considering the spectrum of environments in which clasts are produced, and the possibility that clasts can be moved after formation, interpretation of the environment of deposition of intraclastic texture is equivocal.

Clasts on modern tidal flats range from sand size up to three feet (lm) in long dimension. Plattin clasts, most of which are no

larger than one to two inches (2 to 4.5cm), match in scale the fine mudcracks that are common in the mud laminates of the unit. Compositionally, they are also similar to these mud rocks (Plate 2:A). These observations, associated with the absence of a diverse fauna that would indicate a subtidal origin, suggests that most Plattin clasts formed in high intertidal to supratidal environments and were moved by storms a greater or lesser distance on the tidal flat. The presence in lithic type 5 of mudcracks and evaporite traces reinforces this interpretation. Roehl (1967) reached a similar conclusion for flat-pebble breccias in the Silurian Interlake Formation of the Williston Basin. Hardie and Ginsburg (1977) assign an exposure index of 70-99 to the intertidal-supratidal intraclasts of Andros Island.

Reports of intraclastic rock from lower intertidal and subtidal settings are provided by Walker (1973, lithology 4b) and Jee (1984, lithofacies 9: fossiliferous, intraclastic, peloidal lime packstone to grainstone). In both of these examples the intraclastic rock carries a rather diverse biota. Burrowed examples of lithic type 5 also might have accumulated lower on the tidal flat.

Lithic type 4 and 5 differ in that peloids from the matrix of lithic type 4 (Plate 1:E), whereas the matrix of lithic type 5 is mostly lime mud (Plate 2:A). Roehl (1967) termed the latter "float breccia" and suggested that it was the product of a lower energy environment than texture like that of lithic type 4. However, he also interpreted disoriented clasts as products of higher energy conditions and some of the Plattin mud-supported intraclasts are disoriented (Plate 2:A). As Hardie and Ginsburg (1977) point out, the problem of the origin and accumulation of intraclasts, and in particular the significance of grain-supported versus mid-supported texture, needs more attention in studies on modern tidal flats.

Lithic type 6 - interlaminated lime mudstone and peloid lime packstone/ grainstone: Lithic type 6 is volumetrically the most important rock in the Plattin. It is particularly prevalent in the lower two-thirds of the unit, especially in the eastern sections. To the west (sections SM, GIL, TCB, CC, and CAR; Figures 19-23) it is replaced in prominence by lithic types 3, 4, and 5. For several reasons, lithic type 6 is unequivocally interpreted as a product of the high-intertidal to supratidal environment.

The most diagnostic character of lithic type 6 is its "Andros-type" lamination (Plate 2:C; Plate 3:A), which has been discussed under the interpretation of lithic type 3. this type lamination occurs in lithic type 6 primarily as disrupted flat lamination (mud cracked) (Plate 2:C; Plate 3:A,B) and crinkled fenestral lamination (Plate 2:B), which are characteristic of a variety of supratidal environments (exposure index >85) on Andros Island (Hardie and Ginsburg, 1977). Another strong argument for interpreting lithic type 6 as high intertidal to supratidal is the presence of well-developed fine to medium horizontal fenestrae (Plate 3:A), which is considered by Shinn (1983a,b) as an infallible indicator of tidal flat sediments. In addition, many examples of lithic type 6 exhibit evidences of evaporites in the form of calcite pseudomorphs after selenite and halite (Plate 2:C,D; Plate 3:A-C; Plate 4:A,B). As is also the case with evaporites in lithic type 3 (Plate 1:D), individual porphyroblastic crystals have become laterally linked to form irregular fenestrae of different shapes and sizes (Plate 2:C,D; Plate 3:B,C). Gypsum is forming presently in the high intertidal and supratidal sediments of Andros Island (Hardie and Ginsburg, 1977), Shark Bay (Logan, 1974) and along the Trucial Coast of the Persian Gulf (Bush, 1973). Because of the humid climate, gypsum does not survive in the Andros Island setting. Halite is deposited as ephemeral crusts on the supratidal flats of the Trucial Coast and Shark Bay.

Jee interpreted this same rock type (1984, lithofacies 5 and 5a: interlaminated lime mudstone and peloidal lime packstone and evaporite-bearing interlaminated lime mudstone and peloidal lime packstone) from the Plattin of Izard and Independence counties as indicative of the intertidal and supratidal realms. Cressman and Noger (1976) included similar, but somewhat thicker layered rock in their category "micrite and interlayered pelsparite," which they interpreted as intertidal in origin. Walker reported an equivalent rock type (1973, lithology 3), which he interpreted as

intertidal, from the Black River Group of New York.

Lithic type 10 - stromatolitic limestone: Stromatolites are rare in the Plattin, especially compared to their occurrence in the underlying Joachim, where in some intervals they abound. LLH-C stromatolites closely resemble those forms assigned to the genus Collenia in the literature and are believed to form an protected intertidal flats where there is only slight wave action (Logan and others, 1964). The SH-V forms resemble Cryptozoan and have been interpreted as forms that grow in exposed intertidal zones, where the scouring action of waves prevents the growth of cyanobacterial mats between adjacent stromatolites. Except that they are larger in scale, the Plattin stromatolites (Plate 6:C) resemble in external form and internal layering the smooth domal and "raised disc" protostromatolites now forming in the intertidal-supratidal environments on Andros Island (Hardie and Ginsburg, 1977). Probably the most convincing evidence for placing these stromatolitic structures in the intertidal-supratidal zones is that their dominant internal layering is that of lithic type 6 with lamination disrupted by mudcracks and calcite casts of evaporites (Plate 6:B).

LOWER INTERTIDAL-SUBTIDAL

Lithic type 7 - mollusc lime wackestone: The nearly total lack of laminations, presence of burrow mottling, and common occurrence of mollusc skeletons (Plate 4:C) suggest close affinity of this rock to sediment collecting in subtidal and bordering intertidal low algal marsh environments of the channeled belt ponds on Andros Island (Hardie and Ginsburg, 1977). Lack of laminations probably reflects burrowing activity of animals, possibly the associated molluscs. Lithic type 7 is gradational with lithic type 3 through the addition of faint laminations, mudcracks and calcite pseudomorphs after evaporites.

Lithic type 9 - ooid-peloid lime grainstone/packstone: Lithic type 9 is rare in the Plattin. Interpretation of its environment of deposition is a problem because it is associated with rocks of both subtidal and intertidal-supratidal affinity. Loreau and Purser (1973) report ooid formation in the Persian Gulf in both shallow, agitated water and less agitated waters of lagoons and protected tidal flats. Furthermore, ooids are commonly moved from their site of formation to ultimate resting places on beaches, tidal flats, and aeolian dunes. It is our conclusion that most Plattin ooids probably formed in shallow-subtidal environments and either accumulated there, as seems to the case for the ooids associated with subtidal rocks high in the Gunner Pool and Big Creek sections (Figures 15, 18), or were driven by storms onto the tidal flat. The latter almost certainly seems to be the explanation of ooids associated with intraclasts and containing a lime mud matrix or interlaminated with mudcracked, laminated lime mudstone (Plate 5:B,D). In addition, in these latter examples ooids are commonly partially to completely altered to micrite (Plate 6:A), suggesting a process similar to that in Shark Bay where grains washed from subtidal environments onto the cyanobacterial mats of the tidal flat are micritized by boring algae.

Lithic type 9 is the same as Jee's (1984) lithofacies 10 (fossiliferous intraclastic, peloidal, oolitic lime packstone to grainstone), which he interprets as protected subtidal. Walker interprets a similar rock (1973, lithology 5) as a product of the intertidal environment.

SUBTIDAL

Lithic type 8 - skeletal lime wackestone/packstone: The abundant, diverse fauna and unlaminated, burrow-mottled character of lithic type 8 (Plate 5:A) makes its placement in the shallow subtidal environment unquestionable. this rock type seems to be the same as Walker's (1973) lithology 6a of the Black River Group of New York, and shows similarities to Cressman and Noger's (1976) "micrite containing Tetradium fragments" and "biopelsparite" of the High Bridge Group of Kentucky. Jee's (1984) lithofacies 11, (coral, skeletal lime wackestone to packstone), which he interpreted as protected, shallow subtidal, is the same as our lithic type 8.

Lithic type 11 - coral lime boundstone: The most diagnostic feature of lithic type 11 is the occurrence of Tetradium

colonies in growth position (Plate 7:A). It is essentially the same rock type as Walker's (1973) lithology 6B and Jee's (1984) lithofacies 11a (coral-algal, lime boundstone).

COMPARISON TO MODERN AND ANCIENT TIDAL FLATS

A remarkable similarity exists between the lamination and bedding style of the Plattin and the modern carbonate tidal flat deposits of Andros Island as detailed by Harkie and Ginsburg (1977). Although some comparison does exist between the Plattin and the Shark Bay (Logan and others, 1974) and Persian Gulf (Purser, 1973) settings with respect to evaporite formation, apparently the overall character of sedimentation is much more influenced by energy conditions than climate. Both the Plattin and the Andros Island sediments are mud-rich records of low-energy shelf conditions. Skeletal and other grainstones, which are characteristic of strand line deposits of Shark Bay and the Persian Gulf, are virtually absent in the Plattin and on Andros Island. The transition from intertidal-supratidal deposits of the lower Plattin to distinctly subtidal deposits of the upper Plattin is marked in a few places (sections GP, BC and Jee's [1984] sections along the White River) by a thin ooid-peloid grainstone, but most commonly is gradational through low-energy mud-rich rock.

The climate under which the Plattin was deposited is difficult to ascertain. The presence of widespread evaporites in the unit suggests arid or semi-arid conditions like the present-day carbonate tidal flats of the Persian Gulf Trucial Coast and Shark Bay. The climate of the Trucial Coast is so dry that evaporitic pans (sabkhas), which prohibit growth of cyanobacterial mats, develop. Brines, which develop by evaporation of waters from the surface of the sabkha, sink into the sediments beneath and deposit layers of gypsum. Although sabkha conditions do not develop on the intertidal-supratidal flats of Shark Bay, brines concentrated by evaporation are of sufficiently high chlorinity to deposit gypsum as layers and crystals within the sediment beneath the flats. Algal mats do survive on the Shark Bay supratidal Flats, particularly in the low areas that stay wetted longer, although their growth is not as vigorous as in the more humid Andros Island setting. Porphyroblastic gypsum, in some examples as crystals several centimeters across, grows within the substrate of the Shark Bay intertidal zone. In places gypsum is so abundant that primary textures of the carbonate sediment are destroyed as grains are displaced into intercrystalline spaces. There is no suggestion of sabkha conditions on the Plattin tidal flat. Evaporites were not deposited as layers in salt pans, but rather grew as porphyroblasts that pushed the host sediment aside or as crystals that encompassed the sediment (Plate 4:A,B). Although individual crystals became laterally linked as they grew, forming irregular fenestrae of different shapes and sizes, gypsum did not form continuous layers of any extent as it did in the sabkhas of the Silurian Interlake Formation of the Williston Basin (Roehl, 1967). We have not recognized texture attributable to solution breccia or breccia caused by the force of prophyroblastic crystal growth in any of the Plattin evaporite-bearing strata. In short, evaporites did not form on or in Plattin tidal flat sediments in nearly the abundance that it is presently forming in the semi-arid Shark Bay and arid Persian Gulf climates. We therefore conclude that the climate during Plattin deposition was more humid than these modern sites of evaporite accumulation. This is consistent with the Plattin's characteristic laminate fabric, which suggests a tidal flat on which chlorinity was not persistently so high as to prevent vigorous growth and widespread development of cyanobacterial mats.

Halite has not been reported as porphyroblasts in the sediment of modern tidal flats, but does occur as ephemeral crusts on the supratidal flats on the Trucial Coast (Bush, 1973) and Shark Bay (Logan, 1974). In both locations halite crystals apparently are not preserved because of their susceptibility to resorption by atmospheric water (rain or dew), tidal water, or groundwater. If the conclusion that the Plattin climate was not as arid as those of the Trucial Coast or Shark Bay is correct, then the preservation of porphyroblastic halite for a time sufficient to allow it to be casted is a mystery. If it is presumed that the halite was resorbed shortly after formation, which is likely considering its solubility, then it can only be concluded that soon after deposition, Plattin

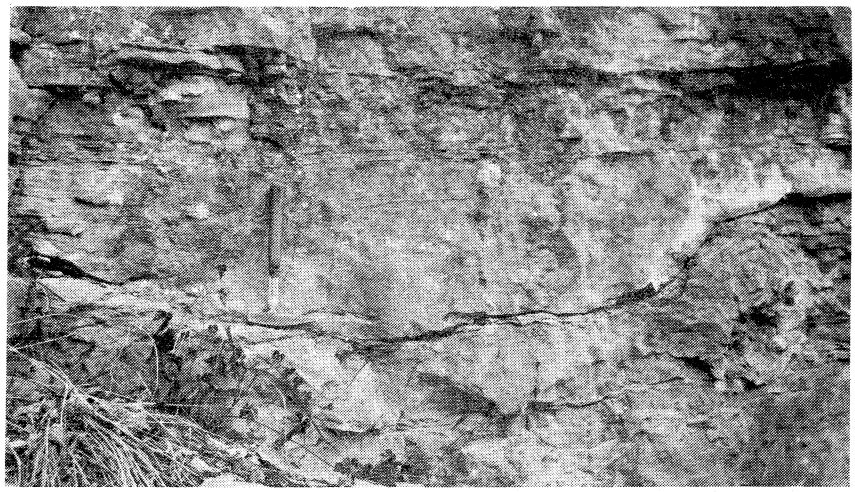

FIGURE 12. *Tidal-channel(?) scour in Plattin. Hammer rests on scoured surface.*

sediment became sufficiently lithified to allow preservation of halite molds.

Although we have compared some of the Plattin textures and structures to specific positions on the Andros Island channeled belt, there is no evidence that the Plattin tidal flat was geomorphically as varied as that on Andros. For instance, we have not recognized in outcrop morphologies that would identify distinct tidal channels with attendant levees and inter-channels ponds. Nor has the construction of facies diagrams identified vertical sequences suggestive of the migration of typical tidal flat environments. Some small channel-like ponds. Nor has the construction of facies diagrams identified vertical sequences suggestive of the migration of typical tidal flat environments. Some small channel-like features do occur at the Gilbert locality (Figure 12), but these are not floored by intraclasts as are the Andros Island Channels and could very well be nothing more than storm scour of the tidal flat. Our failure to recognize in outcrop different tidal flat environments may result from a general lack of lateral exposure sufficient enough to allow observation of facies changes, or it might be simply that the Plattin flat was essentially featureless. We suspect the latter is the case.

As mentioned earlier, the Plattin Limestone of Arkansas represents a small portion of a widespread tidal flat that extended from Oklahoma through Kentucky, Ohio, New York and into Ontario. The Oklahoma Fite Formation and its lateral equivalent, the Corbin Ranch Submember (Bromide "dense") of the Bromide Formation (Amsden, 1983), are composed of interbedded mudcracked, fenestral lime mudstone with restricted fauna and Tetradium-bearing skeletal wackestone/packstone, representing lithic types 3 and 7/8, respectively, of this study. The Oklahoma rocks do not appear to be particularly laminated, nor apparently do they contain traces of evaporites. The distinct interbedding of fossiliferous subtidal rock with fenestral tidal flat rock suggests an overall lower position on the tidal flat for the Oklahoma rocks.

The Plattin compares closely with the High Bridge Group of Kentucky (Cressman and Noger, 1976) and the Black River Group of Ohio, (Stith, 1979), New York (Walker, 1973), and Ontario (Mukherji, 1969) in that these formations are characterized by "Andros-type" lamination in both peloid rocks and mudrocks, flat-pebble breccias, and Tetradium-bearing skeletal wackestone/packstone. In contrast, traces of evaporites have not been reported from the Kentucky and Ohio rocks and are rare to absent in the Black River of New York. In general, these units seem to be more fossiliferous (body and trace fossils) throughout than the Plattin, indicating that they represent a greater accumulation of lower intertidal-subtidal

rocks as compared to a dominance of high intertidal-supratidal rocks in the Plattin. This is particularly true for Plattin sections west of the White River. Rock with a diversity of fossils is more common in Jee's (1981, 1984) sections east of the White River (Figure 2). These sections compare more favorably with the Black River of Kentucky, Ohio and New York.

The Black River of Southwestern Ontario contains calcite nodules interpreted to be casts of supratidal gypsum. The nodules are up to six inches (15cm) in diameter and could very well have formed under sabkha conditions. Other than what appears to be a more intensely evaporation environment, the deposition of the Ontario rocks took place under conditions quite similar to those of the Arkansas Plattin.

In summary, we envision the Plattin environment as a rather featureless tidal flat bordered by a low-energy, shallow, subtidal shelf. Storm tides frequently wetted the tidal flat, encouraging vigorous growth of cyanobacterial mats. The bordering marine water of normal salinity supported a moderately diverse fauna that destroyed cyanobacterial mats in the subtidal environment through their browsing and burrowing activity. Storms delivered to the tidal flat lime mud that was trapped by the mat, which during periods of exposure dried and cracked to provide intraclastic grains that were periodically eroded by storms and redistributed in layers of greater or lesser extent on the tidal flat. Toward the seaward extent of the flat, shallow subtidal pools populated by marine organisms, dominantly molluscs, existed for short periods of time.

The Plattin climate probably was not persistently arid. Sabkhas did not develop, nor did layers of evaporites accumulate. Seasonal or longer term dry periods no doubt did occur. These dry periods caused evaporation of tidal flat waters to form brines from which porphyroblastic evaporite crystals formed within the sediments. Intervening wetter periods dissolved the evaporite minerals. The tidal flat sediment apparently became semi-lithified soon after deposition because molds of the evaporite crystals persisted to become filled by pore-filling calcite.

HISTORY OF DEPOSITION

The Plattin shows distinct east-west trends in the distribution of lithic types across northern Arkansas. Jee (1981, 1984) subdivided the Plattin of Izard and Independence Counties into five informal units. The basal few feet of his unit I, which comprises about 1/4 to 1/3 of the Plattin, are intertidal to supratidal deposits of dolostone, intraclastic-peloidal grainstone (our lithic type 4) and mudcracked, peloidal lime mudstone (our lithic types 3 and 6). Layers of coral, skeletal lime wackestone (our lithic type 7) dominates the upper part of unit I, where it is interbedded with evaporite-tract-bearing interlaminated lime mudstone and peloidal lime packstone/grainstone (our lithic type 6). This association Jee interprets as "competitive sedimentation" between subtidal and tidal flat environments. In Eastern Stone County sections (GF and HER, Figures 13, 14; and Jee's section at Allison, Figure 2), the lower portion of the Plattin is dominated by intertidal to supratidal deposits (mostly lithic types 3 and 6). These sections contain some fossiliferous beds (lithic type 7), the presence of which documents a subtidal influence, but fossiliferous beds are not as common as in Jee's unit 1 to the east. Sections farther west in Stone County (GP, BN, and BS; Figures 15-17) exhibit little, if any, subtidal influence. The basal Plattin in sections further to the west in Searcy and Newton Counties (Figures 18-23), is composed almost entirely of high intertidal-supratidal rocks (lithic types 1-6). This distribution of rock types suggests that initial Plattin deposition to the east was lower on the tidal flat than to the west. Although the lower Plattin in Izard and Independence Counties contains a prominent component of intertidal-supratidal rock, the common association of this rock with beds possessing a relatively diverse fauna suggests a subtidal influence either through relative changes in sea level or the presence of ephemeral tidal ponds. Subtidal influence diminishes to the west where initial Plattin deposits record environments exclusively of high intertidal to supratidal settings.

Jee's unit II is dominated by mudcracked, evaporite-trace-bearing interlaminated lime mudstone and peloidal lime

packstone/grainstone (our lithic type 6) similar to the bulk of the lower Plattin to the west in Stone County. The replacement of unit I by unit II in Izard and Independence Counties indicates a progradation of the tidal flat, with at least a component of the progradation taking place from west to east.

Jee's unit III is a thin interval characterized by fossiliferous oolitic lime packstone/grainstone (our lithic type 9). The unit, which records transgression of the prograded tidal flat by subtidal environments, is present in Jee's sections in Izard and Independence Counties (Figure 2), and at Gunner Pool and Bear Creek (Figures 15, 18), but appears to be absent in other sections. This suggests that the leading edge of the transgression was represented by scattered oolitic shoals that did not occur everywhere.

Jee's unit IV, a coral, skeletal lime wackestone/packstone with abundant Tetradium (our lithic type 8), represents maximum Plattin transgression. This unit, which includes a thin bed of coral boundstone (lithic type 11), is well defined in Jee's sections in Izard and Independence Counties and at Allison. It is also well developed at Guion Ferry, Herpel, and Bear Creek (Figures 13, 14, 18), and the basal few feet appear to be present in the top of the Gunner Pool section (Figure 15). Its absence at the two Barkshed sections, which are relatively thin, and its presence to the west at Bear Creek, a relatively thick section, suggests that unit IV has been removed by erosion from the top of the Plattin to the west of eastern Stone County.

Jee's unit V, composed of bioturbated, sparsely bio-clastic lime wackestone containing desiccation features at its top, indicates that the end of preserved Plattin deposition was marked by renewed progradation. Unit V can be recognized at Guion Ferry and Herpel (Figures 13, 14), where it is more prominently marked by desiccation features than in Jee's sections in Izard and Independence Counties to the east. This suggests that the east-west distribution of peritidal environments present during early Plattin deposition persisted into the deposition of its youngest layers. Unit V is not present in western sections where it has been removed from the top of the Plattin by erosion.

The presence to the north of the Ozark Dome, a persistent Paleozoic high, would predict that the major transgressive-regressive pattern during Plattin deposition be oriented north-south. The facies distribution in the Plattin, however, suggests that at least a minor component of this pattern is oriented east-west. This indicates the presence of a high somewhere in western Arkansas. The distribution of lithic type 12 (calcareous shale and argillaceous limestone), which is more prevalent in western sections of the Plattin, supports this notion. Ordovician erosion patterns in northern Arkansas also are instructive. The apparent overstep of the Plattin onto the St. Peter Sandstone and Fernvale Limestone onto the Plattin in a westerly direction is best explained by a persistent high to the west. The Plattin along Polk Bayou (Figure 2), from where the greatest thickness of the unit is reported (Miser, 1922), could serve as a test as to whether this rise to the west is real or only apparent. If real, the Plattin north of Batesville should show a greater marine influence than that along the White River and to the west.

SELECTED REFERENCES

Aitken, J.D., 1967, Classical and environmental significance of cryptalgal limestone and dolomites, with illustrations from the Cambrian and Ordovician of southeastern Alberta: Jour. Sed. Petrology, v.37, p. 1163-1178.

Amsden, T.W., 1983, Upper Bromide and Viola Group (Middle and Upper Ordovician) in eastern Oklahoma: Part I - Welling-Fite-Corbin Ranch Strata: Oklahoma Geol. Survey, Bull. 132, p. 1-23.

Bush, P., 1973, Some aspects of the diagenetic history of the sabkha in Abu Dhabi, Persian Gulf: in Purser, B.H., The Persian Gulf, Holocene Carbonate Sedimentation and Diagenesis in a Shallow Epicontinental Sea: Springer-Verlag, Berlin, p. 395-407.

Craig, W.W., 1975, History of investigations on the post-St. Peter Ordovician of northern Arkansas: the art of layercake geology: in Headrick, K., and Wise, O. eds., Contributions to the Geology of the Arkansas Ozarks: Arkansas Geol. Comm., p. 1-17.

_____, Wise, O., and McFarland, J.D., III, 1984, A guidebook to the post-St. Peter Ordovician and the Silurian and Devonian rocks of north-central Arkansas: Second Annual Field Trip, Soc. Econ. Paleont. Mineralogists, Arkansas Geol. Comm., GB-84-1, 49p.

Cressman, E.R., and Noger, M.C., 1976, Tidal-flat carbonate environments in the High Bridge Group (Middle Ordovician) of central Kentucky: Kentucky Geol. Survey, Report of Investigations 18, 15 p.

Deliz, M.J., 1984, Stratigraphy and petrology of the Plattin Limestone (Middle Ordovician) in Newton and Searcy Counties, Arkansas (M.S. Thesis): University of New Orleans, New Orleans, LA, 259 p.

Freeman, T., 1966a, Petrology of the post-St. Peter Ordovician of northern Arkansas: Tulsa Geol. Soc. Digest, v. 34, p. 82-98.

_____, 1966b, Petrographic unconformities on the Ordovician of northern Arkansas: Oklahoma Geol. Notes, v. 26, p. 21-28.

_____, 1972, Carbonate facies in Ordovician of northern Arkansas: discussion: Am. Assoc. Petroleum Geologists Bull., v. 56, p. 2284-2287.

Gebelein, C.D., and Hoffman, P., 1973, Algal origin of dolomite laminations in stromatolitic limestone: Jour. Sed. Petrology, v. 43, p. 603-613.

Ginsburg, R.N., Hardie, L.A., Bricker, O.P., Garrett, P., and Wanless, R., 1977, Exposure index: a quantitative approach to defining position within the tidal zone: in Hardie, L.A., ed., Sedimentation on the Modern Carbonate Tidal Flats of Northwest Andros Island, Bahamas: Baltimore, Johns Hopkins University Press, p. 7-11.

Hagan, G.M., and Logan, B.W., 1974, History of Hutchison Embayment tidal flat, Shark Bay, western Australia: Am. Assoc. Petroleum Geologists Mem. 22, p. 283-315.

Hardie, L.A. ed., 1977, Sedimentation on the Modern Carbonate Tidal Flats of Northwest Andros Island, Bahamas: Baltimore, Johns Hopkins University Press, John Hopkins Univ. Studies in Geology, No. 2, 202 p.

_____, and Ginsburg, R.N., 1977, Layering: the origin and environmental significance of laminations and thin bedding, in Harkie, L.A., ed., Sedimentation on the Modern Carbonate Tidal Flats of Northwest Andros Island, Bahamas: Baltomore, John Hopkins University Press, p. 50-123.

Jee, J.L., 1981, Stratigraphy and paleoenvironmental analysis of the Plattin Limestone (Middle Ordovician), White River region, Independence, Izard, and Stone Counties, Arkansas (M.S. Thesis): University of New Orleans, New Orleans, LA, 168 p.

_____, 1984, Stratigraphy and depositional environments of the Plattin Limestone (Middle Ordovician), Parts of Independence, Izard, and Stone Counties, Arkansas: in Hyne, N.J., Limestones of the Mid-Continent, Tulsa Geol. Society, Special Pub. No. 2, p. 307-326.

Kendall, C.G., and Skipworth, P.A., 1968, Recent algal mats of a Persian Gulf lagoon: Jour. Sed. Petrology, v. 38, p. 1040-1058.

Laporte, L.F., 1967, Carbonate deposition near mean sea-level and resultant facies mosaic: Manlius Formation (Lower Devonian) of New York State: Am. Assoc. Petroleum Geologists Bull., v. 51, p. 73-101.

Legendre, K.J., 1987, Stratigraphy and petrology of the Joachim Dolomite and Plattin Limestone (Middle Ordovician), Stone County, Arkansas (M.S. Thesis): University of New Orleans, New Orleans, LA, 325 p.

Logan, B.W., 1974, Inventory diagenesis in Holocene-Recent carbonate sediments, Shark Bay, western Australia: in Logan, B.W. and others, Evolution and Diagenesis of Quaternary Carbonate Sequences, Shark Bay, Western Australia: Am. Assoc. Petroleum Geologists Mem. 22, p. 195-247.

_____, Hoffman, P.W., and Gebelein, C.D., 1974, Algal mats, cryptalgal fabrics, and structures, Hamelin Pool, western Australia, in Logan, B.W., and others, Evolution and Diagenesis of Quaternary Carbonate Sequences, Shark Bay, Western Australia: Am. Assoc. Petroleum Geologists Mem. 22, p. 140-194.

_____, Rezak, R., and Ginsburg, R.N., 1964, Classification and environmental significance of algal stromatolites: Jour. Geology, v. 72, p. 68-83.

Loreau, J.P. and Purser, B.H., 1973, Distribution and ultra-structure of Holocene ooids in the Persian Gulf: in Purser, B.H., ed., The Persian Gulf: Holocene Carbonate Sedimentation and Diagenesis in a Shallow Epicontinental Sea: Springer-Verlag, Berlin, 471 p.

Lucia, F.J., 1972, Recognition of evaporite-carbonate shoreline sedimentation: in Rigby, J.K., and Hamblin, W.K., eds., *Recognition of Ancient Sedimentary Environments*; Soc. Econ. Paleont. Mineralogists Spec. Pub. 16, p. 160-191.

Matter, A., 1967, Tidal flat deposits in the Ordovician of western Maryland: Jour. Sed. Petrology, v. 37, p. 601-609.

Miser, H.D., 1922, Deposits of manganese ore in the Batesville district, Arkansas: U.S. Geol. Survey Bull. 743, 273 p.

Mukherji, K.K., 1969, *Supratidal carbonate rocks in the* Black River (Middle Ordovician) Group of southwestern Ontario, Canada: Jour. Sed. Petrology, v. 39, p. 1530-1545.

Purser, B.H., ed., 1973, The Persian Gulf, Holocene Carbonate Sedimentation and Diagenesis in a Shallow Epicontinental Sea: Springer-Verlag, Berlin, 471 p.

Read, J.F., and Grover, G.A., Jr., 1977, Scalloped and planer erosional surfaces, Middle Ordovician limestones, Virginia: analogs of Holocene exposed karst or tidal rock platforms: *Jour. Sed. Petrology, v. 47, p. 956-972.*

Roehl, P.O., 1967, Stoney Mountain (Ordovician) and Interlake (Silurian) facies analogs of Recent low-energy marine and subaerial carbonates, Bahamas: Am. Assoc. Petroleum Geologists Bull., v. 51, p. 1079-1132.

Shinn, E.A., 1968, Practical significance of birdseye structures in carbonate rocks: Jour. Sed. Petrology, v. 38, p. 215-223.

_____, 1983a, Tidal flat: in Scholle, P.A., Bebout, D.G., and Moore, C.H., eds., Carbonate Depositional Environments: Am. Assoc. Petroleum Geologists Mem. 33, p. 171-210.

_____, 1983b, Birdseye, fenestrae, shrinkage pores, and loferites: a reevaluation: Jour. Sed. Petrology, v. 53, p. 619-628.

_____, 1986, Modern carbonate tidal flats: their diagnostic features: Colorado School of Mines Quarterly, v. 81, p. 7-33.

_____, Ginsburg, R.N., and Michael, L.R., 1965, Recent supratidal dolomite from Andros Island, Bahamas: in Pray, L.C. and Murray, R.C. eds., Dolomitization and Limestone Diagenesis...A symposium: Soc. Econ. Paleontologists Mineralogists, Spec. Pub. 13, p. 112-123.

_____, Lloyd, R.M., and Ginsburg, R.N., 1969, Anatomy of a modern carbonate tidal-flat, Andros Island, Bahamas: *Jour. Sed. Petrology, v. 39, p. 1202-1228.*

Stith, D.A., 1979, Chemical composition, stratigraphy, and depositional environments of the Black River Group (Middle Ordovician) southwestern Ohio: Ohio Geol. Survey, Rept. Invest. no. 113, 36 p.

Tebbutt, G.E., Conley, C.D., and Boyd, D.W., 1965, Lithogenesis of a distinctive carbonate rock fabric: Wyoming Univ. Contrib. Geology, v. 4, p. 1-13.

Walker, K.R., 1973, *Stratigraphy and environmental* sedimentology of the Middle Ordovician Black River Group in the type area - New York State: New York State Museum and Science Service Bull. No. 419, 43 p.

Young, L.M., Fiddler, L.C., and Jones, R.W., 1972a, Carbonate facies in Ordovician of northern Arkansas: Am. Assoc. Petroleum Geologists Bull., v. 56, p. 68-80.

_____, 1972b, Reply to Tom Freeman: Am. Assoc. Petroleum Geologists Bull., v. 56, p. 2287-2290.

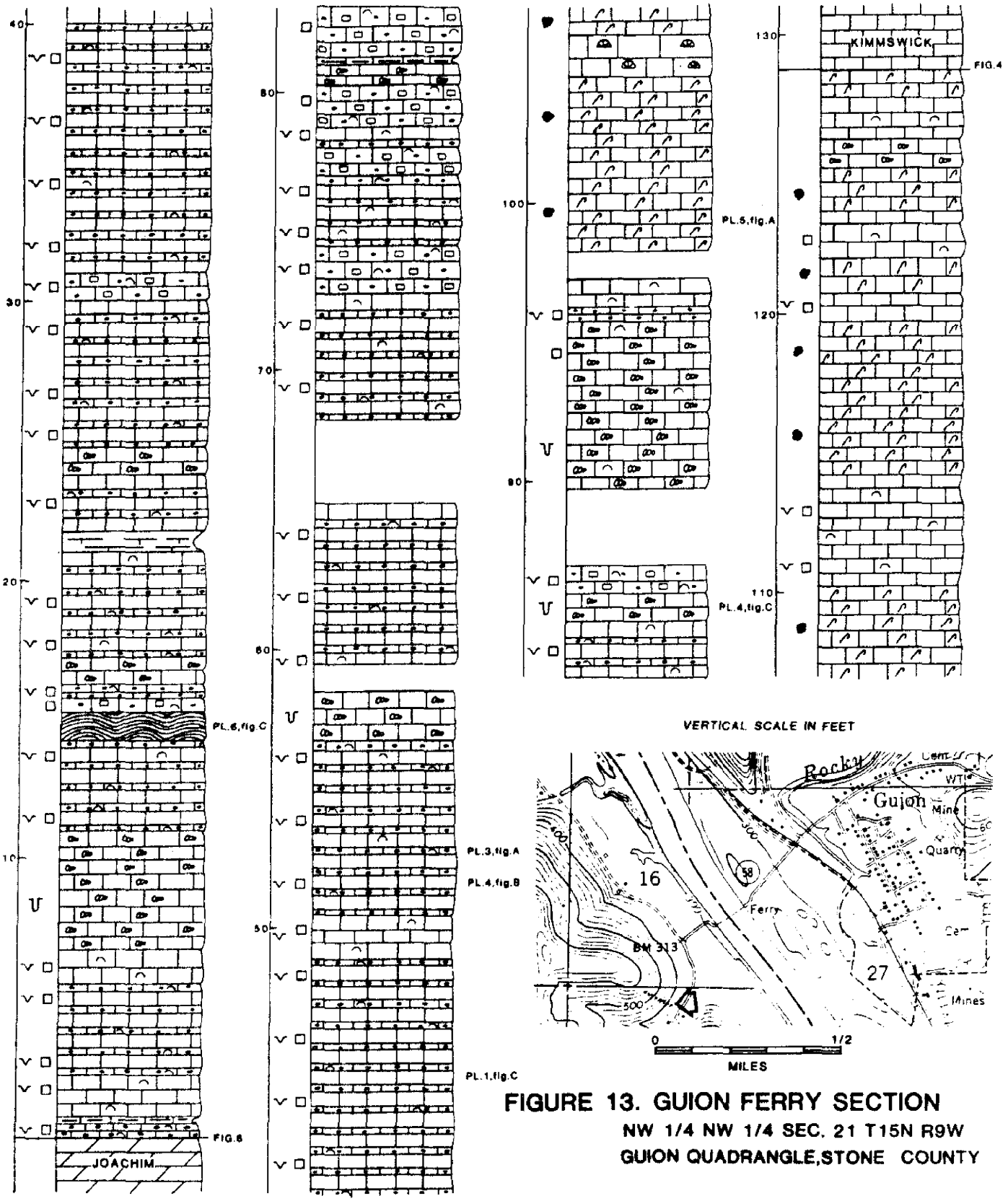

FIGURE 13. GUION FERRY SECTION

NW 1/4 NW 1/4 SEC. 21 T15N R9W
GUION QUADRANGLE,STONE COUNTY

For explanation of Figures 13 - 23 see Figure 21

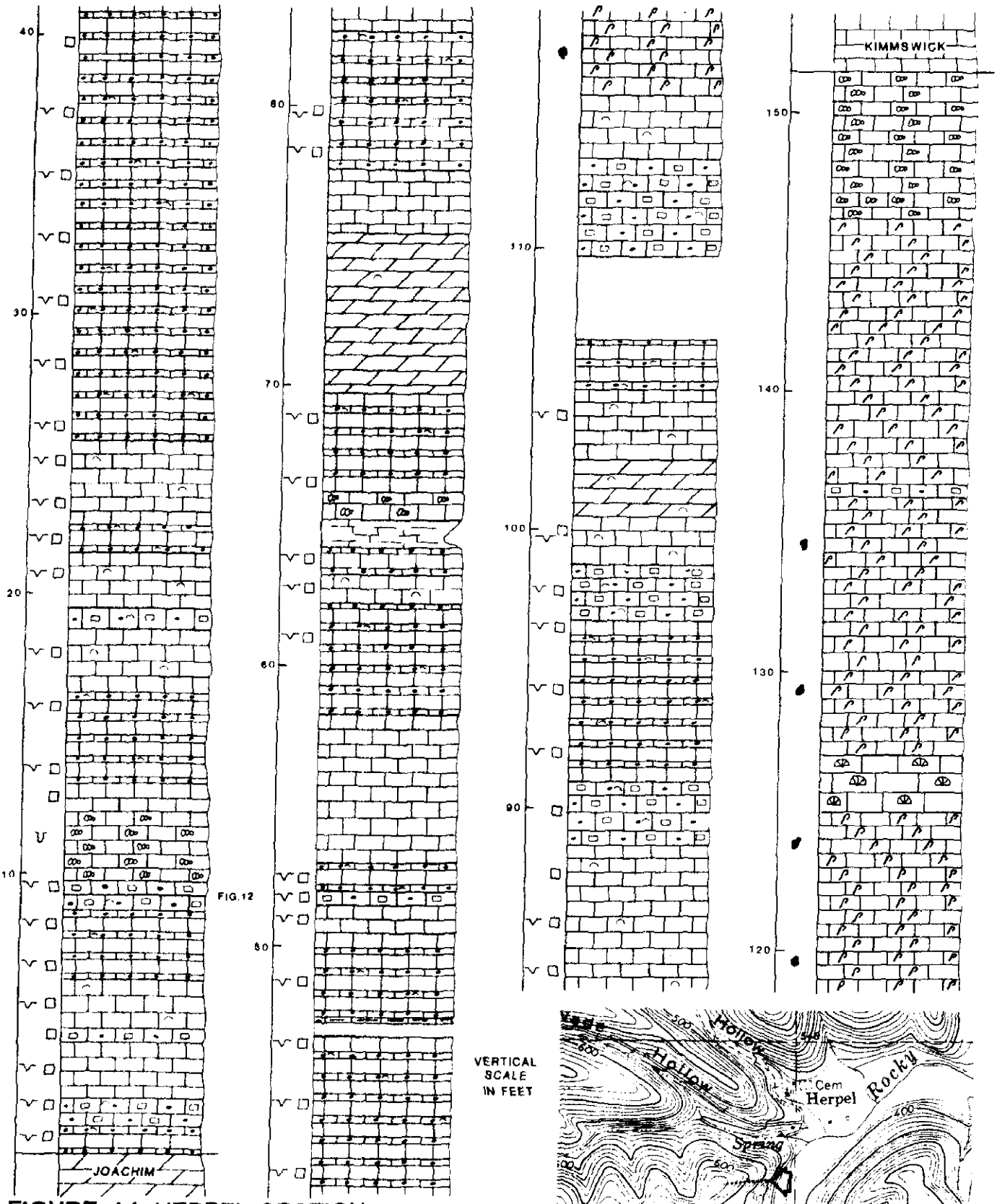

FIGURE 14. HERPEL SECTION
SE 1/4 NE 1/4 SEC. 27 T16N R10W
SYLAMORE QUADRANGLE, STONE COUNTY

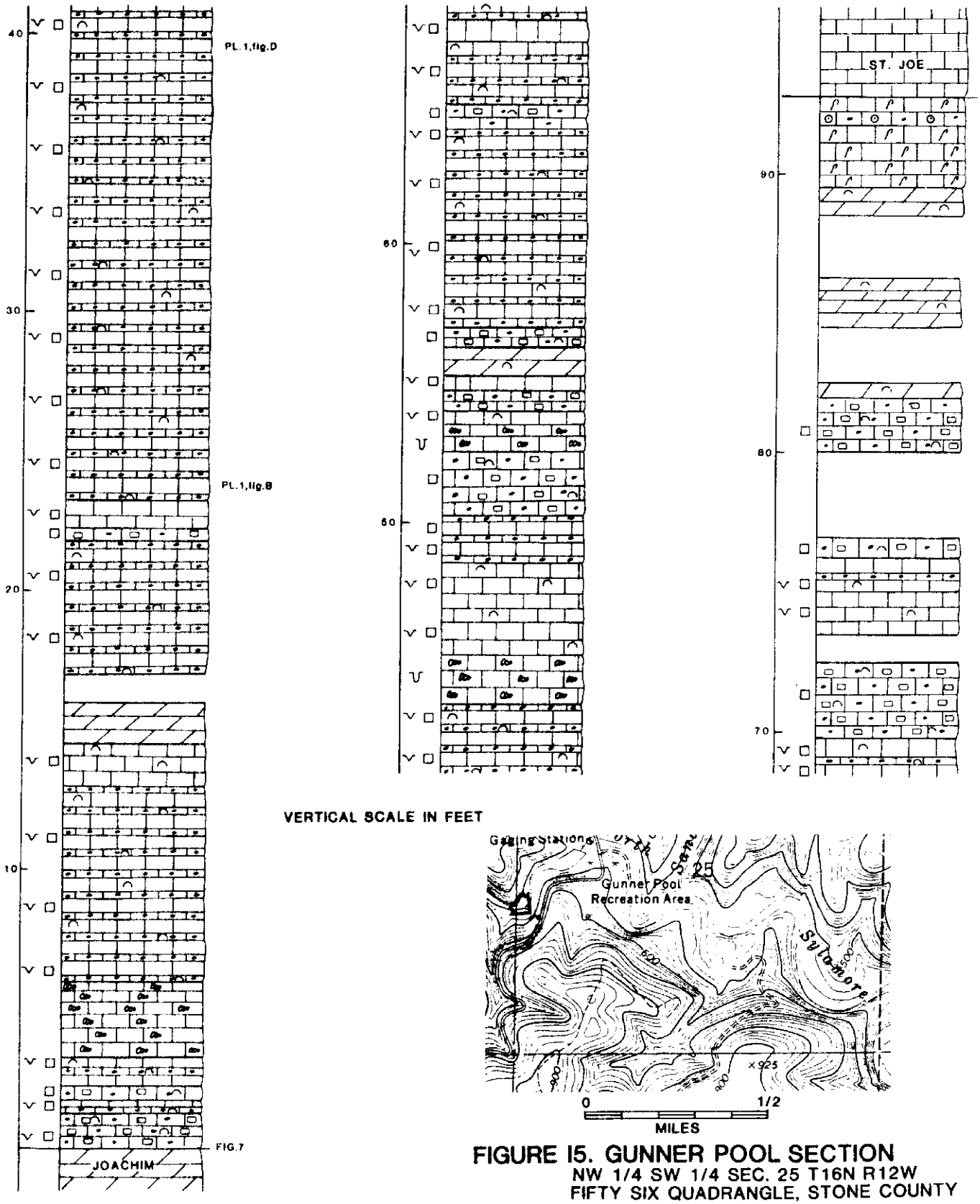

FIGURE I5. GUNNER POOL SECTION
NW 1/4 SW 1/4 SEC. 25 T16N R12W
FIFTY SIX QUADRANGLE, STONE COUNTY

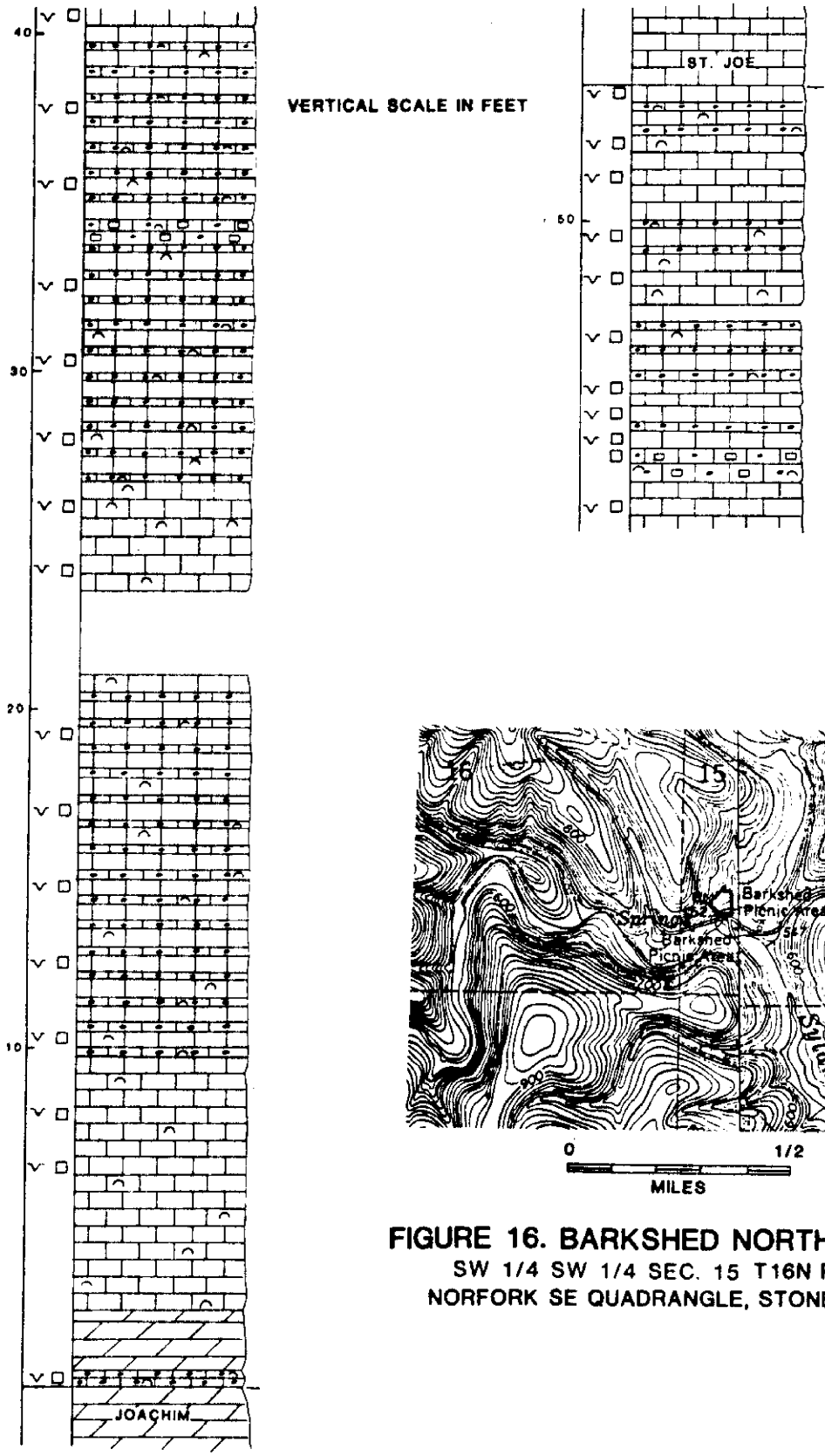

FIGURE 16. BARKSHED NORTH SECTION
SW 1/4 SW 1/4 SEC. 15 T16N R12W
NORFORK SE QUADRANGLE, STONE COUNTY

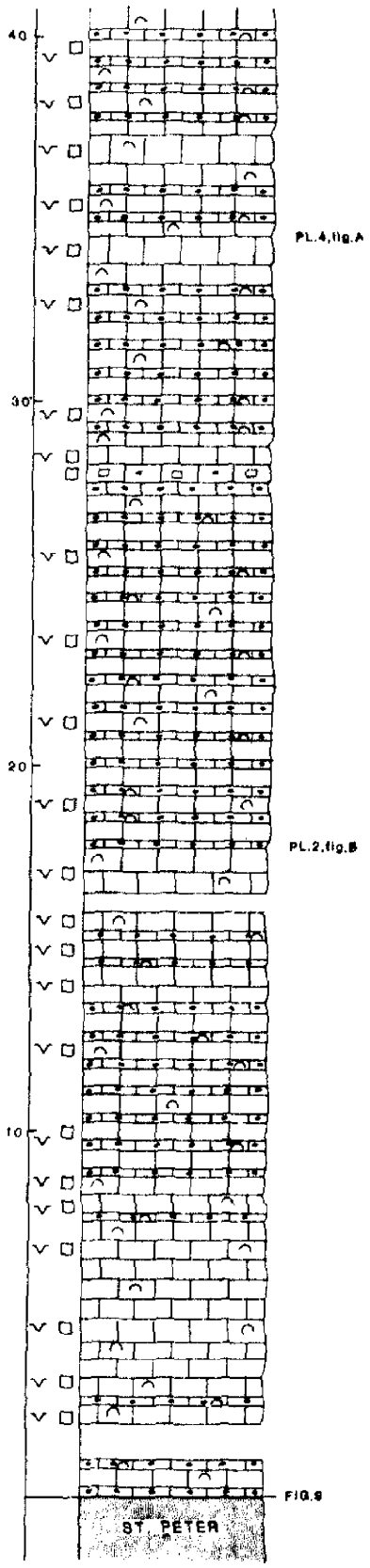

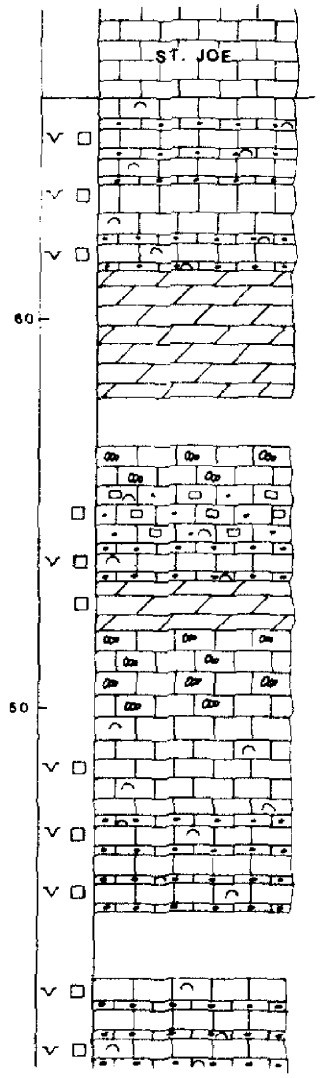

VERTICAL SCALE IN FEET

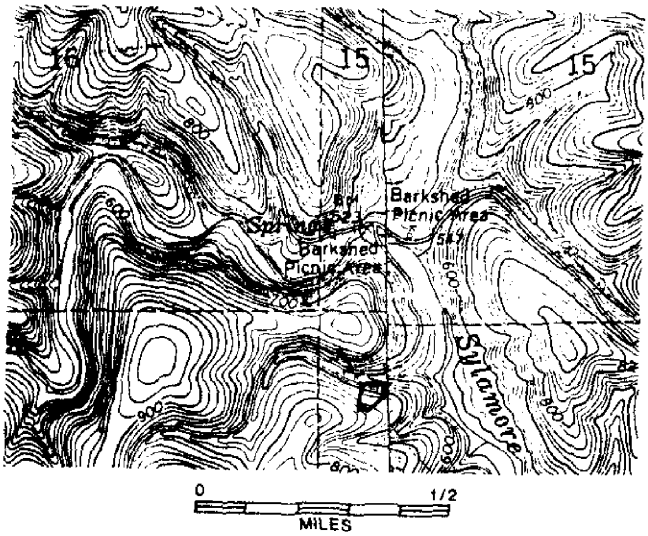

FIGURE 17 BARKSHED SOUTH SECTION
NW 1/4 NW 1/4 T16N R12W
NORFORK SE QUADRANGLE,STONE COUNTY

FIGURE 18. BEAR CREEK SECTION

SW 1/4 NE 1/4 & NE 1/4 SW 1/4 SEC. 33, and NW 1/4 SW 1/4 SEC. 34 T16N R14W LANDIS QUADRANGLE, SEARCY COUNTY

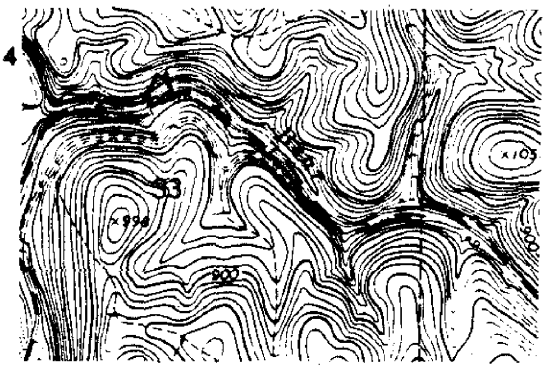

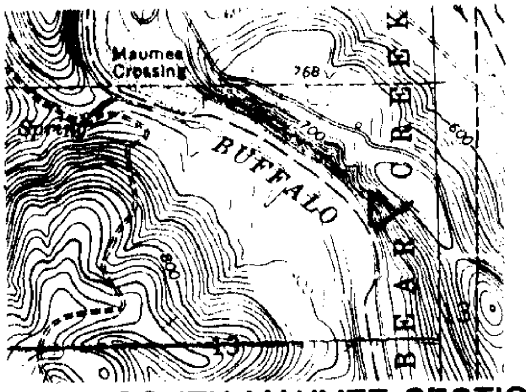

FIGURE 19. SOUTH MAUMEE SECTION
NE 1/4 NE 1/4 SEC. 13 T16N R16W
MAUMEE QUADRANGLE, SEARCY COUNTY

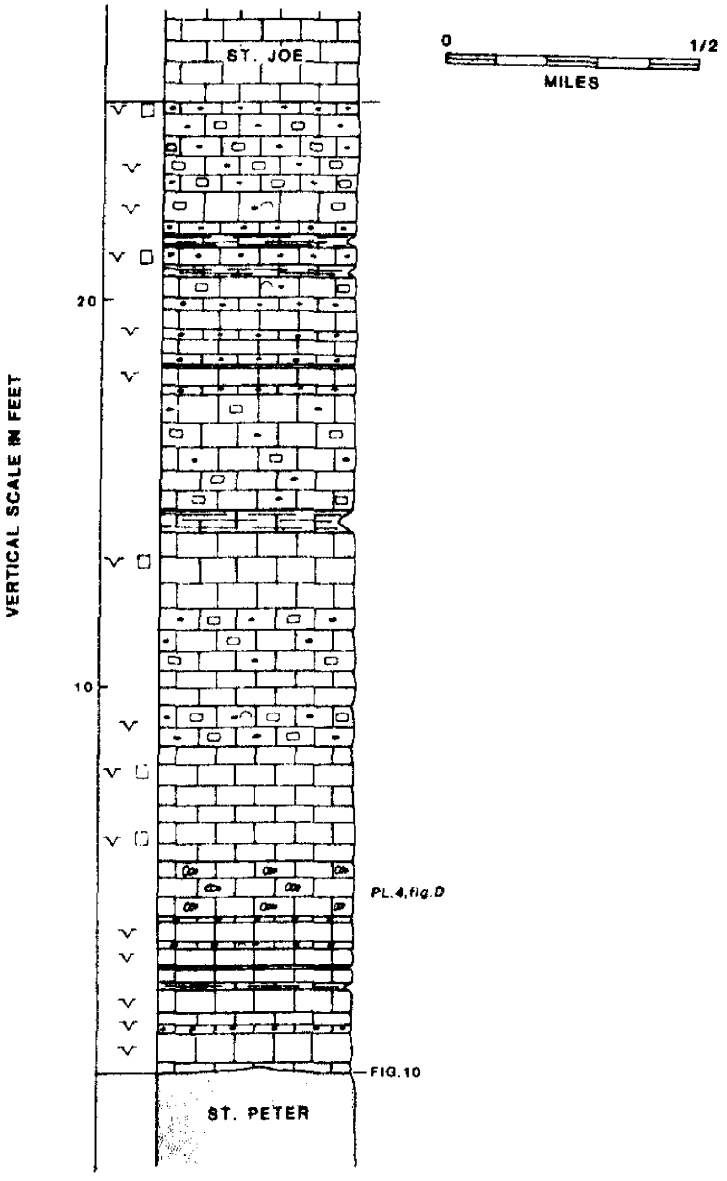

FIGURE 20. GILBERT SECTION

SW 1/4 SE 1/4 SEC. 29 T16N R16W
MARSHALL QUADRANGLE,SEARCY COUNTY

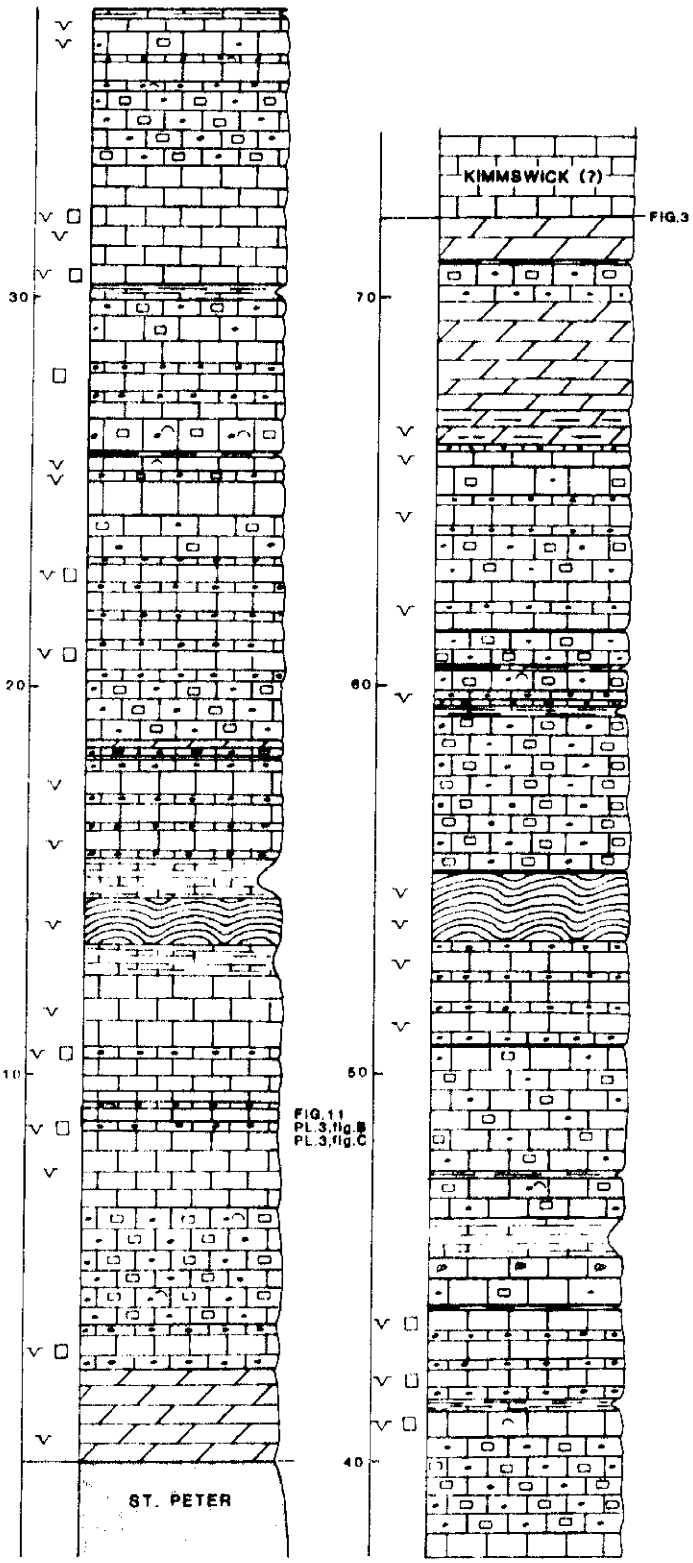

VERTICAL SCALE IN FEET

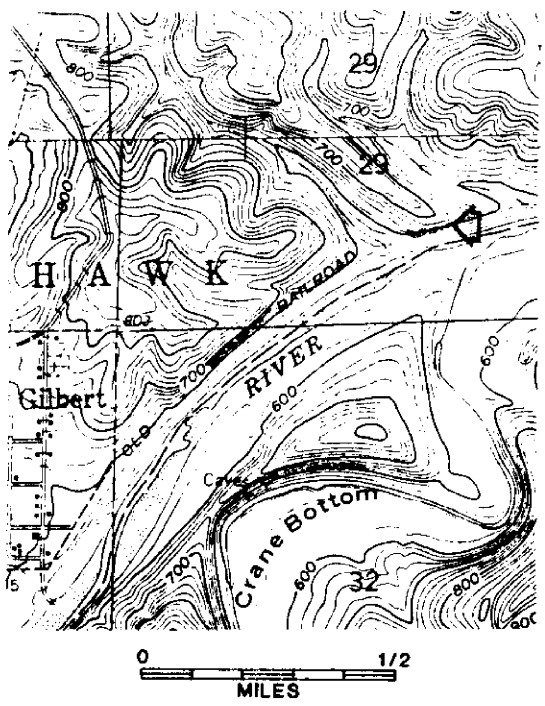

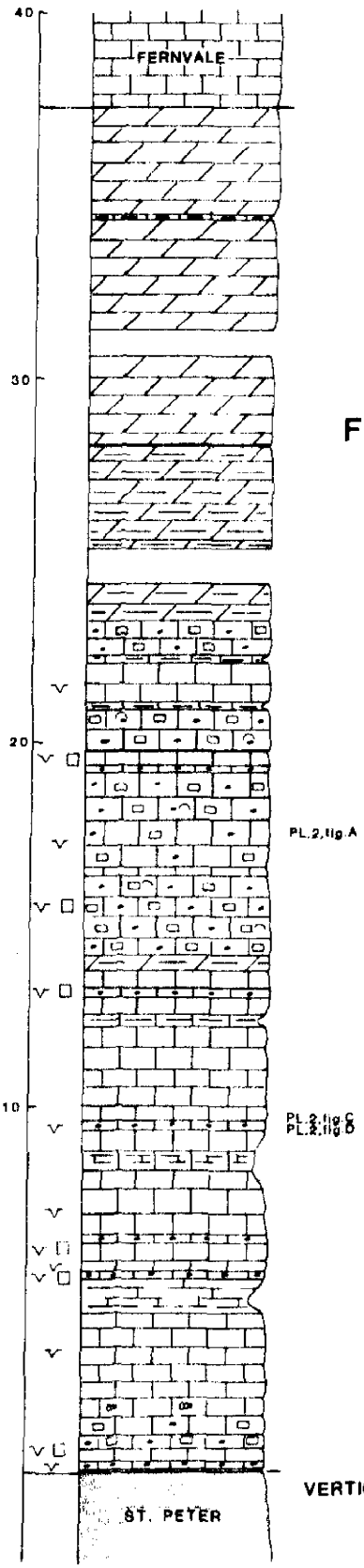

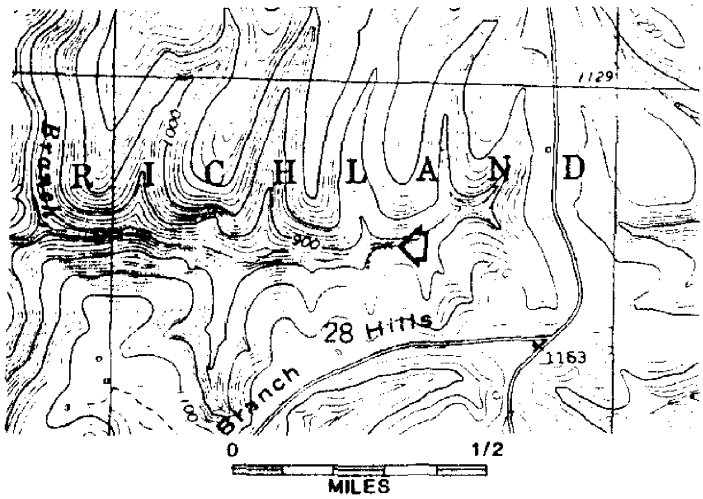

FIGURE 21. TRIBUTARY CANE BRANCH SECTION

SW 1/4 NE 1/4 SEC. 28 T16N R18W
WESTERN GROVE QUADRANGLE, SEARCY COUNTY

EXPLANATION OF FIGURES 13-23

- FINELY CRYSTALLINE DOLOSTONE
- LAMINATED DOLOSTONE
- LIME MUDSTONE
- INTRACLAST-PELOID PACKSTONE/ GRAINSTONE
- PELOID-INTRACLAST WACKESTONE or WACKESTONE/ PACKSTONE
- INTERLAMINATED LIME MUDSTONE & PELOID LIME PACKSTONE/ GRAINSTONE
- MOLLUSC WACKESTONE
- SKELETAL LIME WACKESTONE/ PACKSTONE
- OOID-PELOID PACKSTONE/ GRAINSTONE
- STROMATOLITIC LIMESTONE
- CORAL LIME BOUNDSTONE
- CALCAREOUS SHALE or ARGILLACEOUS LIMESTONE
- MUDCRACKS
- *CALCITE PSEUDOMORPHS AFTER HALITE*
- VERTICAL BURROWS
- MOTTLED
- OSTRACODES
- LOCATION OF SECTION

VERTICAL SCALE IN FEET

PL 2, FIG. A LOCATION OF PLATES AND/OR FIGURES

FIGURE 22. CAVE CREEK SECTION

SE 1/4 SW 1/4 SEC. 14 T15N R19W
EULA QUADRANGLE, NEWTON COUNTY

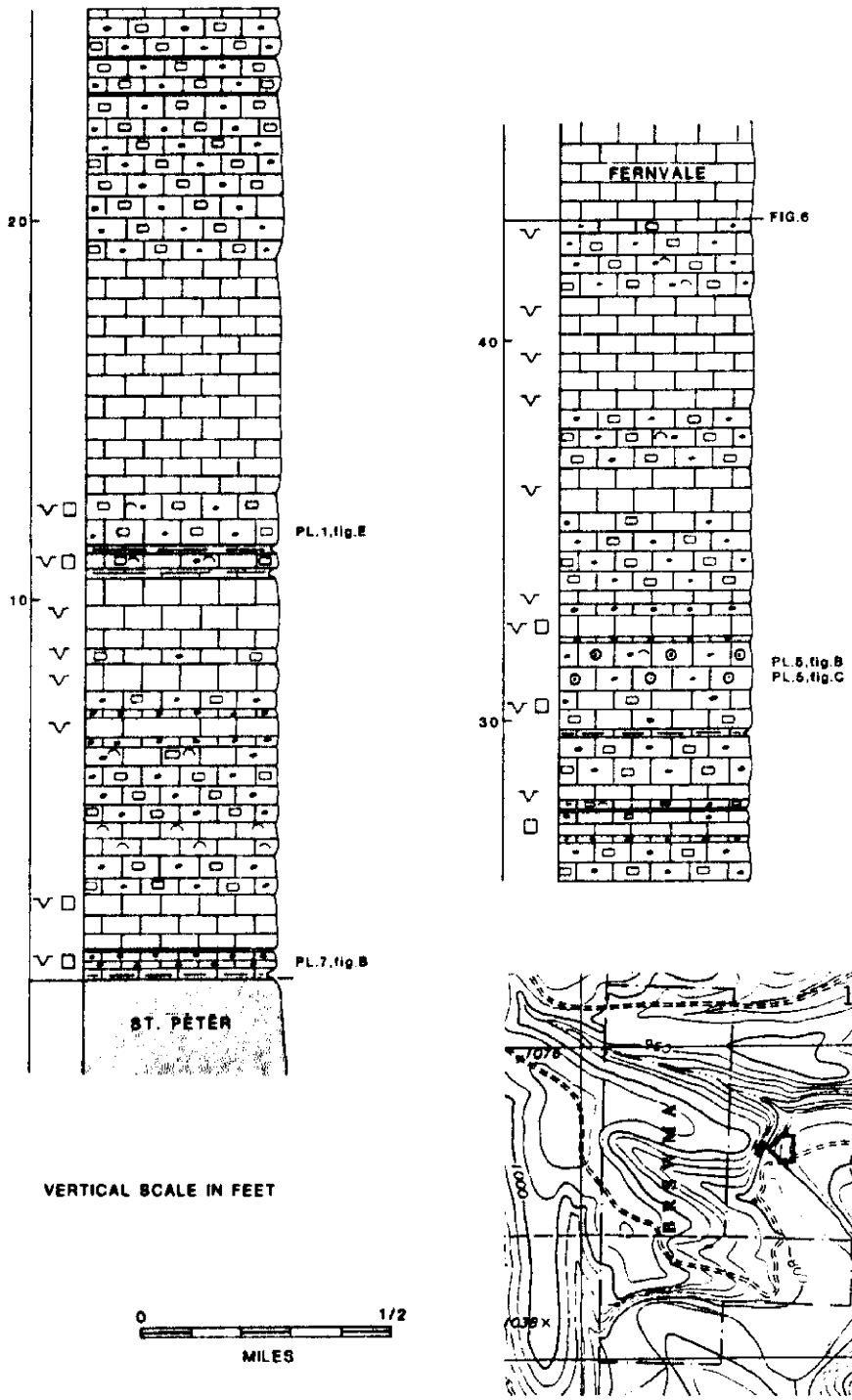

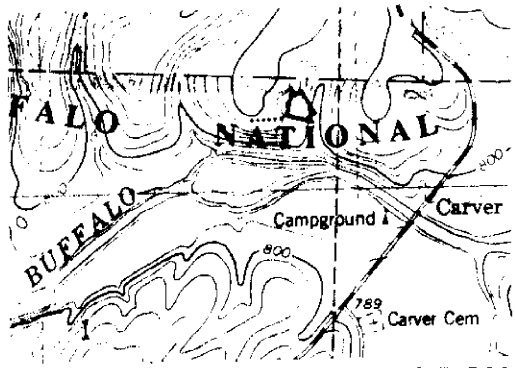

FIGURE 23. CARVER SECTION
NE 1/4 NE 1/4 SEC. 1 T15N R20W
MT.JUDEA QUADRANGLE, NEWTON COUNTY

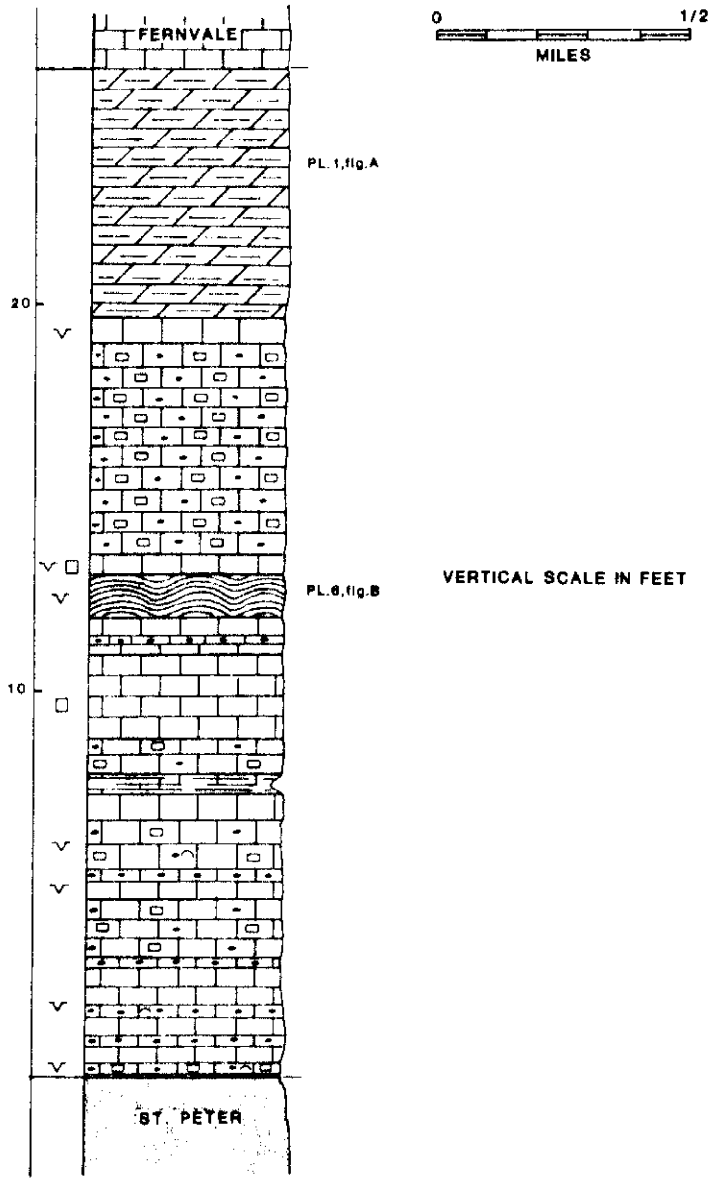

PLATES

EXPLANATION OF PLATE 1

FIGURE A. *Laminated dolostone (lithic type 2). Notice the planar to undulating millimeter laminations that are characteristic of rock type. Similar to smooth flat lamination of Hardie and Ginsburg (1977) (outcrop photograph, CAR-16).*

FIGURE B. *Lime mudstone (lithic type 3). Brecciated fabric produced by intense mudcracking. Note calcite pseudomorphs after halite (arrows) and irregular fenestrae filling interstices between breccia pieces (negative print of acetate peel, GP-47). Bar is 4mm.*

FIGURE C. *Lime mudstone (lithic type 3). Note faint laminations and dolomite-filled, medium-size v-shaped mudcracks in upper 1/3 of photograph. Irregular fenestrae in bottom 2/3 of photograph unidentified, probably desiccation features. (negative print of acetate peel, BS-3). Bar is 4mm.*

FIGURE D. *Lime mudstone (lithic type 3). Irregular fenestrae interpreted as calcite pseudomorphs after porphyroblastic halite crystals that became laterally linked as they grew in sediment. Note straight and angular outlines. Mudcracked nature of rock not visible in this photograph (photomicrograph of acetate peel, GP-59B). Bar is 1mm.*

FIGURE E. *Intraclast-peloid packstone/grainstone (lithic type 4). Note well-sorted, densely packed peloids and angular to rounded intraclasts with long axis parallel to bedding. Laminoid fenestrae common in sheltered areas below intraclasts (negative print of acetate peel, CC-13B). Bar is 5mm.*

PLATE 1

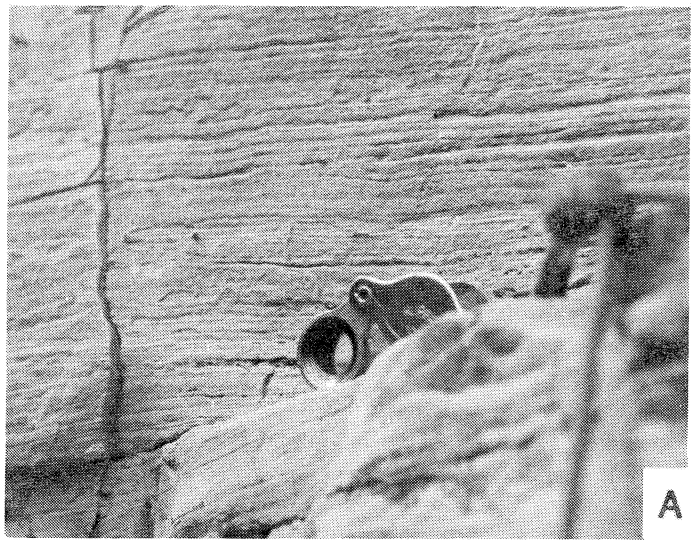
A

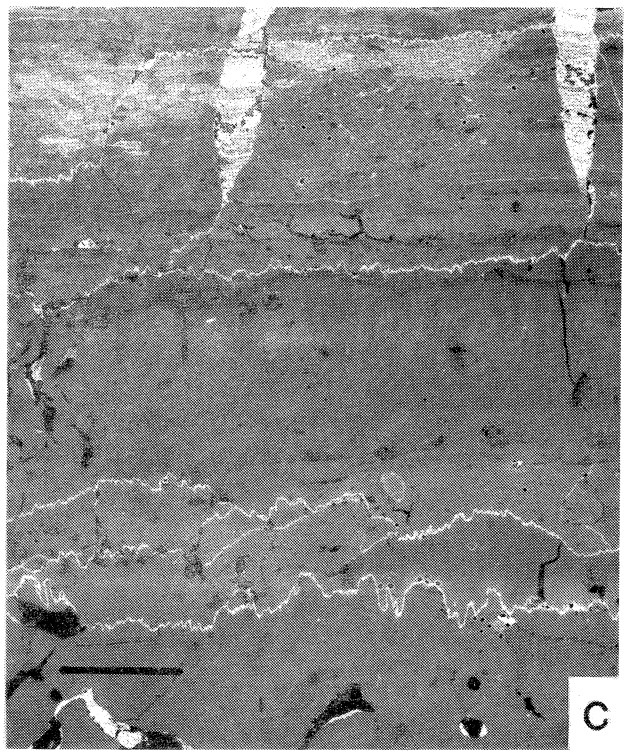
C

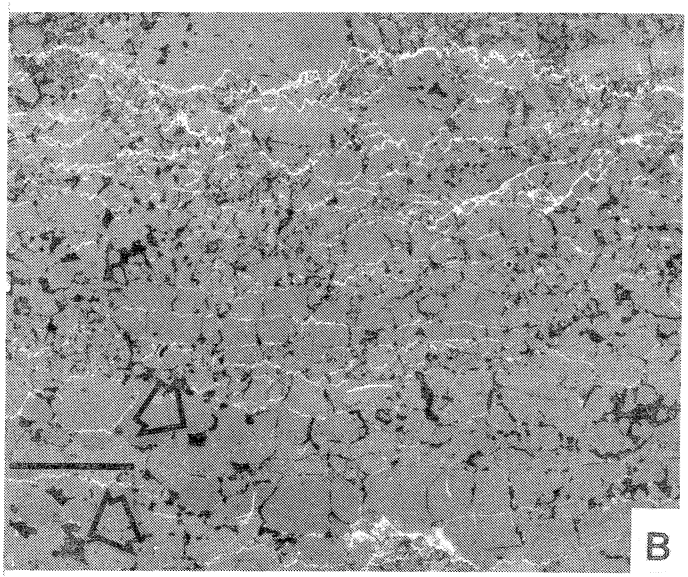
B

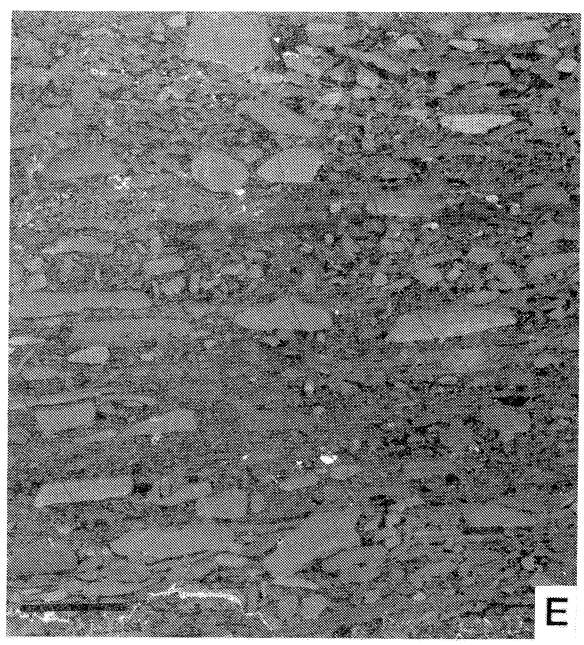
E

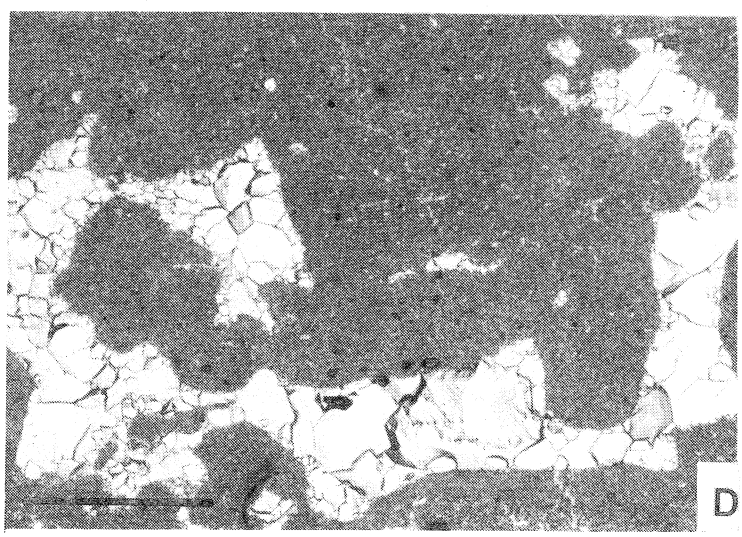
D

EXPLANATION OF PLATE 2

FIGURE A. *Peloid-intraclast wackestone or wackestone/packstone (lithic type 5). Breccia intraclasts are of lithic type 6 with laminoid fenestrae. Random orientation, composition, and angularity of clasts, plus mud matrix, indicates short transport and rapid deposition of algal mat rip-ups on tidal flat. Fabric similar to float breccia of Roehl (1967). Lowest large intraclast is 25 x 9 mm (negative print of acetate peel, TCB-22). Bar is 9mm.*

FIGURE B. *Interlaminated lime mudstone and peloid lime packstone/grainstone (lithic type 6). Rock exhibits planar to wavy laminations, mudcracks (see thick laminae at bottom), and calcite casts of former evaporites. Wavy laminations, similar to crinkled fenestral lamination of Hardie and Ginsburg (1977), apparently records morphology of algal mat (negative print of acetate peel, BS-25). Bar is 4mm.*

FIGURE C. *Interlaminated lime mudstone and peloid lime packstone/grainstone (lithic type 6). Note abundant mudcracks, some which propagate through several layers of mud and peloid composition, and discontinuous peloid laminae. Similar is disrupted flat lamination of Hardie and Ginsburg (1977). Boxed area contains calcite cast of evaporite cluster enlarged in Figure D below (negative print of acetate peel, TCB-12). Bar is 10mm.*

FIGURE D. *Enlargement of boxed area in Figure C above. The spar-filled void contains cast of pseudohexagonal gypsum crystal (arrow). Note other external and internal angular outlines. Bar is 6mm.*

PLATE 2

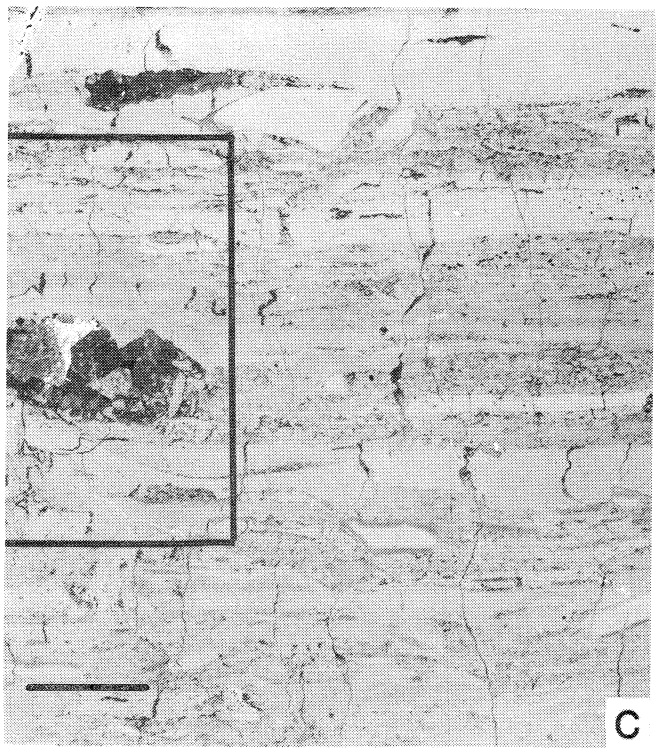

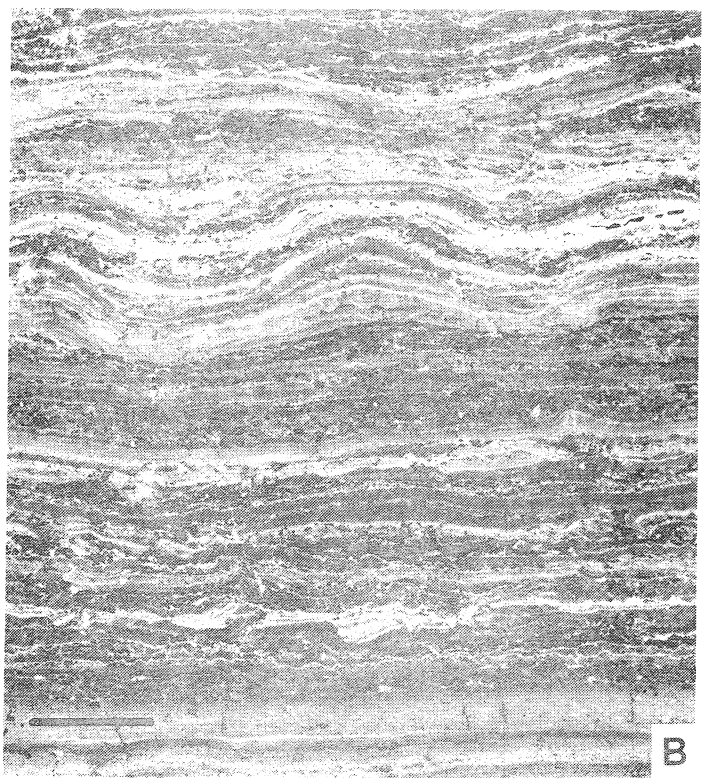

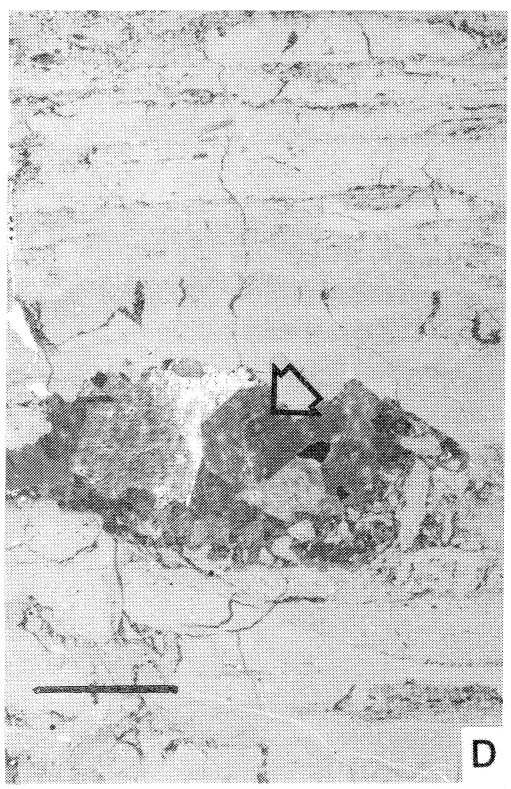

EXPLANATION OF PLATE 3

FIGURE A. *Interlaminated lime mudstone and peloid packstone/grainstone (lithic type 6). Note mudcracks, discontinuous peloid laminae, laminoid fenestrae, and calcite pseudomorphs after halite (arrows). Similar to disrupted flat lamination of Hardie and Ginsburg (1977) (negative print of acetate peel, GF-75). Bar is 4mm.*

FIGURE B. *Interlaminated lime mudstone and peloid lime packstone/grainstone (lithic type 6). Note teepee structure in center of photograph and general disrupted flat laminations resulting from desiccation. Boxed area, enlarged in Figure C below, encompasses evaporite casts (negative print of acetate peel, G1L-10B). Bar is 12mm.*

FIGURE C. *Enlargement of boxed area above. Texture is disrupted by porphyroblastic growth of halite crystals, molds which are now filled by calcite. Note angular corners (arrows) that identify the apparent irregular fenestrae as evaporites. Bar is 2mm.*

PLATE 3

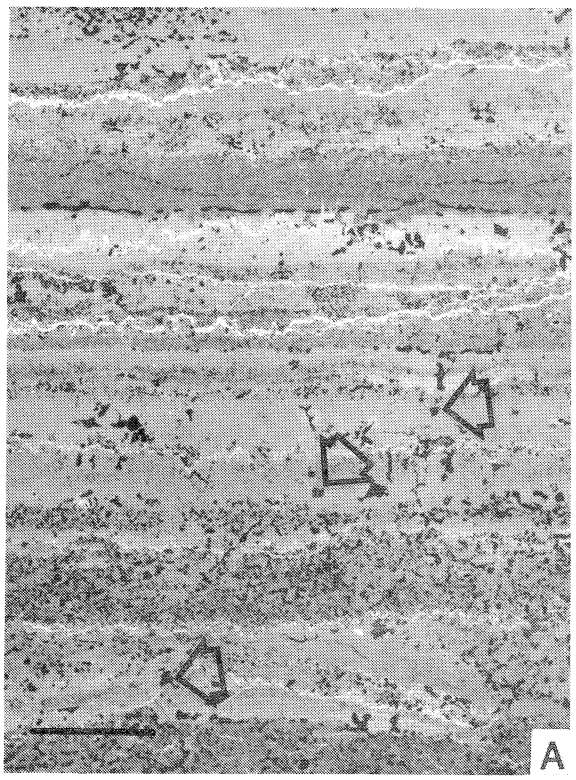

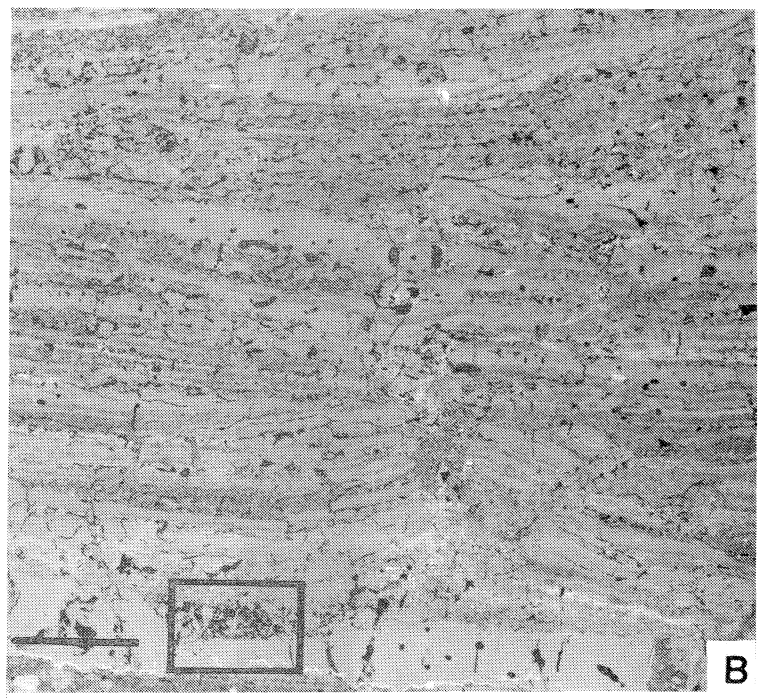

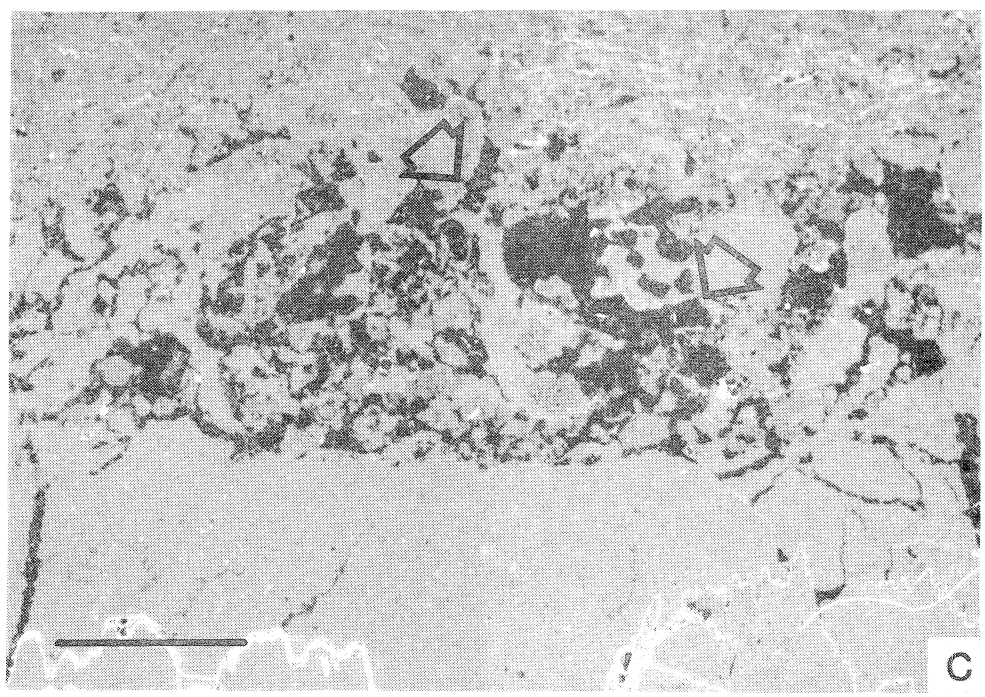

EXPLANATION OF PLATE 4

FIGURE A. *Interlaminated lime mudstone and peloid lime packstone/grainstone (lithic type 6). Pseudohexagonal calcite pseudomorph after selenite. Note encompassed sediment (photomicrograph of acetate peel, BS-41). Bar is 0.5mm.*

FIGURE B. *Interlaminated lime mudstone and peloid lime packstone/grainstone (lithic type 6). Coalesced calcite pseudomorphs after halite. Sediment in bottom of casts either infiltrated in after solution of halite, or during growth crystal encompassed host sediment, which fell to the bottom of mold upon solution of halite (photomicrograph of acetate peel, GF-74B). Bar is 0.5mm.*

FIGURE C. *Mollusc lime wackestone (lithic type 7). Note mollusc fragments, shells, and bioturbated fabric (negative print of acetate peel, GF-111D). Bar is 4mm.*

FIGURE D. *Mollusc lime wackestone (lithic type 7). Rock contains numerous circular skeletal fragments (top arrow) which along with those tests indicated by bottom arrows, have been tentatively identified as tenticulitids. Note cross section of gastropod in upper center of photograph and abundant ostracodes (negative print of acetate peel, SM-7). Bar is 6mm.*

PLATE 4

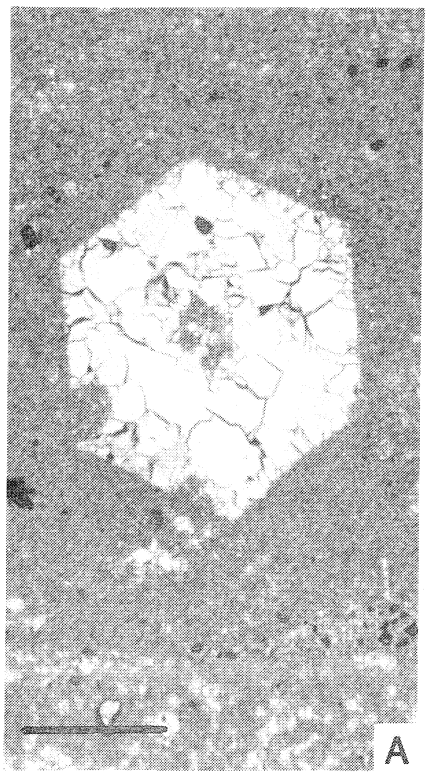
A

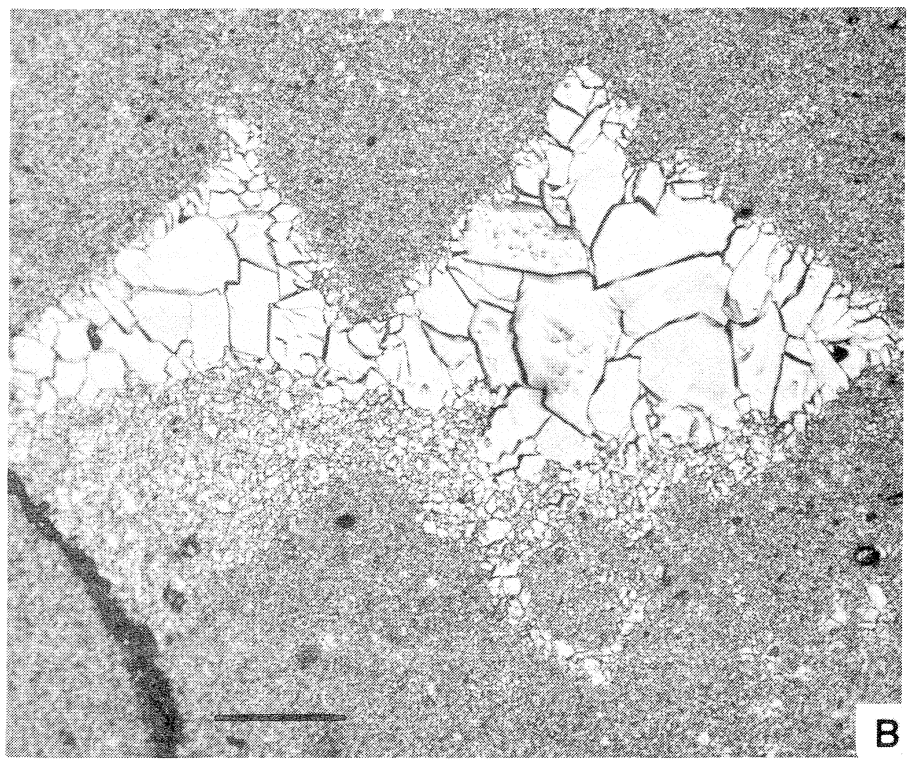
B


C

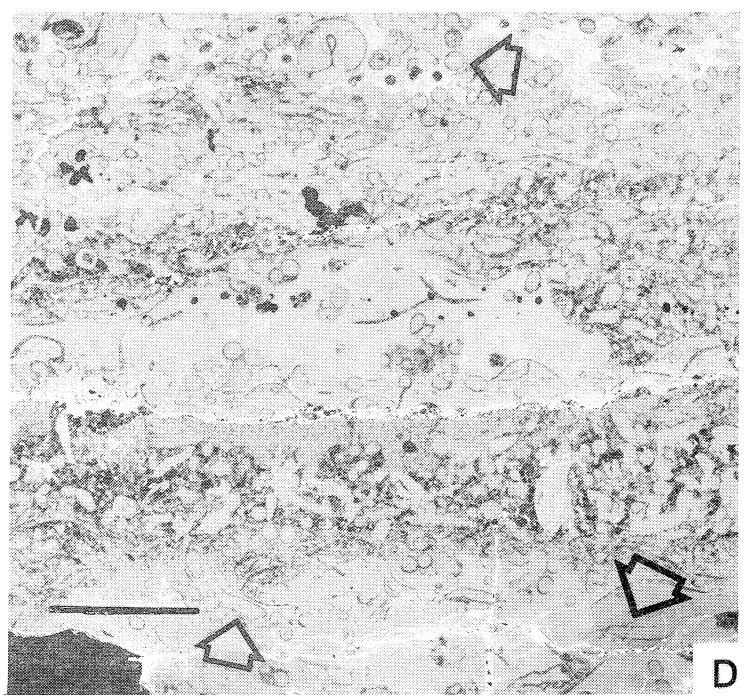
D

EXPLANATION OF PLATE 5

FIGURE A. *Skeletal lime wackestone/packstone (lithic type 8). Note abundant Tetradium corallites (negative print of acetate peel, GF-129). Bar is 5mm.*

FIGURE B. *Ooid-peloid packstone/grainstone (lithic type 9). Note cross lamination in center of photograph bounded by mudcracked lime mudstone above and below (negative print of acetate peel, CC-24L). Bar is 4mm.*

FIGURE C. *Ooid-peloid packstone/grainstone (lithic type 9). Ooids have peloid cores and radial structure (photomicrograph of thin section, CC-23). Bar is 0.5mm.*

FIGURE D. *Ooid-peloid packstone/grainstone (lithic type 9). Allochems are ooids and peloids. Note at bottom of photograph muddier areas that would qualify as packstone (negative print of acetate peel, BC-68B). Bar is 3mm.*

PLATE 5

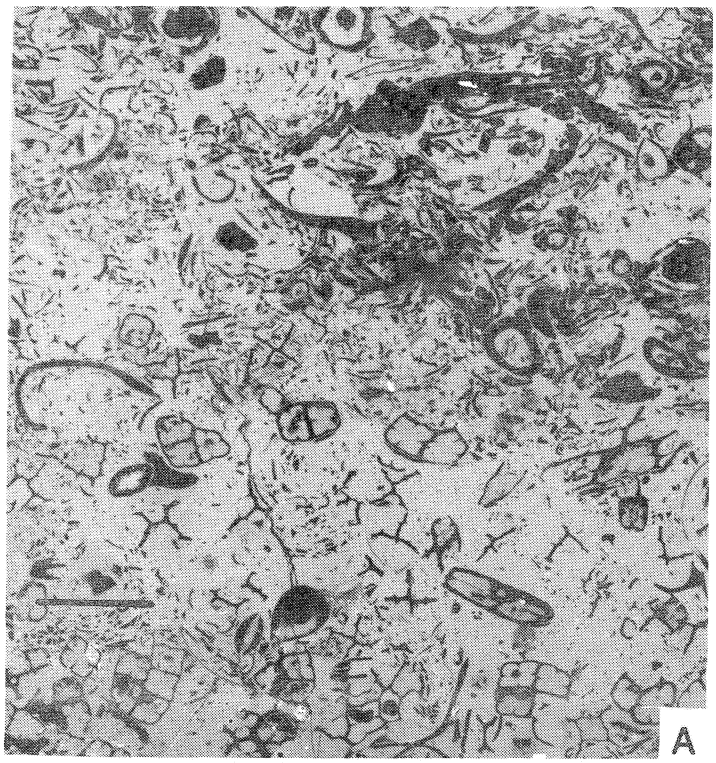
A

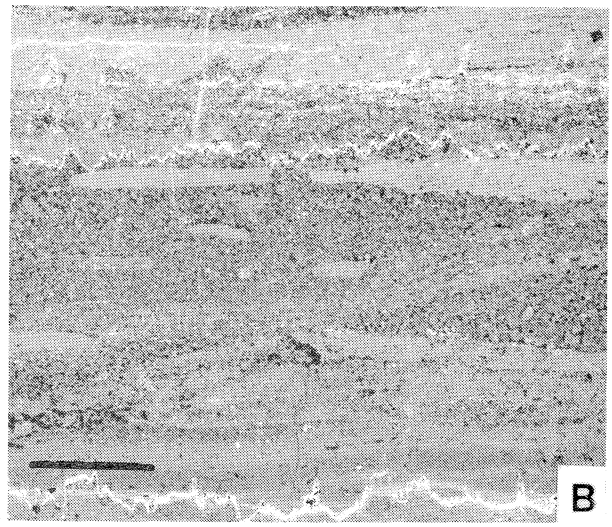
B


C

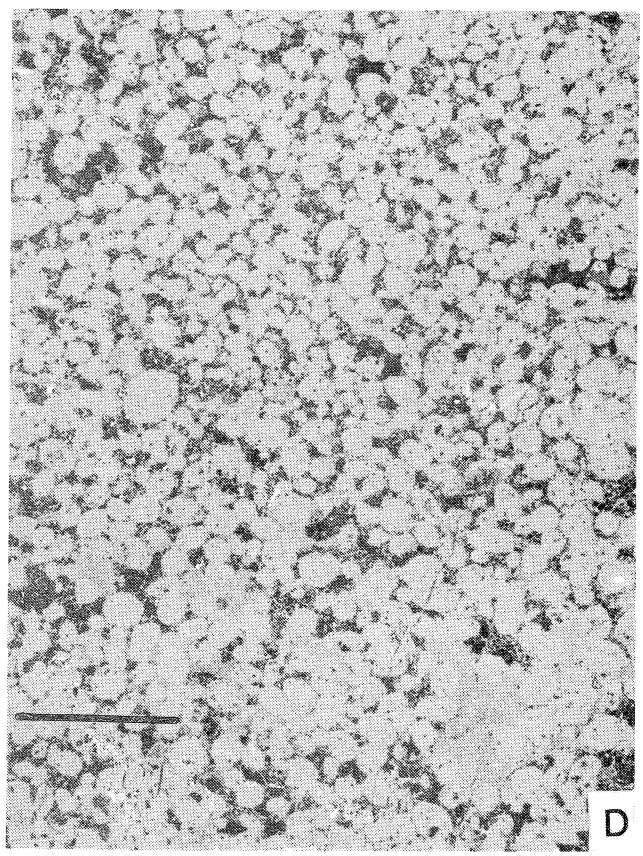
D

EXPLANATION OF PLATE 6

FIGURE A. *Enlargement of Figure 5D. Note micritized ooids with smaller peloids in between (photomicrograph of thin section BC-68B). Bar is 1mm.*

FIGURE B. *Stromatolitic limestone (lithic type 10). Composed of interlaminated lime mudstone and peloid lime packstone/grainstone (lithic type 6). Note mudcracks propagate through several layers (depositional events). Sample is from laterally-linked hemispheroid. Similar to disrupted flat lamination of Hardie and Ginsburg (1977) (negative print of acetate peel, CAR-11B). Bar is 4mm.*

FIGURE C. *Stramatolitic limestone (lithic type 10). Outcrop photo of broad stromatolite head at the Guion Ferry Section.*

PLATE 6

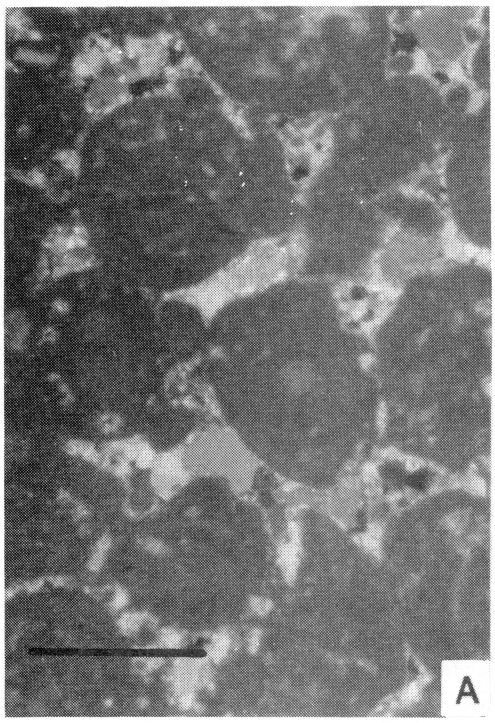
A

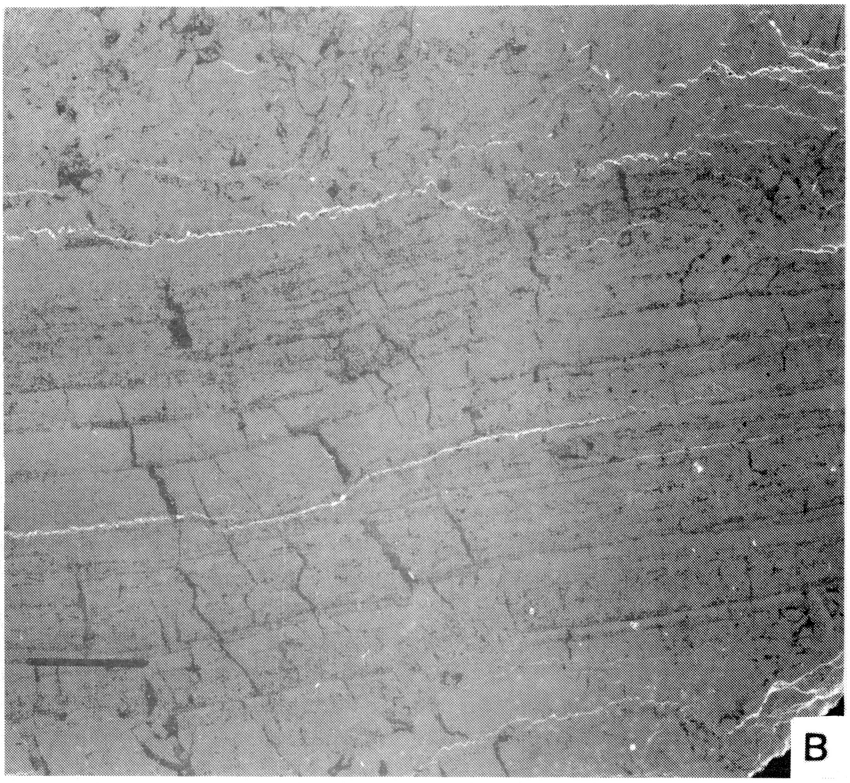
B


C

EXPLANATION OF PLATE 7

FIGURE A. *Coral lime boundstone (lithic type 11). Note Tetradium colony in lower right corner, diversity of fossils, and mottled nature of matrix sediment. Corals are in growth position in outcrop (negative print of acetate peel, BC-71). Bar is 6mm.*

FIGURE B. *Calcareous shale or argillaceous lime mudstone (lithic type 12). St. Peter-Plattin contact at Cave Creek. Note two shale breaks, one which separates the two formations (behind head of hammer) and another that causes the reentrant a few inches above the hammer (outcrop photograph, base of Section CC).*

FIGURE C. *Calcareous shale or argillaceous limestone (lithic type 12). Interbedded calcareous shale to slabby argillaceous limestone. Argillaceous break is overlain by lithic type 6 (note laminations). Pencil for scale (outcrop photograph, BC-40).*

PLATE 7

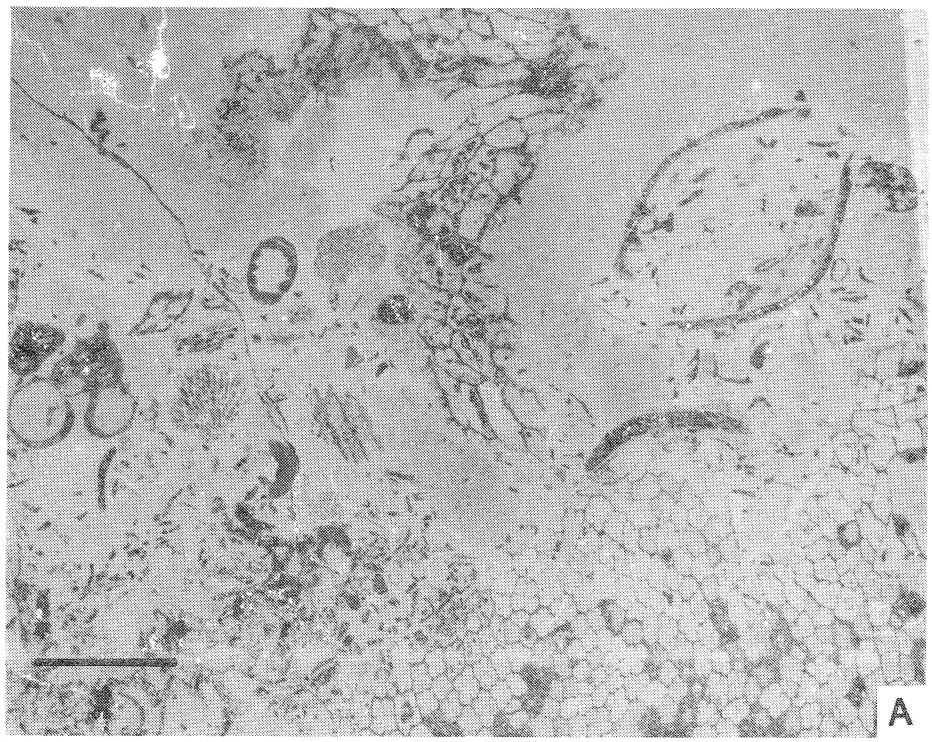

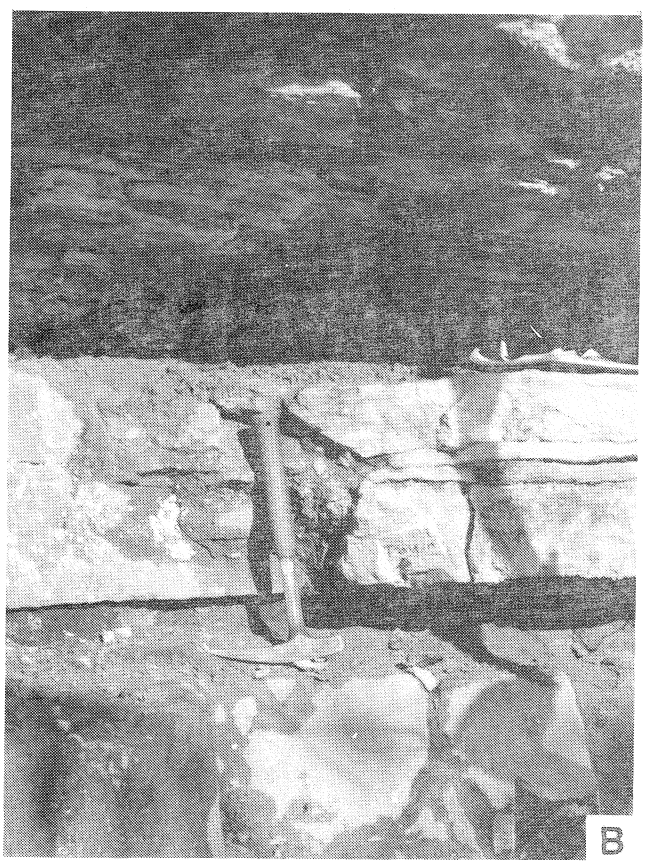

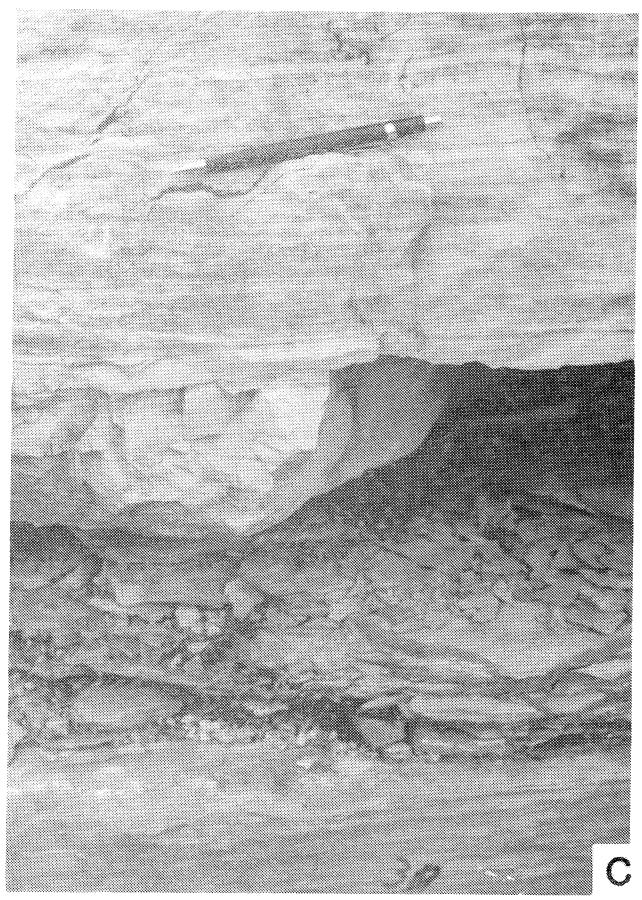

GEOCHEMISTRY OF THE LOWER ORDOVICIAN DOLOMITE OF NORTHERN ARKANSAS

By George H. Wagner, Kenneth F. Steele, and Doy L. Zachry
Department of Geology
University of Arkansas
Fayetteville, AR 72701

ABSTRACT

Dolomite rock from three outcrops of the Cotter and Powell Formations in northern Arkansas were analyzed chemically and by x-ray diffraction. Whole rock purity at three sites averaged 80-90% dolomite with quartz, feldspar, illite, and calcite being the main impurities. For the fraction (15/41) of samples analyzed for these impurities the ranges were: 1.0-20% quartz, 0.2-6% feldspar, 0-0.9% illite and 0.5-1.8% calcite. The acid soluble portion is generally almost pure dolomite. SO_4^{2-} content was generally less than 5 ppm and Cl^- less than 50 ppm indicating almost no residual evaporite minerals. Metal contaminants in the solubles were mainly Fe (2100-3500 average ppm), Mn (200-400 average ppm) and Al (250-1500 ppm average). Other heavy metals averages were low: 1-34 ppm Zn and 0-5 ppm Cu. The Mg content of the dolomites has not favored heavy metal substitution in the lattice as in the case of neighboring limestones. The low metal contents of these unmineralized dolomites indicate they were not a source of the lead and zinc minerals in nearby ores hosted by dolomite rocks.

INTRODUCTION

Little has been published on the dolomites of Arkansas (Freeman, 1966; Young et al., 1972; Handford and Moore, 1976). These publications contain no geochemical data, except for Sr analyses in the latter reference. Data on ancient dolomites are of considerable interest because our knowledge and understanding of the dolomitizing process is still in need of improvement and confirmation.

A further interest in these dolomites arose from geochemical studies of Carboniferous limestones in northern Arkansas (Wagner et al., 1979). These limestone units, because of past erosional episodes and missing strata in the study area, are stratigraphically just above the Ordovician dolomites (Figure 1). The heavy metal contents of the limestone units increased with the magnesium content. It was thus of interest to look to the nearby dolomites with their high magnesium contents for further correlation of this relationship.

The location of the outcrops which were sampled is shown in Figure 2. Sampling sites are further identified as follows: Beaver Dam (BD) samples in Carroll County at NW 1/4, NW 1/4, Sec. 10, R. 27 W., T 20 N; Route 281 samples (R-281) in Boone County at NW 1/4, NE 1/4, Sec. 8, T. 20 N., R. 19 W. and SW 1/4, SE 1/4, Sec. 5, T. 20 N., R. 19 W.; and samples along Highway 14 near Monarch, Arkansas in Marion County (denoted by Mon) at NE 1/4, Sec. 29, T. 20 N., R. 17 W.

METHODS

Chips totaling 10-15 g from unweathered portions of the field samples were ground to minus 100 mesh with mortar and pestle. 10 ml of concentrated HCl or HNO_3 were added to 1 g of this powder in a 50 ml Erlenmeyer flask. After heating to 50°C, then standing overnight, the contents were filtered quantitatively through a preweighed 0.45 micron Millipore filter and diluted to 50 ml with

TABLE 1

Major Cations and Anions in Odovician Dolomites

Sample	Column Height (ft)	Wt. % of HC1 Solubles				ppm of whole rock			HCl solubles Empirial Formula	
		Acid Solubles*	Ca	Mg	CO_2	PO_4^{3-}	SO_4^{2-}	Cl^-	Ca/CO_3	Mg/CO_3
					Site 1					
BD-10	38	88.5	24.9	10.3	46.2	215	-**	-**	0.594	0.401
BD-1	37	97.3	20.8	12.5	46.6	25	–	–	0.491	0.484
BD-5	35	80.5	20.8	12.6	47.5	420	–	–	0.481	0.479
BD-4a	29	95.6	22.4	12.7	–.-**	84	0	38	-.—**	-.—**
BD-4	20	90.9	21.2	12.8	47.1	235	–	–	0.495	0.492
BD-3	16	98.4	20.8	12.8	46.6	25	–	–	0.492	0.497
BD-2	12.9	89.0	20.7	12.6	47.2	250	–	–	0.484	0.485
BD-8	11.5	84.3	21.4	12.7	47.0	285	–	–	0.500	0.490
BD-7a	10.1	42.4	22.1	12.0	–.-	71	566	19	-.—	-.—
BD-7	9.3	95.0	21.7	13.1	46.8	90	–	–	0.511	0.507
BD-9	9.2	96.8	22.5	13.4	47.0	75	–	–	0.525	0.516
BD-6	5	98.8	21.5	13.0	46.5	25	–	–	0.504	0.503
BD-11a	4	96.6	22.6	12.6	–.-	169	0	29	-.—	-.—
BD-11	3	94.2	21.8	13.0	47.4	115	–	–	0.504	0.494
Site I, average		89.2	21.8	12.6	46.9	149	–	–	-.—	-.—
					Site II					
R-281-1	91.5	89.0	20.8	12.9	46.0	105	–	–	0.495	0.506
R-281-2	91	78.5	20.3	12.2	47.0	510	–	–	0.474	0.469
R-281-3	21	77.5	20.3	12.3	45.3	470	–	–	0.493	0.488
R-281-4	14	95.0	21.3	12.8	46.7	125	–	–	0.503	0.497
R-281-5	7	90.7	21.5	13.0	47.3	55	–	–	0.502	0.500
R-281-6	0	91.6	21.0	13.0	47.2	260	–	–	0.491	0.497
Site II, average		87.1	20.9	12.7	46.6	254	–	–	–	–

TABLE 1 (cont.)

Sample	Column Height (ft)	Wt. % of HC1 Solubles				ppm of whole rock			HCl solubles Empirial Formula	
		Acid Solubles*	Ca	Mg	CO_2	PO_4^{3-}	SO_4^{2-}	Cl^-	Ca/CO_3	Mg/CO_3
					Site III					
Mon-118	118	94.4	22.5	12.3	–	162	0	81	–	–
Mon-106	106	71.6	21.4	12.0	–	542	0	11	–	–
Mon-103	103	90.2	22.1	12.4	–	300	0	40	–	–
Mon-95	95	53.1	21.1	11.8	–	1426	0	23	–	–
Mon-86	86	77.8	22.2	13.1	–	81	0	0	–	–
Mon-84	84	76.3	22.0	13.2	–	525	0	16	–	–
Mon-78	78	81.7	22.0	13.1	–	349	0	24	–	–
Mon-52	52	61.9	21.9	11.6	–	1131	0	32	–	–
Mon-47	47	73.2	21.1	12.7	–	546	16	27	–	–
Mon-43	43	88.1	21.5	13.1	–	392	0	91	–	–
Mon-42	42	97.7	21.4	13.1	–	80	0	193	–	–
Mon-36	36	66.5	22.2	12.2	–	1296	0	24	–	–
Mon-34	34	95.1	22.4	13.0	–	216	0	143	–	–
Mon-27	27	76.5	22.5	12.3	–	573	0	31	–	–
Mon-22	22	76.0	21.9	12.8	–	510	0	11	–	–
Mon-20	20	71.3	21.9	11.9	–	755	281	39	–	–
Mon-15.5	15.5	84.7	21.8	12.0	–	518	0	9	–	–
Mon-12	12	91.4	21.9	12.2	–	304	0	35	–	–
Mon-7.5	7.5	81.5	21.0	12.5	–	1090	0	10	–	–
Mon-5	5	78.8	21.8	12.0	–	793	0	45	–	–
Mon-0	0	88.9	22.6	13.1	–	231	0	32	–	–
Site III, average		79.8	21.9	12.5	–	563	–	44	–	–
Precision ±		0.1	0.1	0.05	0.05	10	5	4	0.003	0.003
U.S. Bu. Standards ***		–	21.8	12.95	47.3	40	–	–	0.507	0.497

* Values reported are for HC1. For the Site III samples HC1, HNO_3 and aqua regia were compared: HC1 and HNO_3 solubles agreed to ± 0.43 wt. %; aqua regia dissolved on the average 0.3 wt. % more than the average of the HC1 and HNO_3 solubles.

** not determined.

*** standard dolomite sample No. 88 (Siegel, 1967)

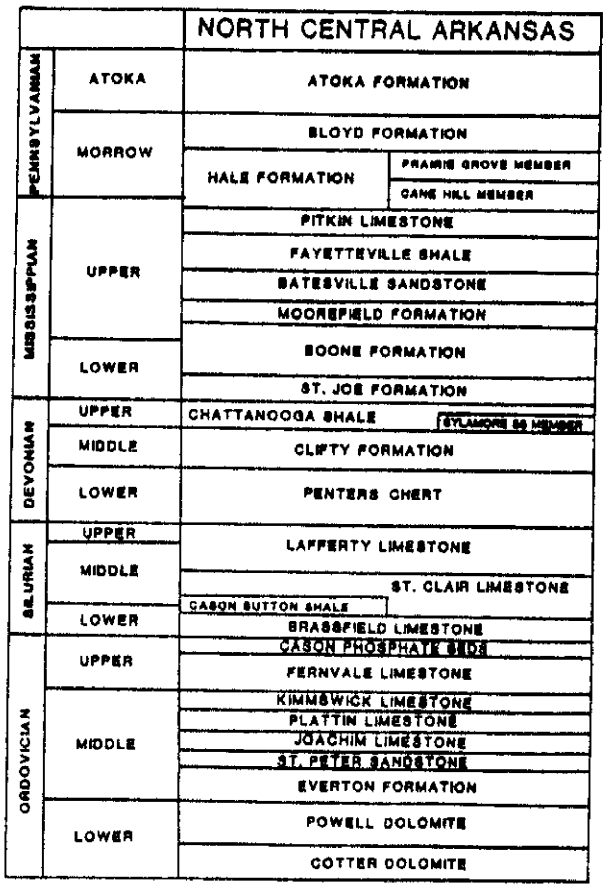

Figure 1. *Stratigraphy of north central Arkansas.*

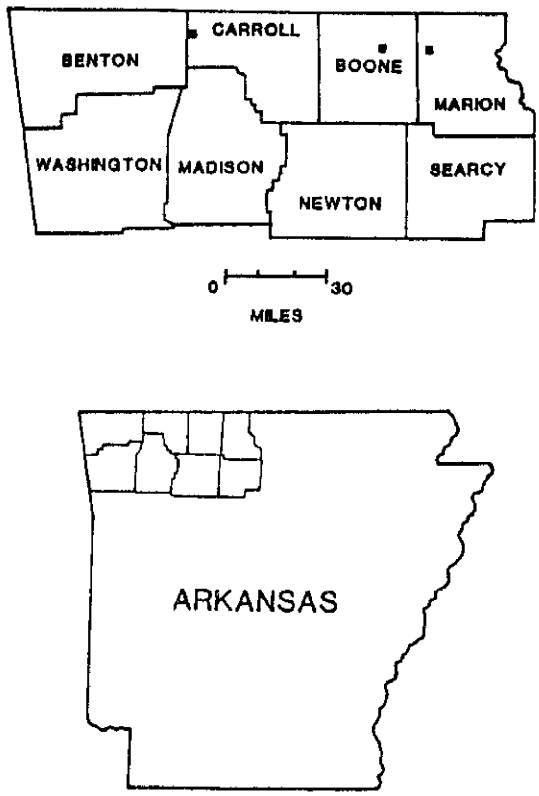

Figure 2. *Location map. Sampled sites denoted by a small black square.*

deionized water. The insolubles and the filter were heated 13 hr. at 80°C, cooled to room temperature and weighed. Three blanks, i.e. all reagents, a Millipore filter, and the complete treatment but without samples, were also run so that corrections for trace metals in reagents could be made.

The solutions were analyzed by atomic absorption (Fe, Zn, Mn, Pb, Al, Ca, Mg) or emission spectroscopy (Sr, K, Na, Li, Rb) using a solid state modernized Model 82-500 Jarrell Ash spectrophotometer. Cs^+ additions to 1000 ppm were made to standards and samples analyzed for Ca, Mg, Sr, Al, K, Na, Li and Rb in order to minimize ionization problems. Three types of flames were used: H_2-air for K, Na, Li and Rb; C_2H_2-air for Fe, Mn, Zn and Pb; C_2H_2-N_2O for Ca, Mg, Sr and Al. The precision of the analyses are given in Table 1 along with the analyses for the major ions which are calculated, as noted in the table, on the basis of the soluble portion for the cations and CO_2, and on the whole rock for PO_4^{3-}, SO_4^{2-} and Cl^-.

CO_2 analyses were by the titration method of Shapiro (1975) with very minor corrections for PO_4^{3-}. PO_4^{3-} analyses were by APHA (1971) p. 532 using aliquots of the HCl-dissolved dolomite samples. Analyses were made on the solutions after KOH neutralization to the phenophthalein endpoint. Although PO_4^{3-} analyses proceeded satisfactorily by this scheme, SO_4^{2-} and Cl^- analyses did not. A brownish precipitate, presumably iron oxide hydrate, interfered in the SO_4^{2-} analysis. In the case of Cl^- a fading endpoint and large blanks made the analyses unreliable. The method finally adopted for SO_4^{2-} and Cl^- was to grind the solid dolomite sample to a very finely divided state using a Spex grinder and an alumina ball. Then 1 g of the fine powder was shaken intermittently in 100 ml of deionized-distilled water in a 200 ml BOD bottle for 46 days. Aliquots of the aqueous extract were analyzed:

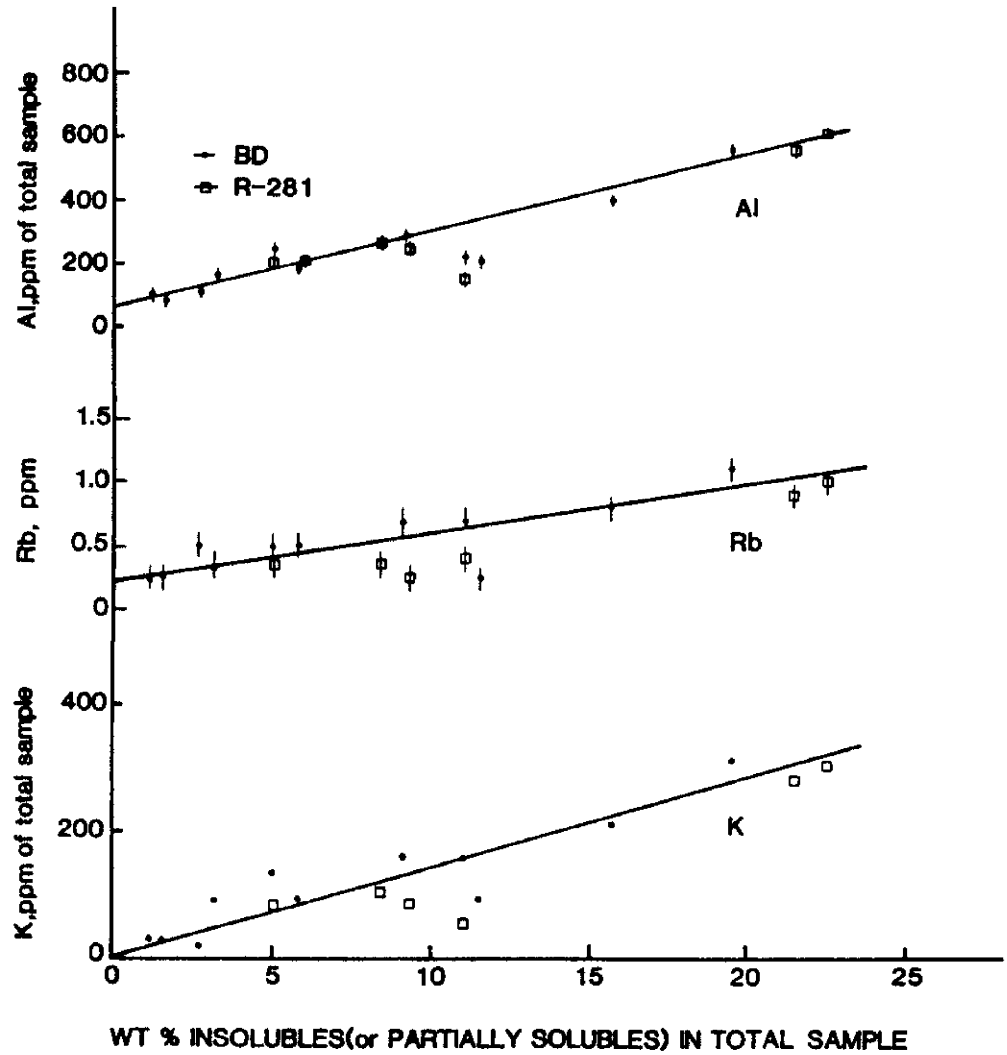

Figure 3. *K, Rb, and Al vs the wt% of insolubles in the BD and R-281 series of samples.*

SO_4^{2-} by APHA (1971) p.334 using a Hach Model 2100A Tubidimeter and Cl^- by APHA (1971) p. 97.

X-ray diffraction analyses were made on a Diano unit using a 40 KV, 20 ma setting and Cu-K alpha radiation. Spex ground samples were used on double-sticky tape on microscope slides. A great deal of effort was spent in preparing standard mixtures of quartz-dolomite, feldspar-dolomite, calcite-dolomite and inter mixtures of quartz, feldspar and calcite in dolomite. These mixtures were prepared in an effort to establish a system where these three impurities - quartz, feldspar, and calcite - could be determined quantitatively in the dolomite by x-ray diffractions as others have done in part (Diebold et al., 1963; Runnells, 1970; Royse et al., 1971). Boone limestone of 95% plus purity was used as a standard source of calcite, St. Peter Sandstone was a standard source of quartz, orthoclase as a standard feldspar and dolomite sample BD-3 as a dolomite standard. All mixtures were ground extensively on the Spex grinder for fineness and homogeneity. Ample dustings of the mixtures were made on double-sticky tape on a glass slide for x-ray diffraction. Standard curves of relative peak heights (peak height of the principal line of the mineral impurity compared to the peak height of the principal dolomite line) versus composition are shown in Figure 7 for

TABLE 2

Minor and Trace Elements in Ordovician Dolomites

Parts Per Million in the HCl Solubles

Sample No.	Column Height (ft)	Fe	Mn	Al	Sr	K	Na	Li	Rb	Zn*	Cu
					Site I						
BD-10	38	3278	329	226	59	104	177	1.2	0.3	4	0
BD-1	37	3335	514	103	60	22	110	0.57	0.5	0	0
BD-5	35	3375	333	671	71	385	118	1.2	1.4	0	0
BD-4a	29	3733	403	261	72	146	117	3.5	1.9	0	0
BD-4	20	2392	313	300	67	176	105	0.95	0.8	0	0
BD-3	16	2251	753	81	43	33	38	0.10	0.3	0	0
BD-2	12.9	2586	426	246	71	174	100	1.3	0.8	0	0
BD-8	11.5	3117	300	451	82	249	117	1.1	0.9	0	0
BD-7a	10.1	2227	260	236	106	128	314	4.5	2.4	0	0
BD-7	9.3	2168	282	253	82	142	123	1.2	0.5	0	0
BD-9	9.2	1932	277	165	80	95	172	1.4	0.4	0	0
BD-6	5	2796	524	101	87	31	138	1.0	0.3	0	0
BD-11a	4	2205	321	207	106	161	209	3.9	2.4	0	0
BD-11	3	2122	333	191	79	102	101	1.2	0.5	4	0
Site I, average		2680	383	249	76	139	139	1.7	1.0	1	0
					Site II						
R-281-1	91.5	854	845	157	84	58	176	1.7	0.4	0	0
R-281-2	91	2624	322	688	82	354	148	1.1	1.1	5	0
R-281-3	21	4955	258	774	74	393	151	1.7	1.3	5	4
R-281-4	14	1316	252	211	99	86	170	2.2	0.4	25	0
R-281-5	7	1378	162	265	108	95	292	2.1	0.3	77	0
R-281-6	0	1556	198	284	77	107	149	1.2	0.4	90	0
Site II, average		2114	340	397	87	182	181	1.8	.7	34	1

TABLE 2 (cont)

Parts Per Million in the HCl Solubles

Sample No.	Column Height (ft)	Fe	Mn	Al	Sr	K	Na	Li	Rb	Zn*	Cu
					Site III						
Mon-118	118	918	101	318	152	238	288	5.3	2.5	0	0
Mon-106	106	3381	204	1392	116	765	225	5.3	4.9	0	0
Mon-103	103	2418	140	885	130	531	257	5.5	3.8	2	0
Mon-95	95	2451	422	3544	112	2360	237	8.0	10.1	180	100
Mon-86	86	871	234	257	152	154	221	5.9	2.1	0	0
Mon-84	84	1875	185	1436	140	757	211	6.1	4.3	13	0
Mon-78	78	2388	198	511	106	389	188	4.9	2.9	0	0
Mon-52	52	3749	268	3180	102	2361	234	6.5	9.1	0	0
Mon-47	47	5872	235	4522	90	2864	270	9.0	10.4	0	0
Mon-43	43	2316	160	910	130	546	230	5.0	3.4	45	0
Mon-42	42	1167	118	307	130	164	396	5.3	2.1	4	0
Mon-36	36	6272	190	1821	121	1403	246	5.5	6.5	13	0
Mon-34	34	1957	138	529	125	307	314	5.5	2.8	8	0
Mon-27	27	5451	226	1850	103	1221	280	6.6	5.4	0	0
Mon-22	22	5998	213	2517	103	1676	261	6.9	7.7	0	0
Mon-20	20	4223	227	2098	101	1462	276	6.0	6.9	0	0
Mon-15.5	15.5	3756	228	1766	92	1114	197	6.4	5.1	2	0
Mon-12	12	3544	177	547	101	339	232	5.6	4.5	0	0
Mon-7.5	7.5	4970	211	1827	95	1126	240	5.5	5.6	0	0
Mon-5	5	5138	218	1137	96	569	249	4.9	3.7	0	0
Mon-0	0	4691	240	676	98	338	222	5.0	3.3	0	0
Site III, average		3496	206	1525	114	985	251	5.9	5.1	13	5
Precision ±		20	14	20	2	1	1	0.05	0.1	2	1
U.S. Bu. Standards **	590	50	350	-	250	590	–	–	–	–	

* Pb was 0 ± 10 ppm on all samples, except sample R-281-5 and R-281-6 which contained 22 ± 10 ppm.

** Standard dolomite sample No. 88 (Siegel, 1967)

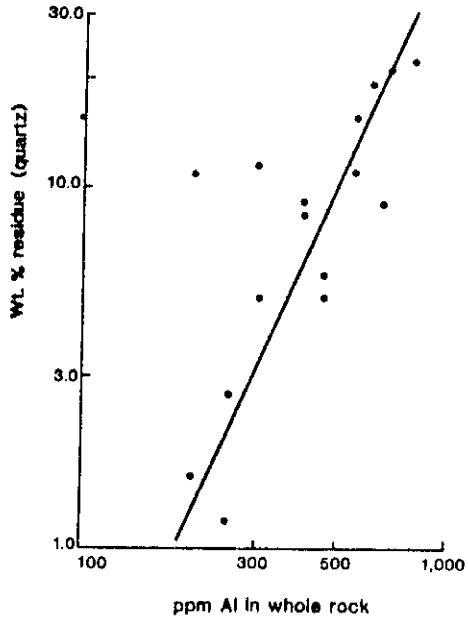

Figure 4. *Wt% of HCl insoluble residue (mainly quartz) vs ppm Al in the BD and R-281 series of samples.*

quartz-dolomite, Figure 8 for calcite-dolomite and Figure 9 for feldspar-dolomite.

In these standard curves Figure 8 shows a smooth relationship for calcite in dolomite and good agreement with previous investigators (Royse et al., 1971). Quartz gives a smooth relationship up to 12 wt.% where the relationship with insoluble residue (equated to quartz) and standard additions of St. Peter Sandstone diverge. Figure 9 is an unsettled enigma for feldspar (orthoclase). This figure shows a standards addition curve for orthoclase in dolomite. The dashed line extension should give at its intersection with the x-axis the amount (9%) of orthoclase in the dolomite. By Al analyses of the solubles and x-ray analysis of the insolubles the orthoclase content can not be greater than 0.4%. Evidently the feldspar in the dolomite provides greater x-ray intensity, because of its fineness, orientation, or composition, than the orthoclase mineral used for the standard mixtures.

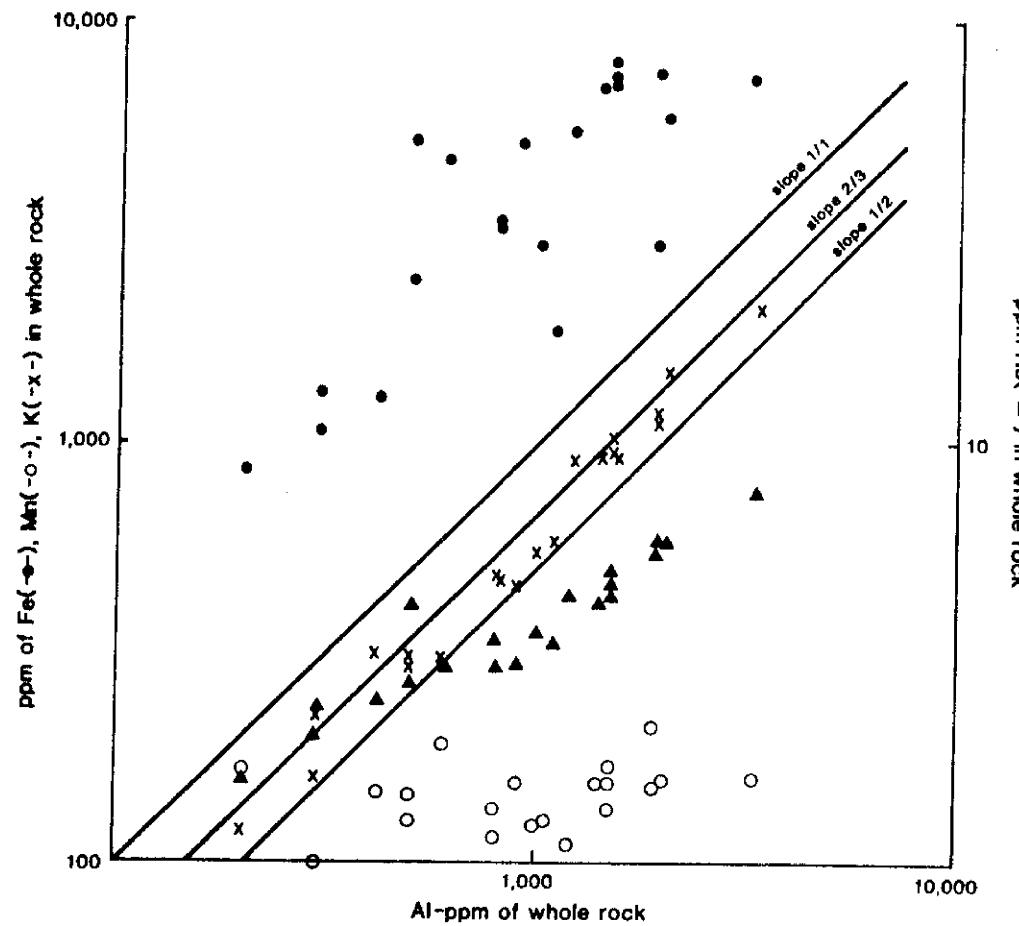

Figure 5. *ppm of Fe, Mn, K and Rb in whole rock vs ppm Al in the Mon series. HNO_3 was the solvent.*

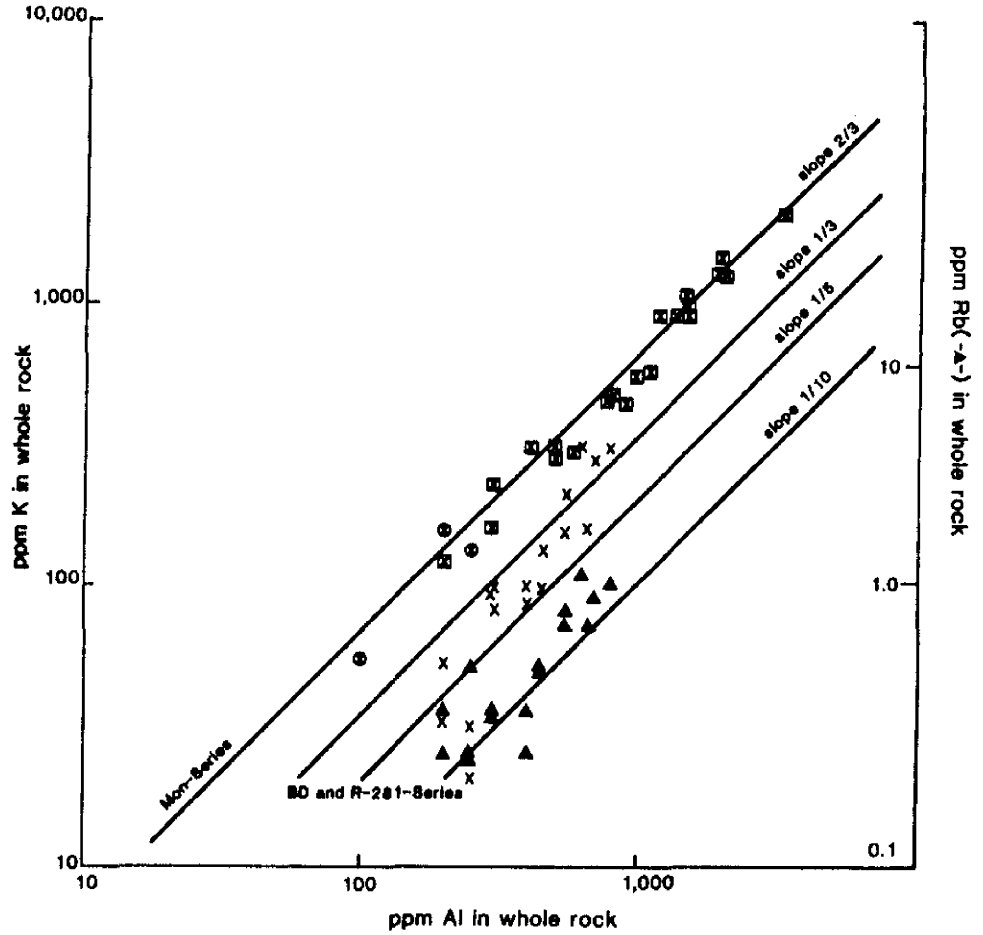

Figure 6. *Comparing the K vs Al for the Mon (⊠), BD, and R-281 (x) series. Rb vs Al is also shown for the BD and R-281 series. Both HCl (x) and HNO_3 (⊗) were used as solvents for BD and R-231 series. The Mon series as well as the ⊗ samples were ground in the Spex grinder whereas the others were ground with mortar and pestle.*

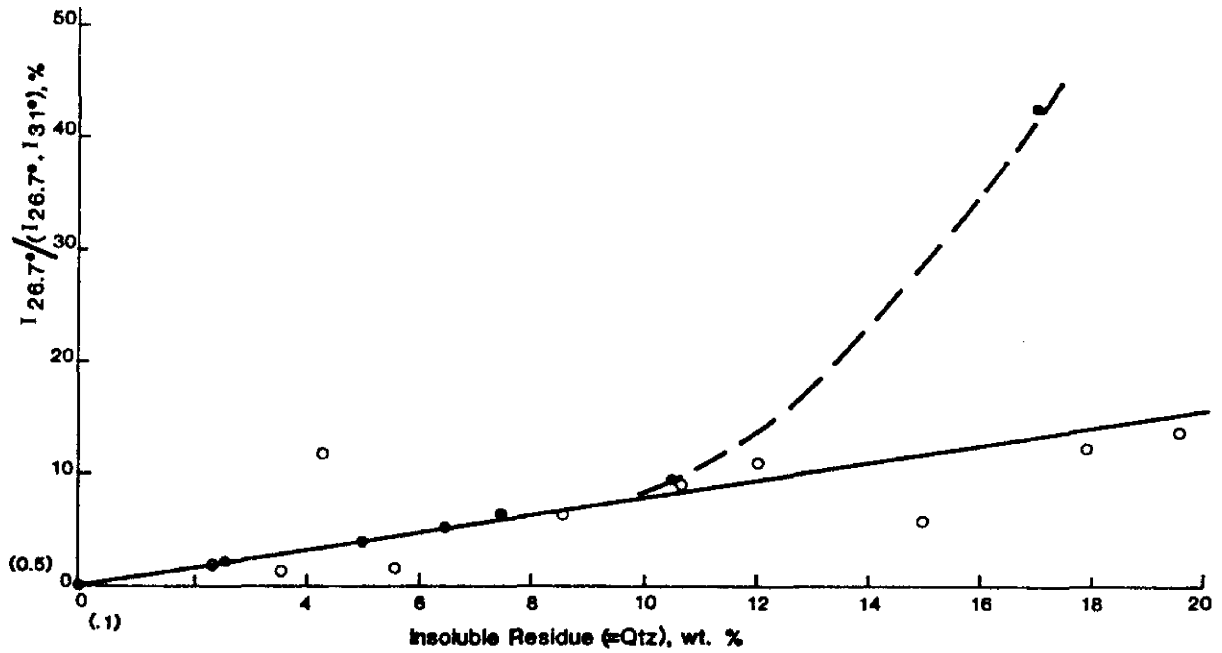

Figure 7. *Relative peak heights for quartz (26.7°) in dolomite from x-ray diffraction data of dolomite samples vs their insoluble residues (○). The insoluble residues are uncorrected for 2-6% of illite. The other points (●) represent quartz (St. Peter Sandstone) additions to dolomite BD-3. The 1.5% quartz in BD-3 has been taken into account. The relative peak height is a % of the height of the principal quartz line (26.7°) in the dolomite to the total of the peak height of pure quartz (26.7°) and pure dolomite (31°).*

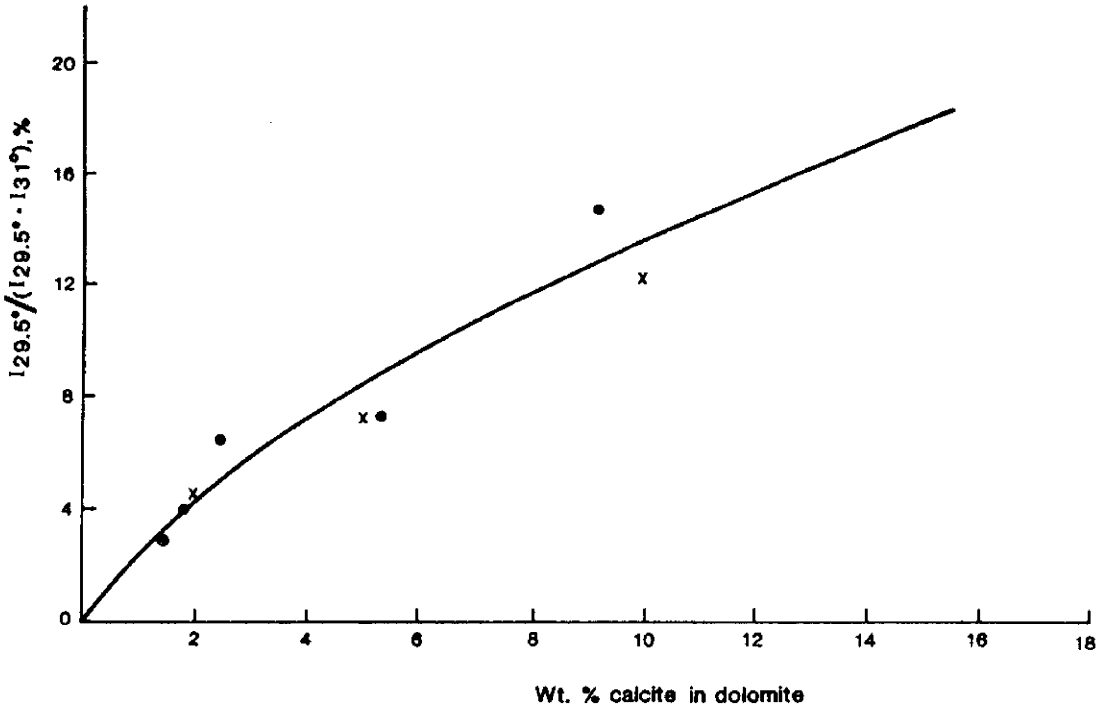

Figure 8. *Relative peak heights of calcite (29.5°) in dolomite vs the wt % of calcite. Literature values (x) are from Royse et al. (1971). Standard additions (●) used Boone limestone mixtures in BD-3 (⊙).*

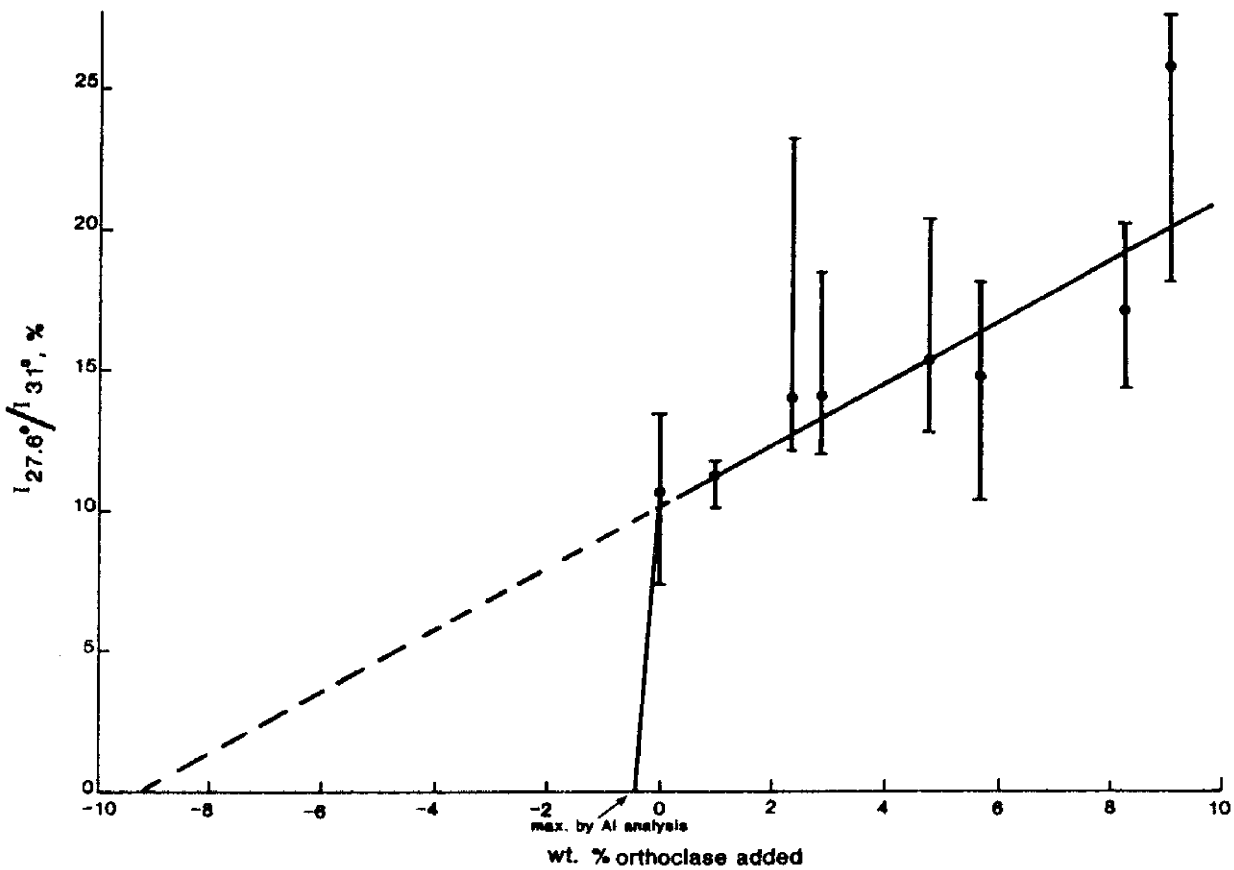

Figure 9. *Relative peak heights for feldspar (orthoclase) at 27.6° vs standard additions of orthoclase to BD-3 dolomite. The extrapolation, dashed line, indicates 9% feldspar in BD-3 whereas its maximum possible content is 0.4% (solid curve). This curve thus is unusable for determining feldspar by x-ray diffraction of unknown samples. It is reproduced here to illustrate a requirement in the standards addition method, i.e. the addition agent must have x-ray sensitivity equivalent to that of material being determined in the unknown. In the present case the unknown material was much more sensitive, possibly because of overgrowths (seen in petrographic examination).*

Clay (illite) was not detectable in the dolomite. However, it was possible to measure it quantitatively by x-ray diffraction on the insoluble residues and back calculate to whole rock percentages. Illite was detectable at 2-theta values of 8.84° and 19.8°.

In summary, the Al content is judged the best measure of the dissolved feldspar content of the dolomite (wt.% Al x 10.3 - wt.% feldspar). X-ray analysis of the insolubles showed a slightly greater amount of feldspar undissolved (60%). Quartz impurity is equated to insoluble residue less feldspar and illite (Table 4), and calcite is determined by chemical or X-ray diffraction analysis (Figure 8). However, the latter requires a CO_2 analysis as % calcite - $2(Ca\text{-}Mg)/CO_2$ x 100 where elemental symbols represent equivalents.

RESULTS

Analyses for the major ions are summarized in Table 1. The acid soluble portion of the samples is generally in the 75-100% range with the BD series being the most soluble, generally over 90%. The acid insoluble residue was analyzed by x-ray diffraction on several samples (Table 4) and was primarily quartz with minor amounts of clay (illite) and potassium feldspar. The soluble portion was in general nearly pure dolomite. The purity can be determined from the empirical formulas for the soluble portion shown in Table 1 where the Ca/CO_3 and Mg/CO_3 equivalent ratios are near 0.5, the theoretical value for dolomite, $CaMg(CO_3)_2$. Also, the analyses correspond well to that of a Bureau of Standards dolomite sample. The PO_4^{3-}, SO_4^{2-} and Cl^- contents are mostly very low indicating little or no residual phosphate or evaporite minerals (NaCl, $CaSO_4$). Apparently these have been weathered out of the deposits.

In Table 2 the minor and trace element contents of the various dolomite samples are summarized. In Table 3 the average analysis of the samples is compared to that found previously in the nearby limestone strata. Fe, Mn and Al tend to be higher in concentration in the dolomite but Zn and Cu contents are low and about the same as in the limestone units.

Dolomite is a host rock in northern Arkansas for Pb-Zn ores (McKnight, 1935). It is of interest that the nonmineralized units of dolomite of the present study which are near mineralized areas have low concentrations of the ore metals and presumably were not a primary source of the metals which might have been concentrated down dip as one theory suggests (McKnight, 1935). The Mg^{++} ion which is thought to help the substitution of other metals into limestone has been of no particular aid in these dolomites for the introduction of heavy metals.

Figure 3 indicates that in the case of K, Rb, and Al these elements are in the insolubles. Because the insolubles are mainly quartz with minor illite and feldspar this is a fortuitous relationship and is really indicative of a correlation between the quartz and feldspar contents, with the latter mineral being the source of K^+, Rb^+, and Al^{+++}. All three of these ions are size and charge misfits for the dolomite lattice and this is indicated by Figure 3, no K, Rb, or Al at zero insoluble residue. This same situation obtained in the limestone units where these same ions are misfits in the calcite lattice (Wagner, et al., 1979).

Figure 4 shows the linear relationship between the amount of quartz and Al in the dolomites. Evidently those conditions favoring quartz also favored the entry of feldspar into the dolomites. Illite is not considered a source of these metals because of the low concentration in the dolomite and because clays are only slightly attacked by the acids used here (Cains, 1980).

Figure 5 shows the relationship between Al and the elements Fe, Mn, K and Rb for the Mon series of samples. Fe shows a rough linear relationship with Al; Mn shows no relationship to Al; whereas, K and Rb show a rather precise linear relationship. The 2/3 slope of the K vs Al plot in Figure 5 equates to 0.5 K per Al on an equivalent basis and suggests that a feldspar is present in the dolomite with the formula $K_{0.5}B_{(1-0.5)}AlSi_3O_8$, where B is probably a mixture of Na and Ca (there is not quite enough Na). Potassium feldspar is an impurity in many Ordovician and Cambrian carbonate rocks (Hearn and Setter, 1985).

TABLE 3

Minor and Trace Elements of Mississippian Limestone Units Compared to Ordovician Dolomite Units

Unit	wt.%		ppm of HCl Solubles								
	HCl Solubles	Mg	Fe	Mn	Al	Sr	K	Na	Li	Zn	Cu
Boone Ls* (4 Sites)	99.4	0.116	361	173	38	107	3	64	1.1	20	1
St. Joe Ls* (7 Sites)	96.0	0.291	1190	791	221	170	57	69	1.2	12	2
Ordovician Dolomites**											
Site I average	89.2	12.6	2680	383	249	76	139	139	1.7	1	0
Site II average	87.1	12.7	2114	340	397	87	182	181	1.8	34	1
Site III average	79.8	12.5	3496	206	1525	114	985	251	5.9	13	5

* Wagner et al., 1979

** Site I (Lower Powell and Upper Cotter Formations); Site II (Upper Cotter and Powell Formations); Site III (Upper Cotter and Powell Formations)

TABLE 4

Mineral Impurities in Selected Dolomite Samples

Sample	wt% of whole rock					
	A Illite[a]	B Quartz[a]	C Feldspar[b]	D Calcite[c]	A+B+C+D	Dolomite
BD-1	0.06	2.6	0.35	0.90	3.91	96.1
BD-2	0.22	10.1	1.06	ND	11.4	88.6
BD-6	0.06	0.95	0.25	ND	1.26	98.7
BD-9	0.13	2.8	0.43	ND	3.36	96.6
BD-11	0.47	4.8	0.85	ND	6.12	93.9
R-281-1	0.11	10.3	0.76	ND	11.2	88.8
R-281-3	0.45	20.9	1.84	ND	23.2	76.8
R-281-4	0.30	4.1	0.92	1.8	5.32	94.7
R-281-6	0.17	7.4	1.05	ND	8.62	91.4
Mon-0	0.45	9.67	1.74	ND	11.9	88.1
Mon-27	0	22.4	3.39	ND	25.8	74.2
Mon-34	0.29	4.16	1.63	ND	6.08	93.9
Mon-84	0.54	20.8	3.21	ND	24.6	75.4
Mon-95	0	12.4	3.91	ND	16.3	83.7
Mon-106	0.87	22.1	6.18	0.5	29.8	70.3

a. Determined from x-ray analysis of acid insolubles. Assumed none dissoved.

b. Determined from x-ray analysis of insolubles plus amount dissolved (10.3 x % Al). For the BD and R-281 samples 46% of the feldspar was dissolved on average. For the Mon samples 35% was dissolved on average.

c. Determined from x-ray analysis of whole rock. ND = none detected. The following additional samples contained calcite (wt%): BD-10 (14.6%), BD-4a (0.6%), BD-3 (6.3%), BD-11a (0.8%), R-281-4 (1.8%), Mon-106 (0.5%), Mon-52 (1.9%), Mon-47 (0.5%), Mon-43 (0.3%), Mon-20 (1%). Other samples did not have detectable amounts.

TABLE 5

Principal X-Ray Lines of Dolomite Samples
(using Cu-K alpha line)

Sample	Relative Intensities (I/Io), %						
	31.0°	33.6°	37.4°	41.2°	45.1°	50.6°	51.1 - 51.3°
ASTM 11-78*	100	10	10	30	15	20	30
BD-2	100	3	7	15	8	10	14
BD-3	100	5	6	15	7	9	10
BD-6	100	6	4	13	7	9	10
BD-11	100	4	4	13	7	9	9
R-281-4	100	3	5	15	12	9	13
R-281-6	100	3	4	14	5	9	9
Mon-12	100	6	5	16	9	10	15
Mon-34	100	3	4	14	6	6	9
Mon-42	100	5	8	20	12	35	18
Mon-103	100	5	5	14	9	12	13
Mon-118	100	5	6	16	9	9	14
Mon-20**	100	8	10	37	16	14	21

* standard dolomite sample
** A slab, all other samples powders

Figure 6 shows the relationship of Al to K and Rb for the BD and R-281 series. On a weight basis the Rb/Al ratio is 0.10; the K/Al ratio is 0.2-0.33 compared to 0.66 for the Mon series. The Mon series has both more feldspar and more K in the feldspar than the other series of samples.

Table 5 summarizes the purity of some selected dolomite samples. These samples were selected because their acid insoluble residues were analyzed by x-ray diffraction for illite, quartz and feldspar while the whole rock was analyzed for calcite by x-rays and the soluble portion chemically for feldspar. Thus, a total rock analysis is available. The average amount of the feldspar dissolved in the acid treatment was 40% of that originally in the dolomite.

X-ray diffraction analyses were run on all the dolomite samples. No clay lines were detected in any samples because of the small amount present but illite was detected in the acid insoluble residues (Table 4). Feldspar was detected in nearly all dolomite samples. Peaks for dolomite corresponded to literature values for 2-theta but secondary line intensities were lower usually than the literature values. This situation is shown in Table 5 where the x-ray diffraction pattern for some selected samples are compared to the ASTM standard. The reason for the low intensities of the secondary lines is probably related to the fineness or impurities of the sample.

All field and powdered samples were examined for fluorescence under ultra violet light. Several fluorescent powdered samples were found and generally these were high in calcite or Mn content. The corresponding field samples showed calcite crystals in fractures. Calcite containing Mn is known to fluoresce. This fluorescence is a rapid method of detecting sizable calcite crystalline domains in dolomite.

ADDITIONAL RESEARCH

Other dolomite deposits in the vicinity of lead zinc ores should be examined for heavy metal content. Dolomite intimately associated with lead-zinc ores should be among those examined and differentiation of metal in lattice and metal in mineral should be made using the methods outlined in Wagner et al. (1979). Such data would help in determining if the dolomite lattice, due to its Mg content, is a favorable host for heavy metals.

REFERENCES

American Public Health Association, 1971, Standard Methods for the Examination of Water and Waste Water, 13th ed., Am. Public Health Assoc., Washington, D.C.

Cains, W. T., 1980, Geochemical investigation of stream sediments in mineralized areas of central Arkansas, unpublished M.S. Thesis, University of Arkansas, Fayetteville.

Diebold, F. E., J. Lemish and C. L. Hiltrop, 1963, Determination of calcite, dolomite, quartz and clay content of carbonate rocks, Jour. Sed. Petrology, 33, 82-98.

Freeman, T., 1966, Petrology of the post-St. Peter Ordovician, northern Arkansas. Tulsa Geol. Soc. Digest, 34, 82-98

_____, "Petrographic" unconformities in the Ordovician of Northern Arkansas, Okla. Geol. Notes, 26, 21-28.

Handford, C. R. and C. H. Moore Jr., 1976, Diagenetic implications of calcite pseudomorphs after halite from the Joachim dolomite (middle Ordovician), Arkansas, Jour. Sed. Petrology, 46, 387-392.

Hearn, P. H. Jr. and J. F. Sutter, 1985, Authigenic potassium feldspar in Cambrian carbonates: evidence of Alleghanian brine migration. Science, 288, 1529-1532.

McKnight, E. T., 1935, Zinc and lead deposits of northern Arkansas. U.S. Geol Surv. Bull., 853, U.S. Government Printing Office, Washington, 311 p.

Royse, C. F., Jr., J. S. Wadell and L. E. Petersen, 1971, X-ray determination of calcite-dolomite: an evaluation, Jour. Sed. Petrology, 41, 483-488.

Runnells, D. D., 1970, Errors in x-ray analysis of carbonates due to solid solution variation in composition of component minerals, Jour. Sed. Petrology, 40, 1156-1166.

Shiparo, L., 1978, Rapid analysis of silicate, carbonate, and phosphate rocks-revised edition, Geol. Surv. Bull. 1401, U.S. Government Printing Office, Washington, 76 p.

Siegel, F. R., 1967, Properties and uses of the carbonates in: T.V. Chilingar, H.J.G. Bissell and R. W. Fairbridge (editors), Carbonate Rocks, Physical and Chemical Aspects (Developments in sedimentology 9B), Elsevier, New York, 413 p.

Wagner, G. H., R. H. Konig, D. A. Smith, K. F. Steele, and D. L. Zachry, 1979, Geochemistry of Carboniferous limestone units in northwest Arkansas, Chem. Geol. 24, 293-313.

INITIAL NATURAL GAS DISCOVERIES FROM THE PALEOZOIC ROCKS OF NORTHERN ARKANSAS

By William M. Caplan
Arkansas Geological Commission
3815 West Roosevelt Road
Little Rock, Arkansas 72204

The commercial production of natural gas from Paleozoic rocks in Arkansas is limited to the Ozark region and the Arkansas Valley (Figure 1). For the purposes of this article, the Ozark region and the Arkansas Valley are grouped under the term "northern Arkansas." With a few exceptions, the gas is dry, sweet, high in methane, low in nitrogen, and has a heating value of about 1000 Btu per cubic foot.

The discovery wells are presented primarily in chronological order, but some exceptions have been made in order to qualify the discovery.

Pennsylvanian Discoveries

The first well in Arkansas to produce gas commercially from the Paleozoic was completed in 1902 in the Arkansas Valley region, now known also as the Arkansas portion of the Arkoma basin. The well was drilled in Sebastian County near the town of Mansfield, from which the field name was taken. The discovery well was the Choctaw Oil and Gas Company No. 2 Duncan, Lot 7, sec. 1, T.4N., R.31W. (Table 1). The well was drilled to a total depth of 1125 feet and had an initial production of 960,000 cubic feet of natural gas per day

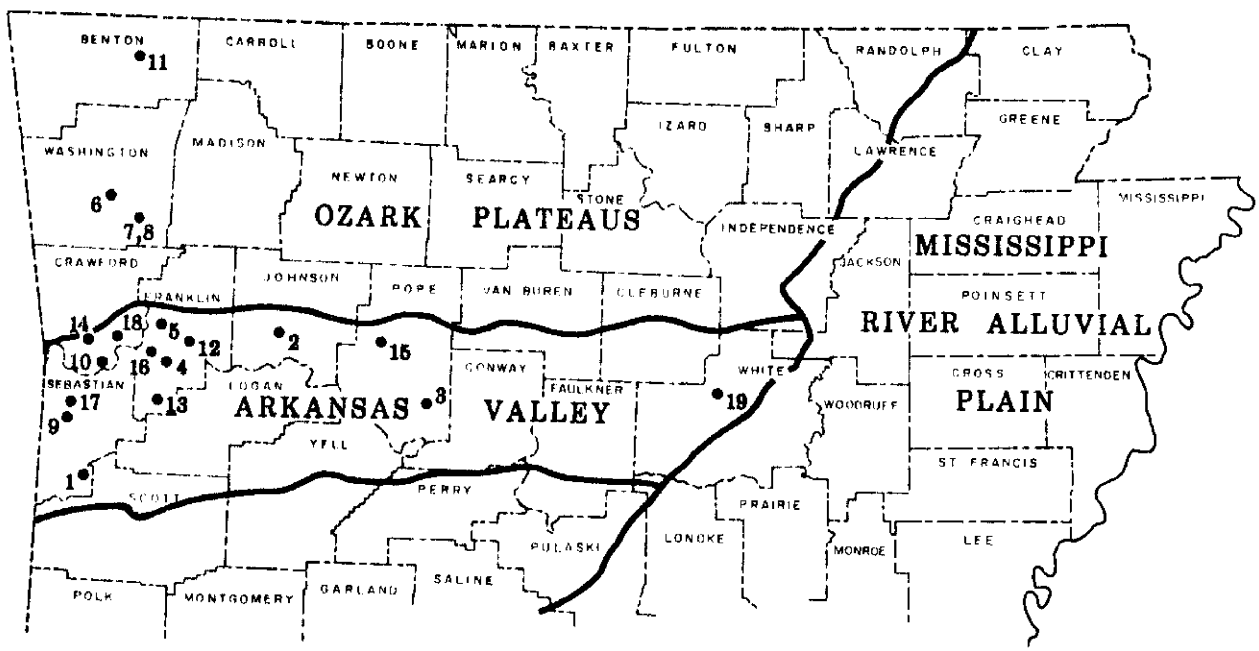

Figure 1. -- *Map showing major physiographic provinces and location of discovery wells discussed in text.*

TABLE 1 - LIST OF REFERENCE WELLS

Map No.	Name	Location	County	Initial Discovery
1	Choctaw O&G No.2 Duncan	1-4N-31W	Sebastian	Atoka
2	Arkansas Louisiana Gas No. 1 Hudson	15-10N-24W	Johnson	Kessler & Brentwood
3	Whitmar Exploration No. 3-28 Roetzel	28-8N-18W	Pope	Brentwood
4	Arkansas Louisiana Gas No. 1 Barton	27-9N-28W	Franklin	Hale
5	Arkansas Western Gas No. 1 Parsley	15-10N-28W	Franklin	Wedington
6	Arkansas Western Gas No. 1 Threlkeld	5-14N-30W	Washington	Sylamore
7	Arkansas Western Gas No. 1 Goad	20-14-29W	Washington	Wedington
8	Arkansas Western Gas No. 1 Harmon	20-14-29W	Washington	Wedington
9	Shell Oil No. 1 Western Coal & Mining	36-7N-32W	Sebastian	St. Clair
10	Stephens Production No. 1 Fontaine	32-9N-30W	Crawford	Boone & Penters
11	Arkansas Western Gas No. 1 Douglass	18-20N-29W	Benton	Everton or Arbuckle
12	Arkansas Western Gas No. 1 Montgomery	33-10N-27W	Franklin	Kimmswick
13	Arkla Exploration No. 1 Turner	3-7N-28W	Franklin	Kimmswick
14	Diamond Shamrock No. 1 Van Matre	12-9N-31W	Crawford	St. Peter
15	Ferguson Oil No. 1 Brigham	33-10N-20W	Pope	St. Peter
16	Arkla Exploration No. 1 Ark. Valley Trust Co.	19-9N-28W	Franklin	Pitkin
17	Texas Oil & Gas Corp. No. 1 Robison	13-7N-32W	Sebastian	Pitkin
18	Diamond Shamrock No. 1 King	1-9N-30W	Crawford	Everton
19	Moran Exploration No. 1 Reaper	12-8N-8W	White	Arbuckle

from the Pennsylvanian Atoka Formation (Figure 2). The well was in Atoka at total depth. The Atoka Formation continues to the present time to be the youngest and most prolific Paleozoic gas-producing formation in northern Arkansas.

From 1902 until 1944 nineteen additional dry gas fields, all Atoka producers, were discovered in the Arkansas Valley. During 1944 the first pre-Atoka production in the Valley was found in Clarksville field, Johnson County, which had produced Atoka gas since 1921. The new gas production, from the Bloyd Formation of the Pennsylvanian Morrow Group, was found in the Arkansas Louisiana Gas Company No. 1 S. M. Hudson, 15-10N-24W. The two Bloyd zones from which the gas was produced were the Kessler Member and the Brentwood Member. The top of the former was at 3402 feet and the top of the latter at 3560 feet. Thirty-foot zones were perforated in each member. A combined initial potential of 3,500 MCFGD was reported. The well was in Lower Ordovician Cotter Dolomite at total depth of 6135 feet.

Wells with good initial gas potentials from the Brentwood continue to be reported occasionally. The most recent is the Whitmar Exploration No. 3-28 Roetzel, 28-8N-18W, completed January 26, 1987, in the Oak Grove field, Pope County. The calculated open flow rate was 20,511 MCFGD from 6437-66 feet, after fracture treatment. The well bottomed at 6800 feet in the Hale.

In 1949 the Arkansas Louisiana Gas Company No. 1 Ralph Barton, 27-9N-28W, Franklin County, opened Cecil field with the first commercial production of gas from the Pennsylvanian Hale Formation of the Morrow Group. The discovery well produced dry gas at the rate of 7,000 MCFGD through perforations from 4850 to 4930 feet. The well was in the Middle Ordovician Everton Formation at total depth of 6650 feet.

PERIOD	FORMATION
Pennsylvanian	Atoka Formation ☼
Pennsylvanian Morrowan Series	Kessler Ls Mbr ☼
	Bloyd Formation
	Brentwood Ls Mbr ☼
	Hale Formation ☼
Mississippian	Pitkin Limestone ☼
	Fayetteville Shale
	Wedington Ss Mbr ☼
	Batesville Formation
	Moorefield Formation
	Boone Formation ☼
	St Joe Ls Mbr
Devonian	Chattanooga Shale
	Sylamore Ss Mbr
	Clifty Formation
	Penters Chert ☼
Silurian	Lafferty Limestone
	St Clair Limestone ☼
	Brassfield/Cason
Ordovician (upper)	Cason Formation
	Fernvale Limestone
Ordovician (middle)	Kimmswick Limestone ☼
	Plattin Limestone
	Joachim Formation
	St Peter Sandstone ☼
	Everton Formation ☼
Ordovician (lower)	Powell Dolomite ☼
	Cotter Dolomite

Figure 2 - *Stratigraphic chart of the Paleozoic rocks of the Arkansas Valley and the Arkansas Ozarks. The units that have yielded natural gas in northern Arkansas are indicated.*

Pre-Pennsylvanian Discoveries

The first pre-Pennsylvanian commercial gas completion in Arkansas was made during 1951, also in Franklin County. The discovery well, the Arkansas Western Gas Company No. 1 Parsley, 15-10N-28W, produced gas from the Wedington Sandstone Member of the Mississippian Fayetteville Shale. The Parsley well had a calculated open flow of 2,000 MCFGD through perforations from 3782-3814 feet. The formation at total depth of 3896 feet was Fayetteville Shale.

The fact that the Parsley well was producing from the Mississippian was not apparent initially, and the well was completed merely as a deeper producer representing a one-mile eastern extension to Lone Elm field, which had been opened by Pennsylvanian production in 1950.

In 1953 the first commercial Devonian production was established in the state, when West Fork field was opened in Washington County, in the Ozark region. The discovery well, the Arkansas Western Gas Company No.1 Threlkeld, 5-14N-30W, reportedly produced gas from the Sylamore Sandstone Member of the Chattanooga Shale. A calculated open flow of 1,500 MCFGD was the reported potential from the open hole interval 566 feet to the total depth of 586 feet.

During 1959 an additional Wedington gas supply was established in northern Arkansas by the opening of Brentwood field, also in Washington County. The discovery well, the Arkansas Western Gas Company No.1 Goad, 20-14N-29W, had an initial potential of 460 MCFGD from open hole between 565 feet and the total depth of 650 feet. Several months later the Arkansas Western No.1 Harmon, also in 20-14N-29W, yielded Wedington gas at a rate of 450 MCFGD from open hole between 757 feet and total depth of 1450 feet. However, the two-well field was abandoned in 1967, without having been produced commercially. The gas was reported to be relatively wet in comparison with gas found in the Arkansas Valley. Brentwood field usually is cited as the Wedington gas discovery field because of the confusion mentioned above regarding the Parsley well, the 1951 Lone Elm field extension well in Franklin County.

During 1962 the first Silurian production in Arkansas was realized with the opening of Bonanza gas field in Sebastian County. The discovery well was the Shell Oil Company No. 1 Western Coal and Mining Company, 36-7N-32W. The well produced at a rate of 9,400 MCFGD from 7936-58 feet in the St. Clair Formation, which is the Arkansas correlative of the Silurian Hunton. Some geologists are of the opinion that the well just touched Precambrian basement at the total depth of 10,924 feet. Others believe the well was still in rocks of Late Cambrian age.

This well had what may be the first valid, substantial show of gas in Arkansas from the Powell Dolomite of Early Ordovician age, which is considered by most Arkoma geologists to be the uppermost Arbuckle-Knox-Ellenburger correlative in Arkansas. The post-Powell Black Rock-Smithville Formations, however, may occupy that position locally in parts of northeastern Arkansas.

In the No.1 Western Coal and Mining well, Shell reported an initial flow of 2,400 MCFGD, with water from the Arbuckle at 8,928 feet, which is 37 feet above the base of the Powell Dolomite. The gas flow eventually decreased to a reported 150 MCFGD. Upon completion, only the gas from the Silurian was reported as commercial.

Later in 1962 the first commercial gas production in the state from both the Mississippian Boone and Devonian Penters formations was achieved in Kibler field, Crawford County, in the Arkansas Valley region. Previously, Kibler field had produced only Pennsylvanian gas since the field was opened in 1915. The well in which the Boone and Penters formations reportedly produced dually was Stephens Production Company No. 1 Fontaine, 32-9N-30W. Calculated open flow from Boone perforations at 5755-75 feet was 2,450 MCFGD. The Penters had a calculated open flow of 7,500 MCFGD through perforations at 5922-34 feet and 5945-54 feet. The Penters is the Arkansas correlative of the Devonian Hunton.

During 1967 Tucks Chapel field was opened in Benton County, in the Ozark region, by an Ordovician gas discovery in the Arkansas Western Gas Company No. 1 Douglass, 18-20N-29W. The open flow potential was reported to be 200 MCFGD, through perforations at 344-89 feet, from either Everton or Arbuckle rocks. The operator first favored the former, then the latter. The one-well field was abandoned in 1968 without having been produced.

Also in 1967 a triple gas producer in Cecil field, Franklin County, yielded Ordovician gas in addition to the dual Atoka production. The Ordovician production in the well, the Arkansas Western Gas Company No. 1 Montgomery, 33-10N-27W, was attributed to rocks of Viola age, a sequence which is post-St. Peter Sandstone (Kimmswick) in age. The calculated open flow through perforations at 5614-24 feet was 4,000 MCFGD.

A subsequent well, the Arkla Exploration Company No. 1 Turner, 3-7N-28W, completed in 1980 in Franklin County, also yielded Viola (Kimmswick) gas in a dual completion with the Hale Formation. The Viola produced through perforations between 9797-9808 feet. The calculated open flow was 49,670 MCFGD. The initial potential, flowing, was 5,061 MCFGD. The well provided a new pay for the Peter Pender field. Also, this became the deepest producer, from the footage standpoint rather than the stratigraphic standpoint, in northern Arkansas.

During 1968 the first commercial production in the state from the Middle Ordovician St. Peter Sandstone was reported. The gas was found in the Diamond Shamrock No. 1 Van Matre, 12-9N-31W, Hollis Lake field, Crawford County. The calculated open-flow potential, through perforations at 3981-4004 feet, was 2,250 MCFGD.

An interesting although non-productive test involving the St. Peter Sandstone had been drilled in 1966. The well was the Ferguson Oil No. 1 Brigham, 33-10N-20W, Booger Hollow field, Pope County, It was abandoned at 6317 feet in Ordovician rocks of possible Cotter age. The well initially flowed about 7,000 MCFGD from the St. Peter on drill-stem test at intervals between 5350-5466 feet. The flow subsequently dropped to about 100 MCFGD or less, and salt water. The St. Peter section in the well was described as having an upper gas sand underlain by an oil sand, both of which exhibited low porosity. The oil sand, in turn, was underlain by a 5-or 10-foot water sand. The well yielded a smoky gas flare. In addition to the St. Peter gas show, a 20-foot section in the interval 5650-4700 feet, thought to be in the Everton Formation, yielded a small quantity of gas.

The first commercial gas production from the Mississippian Pitkin Limestone is generally considered to have been from the Arkansas Louisiana Gas Company (Arkla Exploration) No. 1 Arkansas Valley Trust Company, 19-9N-28W, Cecil field, Franklin County. The well was completed January 1, 1969, as a triple gas producer. Two of the zones were in the Atoka, the third was in the Pitkin. The latter had a calculated open flow of 319 MCFGD through perforations from 4610-14 feet. The well bottomed in the Precambrian at 8638 feet.

Some geologists, however, consider the first commercial Pitkin production to have been from the Texas Oil and Gas Corporation No. 1 Robison, 13-7N-32W, in the Bonanza field, Sebastian County. Completed February 25, 1981, the well was a dual Atoka and Pitkin producer. The latter had a calculated open flow of 100 MCFGD through perforations between 7188 and 7202 feet. The well bottomed in the Hunton at 7745 feet.

In late 1969 a gas well completed in Kibler-Williams field, Crawford County, was reported to be producing from rocks of Ordovician Simpson age. The Diamond Shamrock No. 1 King, 1-9N-30W, had a calculated open flow of 3,000 MCFGD from three zones within a perforated interval from 6221-6390 feet overall. It is possible that at least part of the gas was coming from rocks of Everton age. If so, this probably would be the first commercial Everton production in the state, based on the questionable gas-yielding interval in the Arkansas Western No. 1 Douglas, Benton County, as noted in an earlier paragraph.

On December 3, 1981 the Moran Exploration No. 1 Reaper, 12-8N-8W, White

County, was finaled as the discovery well of Letona field. The operator reported a calculated open flow of 740 MCFGD from 6634-44 feet, in the Arbuckle Group (lower Ordovician and Cambrian units immediately underlying the Everton Formation). If this was, in fact, Arbuckle production as reported, it was the first commercial gas production from this group in Arkansas. Also, this was the easternmost gas production in northern Arkansas. The Reaper well was connected to the Arkansas Louisiana Gas Company gathering system, but was abandoned after producing for about nine months.

REFERENCES

Bacho, A. B., Jr., 1962, Pre-Pennsylvania is good target: Oil and Gas Journal, v. 60, no. 19, May 17, p. 161-167.

Caplan, William M., Oil and gas developments in Arkansas: Annual reports 1953-1981, inclusive, Tulsa World Newspaper.

Caplan, William M., 1957, Subsurface geology of northwestern Arkansas: Arkansas Geol. and Conserv. Commission, Info. Circular 19, 14p.

Frezon, S. E., and Glick, E. E., 1959, Pre-Atoka rocks of northern Arkansas: U.S. Geological Survey Prof. Paper 314-H, p. 171-189.

Haley, Boyd R., 1965, Geologic formations penetrated by the Shell Oil Company No. 1 Western Coal and Mining Co. well on the Backbone anticline, Sebastian County, Arkansas: Arkansas Geological Commission, Info. Circular 20-D, 17p.

Lantz, Robert J., 1950, Geological formations penetrated by the Arkansas-Louisiana Gas Company No. 1 Barton well on the Cecil anticline, Franklin County, Arkansas: Arkansas Resources and Development Commission, Bulletin 18, 26p.

Maher, J. C., and Lantz, R. J., 1953, Correlation of pre-Atoka rocks in the Arkansas Valley, Arkansas: U.S. Geological Survey Oil and Gas Inv. Chart OC-51.

OVERVIEW OF NATURAL GAS PRODUCTION WASHINGTON AND MADISON COUNTY, ARKANSAS

By J. A. McEntire III
Little Rock, Arkansas

HISTORY OF THE AREA

The Threkeld #1 well drilled by the Arkansas Western Gas Company in 1953 at West Fork in Washington County, recorded the first natural gas commercially produced in northwest Arkansas. The two active wells in this field have produced in excess of 1.1 BCF.

Exploration was sporadic for some twenty-four years because of a limited commercial gas market. A second field at Huntsville was discovered and brought into production in 1977. This was followed by the discovery of the Brentwood field in 1978, the Hazel Valley field in 1981, and the Wedington field in 1984.

Between August 1985, when the Baldwin field was discovered, and the present time, nine new fields have been discovered in northwest Arkansas.

An increase in drilling activity in the last few years has been brought about because of an increased demand for gas in this area of northwest Arkansas and because of favorable gas purchase contracts from the local utility. Figure 1 shows the location of producing gas fields, developing fields, and new discoveries in Washington and Madison counties. The pipeline gathering and distribution system is also shown. The explanation at the bottom of the figure shows the cumulative production from each field.

REGIONAL GEOLOGY

The area of interest is located on the Northern Arkansas structural platform. The regional dip is to the south at less than 1 degree. Minor structure is present on the platform, but occasional folds, faults, and subsidence structures are present locally. Structural features are predominantly northeast/southwest trending. The Precambrian basement is overlain by about 2,000 feet of Cambrian through Pennsylvanian age, mostly shallow marine, sedimentary rock. The platform is bounded on the north by the Ozark uplift and by the Arkoma basin to the south.

Anticlinal structures associated with faulting appear to be the primary controlling factor in the accumulation and production of natural gas in the producing fields from pre-Mississippian age formations. Local variation in permeability and porosity controls production in individual wells.

A tectonic map of northwest Arkansas is shown in Figure 2. The location of existing gas fields and their position relative to mapped structures is shown. The two major northeast trending structures known as the Fayetteville fault structural lineament and the Drakes Creek fault structural lineament are highlighted. Their extension into the Arkoma Basin is shown. Both of these features extend for over 50 miles.

PRODUCING ZONES

The primary producing zones are from sandstone found in the St. Peter and the Sylamore Formations. The St. Peter Formation is Middle Ordovician in age. Subsurface samples show it to be a fine to medium grained, clean, white, quartz sand. Individual grains are well rounded and frosted. The Sylamore Formation is Mississippian-Devonian, in age. Subsurface samples show a fine to coarse-

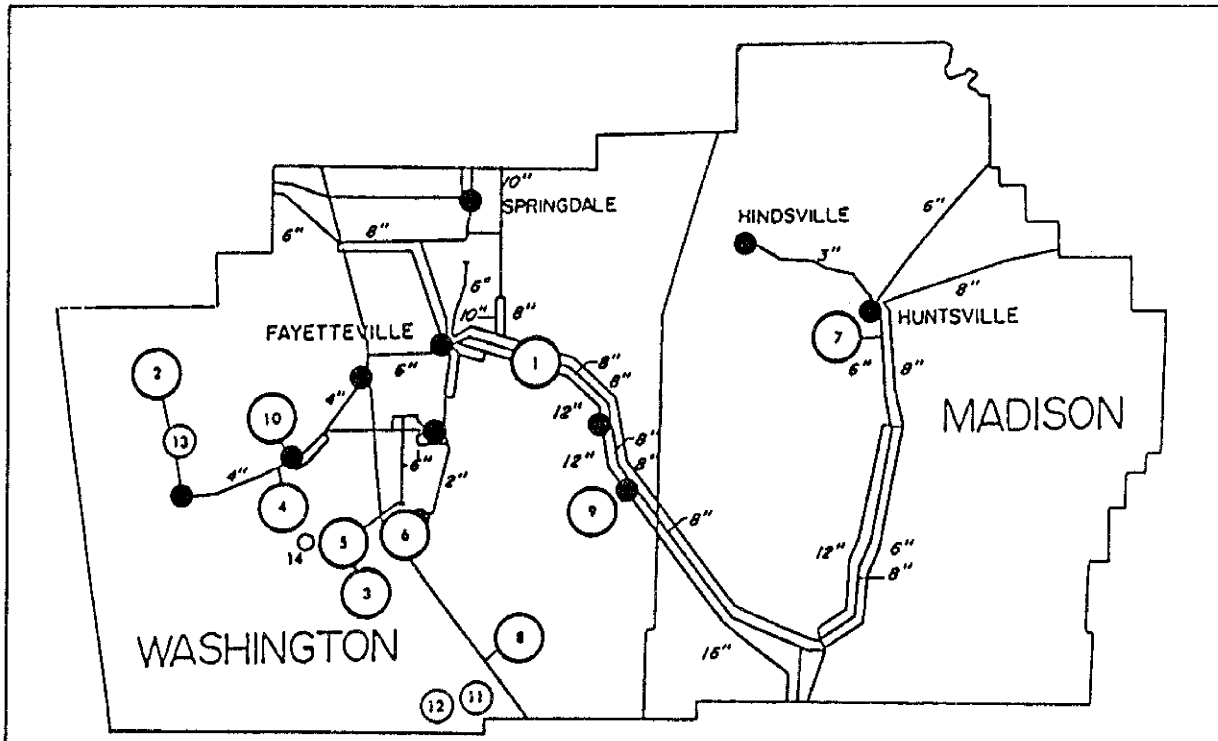

Location Number		Producing Gas Fields	Production Dates	Cumulative Production MCF
1		Baldwin	8/85 - 3/87	788,253
2		Wedington	12/84 - 5/87	438,375
3		Hardt	12/87 -	--
4		Blair Creek	1/88 -	--
5	○	Friendship Church	3/87 - 12/87	81,000
6		West Fork	6/53 - 3/87	1,189,472
7		Huntsville	1/77 - 3/87	745,345
8		Brentwood	4/78 - 3/87	1,738,744
9		Hazel Valley	11/81 - 3/87	470,554
10		Goose Creek	9/85 - 3/87	196,900
		Developing Fields Not In Production	**Discovery Date**	**Discovery well IP Rate - MCF**
11		Sugar Tree Hollow	4/87	250
12	○	Signal Hill	8/87	150
13		High Ocean	12/85	100
		Recent Discovery		
14	○	Blue Ridge	12/87	1000

Figure 1. *Gas fields and pipeline system of Washington and Madison Counties, Arkansas.*

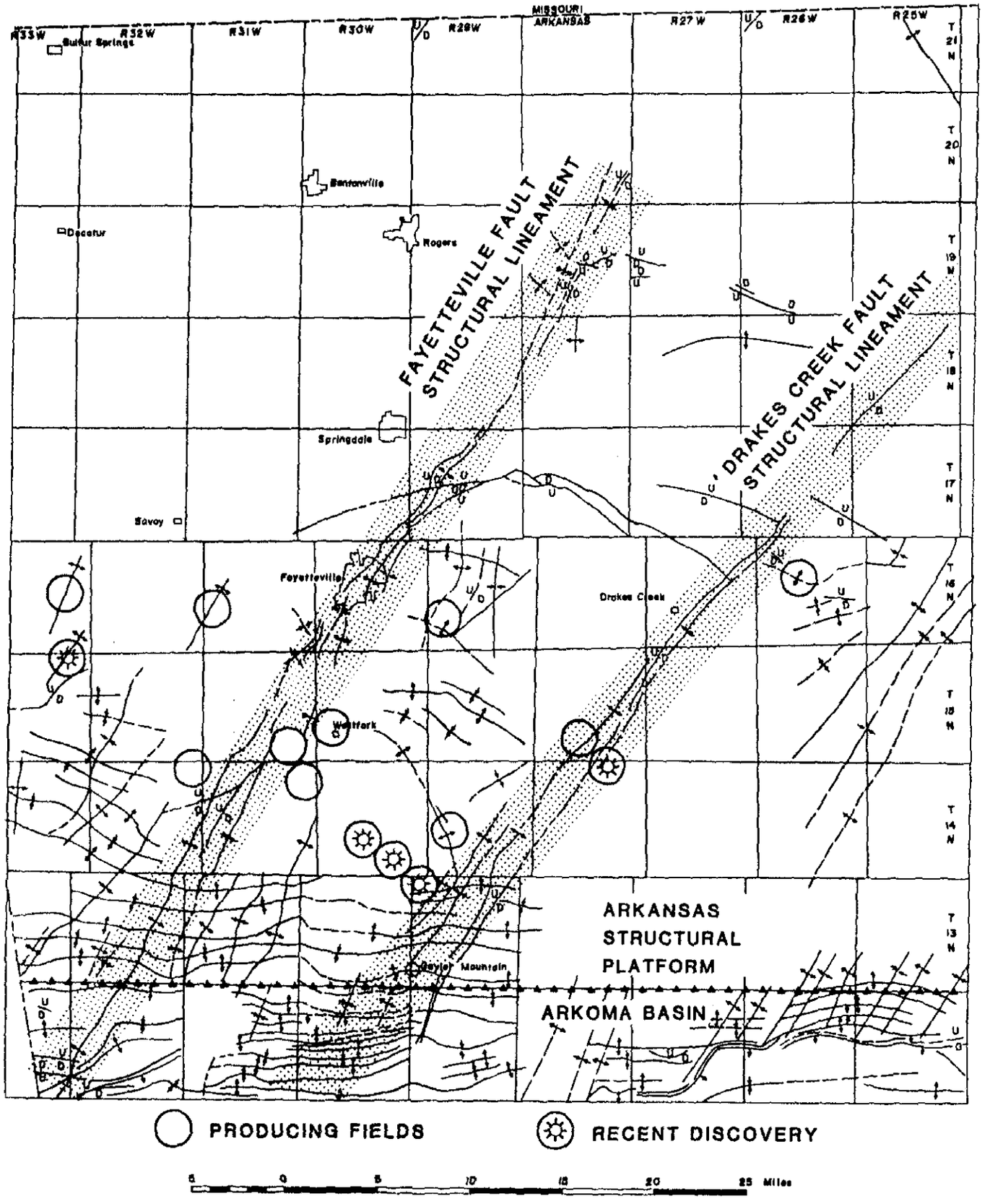

Figure 2 – *Generalized tectonic map of northwest Arkansas. Modified from Chinn & Konig (1973).*

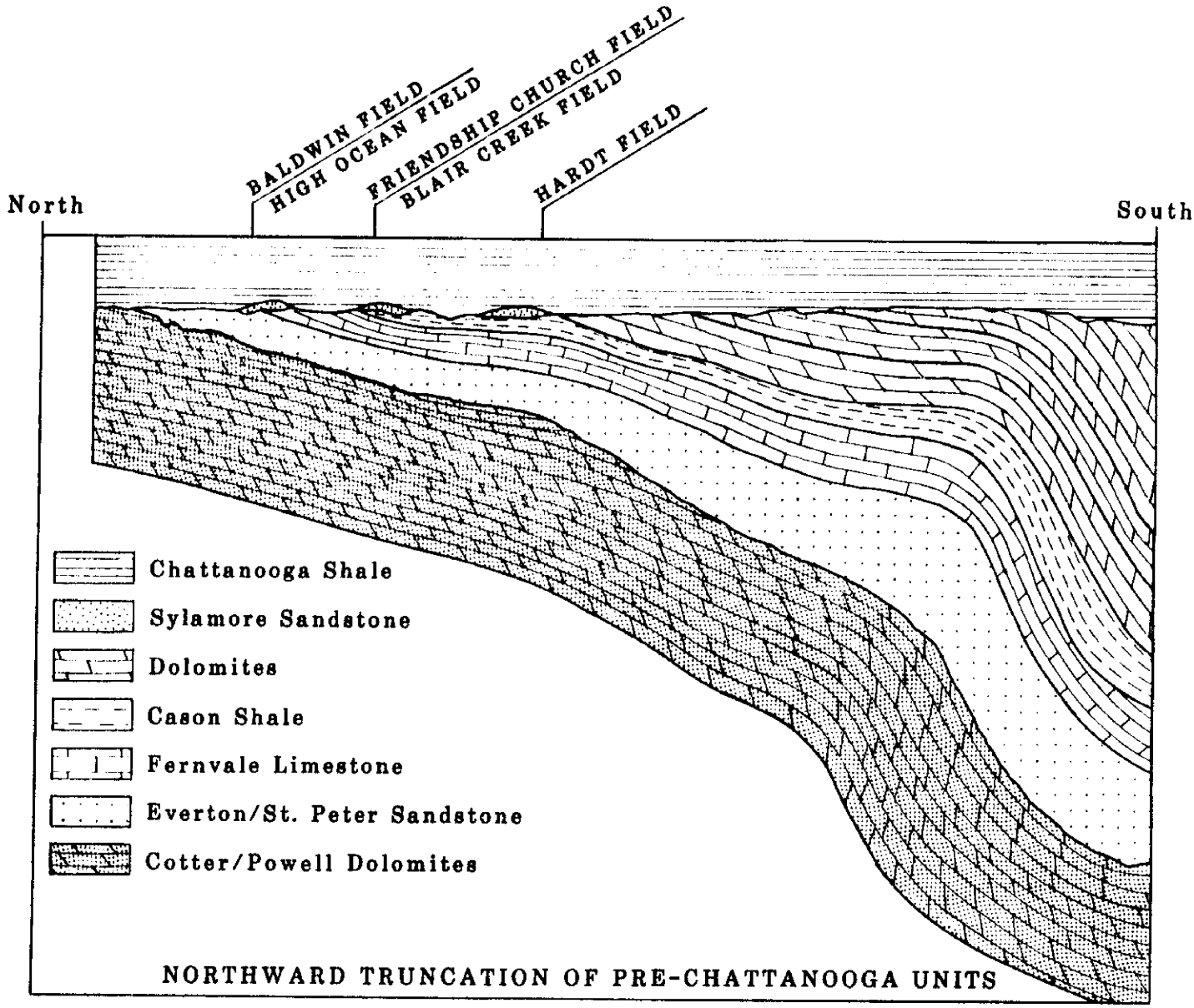

Figure 3 - *Idealized cross section showing the regional unconformity at the base of the Sylamore Sandstone Member of the Chattanooga Shale.*

grained sand with brown to white coloration. Minor shale stringers occur in the formation.

The Sylamore appears to be a transgressive unit and may have been deposited in the form of an offshore bar. This may help to explain the discontinuous nature of the deposit. Its base marks a regional truncating unconformity and it overlies units from Middle Devonian-Middle Ordovician age. The relationship between the St. Peter and Sylamore Formation and the truncating unconformity is shown in the cross section in Figure 3. Figure 4 shows a subcrop map of the pre-Sylamore Unconformity and the location of natural gas fields producing from St. Peter and Sylamore Formations.

The St. Peter and Sylamore "sands or sandstones" are productive on structural highs that are often found associated with faults and where secondary cementation is minor. Wells completed in these "sands or sandstones" usually have initial production (IP) rates from 50 to 1,000 MCFD. Rates as high as 3,000 MCFD have been reported.

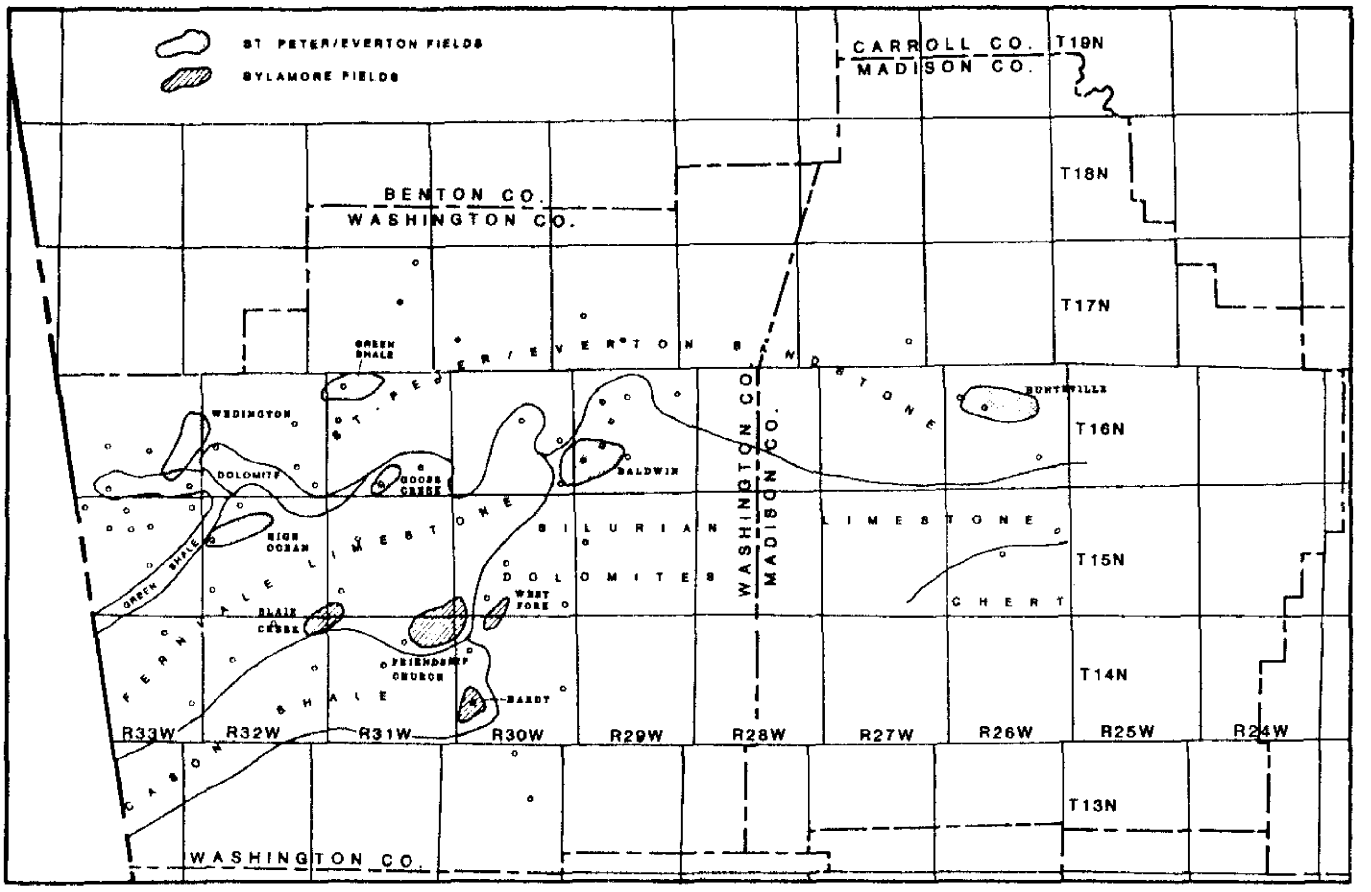

Figure 4 - *Subcrop map of pre-Sylamore Member of the Chattanooga Formation in northwest Arkansas showing location of natural gas fields. (After Robert Liner.)*

The Boone Formation is Mississippian in Age and represents a secondary target zone in the area. The Boone is dominantly a gray fossiliferous limestone interbedded with blue to light gray, dense chert. At this time it is not known if production from the Boone Formation is from primary, secondary, or fracture porosity. Within the area of interest, Boone production has been found from two wells in the Friendship Church field and one well in the Hardt field. (Figure 1)

A fourth producing zone is the Wedington Sandstone Member of the Fayetteville Shale. The Wedington is a fine to medium-grained iron stained sandstone. This sandstone is thought to have been deposited in deltaic and near shore beach environments. The Wedington is not present everywhere but its thickness in some places is over 100 feet. The largest field in the area of interest, the Brentwood field, produces from the Wedington.

A stratigraphic section showing the relative positions and depths of the producing zones in Washington and Madison Counties is shown in Table 1.

RESERVOIR CHARACTERISTICS

Gas produced from the St. Peter, Sylamore, and Wedington Formations is considered a "sweet gas" by industry standards. Chemical analysis shows the gas to be predominantly methane, ethane, and nitrogen. These constituents can vary several percentages points, but are approximately 94%, 4%, and 1%, respectively. Trace amounts of carbon dioxide, propane, isobutane, normal butane, isopentane, normal pentane, hexane,

PERIOD	FORMATION	
Pennsylvanian	Atoka Formation	
Pennsylvanian Morrowan Series	Kessler Ls Mbr	
	Bloyd Formation	
	Brentwood Ls Mbr	
	Hale Formation	
Mississippian	Pitkin Limestone	
	Fayetteville Shale	
	Wedington Ss Mbr	☼ 200'- 1400'
	Batesville Formation	
	Moorefield Formation	
	Short Creek Oolite Mbr	☼ 400'- 1600'
	Boone Formation	
	St Joe Ls Mbr	
Devonian	Chattanooga Shale	
	Sylamore Ss Mbr	☼ 1000'- 1200'
	Clifty Formation	
	Penters Chert	
Silurian	Lafferty Limestone	
	St Clair Limestone	
	Brassfield/Cason	
Ordovician (upper)	Cason Formation	
	Fernvale Limestone	
Ordovician (middle)	Kimmswick Limestone	
	Plattin Limestone	
	Joachim Formation	
	St Peter Sandstone	☼ 600'- ?
	Everton Formation	
Ordovician (lower)	Powell Dolomite	
	Cotter Dolomite	

Table 1 - *Chart showing the stratigraphic column in Northwest Arkansas and the adjoining Arkhoma basin. Symbols indicate producing zones and list approximate depth in Washington and Madison Counties.*

and oxygen make up the balance. The BTU value ranges from a low of 960 to a high of 1,100 in a recent discovery well from the Wedington Sand in the Signal Hill field. The gas is not corrosive and requires only minor treatment, usually for CO_2, prior to sale.

Producing wells form the Boone Formation show some hydrogen sulfide. It is not known presently if this is a localized situation or a characteristic of the formation in general. Hydrogen sulfide is an objectionable constituent and must be removed before sale.

For the most part, only minor amounts of water are associated with the gas production. The water is generally fresh and disposal is not a problem. However, on occasion salt water is encountered and it must be disposed of in an acceptable manner.

Initial shut in pressures range from 90 to 130 psi for well depths to 1,400 feet. Pressure declines from production is from 20% to 30% for the first year and from 10% to 20% per year thereafter. It is estimated that economic limits will be reached at approximately 10 psi shut in pressure.

Arkansas Oil and Gas Commission field rules are variable for the structural platform area in Arkansas. Well spacing requirements have been approved for a minimum of 40 acres. Present information indicates that 80-acre spacing may be most economical for much of this natural gas production.

NEW HEAT FLOW INVESTIGATIONS IN ARKANSAS

By Douglas L. Smith and Len Fishkin
Department of Geology
University of Florida
Gainesville, FL 32611

ABSTRACT

Seven new heat flow values determined in Arkansas are helping to characterize the southern Ozark Plateaus as a region of anomalously low heat flow. The values augment twelve previously determined Arkansas values and, collectively, portray the geothermal regime as complex and as requiring significant contrasts in the nature of the basement rocks. Excluding one value obviously influenced by hydrologic activity, heat flow in Arkansas ranges from 18 mW/m^2 at Prairie Grove in Washington County to 87 mW/m^2 near Pine Bluff.

INTRODUCTION

Although geological investigations in Arkansas are replete with descriptions of thermal springs, igneous rocks, and continuing dynamic activity, more detailed knowledge of the geothermal nature of the subsurface has been obtained only recently and remains incomplete. Temperature gradient data for southern Arkansas, essentially compiled from oil well and other deep borehole logs, were initially included in broader reconnaissance studies of the Mississippi Valley (Van Orstand, 1932; Spicer, 1964). This report summarizes subsequent temperature gradient investigations, and presents the results of continuing heat flow research conducted in Arkansas.

Prior to this decade, gradients at depths deeper than 600 m were known for nine well sites and ranged from 36°C/km to 47°C/km (Guffante and Nathenson, 1981). Substantial temperature gradient and heat flow measurements in the Gulf Coastal Plains established northern Louisiana and west-central Mississippi as regions of potential low-temperature geothermal resources (Smith et al., 1981; Smith and Dees, 1981, 1982a, 1982b). Jarrett (1982) reported temperature gradient values from shallow depths (less than 500 m) for an additional 40 sites in the Mississippi Valley region, including nine measurements in Arkansas. The values ranged from 14°C/km at Helena to 36°C/km at Pine Bluff. Jarrett's preliminary data were incorporated with other existing gradient values to identify possible shallow geothermal resources in the central segment of the Northern Gulf Coastal Plains (Staub and Treat, 1981). Economic extraction of thermal waters in this zone (including southern Arkansas) is not feasible, and only isolated areas in Arkansas were described by the U.S. Geological Survey (Reed, 1983) as potential geothermal resource sites.

The first determinations of heat flow in Arkansas were reported by Roy et al. (1980), but later discussions (R. F. Roy, pers. corres., 1984) resulted in the retraction of all but two of the measurements. Heat flow values of 46 mW/m^2 (western Arkansas) and 44 mW/m^2 (central Arkansas) were considered valid. Subsequent heat flow measurements (Jarrett, 1982; Jarrett et al., 1984; Collins, 1985; Smith et al., in prep.) yielded ten new values, ranging from 25 mW/m^2 at Helena to 87 mW/m^2 at Pine Bluff. Table 1 summarizes the locations and values of the heat flow determinations.

GEOLOGIC/TECTONIC SETTING

Geothermal regimes are basically a function of (1) radioactive heat generation

Site	Lat.	Long.	Depth (m)	Gradient (°c/Km)	K(W/m°K)	Q(mW/m^2)	Source
Blytheville	35° 55' 22"	89° 54' 19"	420	19.93	2.75	54.8	1
Pine Bluff #1	34° 12' 40"	91° 55' 30"	220	32.06	2.39	76.5	1
Pine Bluff #2	34° 12' 39"	91° 55' 30"	240	24.67	2.39	58.9	1
Pine Bluff #3	34° 12' 39"	91° 55' 30"	265	36.42	2.39	86.9	1
International Paper	34° 32' 43"	91° 55' 16"	337	32.67	2.39	78.0	1
Helena	34° 32' 43"	90° 38' 43"	186	13.76	1.79	24.7	1
Mariana	34° 46' 31"	90° 45' 58"	180	19.99	1.93	38.5	1
Thompson Grove	34° 56' 29"	90° 20' 06"	500	22.09	1.93	42.6	1
Evandale	35° 33' 06"	90° 05' 08"	360	15.78	2.76	43.5	1
Well #24	34° 42' 00"	92° 15' 00"	175	25.50	1.74	44.3	2
Well #28	34° 23' 00"	93° 50' 00"	530	18.70	2.44	45.6	2
Jerome	33° 24' 24"	91° 27' 00"	240	41.41	1.63	67.7	3
Fayetteville	36° 07' 36"	94° 00' 30"	20-100 120-195	31.85 17.90	1.64	41.2*	4
Elkins	36° 00' 00"	93° 57' 30"	100-180 180-215	16.60 27.92	1.53	30.4*	4
Prairie Grove	35° 59' 30"	94° 18' 00"	573	12.47	1.42	17.8	4
Bull Shoals	36° 23' 12"	92° 36' 00"	137	4.02	2.05	8.2	4
Leslie	35° 49' 12"	92° 34' 30	1061	11.40	2.12	24.2	4
Green Forest	36° 19' 12"	93° 26' 33"	715	11.25	2.18	24.5	4
Winslow	35° 49' 36"	94° 10' 00"	300	33.23	1.85	61.5	4

Table 1. Locations, depths, gradient values, thermal conductivity values (K), and heat flow values (Q) for Arkansas. Those value with (*) are weighted averages. Sources: 1: Jarrett (1982); 2: Roy et al (1980); 3: Collins (1985); 4: this report.

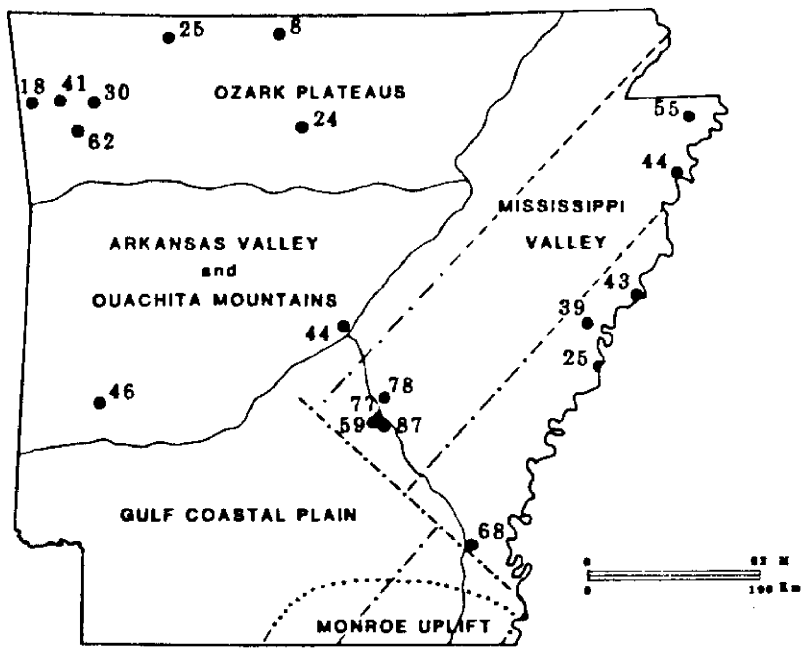

Figure 1. Distribution of heat flow values in Arkansas (values in mW/m^2). Solid lines depict the physiographic province boundaries. Dashed lines show the general subsurface configuration of the Mississippi Valley Graben; the combination dash-dot lines represent the theoretical extension of this feature as determined by Collins (1985) from thermal effects. The dotted line shows the general subsurface extent of the buried Monroe Uplift.

within the crust and (2) the upper mantle-lower crust temperature which is often governed by tectonic conditions in the upper mantle. The conveyance of heat through the crust, by either conduction or convective waters, is related to the rock type and the structure. Thus, crustal units with various origins or physical properties are expected to exhibit various thermal conditions. Conversely, contrasting thermal properties can be indicative of basic differences associated with diverse crustal units.

Arkansas has a significant variety of contrasting crustal units; the near surface heat flow values should reflect these underlying heterogeneities. The complexly folded and thrust faulted Ouachita Mountains (Viele, 1974) have often been described as the result of Paleozoic lithospheric subduction and continental convergence (e.g. Lillie, 1984). North of the Ouachita Mountains and forming the southern terminus of the undeformed North American craton is the Ozark Plateaus, a gently upwarped and stable sequence of Paleozoic sedimentary rocks.

The Gulf Coastal Plains sedimentary sequence buries the southern and eastern extents of the Ouachita tectonic belt and, in the extreme southeastern portion of the state, the Monroe Uplift (Figure 1). The Monroe Uplift, situated on the flank of the Mississippi Embayment, is a broad, subsurface, asymmetrical feature associated with Mesozoic and Cenozoic alkalic igneous rocks (Zartman, 1977). Smith and Dees (1982a) attributed anomalously high heat flow values in northern Louisiana to radiogenic heat sources in the igneous rocks of the Monroe Uplift.

In northeastern Arkansas the Mississippi Valley Graben is buried by Coastal Plain sedimentary rocks and is a source of seismic activity (Kane et al., 1981; Crone et al.,

1985). The graben is a broad, parallel sided structural depression attributed to late Precambrian or early Paleozoic continental rifting (Ervin and McGinnis, 1975). It trends southwest to northeast and has been depicted through interpretations of geophysical surveys as an intensely block-faulted region with basement relief of 2 km (Hildenbrand, 1982, 1985). Thermal modeling of extrapolated temperature gradients and heat flow determinations for the lower crust suggest that the rift structure of the Mississippi Valley Graben may extend through central Arkansas into northern Louisiana (Collins, 1985; Jarrett et al., 1984; Smith et al., in prep.).

METHODS

Field work conducted in autumn 1986 and summer 1987 yielded additional heat flow values to those originally determined. All values, except those attributed to Roy et al. (1980) (table 1), were acquired with the same equipment and procedures.

Temperature values and geothermal gradients were measured in the field with thermistor probes coupled to a Mueller-type Wheatstone Bridge with a 1000-meter, four-conductor cable. The thermistor probes were calibrated in a constant temperature bath with a platinum resistance thermometer and were considered accurate to $\pm$ 0.1°C. The accuracy of gradient values is placed at 0.01°C/km. The temperature values for the measurement at Leslie, Arkansas, were recorded by the U.S. Geological Survey.

Deep drill holes were sought on an opportunistic basis, and temperature measurements were made at discrete intervals in the wells. Wells undisturbed by pumping or recent drilling and at least 150 meters deep were preferred, but the paucity of suitable wells in some areas necessarily introduced a bias of unequal spatial distribution of the data. The local relief at each of the measurement sites was considered insufficient to justify topographic corrections.

Only cuttings samples were available for each of the boreholes logged, thus, the thermal conductivity values were determined in the laboratory using a standard divided-bar apparatus and the procedures described by Sass et al. (1971). Porosity values of 30% were assumed for those samples from the Coastal Plains sediments; samples from the Ozarks Plateaus were assigned porosity values of 30% for sandstone and 15% for shale and limestone samples. Fused quartz and natural quartz cylinders were used as calibration standards.

Thermal conductivity values for all cuttings samples from a given borehole were averaged using the harmonic mean method. The conductivity values are estimated to be accurate to within 15%. Cuttings samples were unavailable for several of the boreholes logged. Conductivity measurements for those sites were determined using representative samples from nearby boreholes with the same lithology.

The computed heat flow values are the product of the geothermal gradient and the harmonic mean thermal conductivity. Weighted average values were determined for those sites with different depth zones of the measured borehole. An accuracy of $\pm$ 20% is assigned to the heat flow values.

RESULTS/DISCUSSION

Table 1 lists the heat flow values for Arkansas with thermal gradients and thermal conductivity values and includes the seven new values reported herein. The distribution of the values is shown in Figure 1. They range from a high of 87 mW/m^2 at Pine Bluff to a low of 18 mW/m^2 at Prairie Grove. A typical continental heat flow value for stable regions is approximately 45 mW/m^2.

The anomalously low value (8 mW/m^2) listed for Bull Shoals in table 1 is regarded as suspect because the very low geothermal gradient value was recorded in a relatively shallow borehole (137 m), and ground water circulation may have affected the temperature gradient. An atypical high heat flow value recorded near Pine Bluff (86.9 mW/m^2), however, is supported by two other measurements in the same region that yielded significant, but lessor values of 76 mW/m^2 and 59 mW/m^2.

The single heat flow measurement (68 mW/m^2) at Jerome in southeastern Arkansas (Figure 1) can be interpreted as representing a northward extension of the positive thermal regime reported for the Monroe Uplift region in northern Louisiana. Collins (1985) described a submerged extension (Figure 1) of the Mississippi Valley Graben trending southwestward beneath the Pine Bluff area of higher heat flow values and, through a transform offset, continuing under the Monroe Uplift. He suggested that the positive anomalies may result from radiogenic heat production in igneous intrusions associated with an aulacogen.

The four low to normal heat flow values flanking the Mississippi River augment other adjacent values in Mississippi and Tennessee (Smith et al., in prep.) and represent a possible negative thermal effect of a synclinal downwarp in the upper crust underlying the river axis. The relatively thick accumulation of low-conductivity sedimentary rocks may act as a thermal barrier to the natural upward conductive transfer of heat. The thermal effects of circulating groundwater may represent a significant influence on the individual heat flow measurements in this portion of the state.

Contrasting heat flow values in northwestern and north-central Arkansas also suggest isolated hydrologic interference with the thermal regime in the Ozark Plateaus. This region of sedimentary rocks contains several prominent aquifers which are manifested locally by springs and producing water wells. Despite the relatively high heat flow value (62 mW/m^2) recorded at Winslow in Washington County, other values recorded in the Ozark region of Arkansas characterized that physiographic province as one with anomalously low heat flow. Unpublished values recently measured in southern Missouri (Smith and Meert, in prep.) substantiate this characterization.

The low heat flow values for the Ozark Plateaus are a result of anomalously low geothermal gradients recorded in boreholes. The measured thermal conductivity values for samples from the Ozarks are similar to those for corresponding rock types from other areas. The wide distribution of anomalously low heat flux within the Ozarks is similar to that encompassing negative thermal anomalies for the Appalachian Plateau and Valley and Ridge provinces of northwestern Georgia and northeastern Alabama (Smith et al., 1981) and the Black Warrior Basin of northern Mississippi (Jarrett, 1982).

Unless near-surface hydrologic conditions can be shown to dominate the thermal regime, anomalies throughout areas of such magnitude must be attributed to deep-seated crustal or upper mantle zones lacking either in normal radiogenic heat production or in direct conduction of heat. Although theories describing the Black Warrior Basin as a thick sediment pile filling a void created by a lateral discontinuity in continental lithosphere (Smith et al., in prep.) may also be applicable to parts of northern Alabama and Georgia, such causal conditions seem unlikely for the Ozark Plateaus. No known evidence exists to suggest that the lithosphere beneath the Ozarks is extraordinarily diminished in heat generation; thus, the attribution of cause for the anomaly is elusive without additional research.

CONCLUSION

The twelve heat flow values previously determined (Roy et al., 1980; Jarrett, 1982; Collins, 1985) were concentrated in the central and eastern portions of Arkansas. They may be interpreted to suggest a zone of relatively low heat flow along the Mississippi River. However, the relatively high values are interpreted (Jarrett et al., 1984; Collins, 1985) to be caused by a southwesterly extension of the thermal effects associated with the Mississippi Valley Graben.

The seven additional heat flow values reported here are all concentrated in the sedimentary rock formations comprising the Ozark Plateaus. Although one anomalous value may be excluded as plausibly influenced by near surface ground water circulation, the remainder seem to characterize the Ozark Plateaus province in Arkansas as an area of anomalously low heat flow. Hydrologic conditions within the Ozark Plateaus may convectively convey some heat, effectively reducing the measured conductive heat flow. Other causal factors for the anomaly require speculation concerning the composition of the

lower crust and upper mantle underlying the Ozark Plateaus.

ACKNOWLEDGEMENTS

We are sincerely grateful for the courteous and professional cooperation afforded us by the Arkansas Geological Commission. State Geologist N. F. Williams and C. G. Stone, among others, were particularly helpful. D. Freiwald, G. Gand, and G. Ludwig of the U.S. Geological Survey, Water Resources Division, in Little Rock provided generous assistance with borehole locations. J. A. McEntire of Big Rock Petroleum, and E. Smith of the Arkansas State Park system were also instrumental in providing access to boreholes. J. Meert and E. Arenberg assisted with the field measurements. This research was sponsored by the University of Utah Research Institute, Contract RI-1291.

REFERENCES

Collins, W. E., 1985, Thermal anomalies in the Mississippi Embayment and their tectonic implications, M.S. Thesis, Univ. of Florida, 190 p.

Crone, A. J., McKeown, F. A., Harding, S. T., Hamilton, R. M., Russ, D. P., and Zoback, M. D., 1985, Structure of the New Madrid seismic source zone in southeastern Missouri and northeastern Arkansas, Geology, v. 13, 547-550.

Ervin, C. P., and McGinnis, L. D., 1975, Reelfoot Rift: Reactivated precursor to the Mississippi embayment, Geol. Soc. Amer. Bull., v. 86, 1287-1295.

Guffanti, M., and Nathenson, M., 1981, Temperature-depth data for selected deep drill holes in the United States obtained using maximum thermometers, U. S. Geol. Surv. Open File Rept. 81-155, 100 p.

Hildenbrand, T. G., 1982, Model of the southeastern margin of the Mississippi Valley Graben near Memphis, Tennessee, from interpretation of truck-magnetometer data, Geology, v. 10, 476-480.

Jarrett, M. L., 1982, Heat flow of the Mississippi Embayment, M.S. Thesis, Univ. of Florida, 143 p.

Jarrett, M. L., Smith, D. L., and Collins, W. H., 1984, Heat Flow in the Mississippi Embayment, Geol. Soc. Amer. Abs. with Prog., v. 16, 550.

Kane, M. F., Hildenbrand, T. G., and Hendricks, J. D., 1981, A Model for the Tectonic evolution of the Mississippi Embayment and its contemporary seismicity, Geology, v. 9, 563-567.

Lillie, R. J., 1984, Tectonic implications of subthrust structures revealed by seismic profiling of Appalachian-Ouachita orogenic belt, Tectonics, v. 3, 619-646.

Reed, J. J., 1983, Assessment of low-temperature geothermal resources of the United States - 1982, U.S. Geol. Surv. Circ. 892, 73 p.

Roy, R. F., Taylor, B., Pynn, A. J., and Maxwell, J. C., 1980, Heat flow measurements in the state of Arkansas, Los Alamos Nat. Lab. Rpt. LA-8569-MS, 15 p.

Sass, J. H., Lachenbruch, A. H., and Monroe, R. J., 1971, Thermal conductivity of rocks from measurements on fragments and its application to heat flow determinations, J. Geophys. Res., v. 76, 3391-3401.

Smith, D. L., Dees, W. T., and Harrelson, D. W., 1981a, Geothermal conditions and their implications for basement tectonics in the Gulf Coast margin, Trans. Gulf Coast Assoc. Geol. Soc., v. 31, 181-190.

Smith, D. L., Gregory, R. G., and Emhof, J. W., 1981b, Geothermal measurements in the southern Appalachian Mountains and southeastern Coastal Plains, Am. Jour. Sci., v. 281, 282-298.

Smith, D. L., and Dees, W. T., 1981, Low-grade geothermal resources in northern Louisiana, Trans., Geothermal Res. Council, v. 5, 127-128.

Smith, D. L., and Dees, W. T., 1982a, Heat flow in the Gulf Coastal Plain, J. Geophys. Res., v. 87, 7687-7693.

Smith, D. L., and Dees, W. T., 1982b, Indicators of low-temperature geothermal resources in northern Louisiana and central Mississippi, J. vol. and Geother. Res., v. 14, 389-393.

Staub, W. P., and Treat, N. C., 1981, A geothermal resource appraisal of the Tennessee Valley region, Inst. Energy Analysis Report, Oak Ridge Assoc. Univ., Oak Ridge, Tenn., 132 p.

Viele, G. W., 1974, Structure and tectonic history of the Ouachita Mountains, Arkansas, in Gravity and Tectonics, DeJong, K. A., and Scholten, R., editors, John Wiley Publ., New York, 361-377.

Zartman, R. E., 1977, Geochronology of some alkalic rock provinces in eastern and central United States, Ann. Rev. Earth Planet. Sci. Ltrs., v. 5, 257-286.

MACROSCOPIC STRUCTURAL GEOLOGY OF THE CENTRAL COSSATOT MOUNTAINS AND SURROUNDING AREAS, BENTON UPLIFT, ARKANSAS

By John C. Weber and Jay Zimmerman
Department of Geology
Southern Illinois University
Carbondale, IL 62901

ABSTRACT

The central Cossatot Mountains comprise a series of closely spaced ridges of Arkansas Novaculite separated by valleys underlain by adjacent stratigraphic units. The spatial distribution of all units is controlled by macroscopic-scale folding and thrust faulting. The mapped area has been divided into two structural domains based on internally consistent plunge direction and geometry of macroscopic folds. In the northern domain, which includes part of the narrow, westward extension of the Mazarn basin, very tight, symmetric, cylindrical kinks plunge about 10° ESE. In the southern domain, which includes the northernmost part of the Athens plateau, tight, rotated north-vergent, monoclinic kink folds plunge 10° WSW. Macroscopic folding accounts for 96.5% of the total stratal shortening in the area, which is estimated palinspastically to be about 6.5 km. The average macrofold wavelength of 1.2 km suggests that a viscosity contrast of 3.1:1 existed between the Arkansas Novaculite and adjacent shale-rich units during orogenic fold formation.

The two structural domains are separated by the Albert thrust fault along which an estimated 1,524 m of relative dip-slip has occurred. Three additional thrust faults in each of the two domains have been recognized. All faults dip very steeply, display a northward sense of transport and appear to be frontal segments of listric thrust faults.

The sense of asymmetry together with present geometry of macrofolds in the southern domain suggest that these structures, like those in much of southern Benton uplift, have been rotated in a clockwise sense (looking east) about a nearly horizontal E-W axis. Our interpretation of local thrust tectonics suggests that at least part of this bulk rotation can be attributed to ramping of the Albert thrust sheet during north-directed transport.

INTRODUCTION

The Cossatot Mountains form the southernmost arm of the Benton uplift (Figure 1) and comprise a series of nearly east-west trending ridges of Arkansas Novaculite (Mississippian-Devonian) separated by valleys of older strata and infolded beds of younger (Mississippian) Stanley Shale. The purpose of this paper is to outline the macroscopic structural geology of a 26 km2 area in Pike and Montgomery counties, which includes a complete transect through the central part of the Cossatot range (Figures 1,2). Adjacent segments of the Mazarn basin and Athens plateau flank the Cossatots to the north and south, respectively, and constitute approximately 30% of the total field area (Figures 1,2).

The data presented here originated during a mapping project conducted in 1984 and 1985. Results of the entire project comprise the senior author's thesis (Weber,

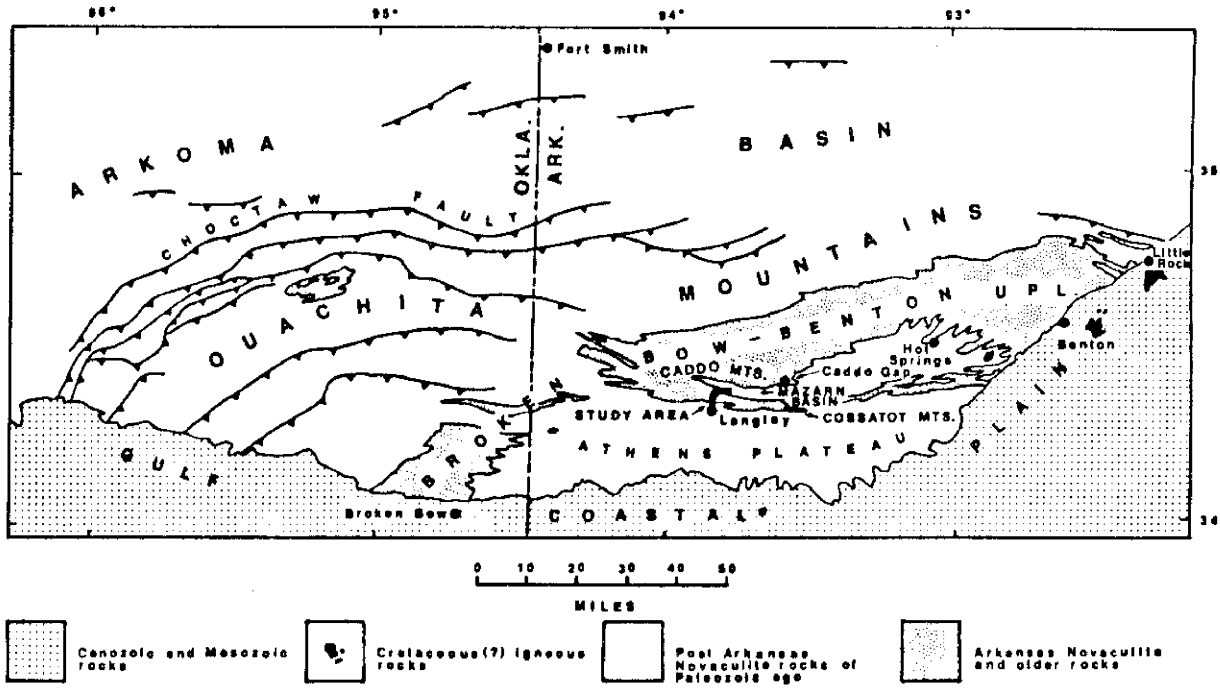

Figure 1. Generalized bedrock geologic map of the Ouachita Mountains and surrounding region. Many faults in the Ouachitas are ommited; those shown are denoted as dark lines with sawteeth on upthrown sides (modified from Miser, 1959).

1987), parts of which have been reported elsewhere (Weber and Zimmerman, 1986). The study was undertaken to add to the structural detail available from previous work in the area (Miser and Purdue, 1929; Haley et al., 1976) by:1) mapping at a larger scale (1:24,000), and 2) mapping the Arkansas Novaculite as three informal members [lower (135 m), middle (71 m) and upper (33 m) members-see Figure 3].

Key structural elements in this part of the orogen include seven steeply dipping, north-directed thrust faults and two sets of gently plunging, upright, macroscopic kink folds in the Bigfork (Ordovician) through Stanley (Mississippian) formations (Figure 2). Palinspastic restoration indicates that strata exposed along the transect have been shortened by approximately 6.5 km (43.5%) during orogenesis. Lithologic characteristics of these strata are discussed in some detail by Miser and Purdue (1929) and Stone et al. (1984). Wever (1987) includes sedimentological descriptions as well.

Geologic mapping (Figure 2), structural analyses (Figure 4), and a balanced cross section (Figure 5) indicate that the area can be divided into two macroscopic structural domains (northern and southern) based on internally consistent plunge direction and geometry of macrofolds. The two domains are separated by a major thrust fault that bisects the central Cossatot range and is best exposed at the village of Albert. The Albert thrust possesses an estimated 1,524 m of dip-slip displacement, the greatest amount of throw of all faults present in the area. Mapped macrofold axes plunge an average of 10^{o} to the west (bs=10/262) in the southern domain, while those north of the fault trace average 10^{o} eastward (bn=10/098).

MACROFOLDS

Macroscopic folding accommodates 96.5% of the total stratal shortening (or 42% shortening) along the transect. Nine macrofolds have been mapped in the two structural domains (Figure 2) and were used to define individual subdomains in Wever's (1987) study. Poles to bedding surface (So) orientations collected from each macrofold are

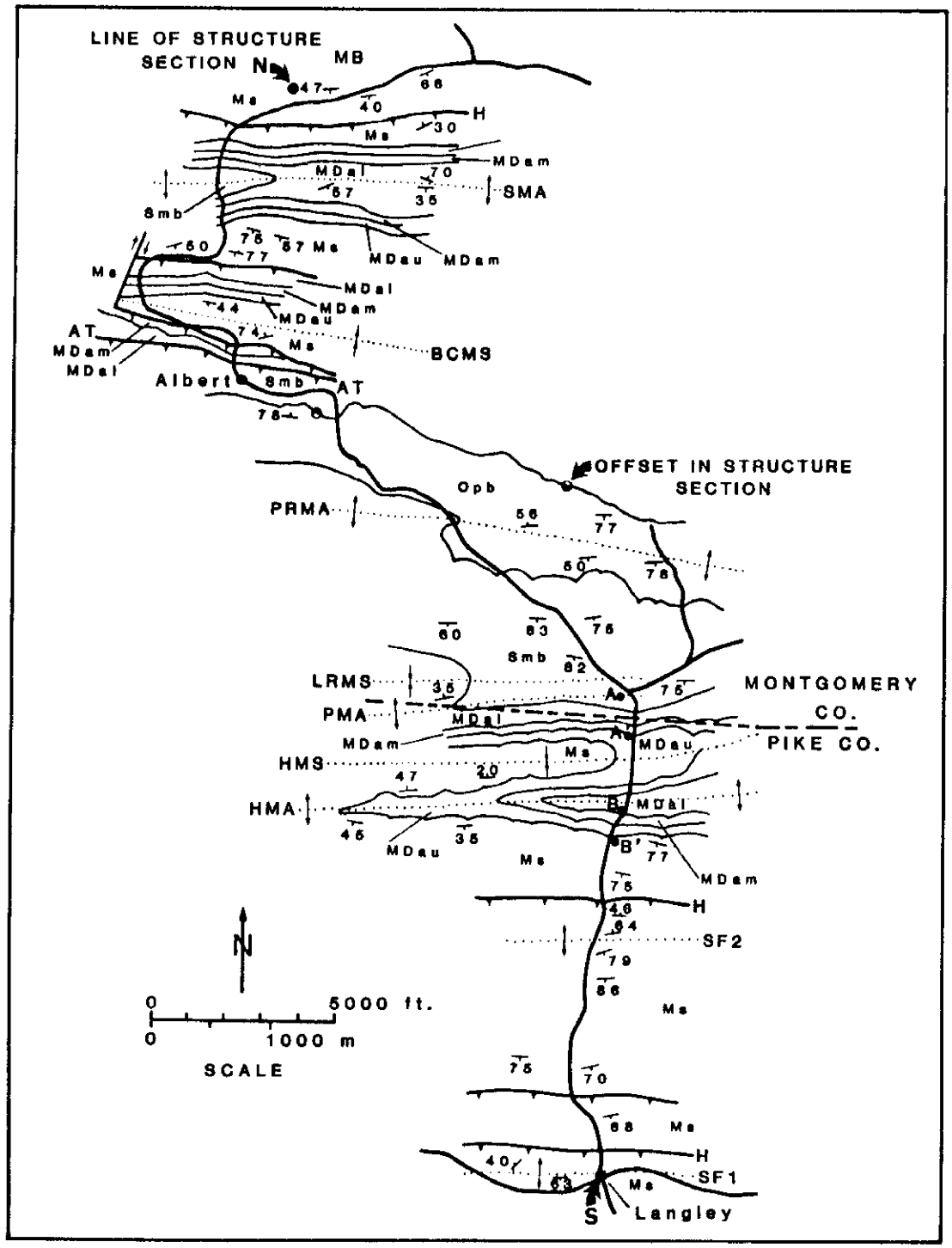

Figure 2. Bedrock geologic map of the study area. Standard symbols are used for thrust faults, bedding orientations, and macrofold trough and crest lines. Explanation: Opb-Bigfork Chert and Polk Creek Shale (Ordovician), Smb-Missouri Mountain Shale and Blaylock Sandstone (Silurian), MDa-Arkansas Novaculite (Mississippian-Devonian) [l-lower member, m-middle member, u-upper member], Ms-Stanley Shale (Mississippian), SF-Stanley flats, HMA-Hogpen Mt. anticline, HMS-Hogpen Mt. syncline, PMA-Paul Mt. anticline, LRMS-Little Raven Mt syncline, PRMA-Pryor Mt. anticline, AT-Albert thrust fault, BCMS-Brier Creek Mt. syncline, SMA-Sherman Mt. anticline, MB-Mazarn basin, H-faults mapped by Haley et al. (1976). The Polk Creek and Missouri Mountain Shales are thin units present only along Opb-Smb and Smb-MDa contacts, respectively.

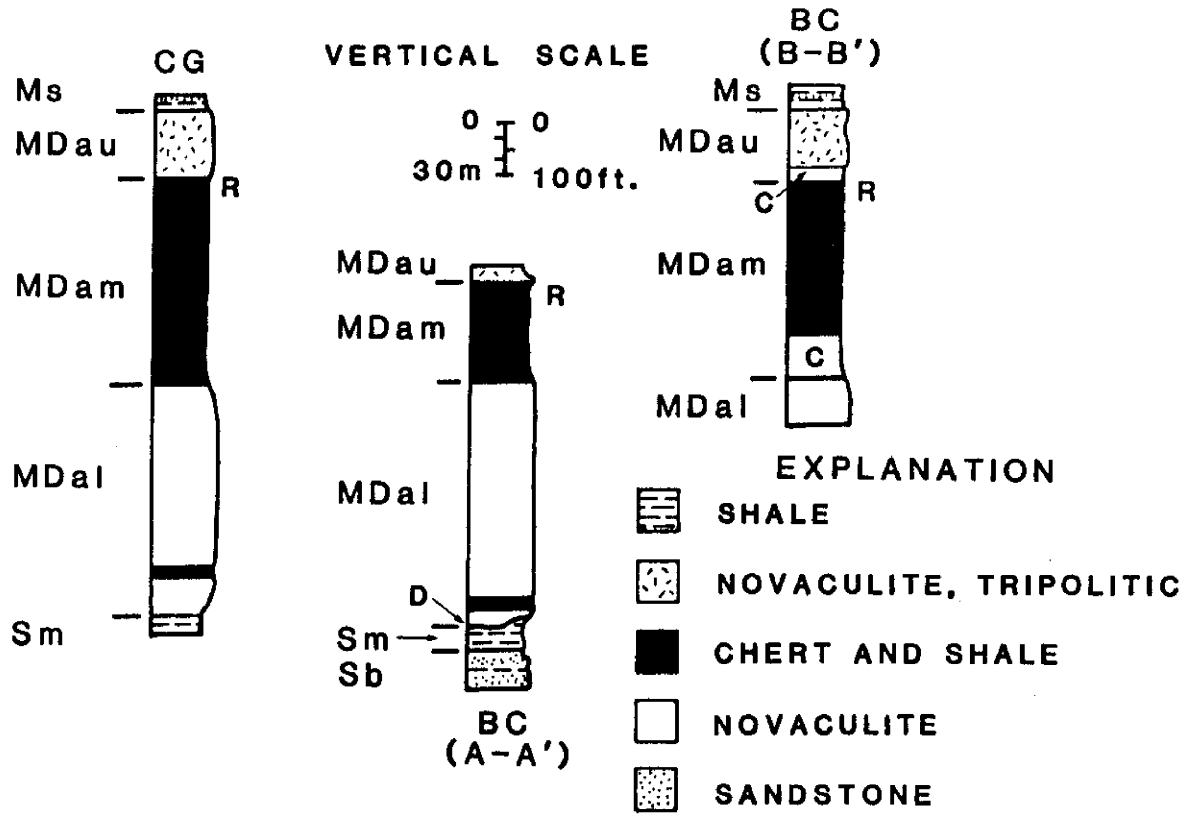

Figure 3. Measured stratigraphic sections through the Arkansas Novaculite and adjacent stratigraphic units. Explanation: CG-Caddo Gap section from Miser and Purdue (1929), see Figure 1 for location; BC-Blocker Creek sections, see Figure 2 for lines of section A-A' and B-B'; C-covered interval; D-disconformity; R-red shale, other cherts and shales are predominantly black in color. See figure 2 for formation and member symbols.

plotted on separate equal-area nets for assessment (Figure 4). All lie along great circles (i.e.-confirm fold cylindricity) and show a tendency to form two clusters in the northern and southern regions of the nets, suggesting a sharp, angular macrofold shape. Our cross section (Figure 5) also includes three blind, macroscopic synclines which are overridden by adjacent thrust faults along the frontal edges of hanging wall blocks.

The average macrofold wavelenght of 1.2 km is controlled by the thick (239 m), competent Arkansas Novaculite and suggests a synorogenic viscosity contrast between the Novaculite and surrounding shale-rich rocks of 3.1:1, according to the dominant wavelength equation of Biot (see Hobbs, et al., 1976, p. 201).

Southern Domain

Macrofold data in the southern domain come from five individual folds in the Cossatots and two in the Athens plateau (Stanley flats area). Folds in the Cossatots, proper, were detailed by subdividing and mapping the Arkansas Novaculite as three informal members [lower, middle and upper (Figure 2,3)]. Stanley rocks in the Athens plateau, for the most part, dips to the south. Since no well exposed marker horizons are present in the Stanley, macrofolds must be recognized by northward dip reversals representing the northern limbs of anticlinal flexures. Two such macrofolds occur

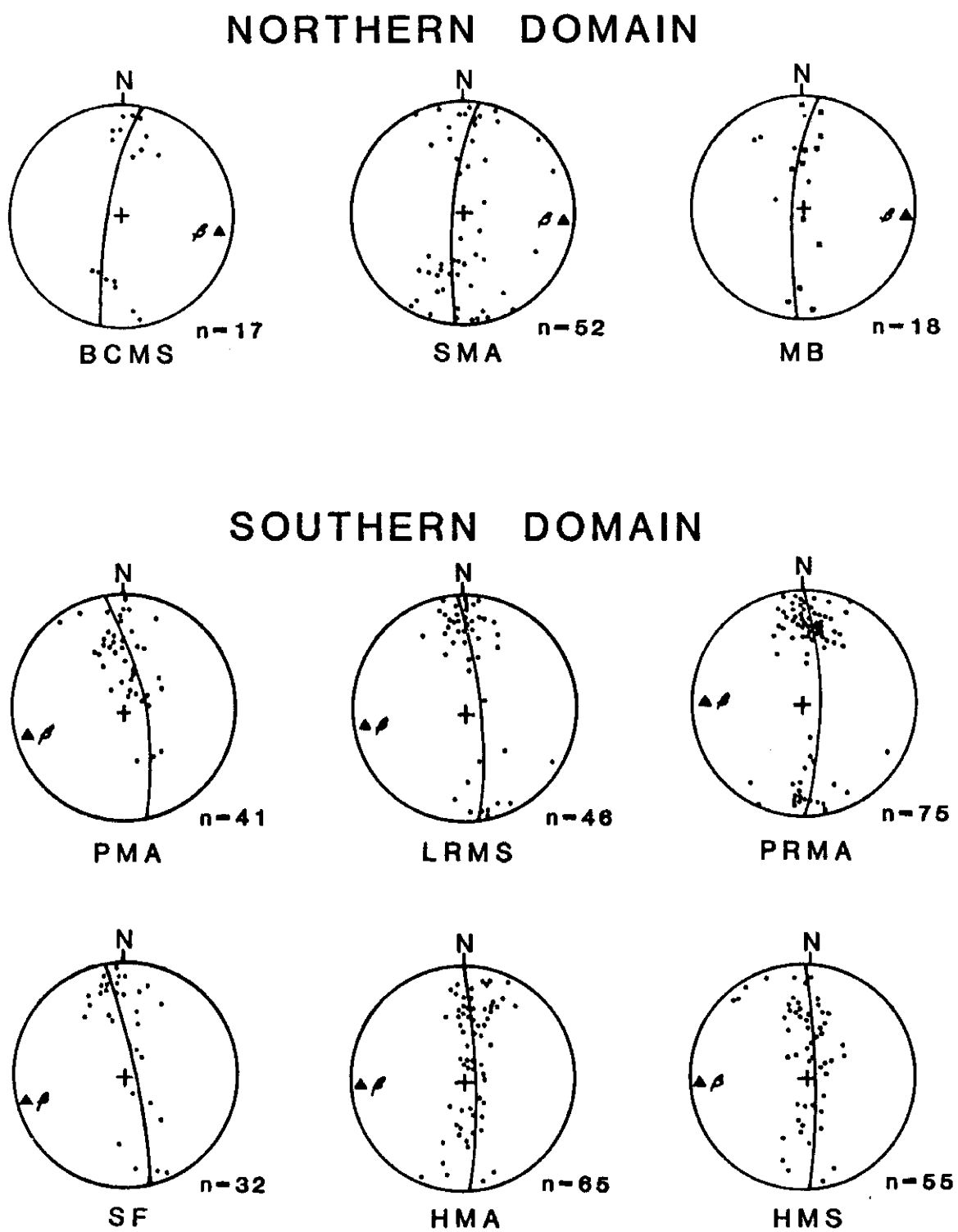

Figure 4. Lower-hemisphere, equal-area synopsis of macrofold data. Circles represent poles to bedding planes (So); squares in MB are poles to bedding (So) from Miser and Purdue (1929); triangles (B0 are statistical macrofold axes; n=number of observations. See Figure 2 for locations of individual macrofolds and explanation of symbols, and see text for discussion of structural domains.

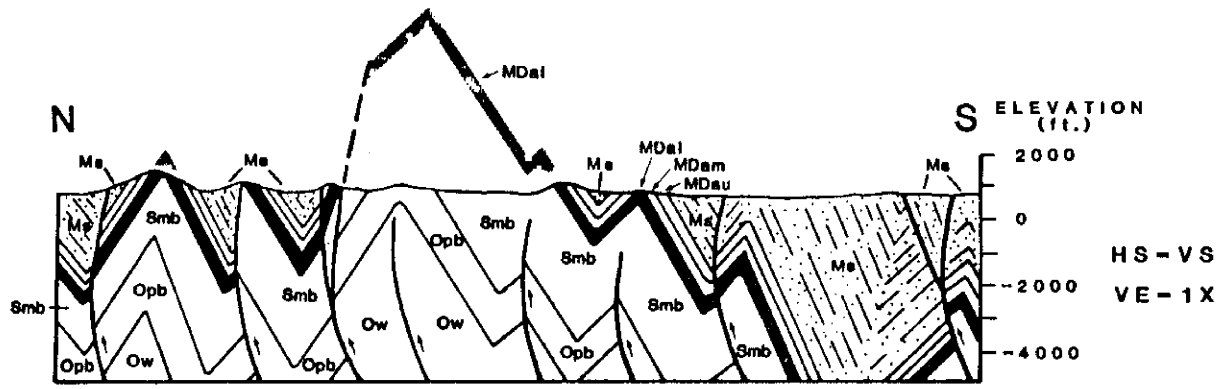

Figure 5. Balanced structural cross section through study area. See Figure 2 for line of section and explanation of symbols. Blackened unit is the lower member of the Arkansas Novaculite (MDal). Stippled MDal is projected up-plunge into the section from ridges west of the line of section (see Figure 2).

as frontal folds (Butler,1982) on faults mapped by Haley et al. (1976). Data from the Stanley flats macrofolds are plotted on a single net (Figure 4) to best represent the limited information obtained from typically poor Stanley outcrops. All macrofolds in the southern domain plunge gently westward (bs=10/262) along a WSW trend.

Down-plunge assesment is an invaluable tool for interpreting map-scale structures (Mackin, 1950; King, 1964; and Ragan, 1973, p. 85) Down-plunge analysis of macrofolds in the Cossatots confirms that they are straight-limbed with tight interlimb angles, sharp and angular hinge areas, and marked asymmetry. Their axial surfaces dip nearly vertically; short limbs face and dip moderately to the north; and long back limbs dip steeply and face southward. Based on this information, they can be considered as kink folds with a northward sense of vergence that have been rotated clockwise (looking east) about an E-W, nearly horizontal axis during or subsequent to their formation. This sense of rotation has long been considered an important element of the structural style in much of the southern Benton Uplift (Viele, 1973, 1979; Arbenz, 1984; Zimmerman et al., 1982).

Macrofolds in the Athens plateau (Stanley flats) also possess similar shapes and geometries, but one must recognize them by the distribution of bedding orientations since there are no mapped contacts to view downplunge. South of our transect, macrofolds in the Athens plateau become less angular and of greater amplitude and wavelenght (Miser and Purdue, 1929), due to the thickness of the Jackfork Sandstone (2,960 m) which probably controls their dominant wavelengths and shapes in the ductile Carboniferous rocks at this structural level in the orogen. It is likely that these folds are cored by kink folds of the Cossatot type at depth.

Northern Domain

Two macrofolds have been mapped in Cossatot portion of the northern domain. When assessed down-plunge these folds display no asymmetry, are very tight, have sharp, angular hinge areas, and appear to be segmented and flattened kinks similar to those in the southern domain. An equal-area plot of poles to bedding from the Mazarn basin, a complex synclinorium (Miser and Purdue, 1929), is included with our Cossatot data (Figure 4) to illustrate that it is geometrically similar to, and probably a structural extension of, the northern domain. Macrofolds in the northern domain, including the Mazarn basin, all plunge gently to the east along an ESE trend (bn=10/098).

THRUST FAULTS

Macroscopic faults are typically poorly exposed along the transect, as they are elsewhere in the Arkansas Ouachitas. Where marker horizions are present, as in the Cossatot range, faults are assessed on the basis of stratigraphic displacement. The three faults mapped here (Figure 2) all place older, hanging wall rocks to the south against younger, footwall rocks to the north (i.e.-display a northward sense of tectonic transport). Their traces are very straight and cut across prominant topographic features, signifying that their dips approach the vertical. All strike ESE.

A major mapping problem exists in Stanley exposures of the Athens plateau (Stanley flats area) and Mazarn basin because: 1) the Stanley Shale is a non-resistant unit and typically forms only scattered outcrops, and 2) *well dispersed marker beds are not present in* the Stanley Shale. 2,593 m of poorly exposed, rythmically bedded sandstone and shale with few marker beds is, at best, difficult to detail structurally. Here, three faults mapped by Haley et al. (1976) from air photographs (Haley, 1985, personal communication) are consistant with our field data and are included on our map (Figure 2). Determining the sense and magnitude of throw along these intra-Stanley faults is also a difficult task. That shown in our cross section (Figure 5) is consistant with the overall structural style of the area and is constrained by down-plunge projection of the Arkansas Novaculite-Stanley contact from out of the field area (Miser and Purdue, 1929) into the section. Several of the 10 fault traces mapped *by Haley et al. (1976) in the area were not* directly confirmed by our field observations and are not included on our map.

Macroscopic faults, which acted as large-scale strain discontinuities during orogenesis (Ramsay, 1976), account for only 3.5% of thef total (43.5%) stratal shortening (or 1.5% shortening) along the transect. Steeply dipping, up-to-the-south faults, of the type exposed in the study area, probably represent the frontal segments of sledrunner thrusts (Roeder, 1973;Boyer and Elliott, 1982) which flatten and become subparallel to bedding surfaces with increasing depth (see the structural sections of Arbenz, 1984; and seismic sections of Lillie et al., 1983). Transport segments (Roeder, 1973) of other thrusts are seen in unroofed outcrops of older rocks in the central core area (Soustek, 1979). These shallowly-dipping faults were formed at structural levels deeper in the orogen than those preserved in the area under discussion. Faults in the field area are responsible for an aggregate 3,500 m of vertical displacement. Their horizontal (shortening) components of displacement probably increase proportionally with increasing depth.

Southern Domain

Three thrust traces are mapped in the southern domain. All crop out in Stanley of the Athens plateau. They are secondary to macrofolds as crustal shortening elements and are shown (Figure 5) to dissect the large, *westward plunging macrofold train present here* by up-to-the-south, vertical displacement. These north-directed thrusts have probably also been rotated (cw looking east) along with macrofolds into their present steep positions late in orogenesis. Several inferred blind thrusts are also included in our cross section. Owing to the importance of thrust faulting in this region, we suspect that kinked macrofolds may be related to the process of fault propagation (Suppe and Medwedeff, 1984).

Albert Thrust

The Albert thrust is a major structural element in the field area because: 1) it separates the two sets (domains) of macrofolds *which plunge in opposite directions, and 2)* posseses the greatest amount of throw of all faults mapped along our transect. A dip-slip displacement of 1,524 m can be obtained for the Albert thrust assuming: 1) the slip vector to lie in the plane of our cross section-which has been constructed parallel to the regional transport direction (Woodard, Boyer and Suppe, 1985), and 2) that the Blaylock Sandstome thins northward. The latter assumptiion is based on the fact that the Blaylock formation is absent in the Caddo Mountains (Figure 1) north of the field area (see Miser and Purdue, 1929; and Lowe, 1985).

MODEL BLOCK DIAGRAM

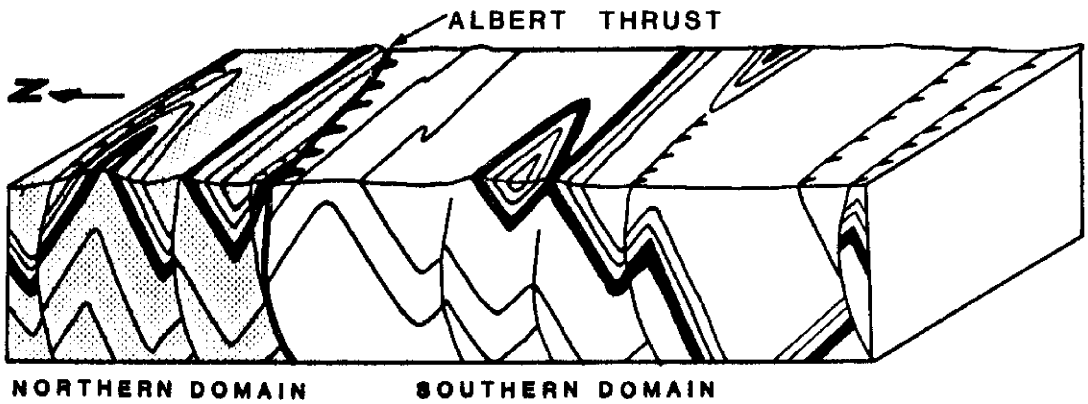

Figure 6. Schematic block diagram of macroscopic structures in the study area. Note northern (stippled) and southern domains separated by the Albert thrust fault. Blackened unit is the lower member of the Arkansas Novaculite (MDal). See text for discussion.

Northern Domain

Three fault traces are present in the northern domain, two in the central Cossatot range and one in the southern Mazarn basin. The two faults in the Cossatots display a northward sense of transport and dip nearly vertically. Based on the argument presented earlier, they probably also represent the frontal segments of listric thrusts. The southernmost fault nearly intersects the Albert thrust along a branch line (Boyer and Elliott, 1982) and is shown to splay off of the latter in our cross section.

The fault trace mapped in the southern Mazarn basin has been adopted from Haley et al. (1976) on the basis of: 1) the sudden presence of incipient pressure solution cleavage surfaces north of the trace, and 2) a reversal of bedding dips across the trace. Our data together with those of Miser and Purdue (1929) show that lower Stanley Shale is present on either side of the trace, which suggests that the magnitude of throw along this fault is minimal. Haley and Stone (1982), however, consider it to define a major tectonic boundry in the Arkansas Ouachitas.

Summary and Conclusions

1). Upright, gently plunging ($B=10^{O}$) macroscopic kink folds, which average 1.2 km in wavelength, define the macrofold style in the central Cossatot range. Asymmetrical kinks in the southern domain display a rotated (cw looking east), northward sense of vergence. Symmetrical macrofolds in the northern domain appear to be tight, flattened kinks.

2). The Albert thrust is the most significant fault in the field area. With an estimated dip-slip displacement of 1,524 m, it appears to mark the leading edge of a large, internally deformed thrust sheet (Figure 6). Faults along the transect dip very steeply and show a northward sense of transport. They probably represent the frontal segments of listric thrust faults. Those present in the southern domain may have been rotated (cw looking east) by upward ramping along the Albert thrust.

3). Mapping the Arkansas Novaculite as three informal members proved usefull in detailing the structure in an area of closely spaced Novaculite ridges.

4). Rocks exposed in the southern domain constiture a large, westward-plunging (Bs=10/262) macrofold train. This segment of the orogen appears to represent the frontal edge (Butler, 1982) of an internally deformed thrust sheet that has been carried upward and rotated externally (cw looking east) along a south-facing and westward-sloping frontal or oblique ramp (Butler, 1982) over rocks of the northern domain. The Albert thrust trace marks the surface expression of this ramp as well as the leading edge of this thrust sheet (Figure 6).

5). The easterly plunge of macrofolds in the northern domain (Bn=10/98) suggests that rocks here comprise the trailing edge of a seperate thrust sheet (Figure 6). This northern thrust sheet has probably experienced a different, more complex (?) structural evolution than that of the overriding southern sheet, but additional data are needed from the Mazarn basin and Caddo Mountains to the north to assess it's geographical extent and to evaluate the structural evolution of this thrust sheet.

AFTERTHOUGHT

A question on the nature of external rotation remains. Did this rotation occur to major parts of the orogen as a whole, late in the process of mountain building, as suggested by Arbenz (1985) and others, or did it occur on discrete thrust sheets as they were ramped upward toward the synorogenic erosional urface? Our data suggests that the latter can ccount for at least part of the bulk rotation experienced by rocks in the central Cossatot range.

ACKNOWLEDGEMENTS

This logistical support provided during field work and later compilation by the Arkansas Geological Commission and the SIU Department of Geology is very much appredlated, Benificial discussion and expertise has been provided by Charles Stone and Boyd Haley who deserve many thanks for showing continued interest in the project. The assistance of Pamela J. Roths, who helped collect data for our measured stratigraphic sections, is also much appreciated. Thanks is due to SOHIO (especially Charles A.O. Titus) and Sigma Xi for partial funding of this mapping project. Finally, deep appreciation goes out to Cleve and Geisla Whisenhunt of Glenwood for their unfailing hospitality during our visits to the Ouachitas.

REFERENCES CITED

Arbenz, J.K., 1984, A structural cross section through the Ouachita Mountains of western Arkansas, in, Stone, C.G., and Haley, B.R., A guidebook to the giology of the central and southern Ouachita Mountains, Arkansas: Arkansas Geol. Comm. Guidebook 84-2, p.76-82.

Boyer, S.E. and Elliott, D., 1982, Thrust Systems: Bull. Amer. Assoc. Petrol. Geol., v.66, no.9, p.1196-1230.

Butler, R.W.H., 1982, The terminoloogy of structures in thrust belts: Jour. Struct. Geol., v.4, p.239-245.

Haley, B.R., et al., 1976, Geologic map of Arkansas: U.S. Geol. Survey and Arkansas Geol. Comm., Scale 1:500,000.

Haley, B.R., and Stone, C.G., 1982, Structural framework of the Ouachita Mountains, Arkansas: Geol. Soc. Amer. Abst. with Programs, South-Central Section, v.14, no.3, p.113.

Hobbs, B.E., Means, D.W., and Williams, P.F., 1976, An outline of structural geology, John Wiley and Sons, New York, 571 p.

King, P.B., 1964, Interpretation of the Garden Springs area, Texas by the "down-structure" method of tectonic analysis: U.S. Geol. Survey Prof. Paper 501-B, p.B1-B8.

Lillie, R.L., et al., 1983, Crustal structure of the Ouachita Mountains, Arkansas: A model based on the integration of COCORP reflection profiles and regional geophysical data: Amer. Assoc. Petrol. Geol. Bull., v.67, n.6, p.907-931.

Lowe, D.R., 1985, Ouachita trough: Part of a Cambrain failed rift system: Geology, v.13, n.11, p.790-793.

Mackin, J.H., 1950, The down-structure method of viewing geologic maps: Jour. Geol., v.58, n.1, p.55-72.

Miser, H.D., 1959, Structure and vein quartz of the Ouachita Mountains of Oklahoma and Arkansas, in, Cline, L.M., et al., eds., The geology of the Ouachita Mountains, a symposium: Dallas and Ardmore Geol. Soc., P.30-43.

_____, and Purdue, A. H., 1929, Geology of the DeQueen and Caddo Gap quadrangles, Arkansas: U.S. Geol. Survey Bull.808, 195 p.

Ragan, D.M., 1973, Structural Geology, an introduction to geometrical techniques, 2nd edition, John Wiley and Sons, New York, 208 p.

Ramsay, J.G., 1976, Displacement and strain, Phil. Trans. R. Soc. Lond., A-283, p.3-25.

Roeder, D.H., 1973, Subduction and orogeny: Jour. Geophys. Res., v.78, p.5005-5021.

Soustek, P.G., 1979, Structural style of the Ouachita core in a portion of the McGraw Mountain quadrangle, Arkansas: M.S. Thesis, Southern Illinois University at Carbondale, 132p.

Stone, C.G., and Haley, B.R., 1984, A guidebook to the geology of the central and southern Ouachita Mountains, Arkansas: Ardkansas Geol. Commk. Guidebook 84-2, 131p.

Suppe, J., and Medwedeff, D.A., 1984, Fault-propagation folding: Geol. Soc. America Abs. with Programs, v.16, no.6, p.670.

Weber, J.C., 1987, Bedrock geology and structural analysis in portions of the Cossatot Mountains, Athens Plateau and Mazarn Basin, Pike and Montgomery counties, Arkansas: M.S. Thesis, Southern Illinois University at Carbondale, 112p.

_____, and Zimmerman, J., 1986, Structural geology of the central Cossatot Mountains, Benton uplift, Arkansas: Geol. Soc. Amer. Abst. with Programs, v.18, no.3, p.271.

Woodard, N.B., Boyer, S.E. and Suppe, J., 1985, An outline of balanced cross-sections, 2nd edition: Univ. of Tenn., Dept. of Geol. Sci., Studies in Geology-11, 170p.

Viele, G.W., 1973, Structure and tectonic history of the Ouachita Mountains, Arkansas, in, DeJong, K.A. and Scholton, R., eds., Gravity and Tectonics, John Wiley and Sons, New York, p.361-377.

_____,1979, Geologic map and cross-section, eastern Ouachita Mountains, Arkansas: Geol. Soc. Amer. Map and Chart Series, MC-28F, Scale 1:250,000.

Zimmerman, J., Roeder, D.H., Morris, R.C., and Evansin, D.P., 1982, Geologic section across the Ouachita Mountains, western Arkansas: Geol. Soc. Amer. Map And Chart Series, MC-28Q, Scale 1:250,000.

PROVENANCE OF THE JACKFORK SANDSTONE, OUACHITA MOUNTAINS, ARKANSAS AND EASTERN OKLAHOMA

By Steven E. Danielson[1], P. Kent Hankinson[2], Kendall D. Kitchings[3], and Alan Thomson[4]

[1] New Orleans, LA, [2] Atlanta, GA, [3] Chevron USA, New Orleans, LA,
[4] University of New Orleans, New Orleans, LA

ABSTRACT

The Jackfork Sandstone represents 6000 feet of Carboniferous flysch deposited in the Ouachita geosyncline in deep water by currents which flowed in a dominantly westward direction. Provenance has been difficult to establish because of the paucity of diagnostic minerals and framework grains. Monocrystalline quartz comprises as much as 96 percent of the framework grain population; with feldspar and mainly metamorphic and sedimentary rock fragments making up the rest.

Samples from widely-spaced outcrops throughout the frontal and southern Ouachitas in Arkansas and central Ouachitas in eastern Oklahoma were collected and over 150 thin sections were prepared. Detailed framework grain analysis showed monocrystalline quartz decreasing in amount to the south, with feldspar and lithic grains increasing in that direction.

Triangular Q_m-F-L_t diagrams and petrographic maps support the notion of a mature Illinois Basin source to the northeast, a less mature metamorphic and igneous source (Llanoria) to the south, and a source to the east which possibly routed sediment from the Ouachita/Appalachian orogen into the geosyncline.

INTRODUCTION

Purpose. The Jackfork Sandstone represents approximately 6000 feet of Carboniferous flysch deposited in the Ouachita geosyncline. The Jackfork has been tentatively subdivided by the Arkansas Geological Commission into three subequal mappable lithic units: lower, middle, and upper.

Facies distributions and paleocurrent data indicate a dominant westward transport of Jackfork siliciclastic sediment in an elongate, east-west oriented basin. Previous stratigraphic and petrographic analyses of Jackfork sandstones suggest possible sourcelands to the north, east, and/or south of the Ouachita trough (Klein, 1966; Briggs and Cline, 1967; Morris, 1974a, 1974b, 1977a; Graham et al, 1975, 1976; Owen and Carozzi, 1986). The purpose of this study was to determine if the framework grain composition of sandstones of the Jackfork Sandstone documents the existence of these various source areas and, if so, to determine to what extent each source area contributed sediment.

Provenance determinations of Jackfork sandstones are inconclusive and somewhat conjectural because the major Paleozoic tectonic elements south and east of the Ouachita trend no longer exist or are too deeply buried to examine. Nevertheless, the nature of the major positive tectonic elements can be inferred from other tectonic environments that have sandstone suites with framework grain compositions similar to those of the Jackfork sandstones. Using this approach, Klein (1966), Morris (1974a, 1974b, 1977a), Graham et al. (1975, 1976), among others, reasoned that the sublitharenites quartzarenites of the Jackfork resulted from contributions from two different

tectonic environments: (1) a stable cratonic interior provenance to the north-northeast, and (2) a recycled orogenic provenance to the south-southeast.

Approach. The approach used to accomplish our goal encompassed two steps: (1) collection of Jackfork sandstone samples from measured sections more or less equally spaced throughout the Ouachita Mountains, and (2) petrographic analysis.

Nineteen surface exposures of the Jackfork Sandstone-- seven in the lower Jackfork, Five in the middle Jackfork, and seven in the upper Jackfork -- were chosen for sampling. Each outcrop was measured, and the stratigraphic succession described using a standard format that recorded the thickness, grain sizes, and sedimentary structures encountered in each bed

The sampling procedure was designed to obtain sandstone samples with similar textures so that the data yielded from their petrographic analysis could be compared easily.

In addition, samples collected were believed to be as fresh as possible, in order to minimize problems with surface weathering.

Fifty-three thin sections were prepared from lower Jackfork samples, forty-eight from middle Jackfork samples and fifty-five from upper Jackfork samples. Each slide was stained with sodium cobaltinitrate in order to facilitate feldspar identification. At least 300 framework grains were counted in each slide.

The study was undertaken by three graduate students from the University of New Orleans; with S.E.D. responsible for the lower, K.D.K. responsible for the middle, and P.K.H. responsible for the upper Jackfork. The entire study was supervised by A.T.

PETROGRAPHY

Bokman (1953), Goldstein and Hendricks (1962), Klein (1966), Morris (1974b, 1977a), Morris, Proctor, and Koch (1979), and Owen and Carozzi (1986) describe the petrology of Jackfork sandstones. Jackfork sandstones are immature-submature quartz-arenites, sublitharenites, and subarkoses (using Folk's 1980 classification system). Framework grains in Jackfork sandstones are dominated by quartz, of which there are three types (Morris, 1977a): unstrained monocrystalline quartz, strained monocrystalline quartz, and polycrystalline quartz.

Monocrystalline quartz types are the most numerous, but they provide no indication of their provenance, although Bokman (1953) states that Jackfork quartz grains are elongate -- indicative of metasedimentary source (Bokman, 1952; Young, 1976). Of the polycrystalline quartz grains, finely polycrystalline quartz dominates (i.e., polycrystalline quartz grains containing more than three sub-crystals). Polycrystalline quartz grains generally exhibit textures indicative of a low-grade metamorphic or sedimentary source; they include stretched, mosaic, and equant recrystallized quartz, metaquartzite, and chert. Morris (1977a) noticed a greater abundance of polycrystalline quartz in the Jackfork Sandstone of the southern Ouachitas than in the Jackfork Sandstone of the frontal Ouachitas.

Recognized feldspars in Jackfork sandstones include twinned and untwinned plagioclase, orthoclase, microcline, and sanidine. Much of the feldspar has been altered or completely replaced by calcite, sericite, kaolinite, or iron oxide (Morris, 1977a).

Of the rock fragments, metamorphic types are the most abundant; they include mica schists, quartz-mica schists, phyllites, and chlorite schists. The schistose rock fragments consist of parallel aligned mica plates and varying amounts of elongate silt-size quartz crystals (Morris, 1977a). Some workers, such as Owen and Carozzi (1986), prefer to classify all polycrystalline quartz exhibiting metamorphic textures as metamorphic rock fragments.

Sedimentary rock fragments include shale, limestone, siltstone, sandstone, siliceous shale, and chert. Volcanic rock fragments are rare in Jackfork sandstones, the most common type being brown, devitrified glassed with minute feldspar laths (Morris, 1977a).

CATEGORIES USED	DESCRIPTION
QUARTZ (Q_m)	total monocrystalline quartz
Unst	unstrained quartz
Stra	strained quartz; undulose and polygonized quartz (undulosity >5°)
FELDSPAR (F)	total feldspar
Plag	plagioclase; twinned and untwinned
K-spar	all potassium feldspar minerals (rarely preserved in original state)
Inde	feldspars that are unidentifiable (as to type) because of extreme diagenetic alteration and/or replacement, but still exhibit relict features indicative of feldspar crystal morphology and/or cleavage; also includes oversized pore-spaces filled with kaolinite.
ROCK FRAGMENTS (L_t)	total lithic rock fragments
MRF	metamorphic rock fragments
Q_p	finely polycrystalline quartz (subcrystals >3) and all polycrystalline quartz exhibiting metamorphic textures; some of the descriptive subcategories used were: equant-recrystallized, stretched-elongate, bimodal-polycrystalline, metachert, and equant recrystallized with some platy minerals.
Schi	Chlorite and mica schist rock fragments
Phyl	phyllitic rock fragments
SRF	sedimentary rock fragments
Stst	siltstone
Shl	shale
Cht	chert
Oth	other sedimentary rock fragments
VRF	volcanic and hypabyssal rock fragments
URF/Unkn	unidentifiable rock fragments

TABLE 1 - *Framework grain categories.*

Muscovite, with minor biotite and chlorite, are the most common light accessory minerals. A stable mineral suite comprises the heavy minerals in Jackfork sandstones; zircon, magnetite-ilmenite, tourmaline, and rutile (Goldstein and Hendricks, 1962).

Texturally, Jackfork sandstones range from immature to submature. Morris (1974b) reports a mean grain size of 2.81 phi units with a standard deviation of 0.87 phi units. Bookman (1953) reports a mean grain size of 2.80 phi units with a standard deviation of 0.85 phi units. Bokman (1953) found no correlation between grain size and bed thickness, and Morris et al. (1979) found no correlation between grain size and facies type; however, the thin turbidite sandstones (<2-3 inches) rarely exceed the fine-grained sand-size range. Morris et al. (1979) did notice a slight decrease in mean grain size and increase in standard deviation of grain sizes from Arkansas to Oklahoma.

Framework grain categories used in point counting are listed in Table 1.

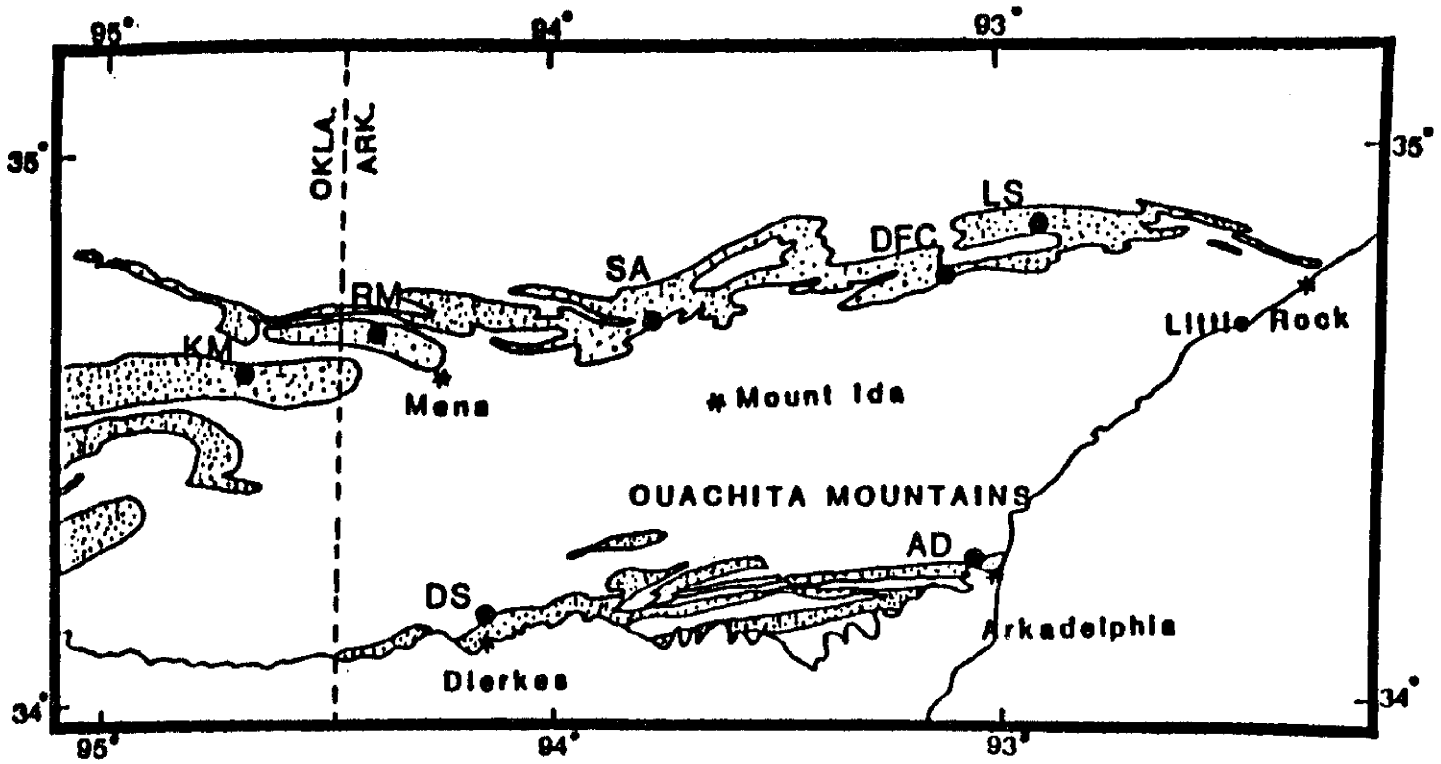

Figure 1 - *Lower Jackfork Sandstone exposures sampled. See Table 2 below for locality names. Stipple pattern indicates Jackfork Sandstone.*

NAME OF EXPOSURE	ABBREV.	COUNTY, STATE	S-T-R
Arkadelphia - DeGray	AD	Clark, AR	11-6S-20W
Dierks spillway	DS	Howard, AR	16-7S-29W
Dry Fork Creek	DFC	Perry, AR	23-2N-20W
Kiamichi Mountain	KM	Le Flore, OK	26-2N-25E
Lake Sylvia	LS	Perry, AR	29-3N-17W
Rich Mountain	RM	Polk, AR	13-1S-31W
Story - Aly	SA	Yell, AR	7-1N-23W

TABLE 2 - *List of lower Jackfork Sandstone exposures samples.*

LOWER JACKFORK SANDSTONE

Seven exposures of lower Jackfork Sandstone were described in detail and sampled. Fifty-three thin sections were prepared and point-counted. The exposures studied are shown in map view in Figure 1 and listed in Table 2.

The results of the thin-section analysis are shown by means of triangular diagram plots and appropriate maps. We have followed the ground rules laid down by Dickinson and Suczek (1977) and Dickinson (1985). Recalculated parameters derived from framework grain categories are listed in Table 3.

Figure 2 is a Monocrystalline quartz - feldspar - total lithics (Q_m-F-L_t) diagram. It indicates that rocks in the northern outcrop belt were derived from a craton interior source whereas many in the southern outcrop belt had a recycled orogen source.

Q_m	=	monocrystalline quartz
F	=	feldspar
L_t	=	rock fragments (RF)
Q_t	=	all quartz
F	=	feldspar
L	=	RF - (polycrystalline quartz + chert)
SRF	=	sedimentary rock fragments
VRF	=	volcanic rock fragments
MRF	=	metamorphic rock fragments

TABLE 3 - *Recalculated parameters derived from framework grain categories.*

The sedimentary - volcanic - metamorphic rock fragments (SRF-VRF-MRF) diagram shown in Figure 3 demonstrates that rock fragments are principally of metamorphic and sedimentary origin, with the former predominating. It also shows sedimentary rock fragments to be more abundant in the northern outcrop belt and metamorphic rock fragments more abundant in the south.

Figure 4 shows in map view monocrystalline quartz as a percent of Q_m-F-L_t.

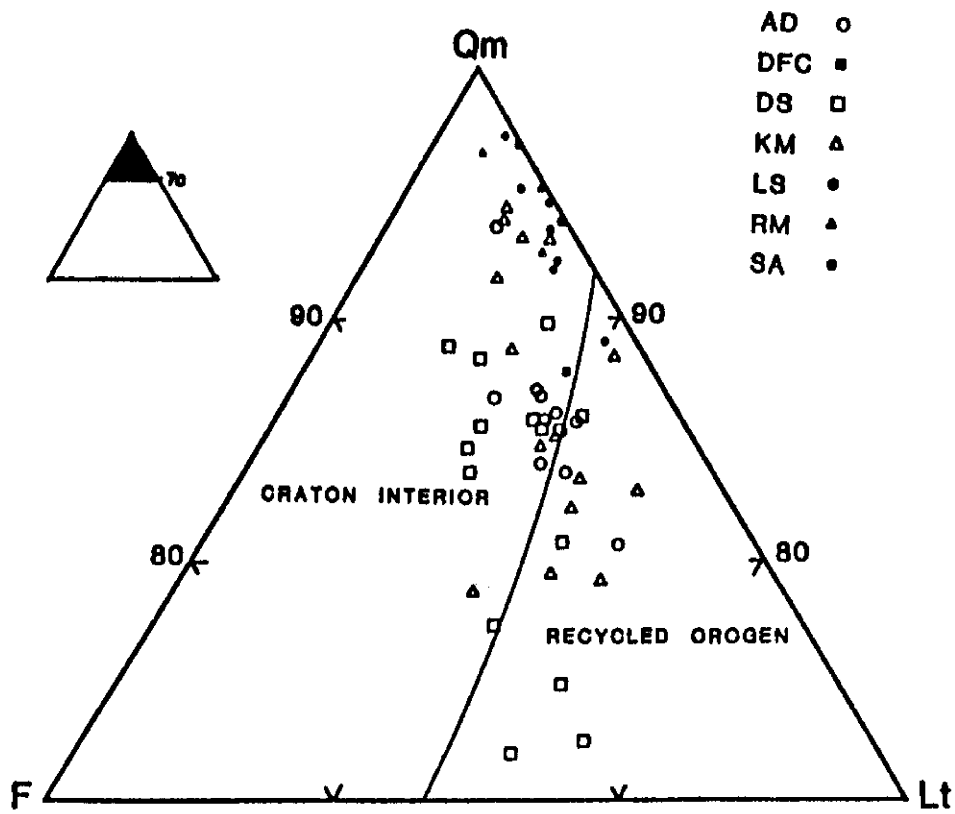

Figure 2 - *Q_m-F-L_t diagram. Lower Jackfork.*

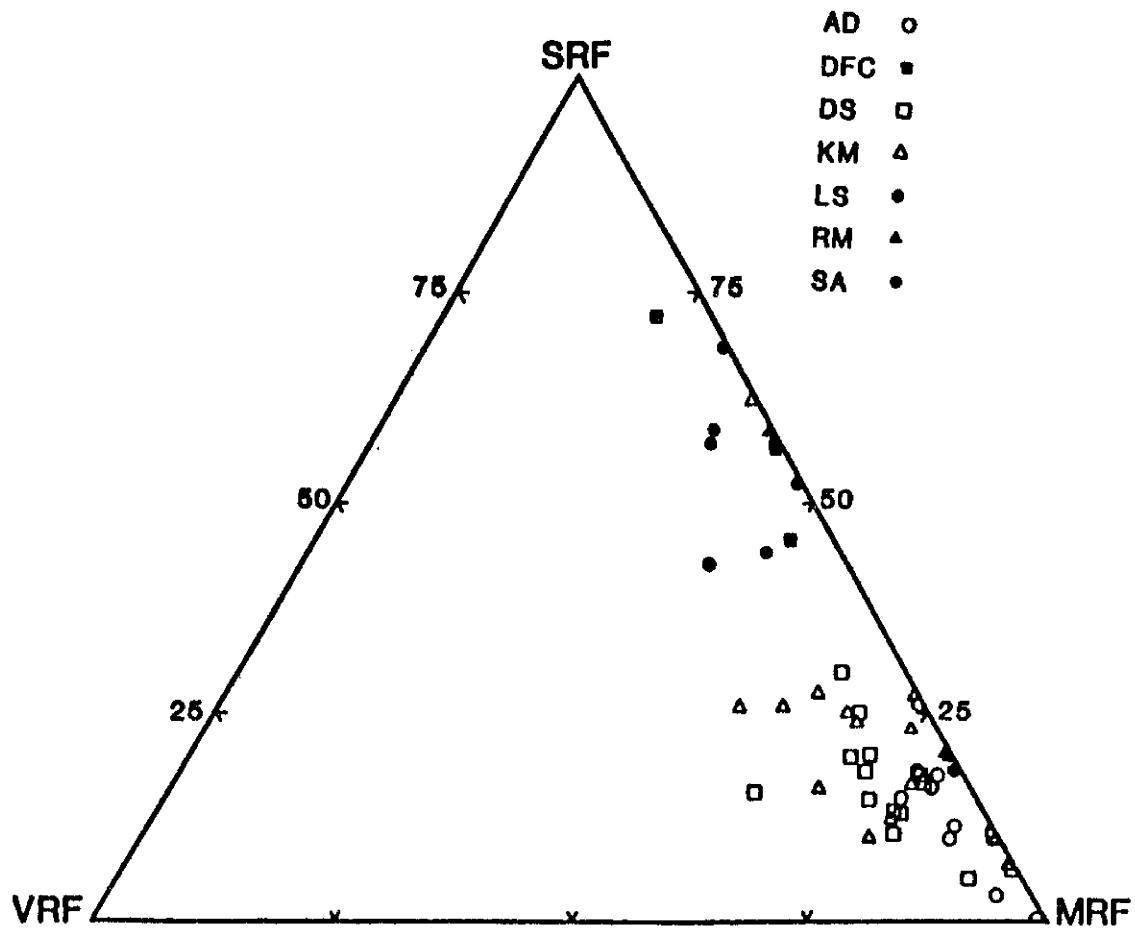

Figure 3 - *SRF-VRF-MRF diagram. Lower Jackfork.*

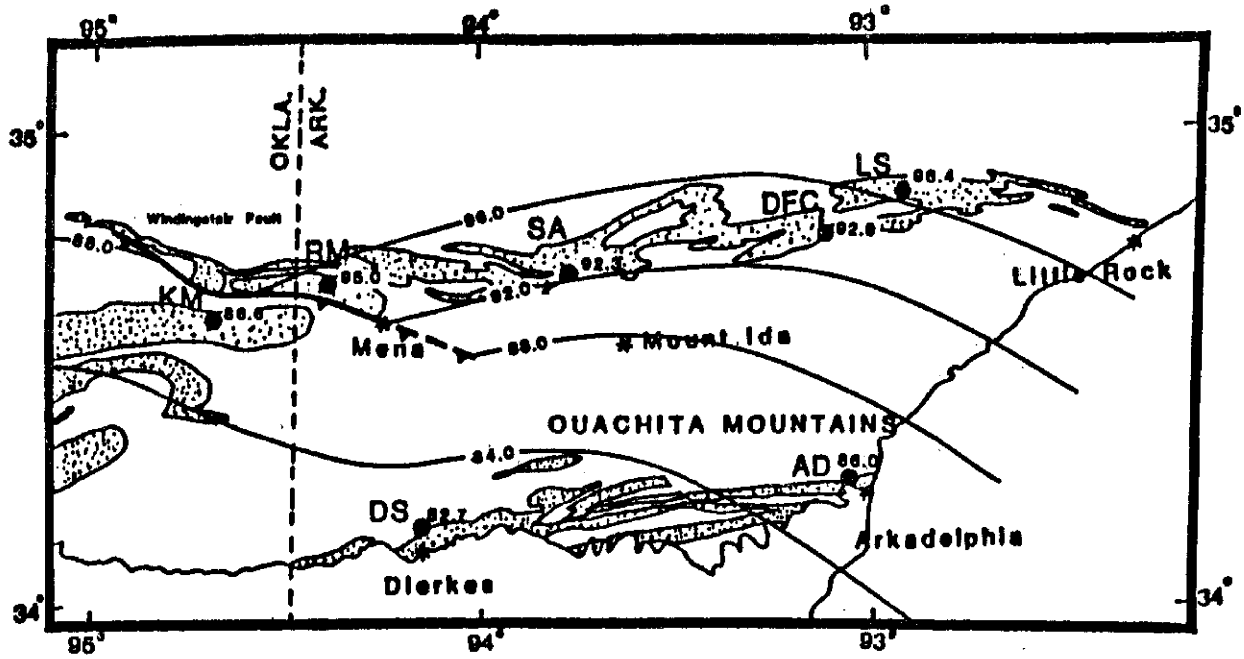

Figure 4 - *Petrographic map of monocrystalline quartz as a percent of Q_m-F-L_t Lower Jackfork.*

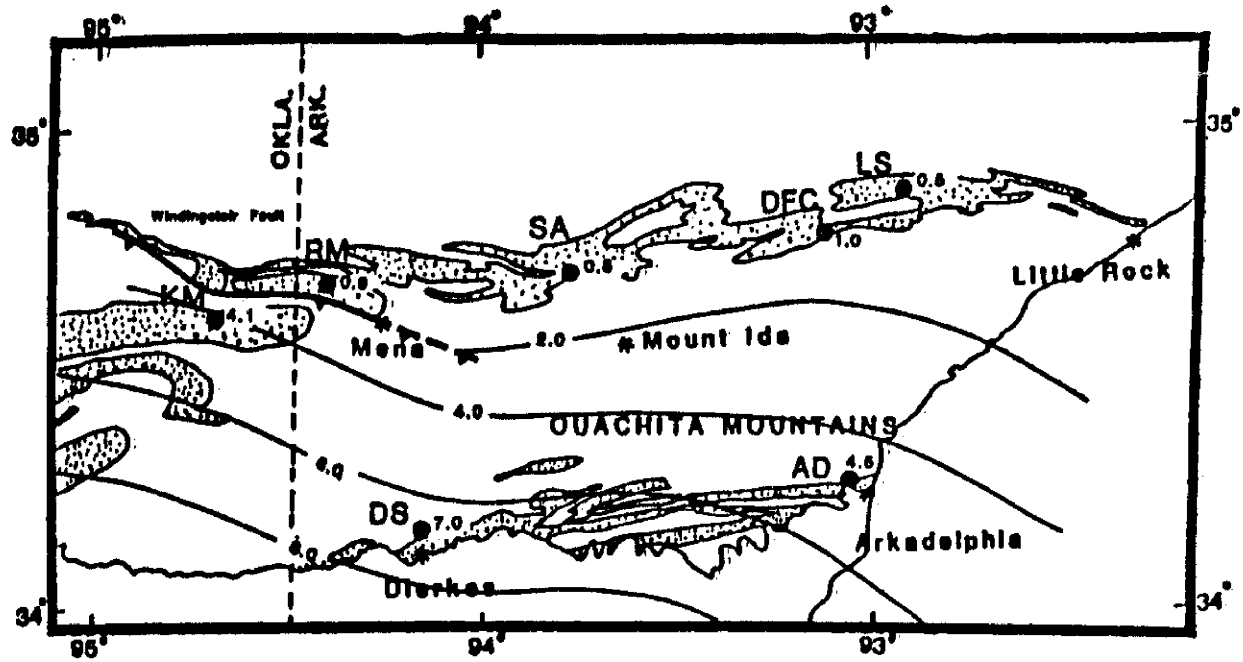

Figure 5 - *Petrographic map of feldspar as a percent of Q_m-F-L_t. Lower Jackfork.*

Monocrystalline quartz diminishes gradually toward the south. This figure also illustrates the dominance of monocrystalline quartz as a framework component.

Figure 5 shows in map view feldspar as a percent of Q_m-F-L_t. The higher feldspar content in the southern outcrop belt is apparent. In a similar fashion lithic fragments increase toward the south as seen in Figure 6, which is a map view of lithic fragments as a percent of Q_m-F-L_t.

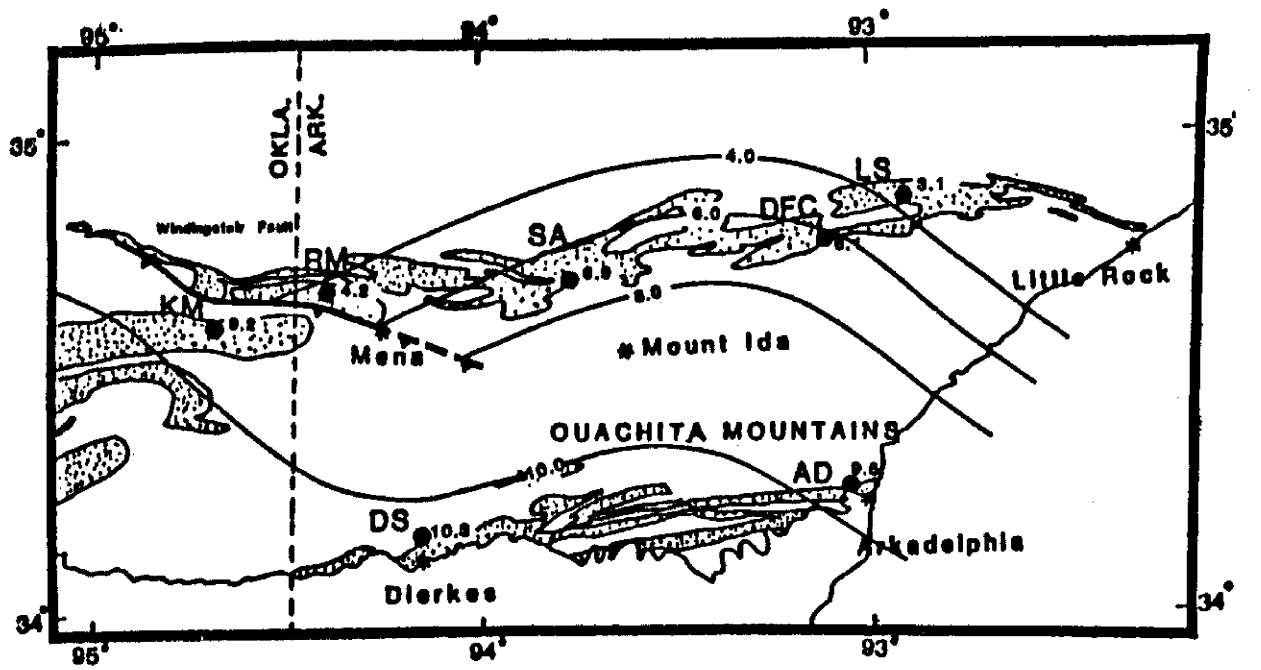

Figure 6 - *Petrographic map of lithic fragments as a percent of Q_m-F-L_t. Lower Jackfork.*

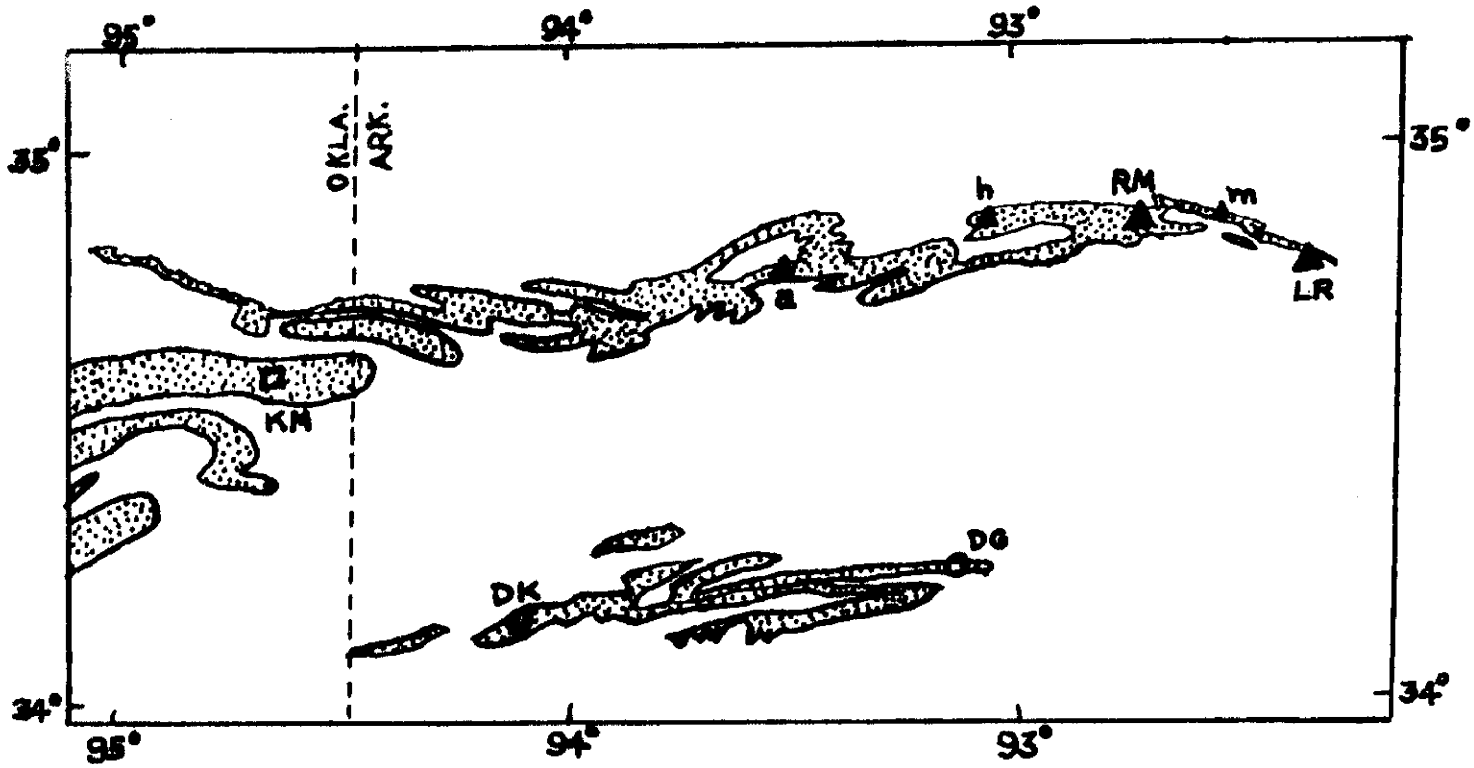

Figure 7 - *Middle Jackfork Sandstone exposures sampled. See Table 4 (below) for locality names.*

NAME OF EXPOSURE	ABBREV.	COUNTY, STATE	S-T-R
DeGray-Arkadelphia	DG	Clark, AR	15-6S-20W
Dierks Spillway	DK	Howard, AR	28-7S-29W
Kiamichi Mountain	KM	Le Flore, OK	28,32-2N-25E
Little Rock	LR	Pulaski, AR	5,6-1N-12W
Round Mountain	RM	Perry, AR	1-2N-17W
Aly	a	Yell, AR	6-1N-23W
Hollis	h	Perry, AR	11-2N-20W
Maumelle	m	Pulaski, AR	28-3N-15W

TABLE 4 - *List of middle Jackfork Sandstone exposures sampled.*

MIDDLE JACKFORK SANDSTONE

Five exposures of middle Jackfork Sandstone were described in detail and sampled. In addition, samples were collected from three smaller outcrops in the frontal or northern belt. A total of 48 thin sections were prepared and point-counted. A map of the exposures studied is shown in Figure 7, and they are listed in Table 4.

Figure 8 is a Q_m-F-L_t diagram for all middle Jackfork samples. Large and small black triangles represent localities in the frontal Ouachitas in Arkansas, open circles represent southern Ouachita localities, and the one open square is from a central Ouachitas locality in Oklahoma. As was seen in a similar diagram of lower Jackfork samples (Fig. 2), rocks in the northern or frontal zone were all derived from a craton interior source. In contrast to the lower Jackfork, however, practically no middle

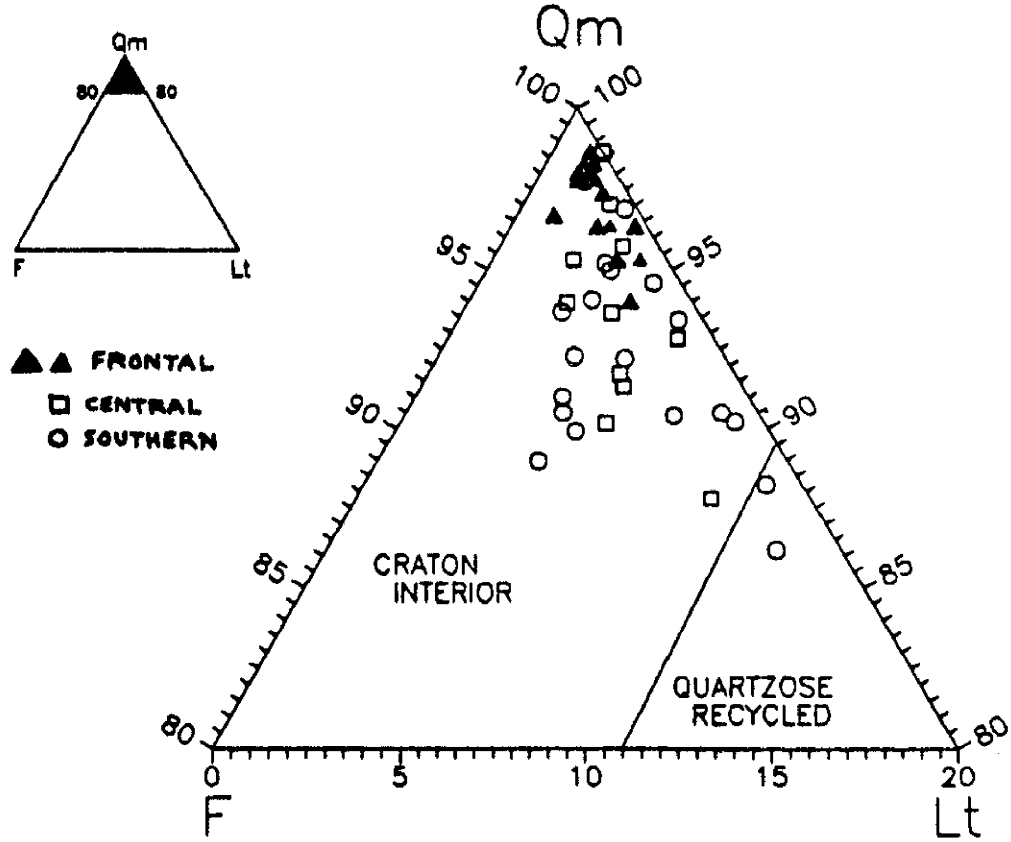

Figure 8 - *Q_m-F-L_t diagram. Middle Jackfork.*

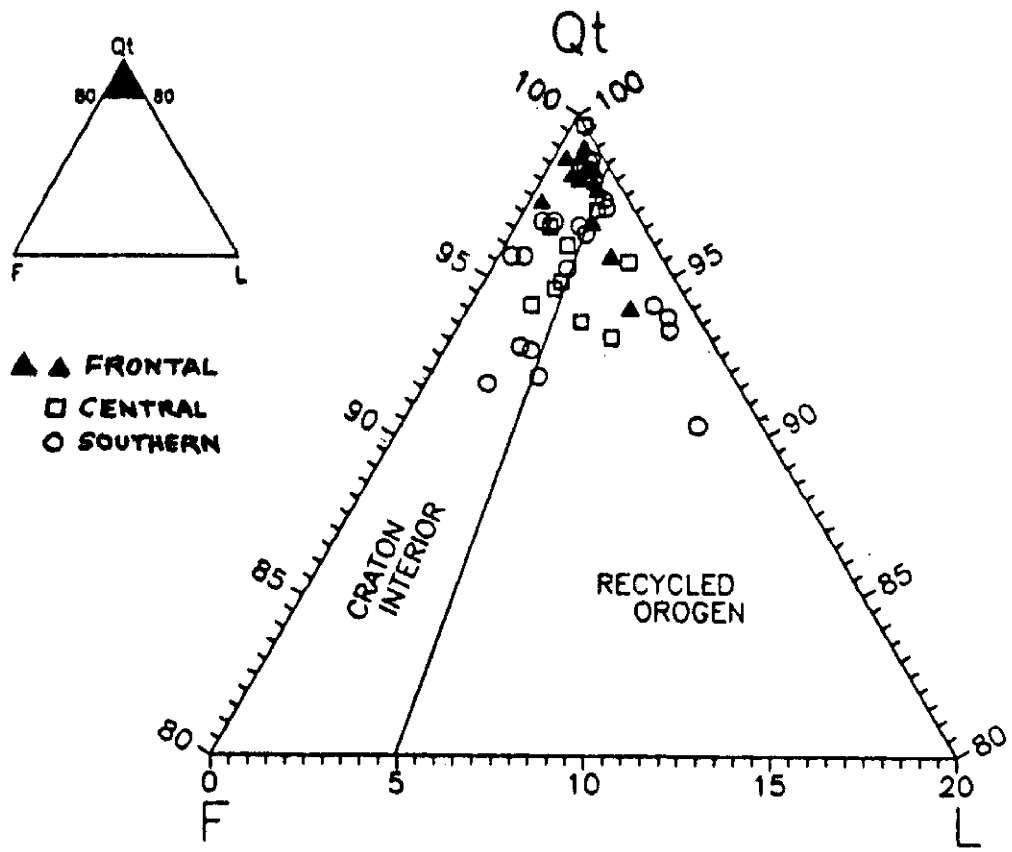

Figure 9 - *Q_t-F-L diagram. Middle Jackfork.*

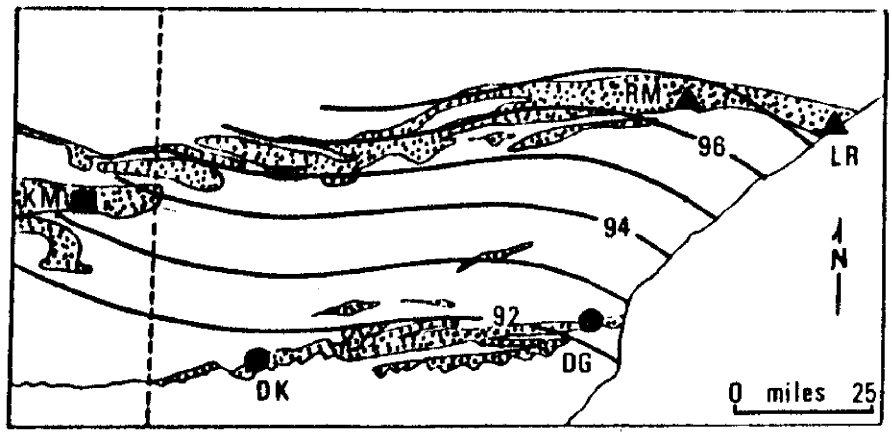

Figure 10 - *Petrographic map of monocrystalline quartz as a percent of total framework. Middle Jackfork.*

Jackfork samples had a recycled quartzose or recycled orogen source.

Figure 9 is a Total quartz - feldspar - lithics (Q_t-F-L) diagram which illustrates the dominance of quartz as a framework grain constituent. Samples from the frontal Ouachitas again show a craton interior source; however, this diagram is not particularly effective in discriminating sources.

A map view in Figure 10 shows total monocrystalline quartz as a percent of total framework. Monocrystalline quartz content remains relatively uniformly high from the frontal to the southern Ouachitas.

Another map view in Figure 11 shows total feldspar as a percent of total framework. Feldspar content in the middle Jackfork is low in contrast to that in the lower Jackfork.

Finally, Figure 12 is a map view showing total lithic fragments as a percent of total framework. Again, this component is considerably less here than in the lower Jackfork

UPPER JACKFORK SANDSTONE

Seven exposures of upper Jackfork Sandstone were described in detail and sampled. A total of 55 thin sections were prepared and point-counted. The exposures studied are shown in map view in Figure 13 and listed in Table 5.

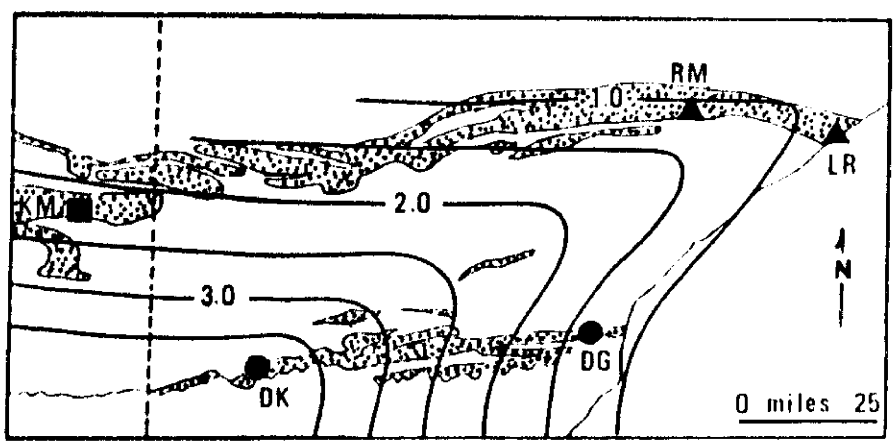

Figure 11 - *Petrographic map of total feldspar as a percent of total framework. Middle Jackfork.*

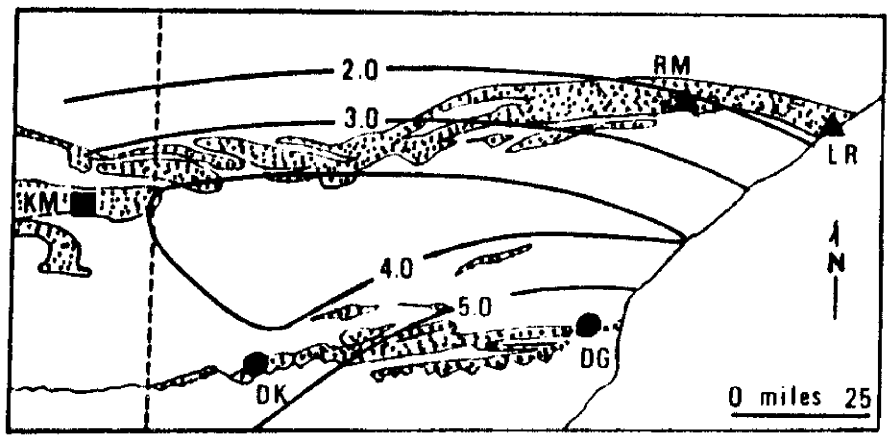

Figure 12 - *Petrographic map of lithic fragments as a percent of total framework. Middle Jackfork.*

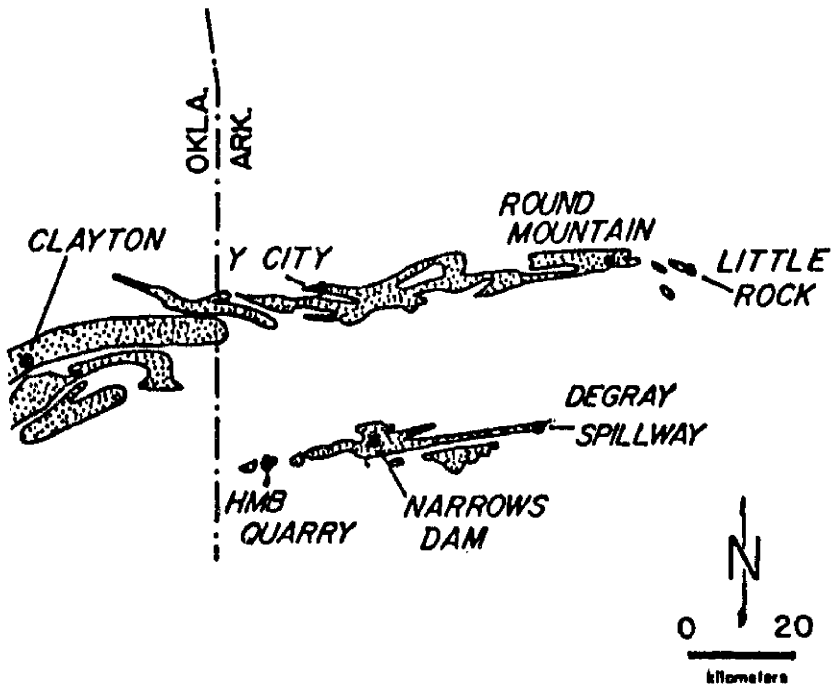

Figure 13 - *Upper Jackfork Sandstone exposures sampled. See Table 5 (below) for locality names.*

NAME OF EXPOSURE	ABBREV.	COUNTY, STATE	S-T-R
Clayton	C	Pushmataha, OK	2-1S-19E
DeGray Spillway	D	Clark, AR	14-6S-20W
HMB Quarry	H	Sevier, AR	31-7S-21W
Little Rock (north)	L	Pulaski, AR	22-2N-13W
Narrows Dam	N	Pike, AR	13-7S-26W
Round Mountain	R	Perry, AR	36-3N-17W
Y City	Y	Scott, AR	15-1N-29W

TABLE 5 - *List of upper Jackfork Sandstone exposures sampled.*

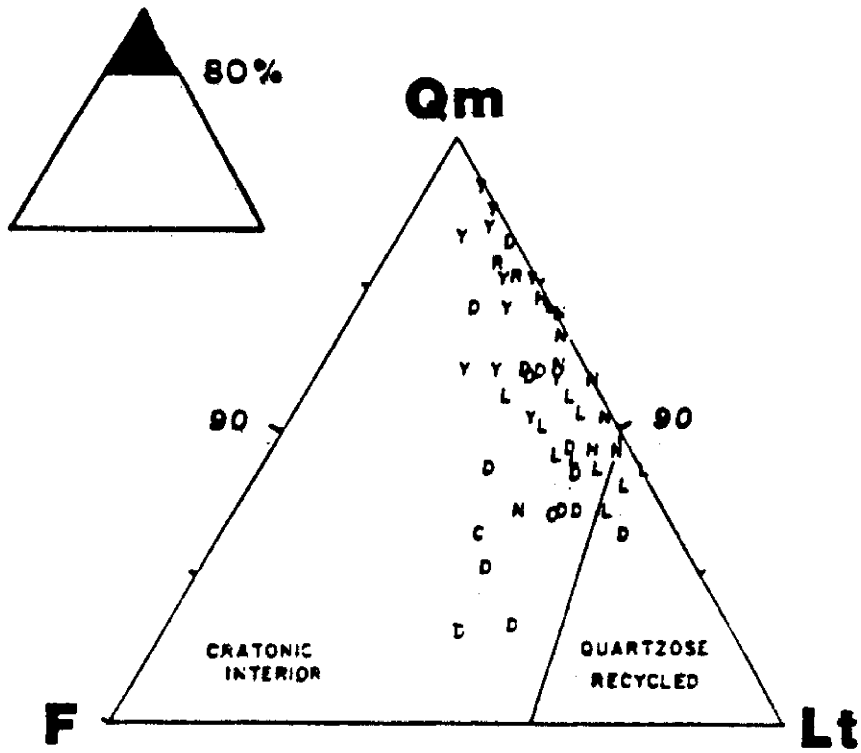

Figure 14 - *Q_m-F-L diagram. Upper Jackfork.*

Figure 14 is a Q_m-F-L_t diagram for all upper Jackfork samples. Rocks from the frontal Ouachitas plot closer to the Q_m pole than those from the southern Ouachitas, and plot even further away from the Q_m pole than middle Jackfork samples (Fig. 8).

A Q_m-F-L_t diagram for the same samples (Fig. 15) shows a preponderance of samples falling in the recycled orogenic field, in contrast to a similar plot of middle Jackfork rocks (Fig. 9).

Total monocrystalline quartz a a percent of total framework is shown in map view in Figure 16. The component gradually decreases toward the south.

Total feldspar as a percent of total framework is shown in map view in Figure 17. The data were not contoured, but two points are significant; viz., 12.0% and 9.7% feldspar at Clayton and DeGray Spillway, respectively. The Clayton value is based on only two thin sections, and, hence, its importance and source can only be speculated upon. The DeGray Spillway value, however, is the average of fourteen thin sections, and is believed to be significant an indication of a southern source.

Total lithic fragments as a percent of total framework is shown in map view in Figure 18. An increase in this component toward the south is again seen here, as it was in the lower and middle Jackfork (Figs. 6 and 12).

ANALYSIS OF PROVENANCE DIAGRAMS

Many workers have correlated sandstone varieties with specific types of source terranes and basins associated with certain plate tectonic regimes (Crook, 1974; Schwab, 1975; Graham et al., 1976; Dickinson and Suczek, 1979; Dickinson and Valloni, 1980; Valloni and Maynard, 1981; Dickinson, 1982; Dickinson et al., 1983). In most of these studies, framework composition is determined quantitatively by point-count analysis, grouped into appropriate end member units (i.e., Q_m-Q_p-L_t etc.) and plotted on triangular diagrams. This procedure is potentially useful for delineating the paleotectonic setting of first-

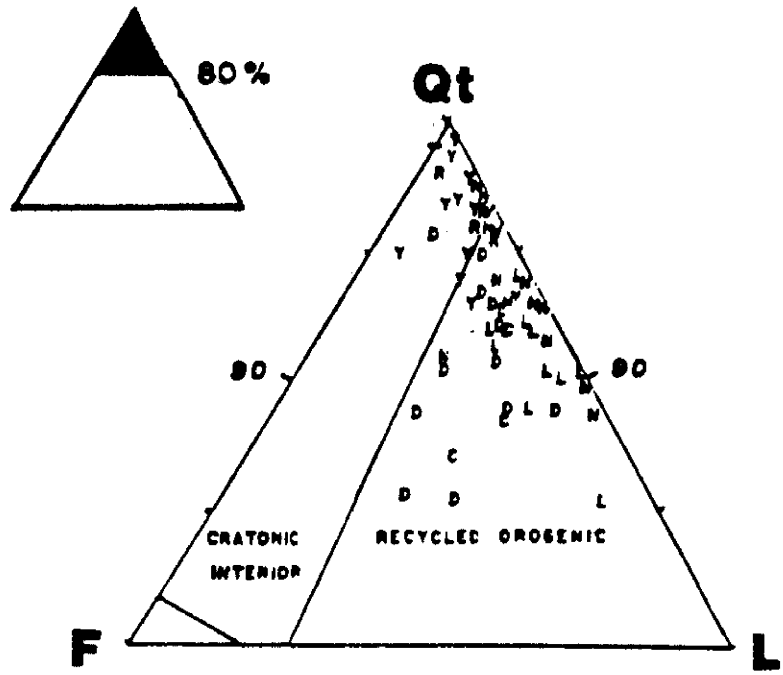

Figure 15 - *Q_t-F-L diagram. Upper Jackfork.*

cycle sandstones; however, usage of these triangles to correlate paleotectonics and polycyclic sandstone composition has pitfalls (Mack, 1984;l Dickinson et al., 1983).

It is a well known fact that sedimentological and weathering processes may alter detrital framework mineralogy (Blatt, 1967; Basu, 1976; Dickinson, 1983; Mack, 1984). Graham et al. (1976) demonstrated that depositional reworking of lithic-rich detritus would probably yield a more quartzose sediment after extensive transportation and reworking. Thorough reworking is suspected of

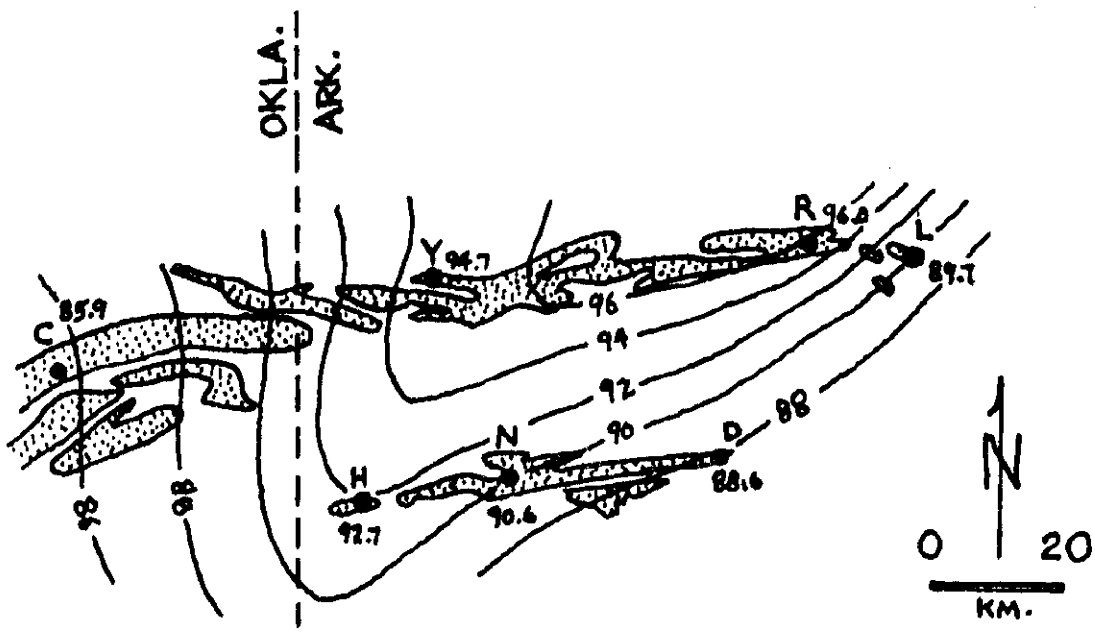

Figure 16 - *Petrographic map of monocrystalline quartz as a percent of total framework. Upper Jackfork.*

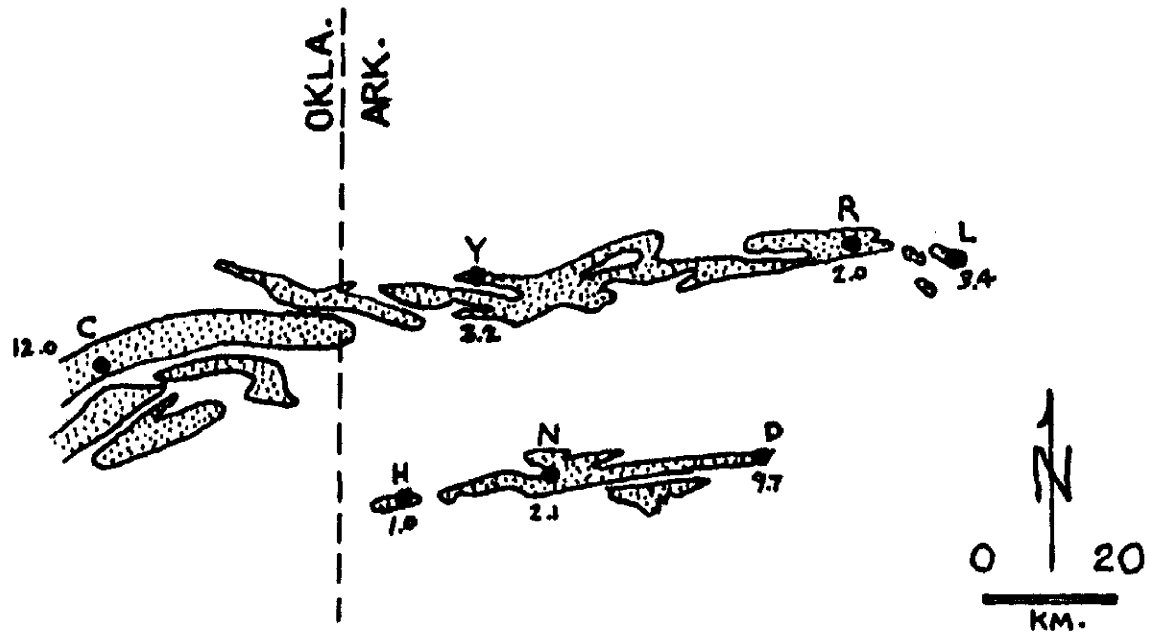

Figure 17 - *Petrographic map of feldspar as a percent of total framework. Upper Jackfork.*

Carboniferous Black Warrior sediments (Parkwood-Hartselle-Pottsville) before they advanced westward toward the Ouachita rough (Thomas, 1972, 1974; Thomas and Mack, 1982; Miller, 1985; Owen and Carozzi, 1986). Therefore, it is possible that a significant proportion of Jackfork sediments are products of intense recycling. As a result, points plotted on triangular diagrams may indicate anomalously high maturity deviating considerably from that of the original source rock. For instance, in the Q_m-F-L_t diagrams constructed for this study (Figs. 2, 8, 14), most sandstones plotted in the cratonic interior field,

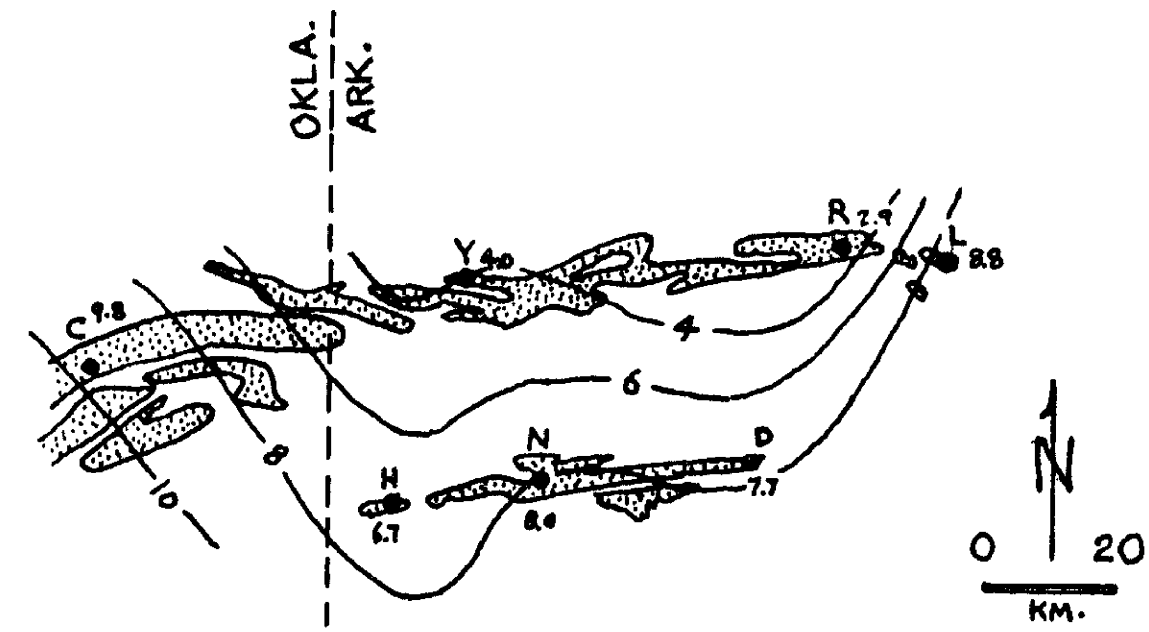

Figure 18 - *Petrographic map of lithic fragments as a percent of total framework. Upper Jackfork.*

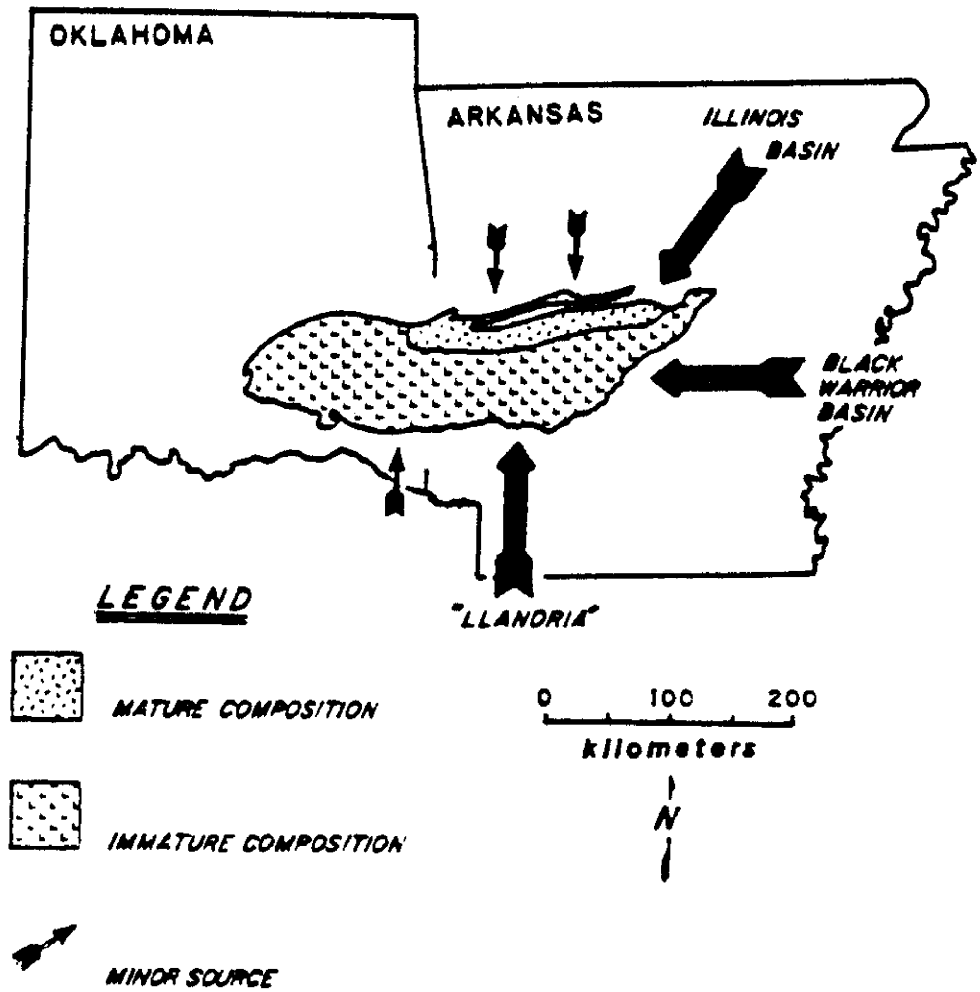

Figure 19 - *Inferred dispersal of sediment into the Ouachita geosyncline during Jackfork time.*

implying derivation from exposed shield areas and/or silica-enriched passive margin sequences (Crook, 1974; Schwab, 1975). Only twenty samples out of more than 150 had the compositional range of Dickinson's quartzose recycled field, which represents provinces such as Collision orogens and foreland uplifts (Dickinson and Suczek, 1979; Dickinson, 1985). It does not seem logical that almost all upper Jackfork samples were derived from the cratonic interior since petrographic maps suggest source(s) south and/or southeast of the Ouachita basin.

Outcrop weathering may have also modified detrital mineralogy to a lesser degree. For instance, kaolinite replacement of feldspar is apparent in many thin sections.

Other problems are more inherent in the nature of the diagrams themselves. Tectonic fields delineated by Dickinson and Suczek (1979) and later revised by Dicknson et al. (1983) land Dickinson (1985) are bounded by empirically-derived subdivisional lines. Tectonic inferences made about points that plot near or on these lines should not necessarily be considered conclusive (Dickinson et al., 1983). At best, it may be said that points near lines separating two fields have affinities for both.

INFERRED SOURCE AREAS

Early geologists in the Ouachita Mountains, most notably Miser (1921, 1934) and Harlton (1934), proposed a southern

provenance for the Jackfork Sandstone based on the occurrence in the Jackfork Sandstone in the southern Ouachitas of a greater sandstone/shale ratio, thicker stratigraphic section, and numerous pebbly sandstones, The proposed landmass, termed Llanoria, supposedly existed in Louisiana and Texas. Bokman (1953) argued for a southern provenance for Jackfork strata; his proposed source area consisted of a northward-migrating foldbelt composed of low-grade metamorphosed sedimentary rocks.

With the recognition of a westward dispersal direction of Jackfork sediment (determined from paleocurrent indicators and facies changes), eastern entry points into the submarine fan complex (eastern source areas) were proposed by Goldstein and Hendricks (1962), Briggs and Cline (1967), Morris (1971a, 1974a), Thomson and LeBlanc (1975), and Stone and McFarland (1981), among many others.

Triangular diagrams and petrographic contour maps delineating geographical lateral variation in Jackfork composition appear to support points of entry along the southern, eastern, and northeastern margins of the Carboniferous Ouachita trough. Jackfork detrital modes manifest their lowest maturity in sandstones collected from southern and northeastern sample localities, whereas mature assemblages of unstrained quartz with minor unstable lithic populations dominate the northwest and north-central portions of the study area.

Comparisons between lower, middle, and upper Jackfork triangular diagrams and petrographic maps show no striking differences. Monocrystalline quartz content decreases systematically in a southward direction in all three. Middle Jackfork rocks have somewhat lower percentages of feldspar and lithic fragments than lower and upper Jackfork rocks. The middle Jackfork section also has a much lower sand/shale ratio (a property which allows the three-part subdivision of the Jackfork). It is believed the middle Jackfork represents a time of increased transgression across the shelf areas to the north. This would lead to a diminishing transport of sand to the basin from all sources, and would also explain the decrease in feldspar and lithic fragments from the south.

Jackfork sandstones display framework compositions principally similar to their less mature Carboniferous counterparts of the Eastern Interior basin and north-central Alabama (Siever, 1957; Potter and Pryor, 1961; Pryor and Sable, 1974; Wanless, 1975; Mack et al., 1981, 1983; Miller, 1985). Therefore, within the context of previous Jackfork provenance studies, it may be argued that dispersal directions implicit in the results of this investigation plausibly support sources from the Illinois basin (Morris, 1971a; Graham et al., 1975, 1976; Pryor and Sable, 1974) and Black Warrior Basin (Morris, 1971a; Graham et al., 1975, 1976; Miller, 1985; Owen and Carozzi, 1986). In addition, a Llanoria-type source to the south can also be supported by lab and field observations. Petrographic maps made for this study show that rock fragments, constituents thought to be especially common in rocks deposited adjacent to their source area (Cleary and Conolly, 1971; Mann and Cavaroc, 1973; Abbott and Peterson, 1978), are most abundant along the southern Ouachitas. In addition, locally coarse conglomeratic sandstones were observed at several localities along the southern outcrop belt.

Estimation of proportional contributions from each source would be unrealistic using the results acquired herein. Miller (1985) has indicated that use of luminescence techniques does not aid in distinguishing between sediments derived from passive and active tectonic provenances; however, it is possible to distinguish between sandstones deposited in different active tectonic settings. For the purposes of this study, it will suffice to assert that intrabasinal trends in petrography support the dispersal of mature Carboniferous polycyclic detritus from the Eastern Interior and Black Warrior basins into the Ouachita trough during Jackfork time. It is also reasonable to acknowledge at least a partial contribution from a southern Llanoria-type source.

Of the three source areas cited herein, the one most difficult to reconcile with the data is the Black Warrior basin to the east. One of (SED) believes, as do Owens and Carozzi (1986), that there is no need to call upon the

Black Warrior basin to act as a conduit for sediment from the Ouachita/Appalachian orogen, as suggested by Graham et al. (1975, 1976).

The inferred dispersal of sediment into the Ouachita geosyncline during Jackfork time is shown in Figure 19.

ACKNOWLEDGMENTS

This overall study could not have been completed without the very generous financial support of the Arkansas Geological Commission and its Director, Norman F. Williams. Additional funding was supplied by the Department of Geology and Geophysics, University of New Orleans.

Very special thanks are due Charles G. Stone of the Arkansas Geological Commission who gave unselfishly of his time and expertise in orienting all of us in the right direction. This study could in "no way" have been completed without his help. He also kindly reviewed the manuscript.

REFERENCES

Abbott, P. L., and G. L. Peterson, 1978, Effects of abrasion durability on conglomerate clast populations: Examples from Cretaceous and Eocene conglomerates of the San Diego area, California: Jour. Sed. Petrology, v. 48, p. 31-42.

Basu, A., 1976, Petrology of Holocene fluvial sand derived from plutonic source rocks: Implications to paleoclimatic interpretation: Jour. Sed. Petrology, v. 46, p. 694-709.

Bokman, J. W., 1952, Clastic quartz particles as indices of provenance: Jour. Sed. Petrology, v. 22, p. 17-24.

_____, 1953, Lithology and petrology of the Stanley and Jackfork Formation: Jour. Geology, v. 61, p. 152-170.

Briggs, Geoffrey and L. M. Cline, 1967, Paleocurrents and source areas of the Late Paleozoic sediments of the Ouachita Mountains, southeastern Oklahoma: Jour. Sed. Petrology, v. 37, p. 985-1000.

Blatt, H., 1967, Provenance determinations and recycling of sediments: Jour. Sed. Petrology, v. 37, p. 1031-1044.

Cleary, W. S., and J. R. Conolly, 1971, Distribution and genesis of quartz in a Piedmont-coastal plain environment: Geol. Soc. America Bull., v. 82, p. 2755-2766.

Crook, K. A. W., 1974, Lithogenesis of geotectonics: The significance of compositional variation in flysch arenites (graywackes) in R. H. Dott and R. H. Shaver (eds.), Modern and ancient geosynclinal sedimentation: Soc. Econ. Paleontologists and Mineralogists Spec. Pub. No. 19, p. 304-310.

Dickinson, W. R., 1982, Compositions of sandstones in circum-Pacific subduction complexes and fore-arc basins: Am. Assoc. Petroleum Geologists Bull., v. 66, p. 121-137.

_____, 1985, Interpreting provenance relations from detrital modes of sandstones, in G. G. Zuffa (ed.), Provenance of Arenites: Reidel Publishing Co., Dordrecht, Holland, p. 333-361.

_____, and C. A. Suczek, 1979, Plate tectonics and sandstone compositions: Am. Assoc. Petroleum Geologists Bull., v. 63, no. 2, p. 2164-2182.

_____, L. S. Beard, G. R. Brakenridge, J. L. Erjavec, R. C. Ferguson, K. F. Inman, R. A. Knepp, F. A. Lindberg, and P. T. Ryberg, 1983, Provenance of North American Phanerozoic sandstones in relation to tectonic setting: Geol. Soc. America Bull., v. 94, p. 222-235.

_____, and R. Valloni, 1980, Plate settings and provenance of sands in modern ocean basins: Geology, v. 8, p. 82-86.

Folk, R. L., 1980, Petrology of Sedimentary Rocks, Hemphill Pub. Co., Austin, Tex., 183 p.

Godstein, A. R., Jr., and T. A. Hendricks, 1962, Late Mississippian and Pennsylvanian sediments in Ouachita Facies, Oklahoma, Texas, and Arkansas, in C. C. Branson (ed.), Pennsylvanian Systems in the United States: Am. Assoc. Petroleum Geologist, p. 385-430.

Graham, S. A., W. R. Dickinson, and R. V. Ingersoll, 1975, Himalayan-Bengal model for flysch dispersal in the Appalachian-Ouachita systems: Geol. Soc. American Bull., v. 86, p. 273-286.

_____, R. V. Ingersoll, and W. R. Dickinson, 1976, Common provenance for lithic grains in Carboniferous sandstones from Ouachita Mountains and Black Warrior Basin: Jour. Sed. Petrology, v. 46, p. 620-632.

Harlton, B. H., 1934, Carboniferous stratigraphy of the Ouachitas -- Special study of the Bendian: Am. Assoc. Petroleum Geologists Bull., v. 18, p. 1018-1049.

Klein, G. D., 1966, Dispersal and petrology of sandstones of Stanley-Jackfork boundary, Ouachita fold belt, Arkansas and Oklahoma: Am. Assoc. Petroleum Geologists Bull., v. 50, p. 308-326.

Mack, G. H., 1984, Exceptions to the relationship between plate tectonics and sandstone composition: Jour. Sed. Petrology, v. 54, p. 212-220.

_____, C. W. James, and W. A. Thomas, 1981, Orogenic provenance of Mississippian sandstones associated with southern Appalachian-Ouachita orogen: Am. Assoc. Petroleum Geologists Bull., v. 65, no. 8, p. 1444-1456.

_____, W. A. Thomas, and C. A. Horsey, 1983, Composition of Carboniferous sandstones and tectonic framework of southern Appalachian-Ouachita orogen: Jour. Sed. Petrology, v. 53, no. 3, p. 931-946.

Mann, W. R., and V. V. Cavaroc, 1973, Composition of sand released from three source areas under humid, low relief weathering in the North Carolina piedmont: Jour. Sed. Petrology, v. 43, p. 870-881.

Miller, M. E., 1985, The use of quartz grain cathodoluminescent colors for interpreting the provenance of the Jackfork Sandstone, Arkansas: unpublished Master's Thesis, University of Cincinnati, 145 p.

Miser, H. D., 1921, Llanoria, the Paleozoic land area in Louisiana and eastern Texas: Am. Jour. Sci., 5th ser., v. 2, p. 61-69.

_____, 1934, Carboniferous rocks of Ouachita Mountains, Am. Assoc. Petroleum Geologists Bull. v. 18, p. 971-1009.

Morris, R. C., 1971a, Stratigraphy and sedimentology of the Jackfork Group, Arkansas: Am. Assoc. Petroleum Geologists Bull., v. 55, p. 387-402.

_____, 1974a, Sedimentary and tectonic history of the Ouachita Mountains, in W. R. Dickinson (ed.), Tectonics and Sedimentation: Soc. Econ. Paleontologists and Mineralogists Spec. Publ. 22, p. 120-142.

_____, 1974b, Carboniferous rocks of the Ouachita Mountains, Arkansas - A study of facies patterns along the unstable slope and axis of a flysch trough, in G. Briggs (ed.), Symposium on the Carboniferous rocks of the southeastern United States: Geol. Soc. America Spec. Paper 148, p. 241-279.

_____, 1977a, Petrography of Stanley-Jackfork Sandstones, Ouachita Mountains, Arkansas, in C. G. Stone (ed.), Symposium on the Geology of the Ouachita Mountains: Ark. Geol. Comm., p. 146-157.

_____, K. E. Proctor, and M. R. Koch, 1979, Petrology and diagenesis of deep-water sandstones, Ouachita Mountains, Arkansas and Oklahoma, in Scholle, P. A. and Schluger, P. R. (eds.), Aspects of Diagenesis: Soc. Econ. Paleontologists and Mineralogists Spec. Publ. 26, p. 263-269.

Owen, M. R., and A. V. Carozzi, 1986, Southern provenance of upper Jackfork Sandstone, southern Ouachita Mountains: Cathodoluminescence petrology: Geol. Soc. America Bull., v. 97, p. 110-115.

Potter, P. E., and W. A. Pryor, 1961, Dispersal centers of Paleozoic and later clastics of the upper Mississippian Valley and adjacent areas: Geol. Soc. America Bull., v. 72, p. 1195-1250.

Pryor, W. A., and E. G. Sable, 1974, Carboniferous of the Eastern Interior basin: Geol. Soc. America Special Paper 148, v. 27, no. 4, p. 281-313.

Schwab, F. L., 1975, Framework mineralogy and chemical composition of continental margin-type sandstone: Geology v. 3, p. 487-490.

Siever, Raymond, 1957, Pennsylvanian sandstones of the eastern interior coal basin: Jour. Sed. Petrology, v. 27, p. 227-250.

Stone, C. G, and J. D. McFarland, III, 1981, Field guide to the Paleozoic rocks of the Ouachita Mountains and Arkansas Valley provinces, Arkansas: Arkansas Geol. Comm. Guidebook 81-1, 140 p.

Thomas, W. A., 1972, Regional Paleozoic stratigraphy in Mississippi between Ouachita and Appalachian Mountains: Am. Assoc. Petroleum Geologists Bull., v. 56, p. 81-106.

_____, 1974, Converging clastic wedges in the Mississippian of Alabama: Geol. Soc. America Special Paper 148, v. 27, no. 4, p. 187-207.

_____, 1976, Evolution of Ouachita-Appalachian continental margin: Journal of Geology, v. 84, p. 323-342.

_____, and G. H. Mack, 1982, Paleogeographic relationship of a Mississippian barrier-island and shelf-bar system (Hartselle Sandstone) in Alabama to the Appalachian-Ouachita orogenic belt: Geol. Soc. America Bull., v. 93, p. 6-19.

Thomson, Alan, and R. J. Leblanc, 1975, Carboniferous deep-sea fan facies of Arkansas and Oklahoma (abst.): Geol. Soc. America Abstracts, v. 7, p. 1298-1299.

Valloni, R., and J. B. Maynard, 1981, Detrital modes of recent deep-sea sands and their relation to tectonic setting: A first approximation: Sedimentology, v. 28, p. 28-83.

Wanless, H. R., 1975, Illinois Basin region, Paleotectonic investigations of the Pennsylvanian System in the United States, Part I: U.S. Geol. Surv. Prof. Paper 853-E, p. 71-95.

Young, S. W., 1976, Petrographic textures of detrital polycrystalline quartz as an aid to interpreting crystalline source rock: Jour. Sed. Petrology, v. 46, p. 595-603.

THE BLAKELY "MOUNTAIN" SANDSTONE (LOWER TO MIDDLE ORDOVICIAN) IN ITS TYPE AREA

By Daryl A. Danielson, Jr. and William W. Craig
Department of Geology and Geophysics
University of New Orleans
New Orleans, LA 70148

ABSTRACT

Excellent exposures of the Blakely Sandstone (upper Lower to lower Middle Ordovician) crop out north of Blakely Mountain Dam along the shores of Lake Ouachita in the Mountain Pine quadrangle, Garland County, Arkansas. At the west end of Blakely Mountain, in the type area of the Blakely, is an overturned exposure of the unit that is remarkable for its completeness, lack of cover, structural integrity, abundance of sedimentary structures, and unweathered nature of many of its beds. This and companion exposures at Whirlpool Rock just to the northwest provide a nearly complete understanding of the internal stratigraphy of the Blakely in this part of the Ouachita core area.

The Blakely in this region attains a thickness of approximately 850 feet (260m) and can be subdivided into three parts. The lowest division is approximately 350 feet (107m) thick and contains prominent intervals, up to 100 feet (30m) thick, of amalgamated channels of conglomeratic, quartz-rich sandstone. The middle division, which is about 170 feet (52m) thick, is distinguished by 1) relatively thin beds of conglomeratic sandstone and shale exhibiting complete Bouma sequences, and 2) a grain and cement composition dominated by carbonate. The upper division is nearly 330 feet (101m) thick and is dominated by shale at its base and top, but contains a middle quartz-rich, conglomeratic sandstone interval similar to the amalgamated channels of the lowest division. Orientation of flute casts in the upper and lower division indicates that paleoslope was to the south and west.

INTRODUCTION

The Blakely Sandstone (uppermost Lower to lowermost Middle Ordovician) is composed of interbedded shale, siltstone, sandstone, and conglomerate, the latter of which contains grains that range from granule to boulder size and represent a spectrum of compositions. Dominant among these compositions are calciclastic grains of shallow-water origin, but siltstone, shale, chert (probably *in situ* replacement of limestone), and plutonic igneous grains can be numerically important in places. The Blakely crops out over a broad region in the core area (Benton Uplift) of the Arkansas Ouachita Mountains. The formation represents an influx of coarse detrital material into a basin that dominantly was accumulating clay and silt of the underlying Mazarn and overlying Womble Shales. Its contacts with both of these units are intercalated and conformable.

The Blakely was first studied by A.H. Purdue and H.D. Miser in 1907-8 during field investigations in the Caddo Gap (30') quadrangle, where it was confused with, and included in, the older Crystal Mountain Sandstone (Miser and Purdue, 1929). During initial field work for the Hot Springs Folio in 1909, the two geologists recognized the Blakely as a separate unit and named it for exposures along Blakely Mountain in the northwest corner of the Hot Springs district. The first appearance of the name Blakely in the literature (Miser, 1917) preceded publication of the folio (Purdue and Miser, 1923), which was several years in preparation.

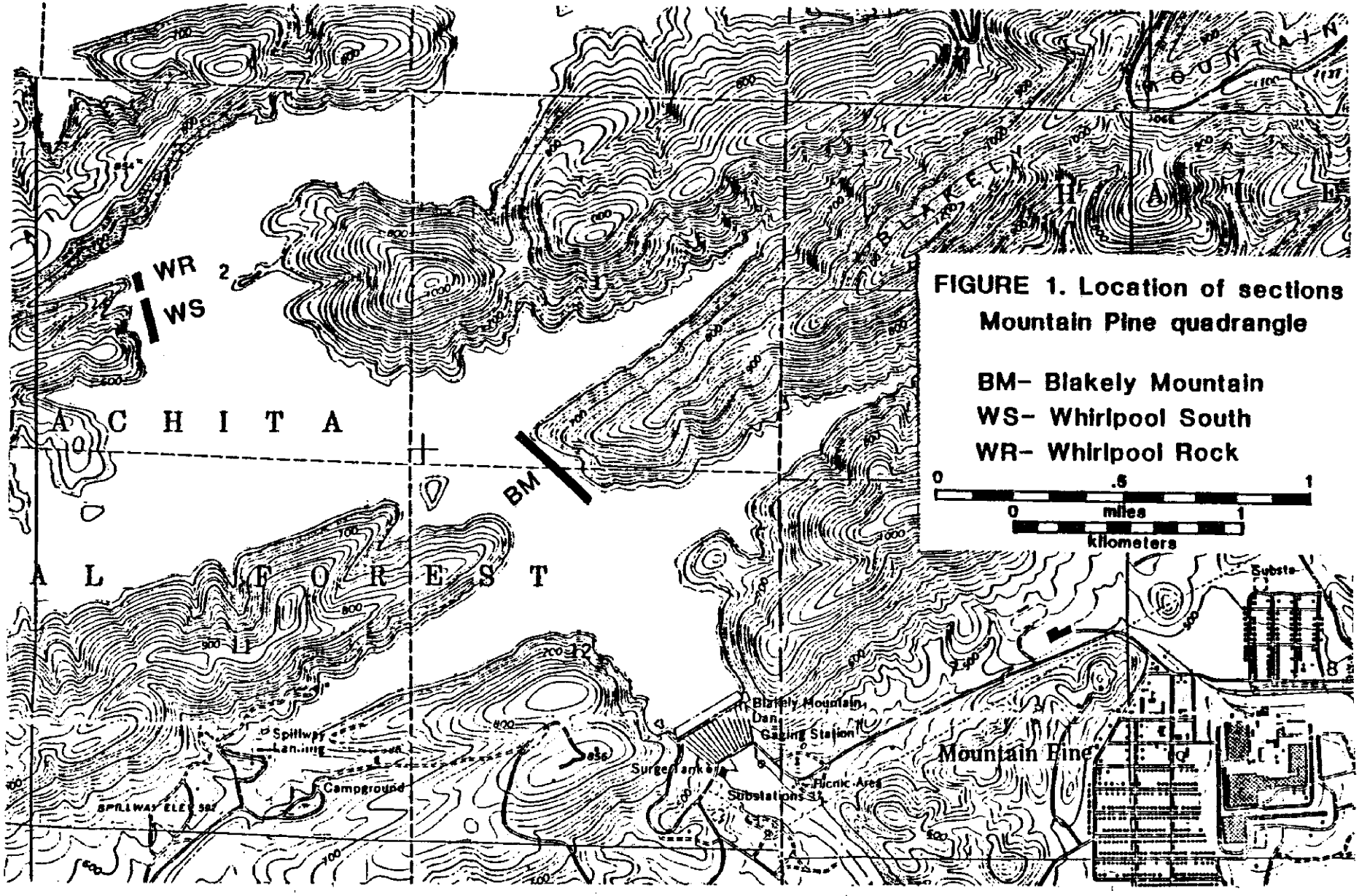

FIGURE 1. Location of sections Mountain Pine quadrangle

BM- Blakely Mountain
WS- Whirlpool South
WR- Whirlpool Rock

Little detailed stratigraphic work has been done on the Blakely because of the structural complexities of the Ouachita core area and the generally poor and deeply weathered exposures in the region. Geologists who have examined sections of the formation report thicknesses that range from less than 200 feet (61m) (Bathke, 1984) to 720 feet (220m) (Stolarz and Zimmerman, 1984). Part of this variation no doubt is because structural complexities make difficult the accurate measurement of sections. However, to a greater extent the different thicknesses reported for the Blakely result from the choice of different formational boundaries by different workers, a natural consequence of the lateral change in the sand content of the unit. As pointed out by Stolarz and Zimmerman (1984), major sand units in the Blakely can pass laterally into shale over relatively short distances. In places, the Blakely interval can be almost entirely shale.

Studies on the Blakely by students at the University of New Orleans (Bathke, 1984; Gaudet, 1986; Danielson, 1987) have been conducted in Montgomery and Garland Counties from the Crystal Mountains east to the vicinity of Blakely Mountain Dam. These studies will be the subject of a future report. The purpose of this report is to document a remarkable section of the Blakely in its type area. The section, which was briefly described by Danielson and Craig (1986), is located on Lake Ouachita at the west end of Blakely Mountain, just north of Blakely Mountain Dam (Figure 1). The Blakely at this locality contrasts with other Blakely sections that we have studied by the near completeness of its exposure, the lack of structural complication, the unweathered nature of many of its contacts with the Mazarn and Womble Shales. The section is overturned and dips about 35^{0} to the north. It and companion exposures just to the northwest at Whirlpool Rock and Whirlpool South (Figure 1) provide a nearly complete understanding of the internal stratigraphy of the formation in this part of the Ouachita core area. The rocks at Whirlpool South, which lie across an anticlinal axis from Blakely Mountain, are upright and face north. The exposure consists of two thick sandstones separated by a shaley unit, all in the Lower Blakely. The nearly vertical sandstone at Whirlpool Rock faces south and apparently is the higher of the two sandstones at Whirlpool South. We interpret a synclinal axis between Whirlpool south and Whirlpool Rock to explain this reversal of facing. For all practical purposes, these Blakely exposures can be reached only by boat, conveniently available at the nearby Spillway Landing Marina (Figure 1).

BLAKELY STRATIGRAPHY

Purdue and Miser (1923) described the Blakely of the Blakely Mountain area as "about 500 feet of interbedded shale and sandstone, of which the shale forms probably 75 per cent." The Blakely at the west end of Blakely Mountain, an exposure mostly not available to Purdue and Miser, is 855 feet (261m) thick and contains only about 40% shale. This is the thickest and sandiest Blakely reported to date. We emphasize, however, that it is apparent from Purdue and Miser's report that the sand content, and no doubt the thickness of the unit, changes laterally within the area. The shale is black and fissile, with silt laminae in places, and is identical to that of the underlying Mazarn and overlying Womble Shales. The conformable transition from Blakely to Womble, well displayed along the shore at the south end of the exposure, is by a decrease in sandstone and an increase in shale. The contact is placed at the top of a five-foot sandstone (Figure 2), above which no sandstone greater than a foot occurs. The Blakely-Mazarn contact is not exposed along the shore-line formed by the point of Blakely Mountain, but can be examined deep in the inlet to the north in ravines running off the mountain. The formational boundary is placed where the conglomeratic base of the thick, lower, ridge-forming sandstone of the Blakely is in contact with the shale of the Mazarn. Below this level only a few thin sandstones occur within the shale and siltstone of the Mazarn. About 100 feet (30m) below the contact, thin bedded, rippled, sandy, pelletoidal limestone dominated the Mazarn, a character that seems consistent for the formation in the region. The Blakely-Mazarn contact is better exposed, during low lake level, at the Whirlpool South locality (Figure 1), where essentially the same stratigraphy prevails.

The basal Blakely sandstone scours into the shale of the upper Mazarn on which it

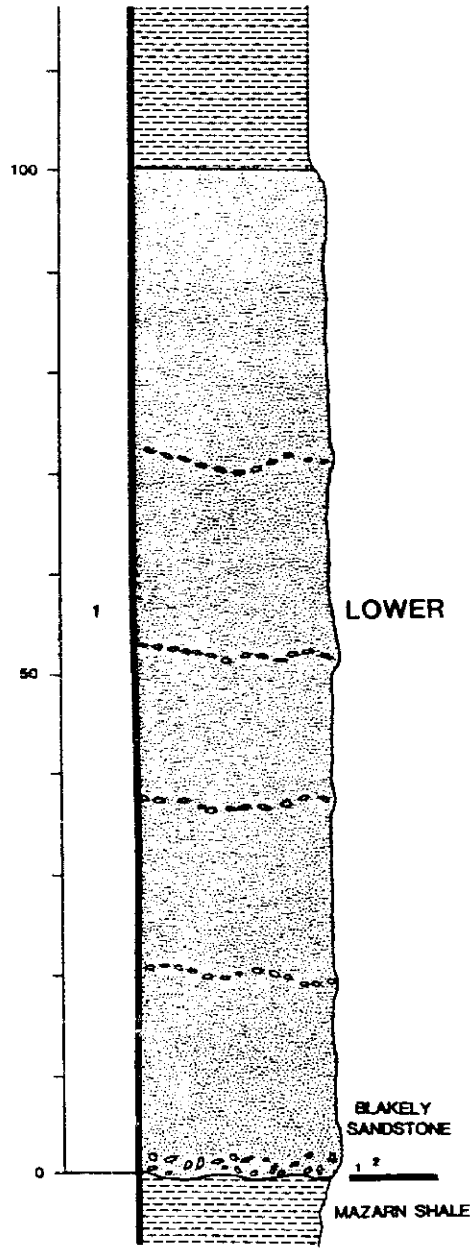
100
50
0
1
LOWER
BLAKELY SANDSTONE
1 2
MAZARN SHALE

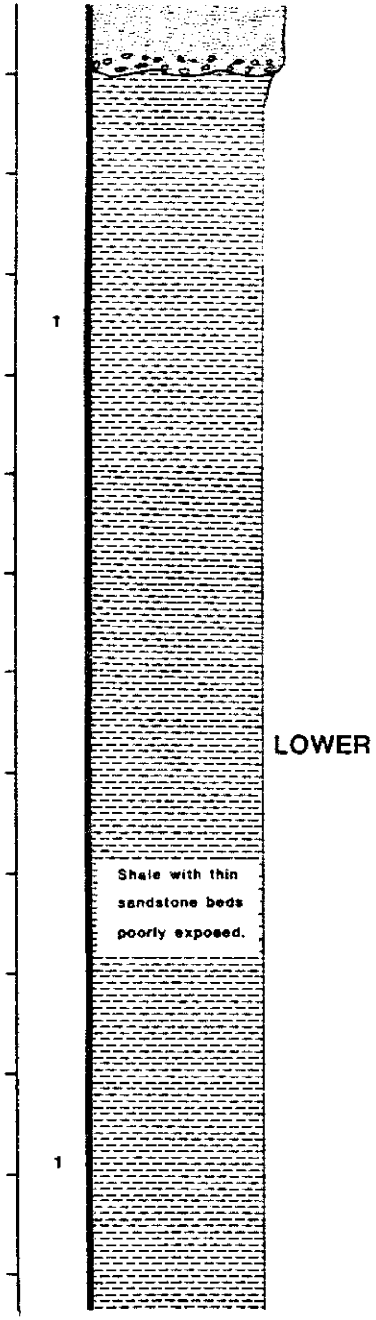
200
150
1
1
LOWER
Shale with thin sandstone beds poorly exposed.

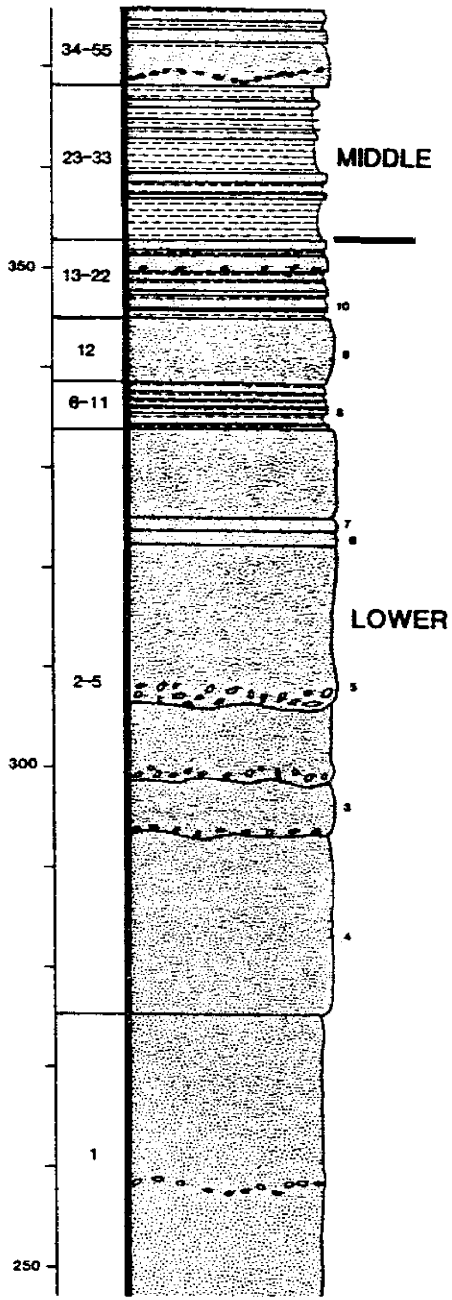
350
300
250
34-55
23-33
13-22
12
6-11
2-5
1
MIDDLE
LOWER
10
9
8
7
6
5
3
4

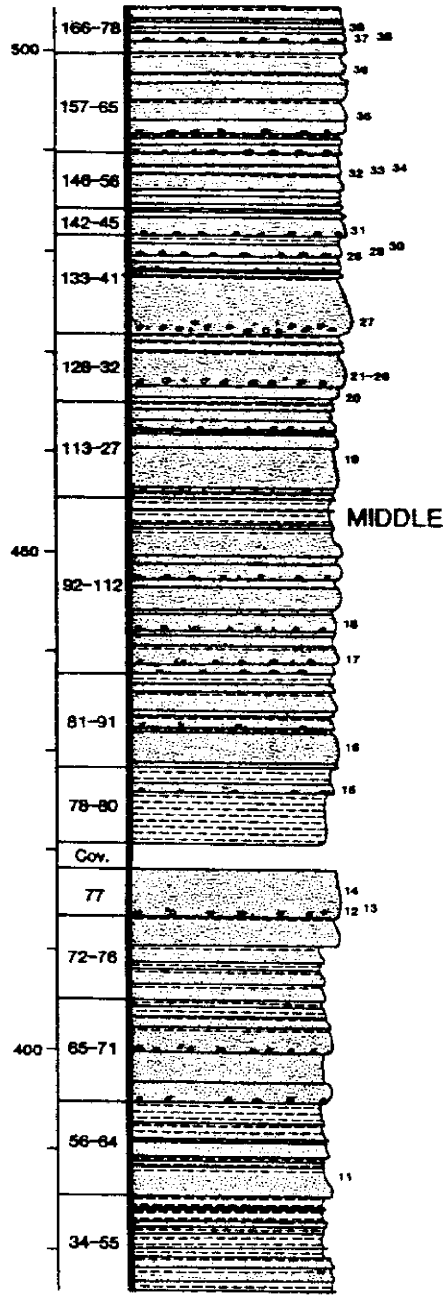
500
450
400
166-78
157-65
146-56
142-45
133-41
128-32
113-27
92-112
81-91
78-80
Cov.
77
72-76
65-71
56-64
34-55
MIDDLE
38
37
36
35
32 33 34
31
28 29 30
27
21-26
20
19
18
17
16
15
14
12 13
11

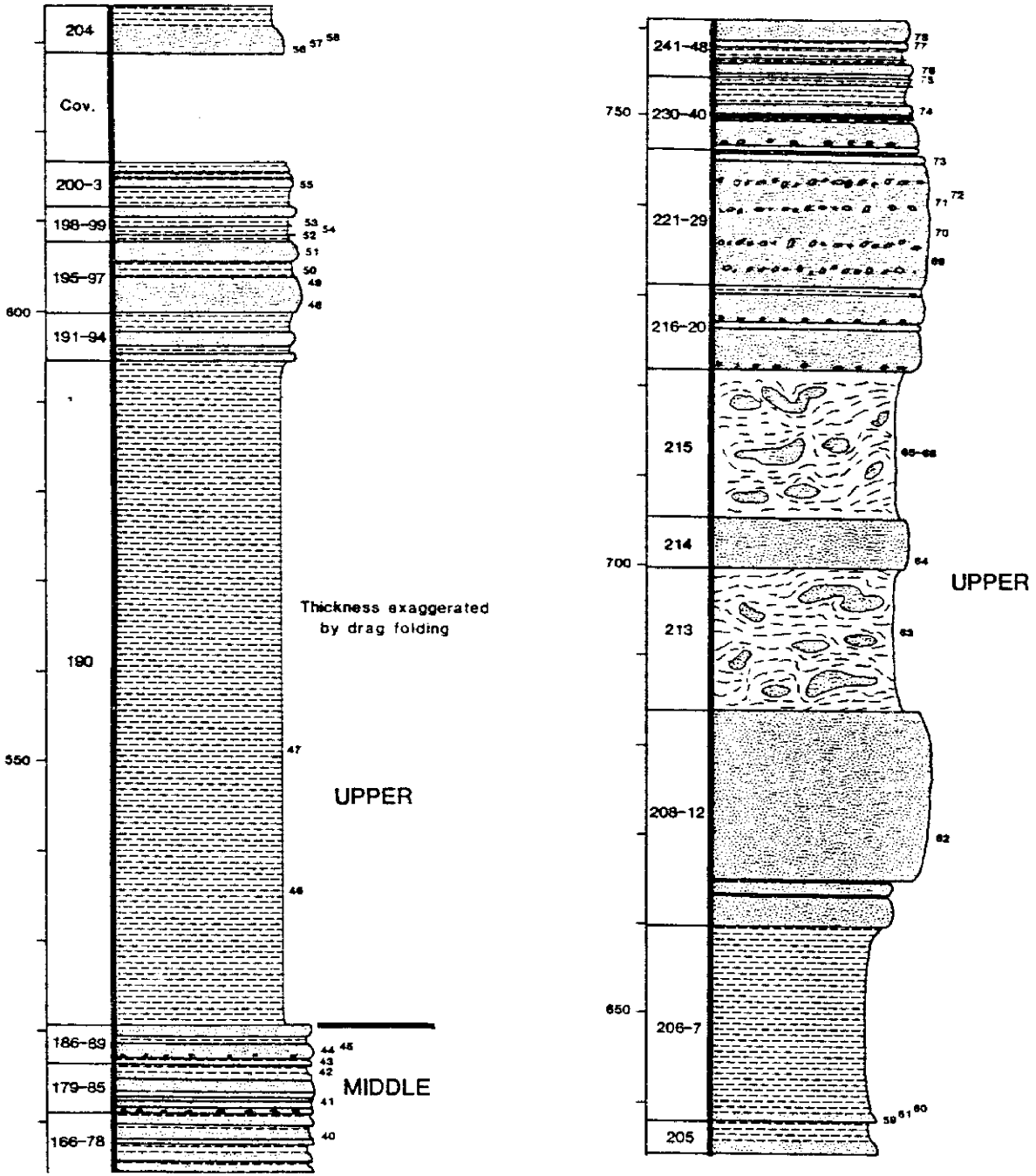

FIGURE 2. BLAKELY MOUNTAIN SECTION

Lithic symbols apparent from text.

rests. Scouring is found at the base of many Blakely sandstones, particularly conglomeratic ones. There is little reason to attach any special historical significance to the basal Blakely conglomerate, as did Purdue and Miser (1923) in suggesting the presence of an unconformity at the top of the Mazarn. The two units are almost certainly conformable on a regional basis.

The Blakely at Blakely Mountain can be subdivided into three units. The thickness of the lower Blakely is 350 feet (107m), 78% of which is sandstone and minor conglomerate; the remaining 22% consists of shale and siltstone (Figure 2). The upper 77 feet (23m) of the lower Blakely are well exposed on the north end of the terminus of the Blakely Mountain peninsula. The lowermost 275 feet (84m) are poorly exposed on the dip-slope (north face) of Blakely Mountain. The thickness for this interval was determined graphically, utilizing a strike and dip of N60E and 35NW, and projecting the Mazarn-Blakely contact westward from its previously mentioned position deep in the inlet north of the Blakely Mountain peninsula. The lower Blakely is well exposed (especially at low-water level) at the Whirlpool South section (Figures 1,3), where it is composed of two thick amalgamated sandstones separated by about 140 feet (43m) of shale with thin sandstone and siltstone interbeds. The exact thicknesses of these sandstones are difficult to determine, but rough measurements indicate that they are 100 feet (30m) or slightly greater. The top of the upper sand (to the north) is not exposed. It is these sandstones that hold up the crest of Blakely Mountain. The lowermost amalgamated sandstone (to the south) contains a graded, deeply weathered, reddish colored, friable, conglomeratic sandstone at its base. The conglomerate is no doubt the one that Purdue and Miser (1923) described at the base of the Blakely. The conglomerate, composed of weathered sedimentary and plutonic grains, is better preserved deep in the inlet north of Blakely Mountain. The prevalent rock type of these lower Blakely sandstones is a friable, medium-grained sandstone, cemented by either calcite or silica, and dominated by well-rounded quartz framework grains.

The upper 77 feet (23m) of the lower Blakely at Blakely Mountain (beds 2-22, Figure 2) is continuous with the upper of the two amalgamated sandstone intervals and contains 95% sandstone. Red, friable, highly weathered, vuggy, lenticular, conglomeratic layers delineate the base of repeated graded sequences, 5 to 16 feet (1.5-4.9m) thick, within the amalgamated sandstone. Interstratal contacts between graded sequences are commonly scoured. The vugs, 1 to 2 1/2 inches (2.5-6.4cm) long, have prismatic outlines and sharp planar boundaries with the surrounding medium-to-coarse-grained sand matrix. These vugs are interpreted as resulting from the leaching of gravel-size framework grains of unknown composition. Pebble and cobble-size, angular, black and gray chert occurs as float within this interval. Similar pebbles are present in place at the base of the upper sandstone at Whirlpool Rock (Figure 4).

Planar laminations are common sedimentary structures; structureless, homogeneous layers are equally common. Partial Bouma sequences consisting of the A and B divisions, with the A divisions either graded or structureless, can be identified. Mutti and Ricci Lucchi's (1972) Facies "A" for the conglomerate-bearing layers and Facies "B" for the structureless sandstone are appropriate characterizations of these lower Blakely sandstones.

The upper 30 feet (9m) (top of bed 2, sample 6, through bed 22, Figure 2) of the lower subdivisions of the Blakely is thinner bedded sandstone, 3 inches to 9 feet (7.6cm to 2.7m) thick, interbedded with shale up to 7 inches (18cm) thick. Basal bedding contacts (superpositional tops in these overturned beds) are sharp and in places commonly exhibit sole marks, including flute casts. These flute casts demonstrate delivery of sediment from the north. The upper contacts of the sandstone are either sharp or gradational with shale. Very fine- and fine-grained sandstone dominate the upper interval in contrast to the medium- to coarse- grained sandstone within the rest of the lower division. The upper 77 feet (23m) of the lower Blakely both fines and thins upward.

The middle Blakely has a measured thickness of 168 feet (51m). Sandstone and conglomerate make up 67% of the division and

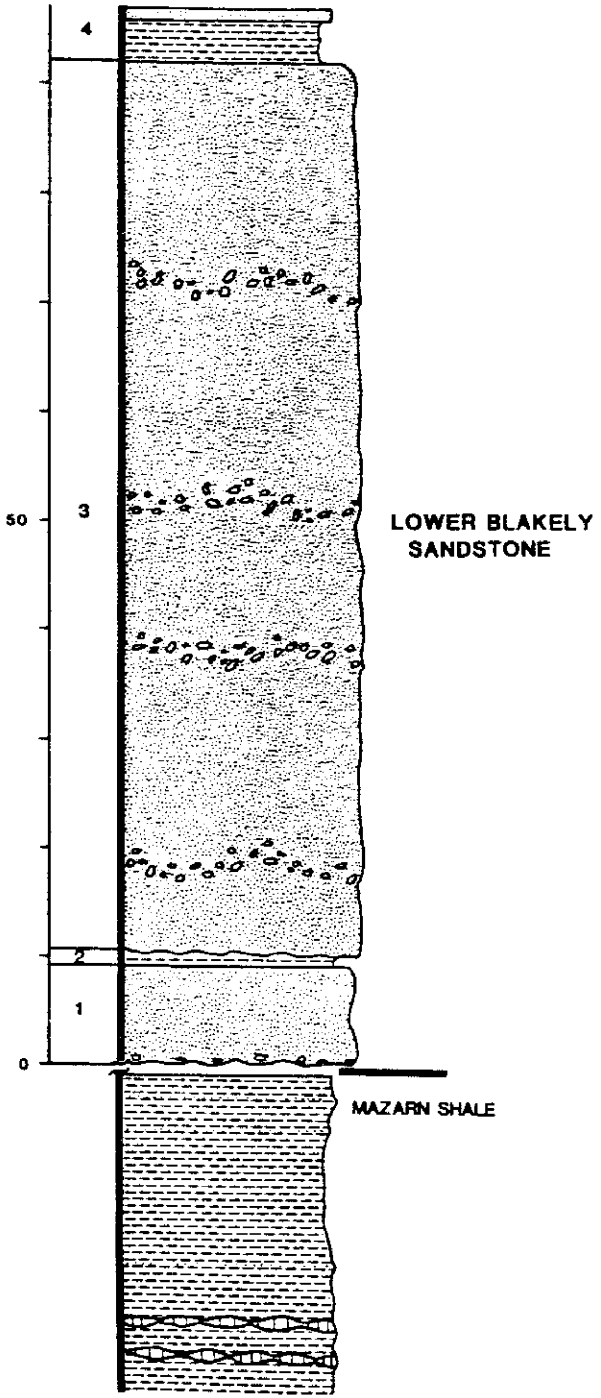

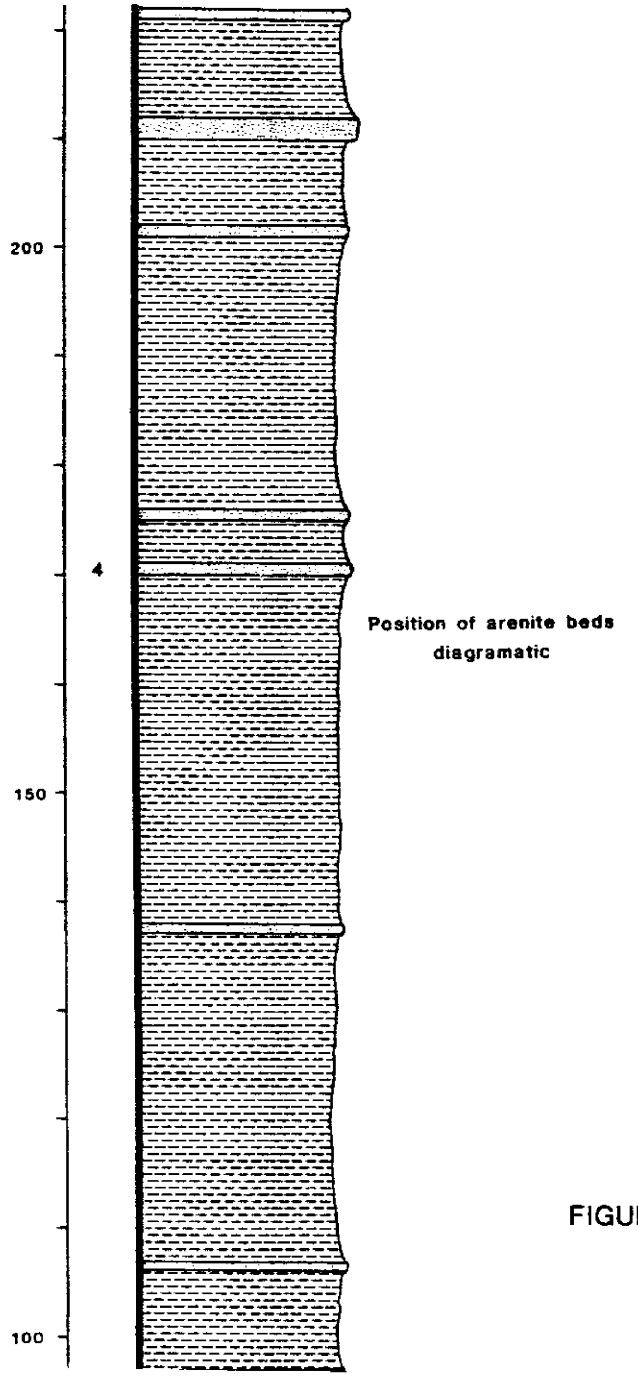

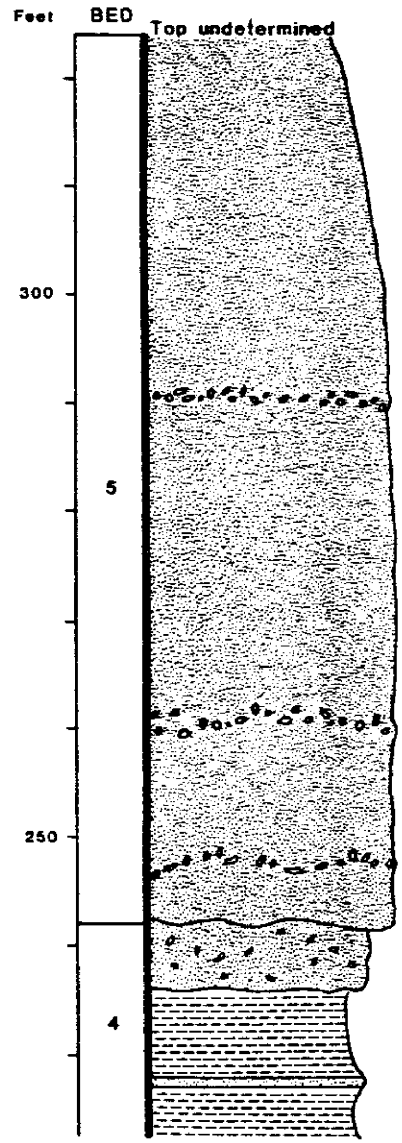

FIGURE 3. WHIRLPOOL SOUTH FIGURE 4.

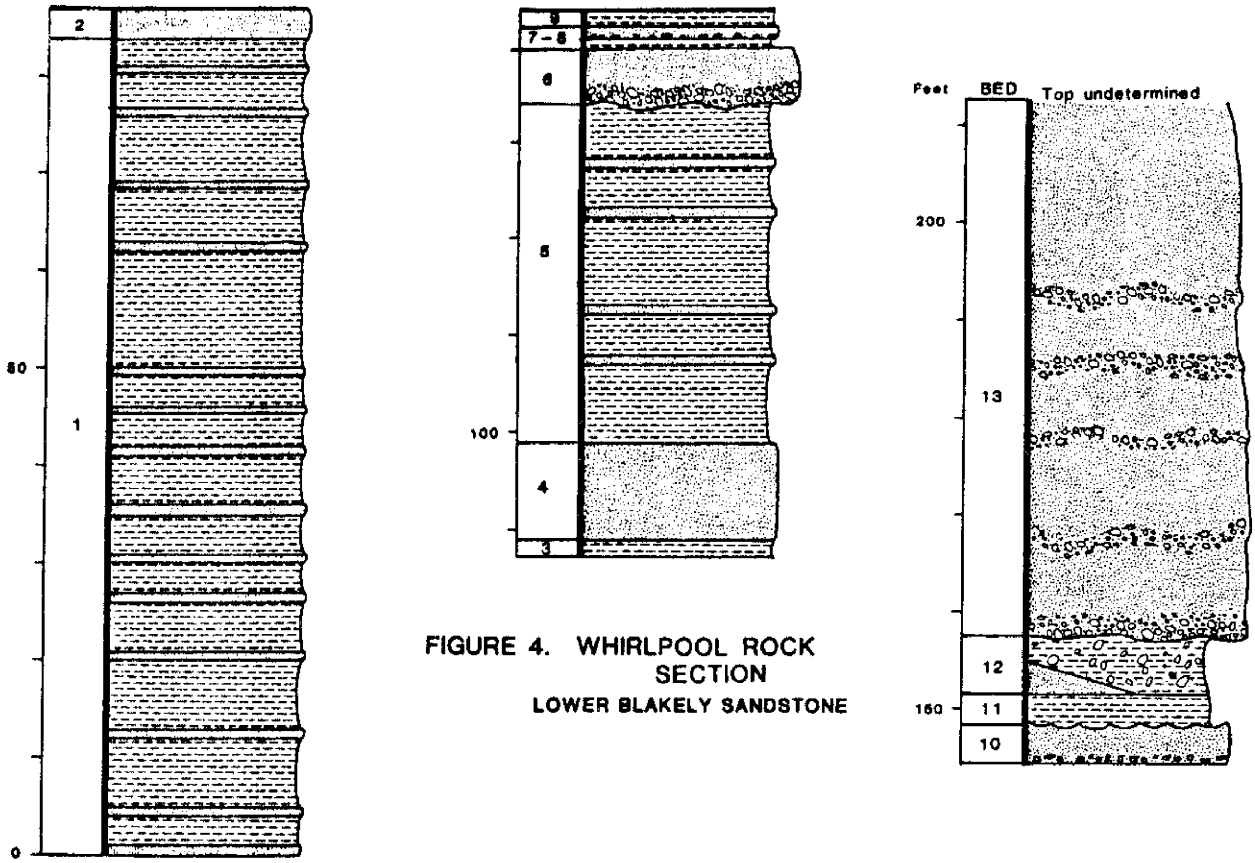

FIGURE 4. WHIRLPOOL ROCK SECTION
LOWER BLAKELY SANDSTONE

the remaining 33% consists of shale and siltstone.

The middle Blakely, thinnest of the subdivisions within the formation, contains 63% of the total number of beds identified at the Blakely Mountain section. Bedding is typically in sandstone-shale couplets, with sandstone layers commonly possessing sharp basal contacts and gradational upper contacts. Both symmetrical and asymmetrical trends in bed thicknesses are present; the asymmetrical trends thicken or thin upward with no second-order trend discernable.

The lower 42 feet (13m) of the middle Blakely (beds 23-64, Figure 2) are composed of 57% shale and siltstone interbedded with <1/2 inch to 4-feet (1.3cm-1.2m) thick sandstone beds. In the field, this shaley interval provides a natural break between the thick-bedded sandstone of the lower Blakely and the thin-bedded sandstone that follows within the remainder of the middle Blakely. The sandstone within the lower portion of the middle Blakely is typically light brown to gray, structureless, very fine to fine grained and quartz rich. Sandstone beds are generally wavy, lenticular and thin, ranging from <1/2 inch to 8 inches (1.3-20.3cm) in thickness. Scoured basal contacts and faint ripple laminations present in these wavy-bedded sandstones suggest a correlation to the traction laid deposits of Mutti and Ricci Lucchi's (1972) Facies "E".

A 4-foot (1.2m), medium-grained, siliciclastic sandstone in the lower shaley interval of the middle Blakely (bed 34, Figure 2) is an excellent example of the amalgamated nature of much of the interval. Toward the stratigraphic base of the bed is a pebbly, vuggy, conglomeratic layer that delineates a scoured contact between successive depositional episodes. The internal conglomeratic layer is undulatory, measuring 2 inches (5.1cm) from the stratigraphic base in one location to 12 inches (30.5cm) from the stratigraphic base in

another. Because the sand grain size is similar between the two depositional episodes, only the thin conglomeratic layer identifies the bed as an amalgamated sandstone layer.

Beds also are lenticular in the upper portion of the middle Blakely, where scouring at basal contacts off sandstone and conglomeratic sandstone has resulted in amalgamated layers. Grains range from silt to pebble size. Beds range in thickness from <1/2 inch to 5 1/2 feet (1.3cm-1.7m). Shale interlayers are thin, commonly present only as discontinuous partings.

Granule- and pebble-size clasts of limestone, chert, (limestone silicified *in situ*), shale, sandstone, siltstone, and granitic-plutonic rock fragments from the composition of the conglomerates, which are commonly deeply weathered. In many beds the gravel content has been completely removed and only suggested by the presence of vugs. The sand component of the turbidite beds in the middle Blakely can be exclusively composed of either siliciclastic or calciclastic grains, or subequal mixtures of the two. Weathering has produced reddish-brown "rotten" layers that are interpreted to result from the leaching of carbonate grains and cement. This is confirmed in that some weathered sandstones can be broken and an unweathered core of carbonate found. It is probable that all the deeply weathered sandstone layers of the middle division were originally dominated by grains and cement of carbonate composition.

Evidence of faunal activity in the form of burrows and trails is present on bedding surfaces. Vertical burrows also are common, particularly in the very thin interbeds of sandstone and shale.

Sedimentary structures within the middle Blakely are abundant and include graded beds, planar laminations, and large- and small-scale ripple bedding. Ripple forms on bedding planes are common. The sequence of these structures is clearly correlative to the Bouma sequence of sedimentary structures in turbidite beds (Bouma, 1962). All Bouma divisions, A through E, are commonly present. One of the interesting features about the sequence of internal structures in these graded units is the presence in some of cross bedding, which indicates the occurrence of a dune phase of deposition. Bouma did not include cross bedding in his sequence of structures. Although flume studies, under certain conditions of current strength and grain size, predict the presence of a dune bed form between the upper plane and ripple bed forms, cross bedding is not common in turbidites. It has been reported, however, in its predicted position by some workers. Allen (1970) reviews the problem and concludes that the dune bed form and its accompanying cross bedding can be expected in turbidites that originated in relative coarse-grained sediment. Dune cross bedding in the Blakely, which is most common in thicker, coarse-grained sandstone and conglomerate, is in agreement with this conclusion. Dune cross bedding is present in all subdivisions of the Blakely, but is most common in the turbidites of the middle division. It can occur either alone or as a part of a Bouma sequence. For instance, in bed 130 (samples 21-26, Figure 2), which is a prominent unit in the exposure (Figures 5 and 6), the sequence is 25 inches (63.5cm) of graded limestone conglomerate (Ta), 14 inches (35.6cm) of parallel-laminated, graded calciclastic sandstone (Tb), and 2" (5.1cm) of siltstone and shale (Tde). Up section (down dip) 5.5 feet (1.7m) from bed 130, bed 133 (sample 27, Figure 2) contains the sequence: 43 inches (109.2cm) of graded, vuggy (conglomeratic) sandstone (Ta), 7.5 inches (19.1cm) of parallel-laminated, medium-grained siliciclastic sandstone (Tb), 10 inches (25.5cm) of cross-bedded, medium-grained siliciclastic sandstone (dune phase Tc), 5 inches (12.7cm) of cross-laminated, fine- to medium-grained siliciclastic sandstone (ripple phase Tc), and 2 inches (5.1cm) of siltstone and shale (Tde). Other examples of sequences containing cross bedding are bed 162 (sample 35, Figure 2), where the order is 3 inches (7.6cm) of parallel-laminated, coarse-grained calciclastic sandstone (Tb), 16 inches (40.6cm) of cross-bedded, coarse-grained calciclastic sandstone (dune phase Tc), 3 inches (7.6cm) of cross-laminated calciclastic sandstone (ripple phase Tc), and 3 inches (7.6cm) of shale and siltstone (Tde); and bed 84 (sample 16, Figure 2), in which is recorded 1 to 5 inches (2.5 to 12.7cm) of structureless, medium- to coarse-grained siliciclastic sandstone (Ta), 21 to 27 inches

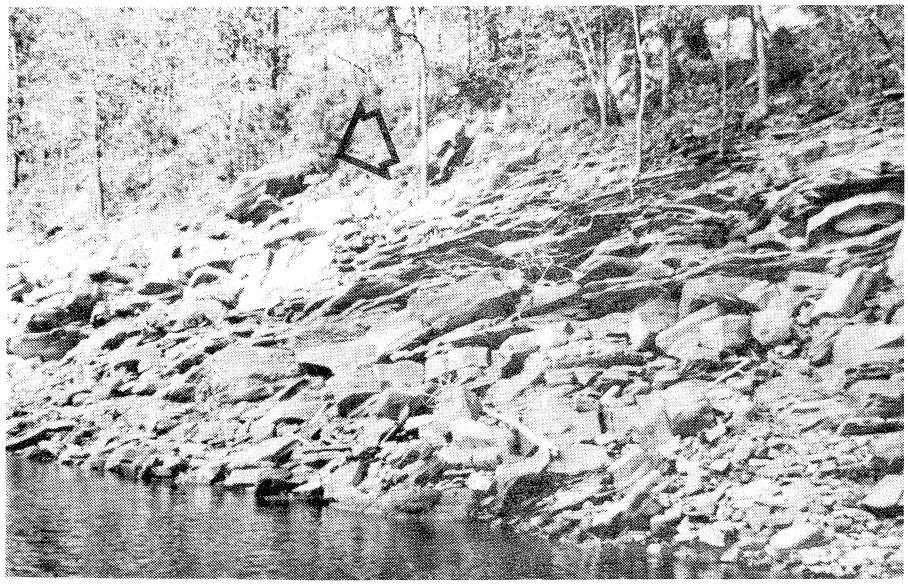

FIGURE 5. *Middle Blakely turbidites, shore of Lake Ouachita, west end of Blakely Mountain. Arrow points to bed 130.*

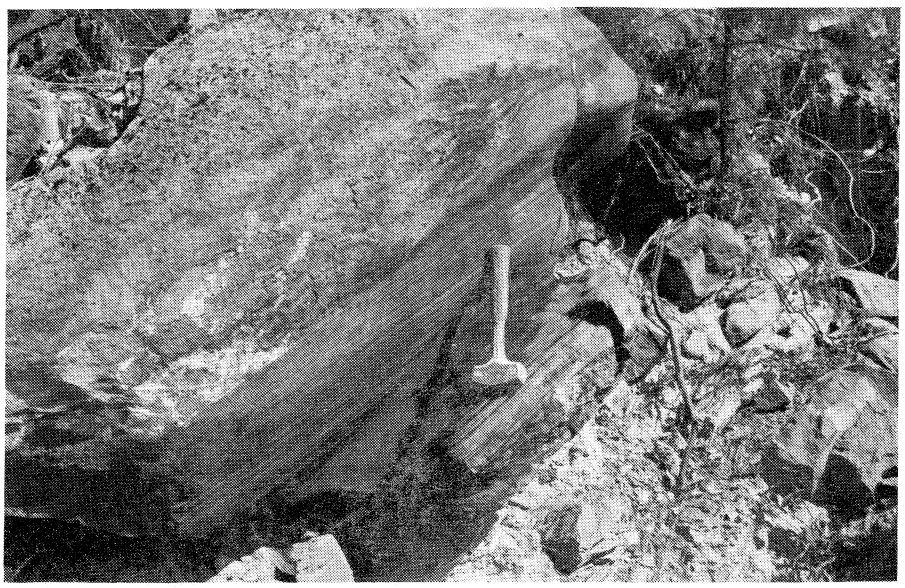

FIGURE 6. *Bed 130 showing sequence from superpositional top to bottom of conglomeratic, graded Ta division, laminated Tb division, and cross bedded Tc division (below hammer at base of ledge). Grains standing in relief are silicified carbonate.*

(53.3cm to 68.6cm) of cross-bedded, medium-grained siliciclastic sandstone (dune phase Tc), and 2.5 inches (6.4cm) of siltstone and shale (Tde). In the latter example, the varying thicknesses of the Ta and Tc Bouma divisions result from scour; the Ta division scours into the unit stratigraphically below it, and in turn is scoured by the overlying Tc division. Several dune and ripple phase Tc units exhibit scour at their bases, suggesting that they are characterized by 3D geometry (Harms and others, 1982).

Other common Bouma sequences found in the Middle Blakely (see Figure 2 for positions) include bed 138 (samples 28-30): 14 inches (35.6cm) of structureless, vuggy (conglomeratic), coarse-grained siliciclastic sandstone (Ta), 0.5 inch (1.3cm) of laminated, fine- to medium-grained siliciclastic sandstone (Tb), 1 inch (2.5cm) of cross-laminated, fine- to medium-grained siliciclastic sandstone (ripple phase Tc), and 1/5 inches (3.8cm) of siltstone and shale (Tde); bed 77 (samples 12-14): 46 inches (116.8cm) of structureless, slightly conglomeratic, fine- to medium-grained siliciclastic sandstone (Ta), 4 inches (10.2cm) of parallel-laminated, very fine-grained siliciclastic sandstone (Tb), 7 inches (17.8cm) of cross-laminated, very fine-grained siliciclastic sandstone (ripple phase Tc), and a thin shale and siltstone layer (Tde); beds 146-160, an interval dominated by 2 to 10 inch (5.1 to 25.4cm) thick units of Tb, Tc, Tde divisions; and beds 119-126, which are characterized by repeated fine-grain siliciclastic sequences of Tc and Tde units that average 2 to 3 inches (5.1 to 7.6cm) in thickness.

The middle division of the Blakely is dominated by strata characteristic of Mutti and Ricci Lucchi's (1972) Facies "C", in which the Bouma A interval is present. Facies "D", in which the Bouma A interval is absent, is common. Thin sandstones with a pinch-and-swell, lenticular bedding style, characteristic of Facies "E", also are present in the middle Blakely.

The upper Blakely begins 521 feet (159m) above the Mazarn-Blakely contact and has a measured thickness of 334 feet (102m). Sandstone and conglomerate make up 40% of the division; the remaining 60% consists of shale and siltstone. An interval of shale (bed 190, Figure 2) measured at 74 feet (23m) in thickness, but considerably exaggerated by subsidiary folding, separates the coarse middle Blakely from the coarse sediments of the upper Blakely and is arbitrarily assigned to the upper subdivision.

Overlying the basal shale are 22 feet (7m) of thin, wavy interbeds of sandstone, shale, and siltstone (beds 191-203) that lack the structural complication found in the underlying shale. The sandstone layers commonly exhibit a pinch-and-swell, lenticular bedding style. Sedimentary structures are poorly preserved, with graded beds the most prominent feature; Bouma sequences beginning with the A or B division are present. These sandstone layers exhibit a thinning upward trend. Burrows are common, and sand-filled burrows within shale layers demonstrate that the beds are overturned.

Within the shallow re-entrant along the shoreline (Figure 1) of the measured section is an interval (beds 204-207, Figure 2), 43 feet (13m) thick, that again is dominated by a black fissile shale, but contains three sandy layers at its base. Each of these sandy layers consists of irregularly bedded sandstone and shale that possess a bedding style suggestive of a combination of flaser and lenticular bedding.

Above the shale interval (beds 206-207), sandstone and conglomerate dominate, comprising 54% of the section, with the remaining 46% made up of shale and siltstone. The most prominent outcrop feature of the upper division of the Blakely is two amalgamated sandstones, each approximately 25 feet (7.6m) thick. The lowermost stratigraphically of the two sandstones (beds 208-212, Figure 2) is a vuggy, structureless, weathered, friable, orange to gray, medium-grained quartz arenite. The vugs are large with elliptical outlines; they do not appear to be the artifact of molds left by weathering equivalent gravel-size clasts. The friable character of the rock, as well as its contained vugs, is interpreted to result from the leaching of calcite cement. At the base of this amalgamated sandstone, separate depositional events are distinguished by the occurrence of discontinuous shale partings. Flute casts are

present on bedding soles, as are burrows. As with flute casts in the lower Blakely, upper Blakely flutes indicate a northerly source for the sediments.

The upper amalgamated sandstone (beds 216-229, Figure 2) is distinguished by conglomeratic zones in an interval dominated by well indurated, medium-grained, silica-cemented quartz arenite. The conglomerates are defined by lenticular horizons of concentrated vugs, which are generally less than an inch (2.5cm) in long dimension. It is a peculiarity of some horizons that the vugs become less abundant both above and below their major level of concentration. The composition of the pebbles that formed them is unknown, possibly shale and/or limestone. At least eight depositional episodes, as outlined by the moldic conglomerates, can be identified. The zones, however, are very lenticular; a short distance along the strike (up the hillside) they are absent.

Less common in the upper amalgamated sandstone are deeply weathered conglomerates that now consist of soft, reddish brown sandstone layers containing common blebs of white kaolinite that contrast sharply with their matrix. These kaolinite blebs are probably altered feldspathic rock fragments. The deeply weathered character of these reddish conglomeratic zones suggests that the parent rock was calcite cemented.

Discontinuous shale partings further attest to the amalgamated character of this sandstone. The few sedimentary structures present consist of faint, planar- and cross-laminated zones. Worm burrows are common on bedding soles.

Between the two amalgamated sandstones is 38 feet (11.6m) of irregularly bedded shale and siltstone (beds 213, 215) separated by a regularly bedded, prominent sandstone (bed 214). The irregularly bedded units contain sandstone and conglomerate lenses, some of which are transverse to normal bedding, and patches of muddy sandstone. We attribute these textures to soft-sediment deformation and correlate this "chaotic" interval with Mutti and Ricci-Lucchi's (1972) Facies "F", which is interpreted as the product of gravity sliding and slumping.

The uppermost 109 feet (33m) of the upper division of the Blakely consists of thin-bedded sandstone and shale, and four covered intervals that total 43 feet (13m). Sandstones are siliciclastic, commonly graded, muddy, and contain shale clasts in their bases.

A mud-supported pebble conglomerate (bed 263), 3 feet (0.9m) thick, occurs 12 feet (3.7m) below the Blakely-Womble contact. The pebbles are weathered, well rounded, randomly distributed, and dominated by siltstone clasts. Purdue and Miser (1923, p. 3) described a similar conglomerate, 18 inches (45.7cm) thick, near the top of the formation.

Asymmetric trends in sandstone bed thicknesses characterize the upper division of the Blakely. Two thinning upward trends are followed by a thickening upward trend to the Blakely-Womble contact, which is placed at the top of a prominent, cross-bedded, 5-foot (1.5m) sandstone (bed 267).

SELECTED REFERENCES

Allen, J.R.L., 1970, The sequence of sedimentary structures in turbidites, with special reference to dunes: Scottish Jour. Geology, v. 6, p. 146-161.

Bathke, S.A., 1984, Stratigraphy, petrology, and environment of deposition of the Blakely Sandstone, Ouachita Mountains, western Garland County, Arkansas [Masters Thesis]: Univ. New Orleans, 148 p.

Bouma, A.H., 1962, Sedimentology of some flysh deposits, a graphic approach to facies interpretation: Elsevier, Amsterdam, 168 p.

Danielson, D.A., 1987, Stratigraphy, petrology, and structure of the Blakely Sandstone, Mountain Pine quadrangle, Garland County, Arkansas [Masters Thesis]: Univ. New Orleans, 244 p.

_____, and Craig, W.W., 1986, Description of the Blakely Sandstone (Middle Ordovician) in its type area, Garland County, Arkansas: Geol. Society America, Abstracts with Programs, v. 18, p. 216.

Gaudet, D.J., 1986, Stratigraphy, Petrology, an depositional environment of the Blakely Sandston Ouachita Mountains, Montgomery County, Arkansa [Masters Thesis]: Univ. of New Orleans, 171 p.

Harms, J.C., Southard, J.B., Walker, R.G., 1982, Structure and sequences in clastic rocks: Soc. Econ. Paleontologist and Mineralogists Short Course no. 9, p. 2-1 - 2-55.

Miser, H.D., 1917, Manganese deposits of Caddo Gap an De Queen quadrangles, Arkansas: U.S. Geological Survey Bull. 660, p. 59-112.

_____, and Purdue, A.H., 1929, Geology of the De Quee and Caddo Gap quadrangles, Arkansas: U.S. Geol. Surve Bull. 808, 195 p.

Mutti, W., and Ricci-Lucchi, 1972, Le turbiditi dell'Appennine settentrionale: introduzione all'analisi di facies: Memorie della Societa Geologica Italiana, v. 11, p. 161-199. (Translated into English by T.H. Nilsen, 1978, International Geology Review, v. 20, no. 2, p. 125-166.)

Purdue, A.H., and Miser, H.D., 1923, Geologic Atlas of the United States: Hot Springs Folio: U.S. Geol. Survey Folio No. 215, 12 p.

Stolarz, R.J., and Zimmerman, J., 1984, Geology of the Blakely Sandstone in eastern Montgomery and western Garland Counties, Arkansas: in McFarland, J.D., III, and Bush, W.V., eds., Contributions to the Geology of Arkansas, v. 2, Arkansas Geological Commission, Misc. Pub. 18-B, p. 135-146.